

Partial Differential Equations of Electrostatic MEMS

by

Yujin Guo

B.Sc., China Three Gorges University, 2000

M.Sc., Huazhong Normal University, 2003

A THESIS SUBMITTED IN PARTIAL FULFILMENT OF
THE REQUIREMENTS FOR THE DEGREE OF

Doctor of Philosophy

in

The Faculty of Graduate Studies

(Mathematics)

The University of British Columbia

July 2007

© Yujin Guo 2007

Abstract

Micro-Electromechanical Systems (MEMS) combine electronics with micro-size mechanical devices in the process of designing various types of microscopic machinery, especially those involved in conceiving and building modern sensors. Since their initial development in the 1980s, MEMS has revolutionized numerous branches of science and industry. Indeed, MEMS-based devices are now essential components of modern designs in a variety of areas, such as in commercial systems, the biomedical industry, space exploration, telecommunications, and other fields of applications.

As it is often the case in science and technology, the quest for optimizing the attributes of MEMS devices according to their various uses, led to the development of mathematical models that try to capture the importance and the impact of the multitude of parameters involved in their design and production. This thesis is concerned with one of the simplest mathematical models for an idealized electrostatic MEMS, which was recently developed and popularized in a relatively recent monograph by J. Pelesko and D. Bernstein. These models turned out to be an incredibly rich source of interesting mathematical phenomena.

The subject of this thesis is the mathematical analysis combined with numerical simulations of a nonlinear parabolic problem $u_t = \Delta u - \frac{\lambda f(x)}{(1+u)^2}$ on a bounded domain of \mathbb{R}^N with Dirichlet boundary conditions. This equation models the dynamic deflection of a simple idealized electrostatic MEMS device, which consists of a thin dielectric elastic membrane with boundary supported at 0 above a rigid ground plate located at -1 . When a voltage λ is applied, the membrane deflects towards the ground plate and a snap-through (touchdown) may occur when it exceeds a certain critical value λ^* (pull-in voltage). This creates a so-called pull-in instability which greatly affects the design of many devices. In order to achieve better MEMS design, the elastic membrane is fabricated with a spatially varying dielectric permittivity profile $f(x)$.

The first part of this thesis is focussed on the pull-in voltage λ^* and the quantitative and qualitative description of the steady states of the equation. Applying analytical and numerical techniques, the existence of λ^* is established together with rigorous bounds. We show the existence of at least one steady state when $\lambda < \lambda^*$ (and when $\lambda = \lambda^*$ in dimension $N < 8$), while none is possible for $\lambda > \lambda^*$. More refined properties of steady states—such as regularity, stability, uniqueness, multiplicity, energy estimates and comparison results—are shown to depend on the dimension of the ambient space and on the permittivity profile.

The second part of this thesis is devoted to the dynamic aspect of the parabolic equation. We prove that the membrane globally converges to its unique maximal negative steady-state when $\lambda \leq \lambda^*$, with a possibility of touchdown at infinite time when $\lambda = \lambda^*$ and $N \geq 8$. On the other hand, if $\lambda > \lambda^*$ the membrane must touchdown at finite time T , which cannot take place at the location where the permittivity profile $f(x)$ vanishes. Both larger pull-in distance and larger pull-in voltage can be achieved by properly tailoring the permittivity

Abstract

profile. We analyze and compare finite touchdown times by using both analytical and numerical techniques. When $\lambda > \lambda^*$, some a priori estimates of touchdown behavior are established, based on which, we can give a refined description of touchdown profiles by adapting recently developed self-similarity methods as well as center manifold analysis. Applying various analytical and numerical methods, some properties of the touchdown set –such as compactness, location and shape– are also discussed for different classes of varying permittivity profiles $f(x)$.

Table of Contents

Abstract	ii
Table of Contents	iv
List of Tables	vi
List of Figures	vii
Acknowledgements	ix
Statement of Co-Authorship	x
1 Introduction	1
1.1 Electrostatic MEMS devices	1
1.2 PDEs modeling electrostatic MEMS	2
1.2.1 Analysis of the elastic problem	2
1.2.2 Analysis of electrostatic problem	4
1.3 Overview and some comments	7
2 Pull-In Voltage and Steady-States	14
2.1 Introduction	14
2.2 The pull-in voltage λ^*	17
2.2.1 Existence of the pull-in voltage	17
2.2.2 Monotonicity results for the pull-in voltage	19
2.3 Estimates for the pull-in voltage	22
2.3.1 Lower bounds for λ^*	22
2.3.2 Upper bounds for λ^*	23
2.3.3 Numerical estimates for λ^*	26
2.4 The branch of minimal solutions	28
2.4.1 Spectral properties of minimal solutions	29
2.4.2 Energy estimates and regularity	31
2.5 Uniqueness and multiplicity of solutions	37
2.5.1 Uniqueness of the solution at $\lambda = \lambda^*$	37
2.5.2 Uniqueness of low energy solutions for small voltage	39
2.5.3 Second solutions around the bifurcation point	40
2.6 Radially symmetric case and power-law profiles	41

Table of Contents

3	Compactness along Lower Branches	47
3.1	Introduction	47
3.2	Mountain Pass solutions	51
3.3	Minimal branch for power-law profiles	55
3.4	Compactness along the second branch	61
3.4.1	Blow-up analysis	61
3.4.2	Spectral confinement	68
3.4.3	Compactness issues	72
3.5	The second bifurcation point	74
3.6	The one dimensional problem	75
4	Dynamic Deflection	76
4.1	Introduction	76
4.2	Global convergence or touchdown	78
4.2.1	Global convergence when $\lambda < \lambda^*$	78
4.2.2	Touchdown at finite time when $\lambda > \lambda^*$	79
4.2.3	Global convergence or touchdown in infinite time for $\lambda = \lambda^*$	82
4.3	Location of touchdown points	87
4.4	Estimates for finite touchdown times	91
4.4.1	Comparison results for finite touchdown time	91
4.4.2	Explicit bounds on touchdown times	93
4.5	Asymptotic analysis of touchdown profiles	97
4.5.1	Touchdown profile: $f(x) \equiv 1$	97
4.5.2	Touchdown profile: variable permittivity	99
4.6	Pull-in distance	101
5	Refined Touchdown Behavior	107
5.1	Introduction	107
5.2	A priori estimates of touchdown behavior	109
5.2.1	Lower bound estimate	112
5.2.2	Gradient estimates	113
5.2.3	Upper bound estimate	116
5.3	Refined touchdown profiles	121
5.3.1	Refined touchdown profiles for $N = 1$	124
5.3.2	Refined touchdown profiles for $N \geq 2$	126
5.4	Set of touchdown points	127
5.4.1	Radially symmetric case	128
5.4.2	One dimensional case	131
6	Thesis Summary	134
6.1	Stationary Case	134
6.2	Dynamic Case	134
Bibliography	Bibliography	136

List of Tables

2.1	<i>Numerical values for pull-in voltage λ^* with the bounds given in Theorem 2.1.1. Here the exponential permittivity profile is chosen as (2.3.21).</i>	27
2.2	<i>Numerical values for pull-in voltage λ^* with the bounds given in Theorem 2.1.1. Here the power-law permittivity profile is chosen as (2.3.21).</i>	28
4.1	<i>Computations for finite touchdown time T with the bounds T_*, $T_{0,\lambda}$, $T_{1,\lambda}$ and $T_{2,\lambda}$ given in Proposition 4.4.3. Here the applied voltage $\lambda = 20$ and the profile is chosen as (4.4.23).</i>	96
4.2	<i>Numerical values for finite touchdown time T at different applied voltages $\lambda = 5, 10, 15$ and 20, respectively. Here the constant permittivity profile $f(x) \equiv 1$ is chosen.</i>	96
4.3	<i>Numerical values for pull-in voltage λ^*: Table (a) corresponds to exponential profiles, while Table (b) corresponds to power-law profiles.</i>	102

List of Figures

1.1	<i>The simple electrostatic MEMS device.</i>	3
2.1	<i>Plots of $u(0)$ versus λ for the constant permittivity profile $f(x) \equiv 1$ defined in the unit ball $B_1(0) \subset \mathbb{R}^N$ with different ranges of N. In the case of $N \geq 8$, we have $\lambda^* = (6N - 8)/9$.</i>	16
2.2	<i>Plots of λ^* versus α for a power-law profile (heavy solid curve) and the exponential profile (solid curve). The left figure corresponds to the slab domain, while the right figure corresponds to the unit disk.</i>	26
2.3	<i>Plots of $u(0)$ versus λ for profile $f(x) = x ^\alpha$ ($\alpha \geq 0$) defined in the slab domain ($N = 1$). The numerical experiments point to a constant $\alpha^* > 1$ (analytically given in (2.6.10)) such that the bifurcation diagrams are greatly different for different ranges of α: $0 \leq \alpha \leq 1$, $1 < \alpha \leq \alpha^*$ and $\alpha > \alpha^*$.</i>	43
2.4	<i>Top figure: Plots of $u(0)$ versus λ for $2 \leq N \leq 7$, where $u(0)$ oscillates around the value λ_* defined in (2.6.12) and u^* is regular. Bottom figure: Plots of $u(0)$ versus λ for $N \geq 8$: when $0 \leq \alpha \leq \alpha^{**}$, there exists a unique solution for $(S)_\lambda$ with $\lambda \in (0, \lambda^*)$ and u^* is singular; when $\alpha > \alpha^{**}$, $u(0)$ oscillates around the value λ_* defined in (2.6.12) and u^* is regular.</i>	45
3.1	<i>Top figure: plots of $u(0)$ versus λ for the case where $f(x) \equiv 1$ is defined in the unit ball $B_1(0) \subset \mathbb{R}^N$ with different ranges of dimension N, where we have $\lambda^* = (6N - 8)/9$ for dimension $N \geq 8$. Bottom figure: plots of $u(0)$ versus λ for the case where $f(x) \equiv 1$ is defined in the unit ball $B_1(0) \subset \mathbb{R}^N$ with dimension $2 \leq N \leq 7$, where λ^* (resp. λ_2^*) is the first (resp. second) turning point.</i>	48
4.1	<i>Left Figure: u versus x for $\lambda = 4.38$. Right Figure: u versus x for $\lambda = 4.50$. Here we consider (4.3.1) with $f(x) = 2x$ in the slab domain.</i>	88
4.2	<i>Left Figure: u versus r for $\lambda = 1.70$. Right Figure: u versus r for $\lambda = 1.80$. Here we consider (4.3.1) with $f(r) = r$ in the unit disk domain.</i>	88
4.3	<i>Left Figure: plots of u versus x for different $f(x)$ at $\lambda = 8$ and $t = 0.185736$. Right Figure: plots of u versus x for different λ with $f(x) = 2x$ and $t = 0.1254864$.</i>	92
4.4	<i>Plots of the pull-in distance $u(0) = u^*(0)$ versus α for the power-law profile (heavy solid curve) and the exponential profile (solid curve). Left figure: the slab domain. Right figure: the unit disk.</i>	102

List of Figures

4.5	<i>Left figure: plots of u versus x at $\lambda = \lambda^*$ for $\alpha = 0$, $\alpha = 1$, $\alpha = 3$, and $\alpha = 10$, in the unit disk for the power-law profile. Right figure: plots of u versus x at $\lambda = \lambda^*$ for $\alpha = 0$, $\alpha = 2$, $\alpha = 4$, and $\alpha = 10$, in the unit disk for the exponential profile. In both figures the solution develops a boundary-layer structure near $x = 1$ as α is increased.</i>	103
4.6	<i>Bifurcation diagram of $w'(0) = -\gamma$ versus λ_0 from the numerical solution of (4.6.6).</i>	103
4.7	<i>Comparison of numerically computed λ^* (heavy solid curve) with the asymptotic result (dotted curve) from (4.6.7) for the unit disk. Left figure: the exponential profile. Right figure: the power-law profile.</i>	104
4.8	<i>Left figure: plots of u versus x at $\lambda = \lambda^*$ in the slab domain. Right figure: plots of u versus x at $\lambda = \lambda^*$ in the unit disk domain.</i>	105
4.9	<i>Left figure: plots of u versus x at $\lambda = \lambda^*$ in the slab domain. Right figure: plots of u versus x at $\lambda = \lambda^*$ in the unit disk domain.</i>	106
5.1	<i>Left figure: plots of u versus x at different times with $f(x) = 1 - x^2$ in the slab domain, where the unique touchdown point is $x = 0$. Right figure: plots of u versus $r = x$ at different times with $f(r) = 1 - r^2$ in the unit disk domain, where the unique touchdown point is $r = 0$ too.</i>	129
5.2	<i>Left figure: plots of u versus x at different times with $f(x) = e^{-x^2}$ in the slab domain, where the unique touchdown point is $x = 0$. Right figure: plots of u versus $r = x$ at different times with $f(r) = e^{-r^2}$ in the unit disk domain, where the unique touchdown point is $r = 0$ too.</i>	130
5.3	<i>Left figure: plots of u versus x at different times with $f(x) = e^{x^2-1}$ in the slab domain, where the unique touchdown point is still at $x = 0$. Right figure: plots of u versus $r = x$ at different times with $f(r) = e^{r^2-1}$ in the unit disk domain, where the touchdown points satisfy $r = 0.51952$.</i>	130
5.4	<i>Left figure: plots of u versus x at different times with $f(x) = 1/2 - x/2$ in the slab domain, where the unique touchdown point is $x = -0.10761$. Right figure: plots of u versus $r = x$ at different times with $f(x) = x + 1/2$ in the slab domain, where the unique touchdown point is $x = 0.17467$.</i>	131
5.5	<i>Plots of u versus x at different times in the slab domain, for different permittivity profiles $f[\alpha](x)$ given by (5.4.5). Top left (a): when $\alpha = 0.5$, two touchdown points are at $x = \pm 0.12631$. Top right (b): when $\alpha = 1$, the unique touchdown point is at $x = 0$. Bottom Left (c): when $\alpha = 0.785$, touchdown points are observed to consist of a closed interval $[-0.0021255, 0.0021255]$. Bottom right (d): local amplified plots of (c).</i>	132

Acknowledgements

My greatest gratitude goes to my supervisor, Nassif Ghoussoub. Without his expert guidance, enormous patience, constant encouragement, and continuing quest for mathematical rigor, this thesis would not have been possible. I deeply acknowledge his generosity with his time, and his invaluable suggestions and insightful comments.

I would like to thank my collaborators Michael J. Ward, Zhenguo Pan and Pierpaolo Esposito, from whom I have benefited a lot. I am particularly grateful to Michael J. Ward, whose graduate course led me to learn about the PDE models of electrostatic MEMS, and the pioneering work of J. Pelesko. I would also like to thank Professor Louis Nirenberg for pointing me to the pioneering work of Joseph and Lindgren, and eventually to the extensive mathematical literature on nonlinear eigenvalue problems. I will always be grateful to the PDE team at UBC (whether faculty, postdocs, or graduate students), and in particular Ivar Ekeland, Tai-Peng Tsai, Stephen Gustafson, Daniele Cassani, Abbas Maomeni, Yu Yan, and Meijiao Guan for their constant support. Many thanks also go to Danny Fan for her great help over the past three years.

Financial support from Research Assistantship under Nassif Ghoussoub (2003-2004), Chi-Kit Wat Scholarship (2004-2005), T. K. Lee Scholarship (2005-2006) and U. B. C. Graduate Fellowships (2004-2007), is gratefully acknowledged.

Finally, I would like to extend my thanks to my parents and my wife who have given me constant support and encouragement during my studies at UBC.

Statement of Co-Authorship

The numerical results in sections 2.3.3 were published in:

[1] Y. Guo, Z. Pan and M. J. Ward, *Touchdown and pull-in voltage behavior of a MEMS device with varying dielectric properties*, SIAM, J. Appl. Math. **66** (2005), 309–338.

Most of the results in Chapter 2 have been published in:

[2] N. Ghoussoub and Y. Guo, *On the partial differential equations of electrostatic MEMS devices: stationary case*, SIAM, J. Math. Anal. **38** (2007), 1423–1449.

The main results of Chapter 3 are due to appear in the following paper in press:

[3] P. Esposito, N. Ghoussoub and Y. Guo, *Compactness along the branch of semi-stable and unstable solutions for an elliptic problem with a singular nonlinearity*, Comm. Pure Appl. Math., accepted (2006).

Sections 4.5 and 4.6 can be found in the paper [1] mentioned above, and while the main results of sections 4.1-4.4 come from the following paper which is also in press:

[4] N. Ghoussoub and Y. Guo, *On the partial differential equations of electrostatic MEMS devices II: dynamic case*, NoDEA Nonlinear Diff. Eqns. Appl., accepted (2007).

The main results of Chapter 5 can be found in the paper:

[5] Y. Guo, *On the partial differential equations of electrostatic MEMS devices III: refined touchdown behavior*, submitted (2006).

Chapter 1

Introduction

The roots of micro-system technology lie in the technological developments accompanying World War II, and in particular the work around radar stimulated research in the synthesis of pure semiconducting materials. These materials, especially pure silicon, have become the main components of integrated and modern technology of Micro-Electromechanical Systems (MEMS). The advent of MEMS has revolutionized numerous branches of science and industry, and their applications are continuing to flourish, as they are becoming essential components of modern sensors in areas as diverse as the biomedical industry, space exploration, and telecommunications.

A comprehensive overview of the rapidly developing field of MEMS technology can be found in the relatively recent monograph by Pelesko and Bernstein [52]. Not only is this book a rich source of information about the incredibly vast area of applications of MEMS, but also it contains justifications and derivations of the fundamental partial differential equations that model such devices. It is the mathematical analysis and the numerical simulations of these equations that concern us in this thesis.

In this introduction, we shall first briefly recall some of the industrial applications of MEMS while referring the reader to the book of Pelesko and Bernstein mentioned above for a more comprehensive survey. For the convenience of the reader, we shall also include a derivation of the simplest PDE modeling electrostatic MEMS devices, which is by now a well known and broadly accepted mathematical model.

1.1 Electrostatic MEMS devices

The state of the art is best summarized by the following description of Pelesko and Bernstein in the book [52]: “Spurred by rapid advances in integrated circuit manufacturing, microsystems process technology is already well developed. As a result, researchers are increasingly focusing their attention on device engineering questions. Foremost among these is the question of how to provide accurate, controlled, stable locomotion for MEMS devices. Just as what has been recognized for some time by several scientists and engineers, it is neither feasible nor desirable to attempt to reproduce modes of locomotion used in the macro world. In fact, the unfavorable scaling of force with device size prohibits this approach in many cases. For example, magnetic forces, which are often used for actuation in the macro world, scale poorly into the micro domain, decreasing in strength by a factor of ten thousand when linear dimensions are reduced by a factor of ten. This unfavorable scaling renders magnetic forces essentially useless. At the micro level, researchers have proposed a variety of new modes of locomotion based upon thermal, biological, and electrostatic forces”. The use of electrostatic forces to provide locomotion for MEMS devices is behind the mathematical model that we address in this thesis.

Experimental work in this area dates back to 1967 and the work of Nathanson et. al. [49].

In their seminal paper, Nathanson and his coworkers describe the modeling and manufacture of, experimentation with, a millimeter-sized resonant gate transistor. These early MEMS devices utilized both electrical and mechanical components on the same substrate resulting in improved efficiency, lowered cost, and reduced system size. Nathanson and his coworkers also introduced a simple lumped mass-spring model of electrostatic actuation. In an interesting parallel development, the British scientist, G. I. Taylor [55] investigated electrostatic actuation at about the same time as Nathanson. While Taylor was concerned with electrostatic deflection of soap films rather than the development of MEMS devices, his work spawned a small body of the literature with relevance to MEMS. Since Nathanson and Taylor's seminal work, numerous investigators have been continually exploring new uses of electrostatic actuation, such as Micropumps, Microswitches, Microvalves, Shuffle Motor and etc. See [52] for more details on how these devices use electrostatic forces for their operation.

1.2 PDEs modeling electrostatic MEMS

A key component of some MEMS systems is the simple idealized electrostatic device shown in Figure 1.1. The upper part of this device consists of a thin and deformable elastic membrane that is held fixed along its boundary and which lies above a parallel rigid grounded plate. This elastic membrane is modeled as a dielectric with a small but finite thickness. The upper surface of the membrane is coated with a negligibly thin metallic conducting film. When a voltage V is applied to the conducting film, the thin dielectric membrane deflects towards the bottom plate. A similar deflection phenomenon, but on a macroscopic length scale, occurs in the field of electrohydrodynamics. In this context, Taylor [55] studied the electrostatic deflection of two oppositely charged soap films, and he predicted a critical voltage for which the two soap films would touch together.

A similar physical limitation on the applied voltage occurs for the MEMS device of Figure 1.1, in that there is a maximum voltage V^* –known as pull-in voltage– which can be safely applied to the system. More specifically, if the applied voltage V is increased beyond the critical value V^* , the steady-state of the elastic membrane is lost, and proceeds to snap through at a finite time creating the so-called pull-in instability (cf. [29, 30, 32, 50]). The existence of such a pull-in voltage was first demonstrated for a lumped mass-spring model of electrostatic actuation in the pioneering study of [49], where the restoring force of the deflected membrane is modeled by a Hookean spring. In this lumped model the attractive inverse square law electrostatic force between the membrane and the ground plate dominates the restoring force of the spring for small gap sizes and large applied voltages. This leads to snap-through behavior whereby the membrane hits the ground plate when the applied voltage is large enough.

Following closely the analysis in [32, 52], we shall now formulate the partial differential equations that models the dynamic deflection $\hat{w} = \hat{w}(x', y', t')$ of the membrane shown in Figure 1.1.

1.2.1 Analysis of the elastic problem

We shall apply Hamilton's least action principle and minimize the *action* \mathcal{S} of the system. Here the action consists of the superposition of the kinetic energy, the damping energy and the potential energy in the system. The pointwise total of these energies is the *Lagrangian* \mathcal{L}

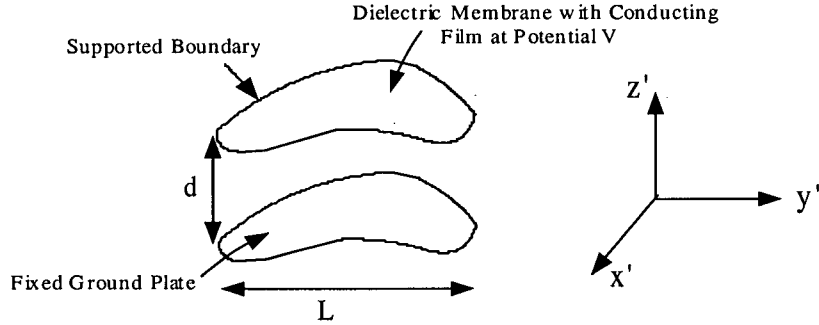


Figure 1.1: *The simple electrostatic MEMS device.*

for the system. We then have

$$\begin{aligned} \mathcal{S} &= \int_{t_1}^{t_2} \int_{\Omega'} \mathcal{L} dX' dt' = \text{Kinetic Energy} + \text{Damping Energy} + \text{Potential Energy} \\ &=: E_k + E_d + E_p, \end{aligned} \quad (1.2.1)$$

where Ω' is the domain of the membrane with respect to (x', y') . In this subsection, dX' denotes $dx' dy'$, and the gradient ∇' (and the Laplace operator Δ') denotes the differentiation only with respect to x' and y' .

For the dynamic deflection $\hat{w} = \hat{w}(x', y', t')$ of the membrane, the kinetic energy E_k is

$$E_k = \frac{\rho A}{2} \int_{t_1}^{t_2} \int_{\Omega'} \hat{w}_t'^2 dX' dt', \quad (1.2.2)$$

where ρ is the mass density per unit volume of the membrane, and A is the thickness of the membrane. The damping energy E_d is assumed to be

$$E_d = \frac{a}{2} \int_{t_1}^{t_2} \int_{\Omega'} \hat{w}^2 dX' dt', \quad (1.2.3)$$

where a is the damping constant.

For this model, the potential energy E_p is composed of

$$E_p = \text{Stretching Energy} + \text{Bending Energy}. \quad (1.2.4)$$

It is reasonable to assume that the stretching energy in the elastic membrane is proportional to the changes in the area of the membrane from its un-stretched configuration. Since we assume the membrane is held fixed at its boundary, we may write the stretching energy as

$$\text{Stretching Energy} := -\mu \left(\int_{t_1}^{t_2} \int_{\Omega'} \sqrt{1 + |\nabla' \hat{w}|^2} dX' dt' - |\Omega'| (t_2 - t_1) \right). \quad (1.2.5)$$

Here the proportionality constant μ , is simply the tension in the membrane. We linearize this expression to obtain

$$\text{Stretching Energy} := -\frac{\mu}{2} \int_{t_1}^{t_2} \int_{\Omega'} |\nabla' \hat{w}|^2 dX' dt'. \quad (1.2.6)$$

The bending energy is assumed to be proportional to the linearized curvature of the membrane, that is

$$\text{Bending Energy} := -\frac{D}{2} \int_{t_1}^{t_2} \int_{\Omega'} |\Delta' \hat{w}|^2 dX' dt'. \quad (1.2.7)$$

Here the constant D is the flexural rigidity of the membrane. For the total potential energy E_p we now have

$$E_p = - \int_{t_1}^{t_2} \int_{\Omega'} \left(\frac{\mu}{2} |\nabla' \hat{w}|^2 + \frac{D}{2} |\Delta' \hat{w}|^2 \right) dX' dt'. \quad (1.2.8)$$

Combining (1.2.1) – (1.2.3) and (1.2.8) now yields that

$$\mathcal{L} = \frac{\rho A}{2} \hat{w}_{t'}^2 + \frac{a}{2} \hat{w}^2 - \frac{\mu}{2} |\nabla' \hat{w}|^2 - \frac{D}{2} |\Delta' \hat{w}|^2. \quad (1.2.9)$$

According to Hamilton's principle, we should minimize

$$\int_{t_1}^{t_2} \int_{\Omega'} \left(\frac{\rho A}{2} \hat{w}_{t'}^2 + \frac{a}{2} \hat{w}^2 - \frac{\mu}{2} |\nabla' \hat{w}|^2 - \frac{D}{2} |\Delta' \hat{w}|^2 \right) dX' dt', \quad (1.2.10)$$

which implies –via Euler-Lagrange variational calculus– that the elastic membrane's deflection \hat{w} satisfies

$$\rho A \frac{\partial^2 \hat{w}}{\partial t'^2} + a \frac{\partial \hat{w}}{\partial t'} - \mu \Delta' \hat{w} + D \Delta'^2 \hat{w} = 0. \quad (1.2.11)$$

1.2.2 Analysis of electrostatic problem

We now analyze the electrostatic problem of Figure 1.1 and we allow the dielectric permittivity $\varepsilon_2 = \varepsilon_2(x', y')$ of the elastic membrane to exhibit a spatial variation reflecting the varying dielectric permittivity of the membrane. Therefore, in view of (1.2.11) we assume the membrane's deflection \hat{w} satisfying

$$\rho A \frac{\partial^2 \hat{w}}{\partial t'^2} + a \frac{\partial \hat{w}}{\partial t'} - \mu \Delta' \hat{w} + D \Delta'^2 \hat{w} = -\frac{\varepsilon_2}{2} |\nabla' \phi|^2, \quad (1.2.12)$$

where the term on the right hand side of (1.2.12) denotes the force on the elastic membrane, which is due to the electric field. We suppose that such force is proportional to the norm squared of the gradient of the potential and couples the solution of the elastic problem to the solution of the electrostatic problem. A derivation of such source term may be found in [42].

We now apply dimensionless analysis to equation (1.2.12). We scale the electrostatic potential with the applied voltage V , time with a damping timescale of the system, the x' and y' variables with a characteristic length L of the device, and z' \hat{w} with the size of the gap d between the ground plate and the undeflected elastic membrane. So we define

$$w = \frac{\hat{w}}{d}, \quad \psi = \frac{\phi}{V}, \quad x = \frac{x'}{L}, \quad y = \frac{y'}{L}, \quad z = \frac{z'}{d}, \quad t = \frac{\mu t'}{aL^2}, \quad (1.2.13)$$

and substitute these into equation (1.2.12) to find

$$\gamma \frac{\partial^2 w}{\partial t^2} + \frac{\partial w}{\partial t} - \Delta w + \delta \Delta^2 w = -\lambda \left(\frac{\varepsilon_2}{\varepsilon_0} \right) \left[\varepsilon^2 |\nabla' \psi|^2 + \left(\frac{\partial \psi}{\partial z} \right)^2 \right] \quad \text{in } \Omega, \quad (1.2.14)$$

where Ω is the dimensionless domain of the elastic membrane. Here the parameter γ satisfies

$$\gamma = \frac{\sqrt{\rho\mu A}}{aL}, \quad (1.2.15)$$

and the parameter δ measures the relative importance of tension and rigidity and it is defined by

$$\delta = \frac{D}{\mu L^2}. \quad (1.2.16)$$

The parameter ε is the aspect ratio of the system

$$\varepsilon = \frac{d}{L}, \quad (1.2.17)$$

and the parameter λ is a ratio of the reference electrostatic force to the reference elastic force and it is defined by

$$\lambda = \frac{V^2 L^2 \varepsilon_0}{2\mu d^3}. \quad (1.2.18)$$

In view of equation (1.2.12), and in order to further understand membrane's deflection, we need to know more about the electrostatic potential ϕ inside the elastic membrane. In the actual design of a MEMS device there are several issues that must be considered. Typically, one of the primary device design goals is to achieve the maximum possible stable steady-state deflection, referred to as the pull-in distance, with a relatively small applied voltage V . Another consideration may be to increase the stable operating range of the device by increasing the pull-in voltage V^* subject to the constraint that the range of the applied voltage is limited by the available power supply. This increase in the stable operating range may be important for the design of microresonators. For other devices such as micropumps and microvalves, where snap-through (or called touchdown) behavior is explicitly exploited, it is of interest to decrease the time for touchdown, thereby increasing the switching speed. One way of achieving larger values of V^* while simultaneously increasing the pull-in distance, is to use a voltage control scheme imposed by an external circuit in which the device is placed (cf. [53]). This approach leads to a nonlocal problem for the deflection of the membrane. A different approach is to introduce a spatial variation in the dielectric permittivity of the membrane, which was theoretically studied in [29–32, 50? ?].

In the following we discuss the electrostatic potential ϕ by introducing a spatial varying dielectric permittivity into our simple MEMS model. The idea is to locate the region where the membrane deflection would normally be largest under a spatially uniform permittivity, and then make sure that a new dielectric permittivity ε_2 is largest –and consequently the profile $f(x, y)$ smallest– in that region.

We assume that the ground plate, located at $z' = 0$, is a perfect conductor. The elastic membrane is assumed to be a uniform thickness $A = 2\iota$. The deflection of the membrane at time t' is specified by the deflection of its center plane, located at $z' = \hat{w}(x', y', t')$. Hence the top surface is located at $z' = \hat{w}(x', y', t') + \iota$, while the bottom of the membrane is located at $z' = \hat{w}(x', y', t') - \iota$. We also assume that the potential between the membrane and ground plate, ϕ_1 , satisfies

$$\Delta\phi_1 = 0, \quad (1.2.19)$$

$$\phi_1(x', y', 0) = 0 \quad \text{in } \Omega', \quad (1.2.20)$$

where we assume that the fixed ground plate is held at zero potential. The potential inside the membrane, ϕ_2 , satisfies

$$\nabla \cdot (\varepsilon_2 \nabla \phi_2) = 0, \quad (1.2.21)$$

$$\phi_2(x', y', \hat{w} + \iota) = V \quad \text{in } \Omega'. \quad (1.2.22)$$

Defining

$$\psi_1 = \frac{\phi_1}{V}, \quad \psi_2 = \frac{\phi_2}{V} \quad (1.2.23)$$

together with (1.2.13), and applying dimensionless analysis again, the electrostatic problem reduces to

$$\frac{\partial^2 \psi}{\partial z^2} + \varepsilon^2 \left(\frac{\partial^2 \psi}{\partial x^2} + \frac{\partial^2 \psi}{\partial y^2} \right) = 0, \quad 0 \leq z \leq w - \iota; \quad (1.2.24a)$$

$$\varepsilon_2 \frac{\partial^2 \psi}{\partial z^2} + \varepsilon^2 \left(\frac{\partial}{\partial x} \left(\varepsilon_2 \frac{\partial \psi}{\partial x} \right) + \frac{\partial}{\partial y} \left(\varepsilon_2 \frac{\partial \psi}{\partial y} \right) \right) = 0, \quad w - \iota \leq z \leq w + \iota; \quad (1.2.24b)$$

$$\psi = 0, \quad z = 0 \text{ (ground plate);} \quad \psi = 1, \quad z = w + \iota \text{ (upper membrane surface),} \quad (1.2.25)$$

together with the continuity of the potential and the displacement fields across $z = w - \iota$. Here ψ is the dimensionless potential scaled with respect to the applied voltage V , and, as before, $\varepsilon \equiv d/L$ is the device aspect ratio.

In general, we note that one has little hope of finding an exact solution ψ from (1.2.24) and (1.2.25). However, we can simplify the system by examining a restricted parameter regime. In particular, we consider the small-aspect ratio limit $\varepsilon \equiv d/L \ll 1$. Physically, this means that the lateral dimensions of the device in Figure 1.1 are larger compared to the size of the gap between the undeflected membrane and ground plate. In the small-aspect ratio limit $\varepsilon \ll 1$, equation (1.2.24) gives $\frac{\partial^2 \psi}{\partial z^2} = 0$. Further, the asymptotical solution of ψ which is continuous across $z = w - \iota$ is

$$\psi = \begin{cases} \psi_L \frac{z}{w - \iota}, & 0 \leq z \leq w - \iota, \\ 1 + \frac{(1 - \psi_L)}{2\iota} (z - (w + \iota)), & w - \iota \leq z \leq w + \iota. \end{cases} \quad (1.2.26)$$

To ensure that the displacement field is continuous across $z = w - \iota$ to leading order in ε , we impose that

$$\varepsilon_0 \frac{\partial \psi}{\partial z} \Big|_- = \varepsilon_2 \frac{\partial \psi}{\partial z} \Big|_+,$$

where the plus or minus signs indicate that $\frac{\partial \psi}{\partial z}$ is to be evaluated on the upper or lower side of the bottom surface $z = w - \iota$ of the membrane, respectively. This condition determines ψ_L in (1.2.26) as

$$\psi_L = \left[1 + \frac{2\iota}{w - \iota} \left(\frac{\varepsilon_0}{\varepsilon_2} \right) \right]^{-1}. \quad (1.2.27)$$

From (1.2.26) and (1.2.27), we observe that the electric field in the z -direction inside the membrane is independent of z , and is given by

$$\frac{\partial \psi}{\partial z} = \frac{\varepsilon_0}{\varepsilon_2 (w - \iota)} \left[1 + \frac{2\iota}{w - \iota} \frac{\varepsilon_0}{\varepsilon_2} \right]^{-1} \sim \frac{\varepsilon_0}{\varepsilon_2 w} \quad \text{for } \iota \ll 1. \quad (1.2.28)$$

In engineering parlance, this approximation is equivalent to ignoring fringing fields. Therefore, in the small-aspect ratio limit $\varepsilon \ll 1$, the governing equation (1.2.14) is simplified from (1.2.28) into

$$\gamma \frac{\partial^2 w}{\partial t^2} + \frac{\partial w}{\partial t} - \Delta w + \delta \Delta^2 w = -\frac{\lambda \varepsilon_0}{\varepsilon_2 w^2} \quad \text{in } \Omega. \quad (1.2.29)$$

We now suppose the membrane is undeflected at the initial time, that is $w(x, y, 0) = 1$. Since the boundary of the membrane is held fixed, we have $w(x, y, t) = 1$ on the boundary of Ω at any time $t > 0$. We now also assume that the membrane's thickness $A = 2d\iota$ satisfies $A = 2d\iota \ll 1$ which gives $\gamma \ll 1$ in view of (1.2.15), and assume that the elastic membrane has no rigidity which gives $\delta = 0$ in view of (1.2.16). Therefore, by using further simplification, the dynamic deflection $w = w(x, t)$ of the membrane on a bounded domain Ω in \mathbb{R}^2 , is found to satisfy the following parabolic problem

$$\frac{\partial w}{\partial t} - \Delta w = -\frac{\lambda f(x)}{w^2} \quad \text{for } x \in \Omega, \quad (1.2.30a)$$

$$w(x, t) = 1 \quad \text{for } x \in \partial\Omega, \quad (1.2.30b)$$

$$w(x, 0) = 1 \quad \text{for } x \in \Omega, \quad (1.2.30c)$$

where the parameter $\lambda > 0$ is called the applied voltage in view of relation (1.2.18), and while the nonnegative continuous function $f(x)$ characterizes the varying dielectric permittivity of the elastic membrane, in the point of the relation

$$f(x) = \frac{\varepsilon_0}{\varepsilon_2(Lx, Ly)}. \quad (1.2.31)$$

Therefore, understanding dynamic deflection of our MEMS model is equivalent to studying solutions of (1.2.30).

1.3 Overview and some comments

The main contents of this thesis are divided into two major parts, each consisting of two chapters.

Part I: Pull-In Voltage and Stationary Deflection

The first part of this thesis is focussed on pull-in voltage and stationary deflection of the elastic membrane satisfying (1.2.30). For convenience, by setting $w = 1 - u$ we study the following semilinear elliptic problem with a singular nonlinearity

$$\begin{cases} -\Delta u = \frac{\lambda f(x)}{(1-u)^2} & \text{in } \Omega, \\ 0 < u < 1 & \text{in } \Omega, \\ u = 0 & \text{on } \partial\Omega, \end{cases} \quad (S)_\lambda$$

where $\lambda > 0$ denotes the applied voltage and the nonnegative continuous function $f(x)$ characterizes the varying dielectric permittivity of the elastic membrane. Mathematically, we consider the domain $\Omega \subset \mathbb{R}^N$ with any dimension $N \geq 1$. $(S)_\lambda$ was firstly studied by Pelesko

in [50], where the author focussed on lower dimension $N = 1$ or 2 , and he considered either $f(x) \geq C > 0$ or $f(x) = |x|^\alpha$. In my joint work with Pan and Ward [32], we studied $(S)_\lambda$ for a more general profile $f(x)$ which can vanish somewhere. In the past two years, $(S)_\lambda$ was further extended and sharpened in our series work [22, 29].

The main results of Chapter 2 can be found in [29]. In §2.2 we mainly show the existence of a specific pull-in voltage in the sense

$$\lambda^* := \lambda^*(\Omega, f) = \sup \left\{ \lambda > 0 \mid (S)_\lambda \text{ possesses at least one solution} \right\}. \quad (1.3.1)$$

The definition of λ^* shows that for $\lambda < \lambda^*$, there exists at least one solution for $(S)_\lambda$; while for $\lambda > \lambda^*$, there is no solution for $(S)_\lambda$. In §2.2 we also study pull-in voltage's dependence on the size and shape of the domain, as well as on the permittivity profile. These properties will help us in §2.3 establish some lower and upper bound estimates on the pull-in voltage, see Theorem 2.1.1. In particular, we shall prove in Theorem 2.1.1(5) that if $f(x) \equiv |x|^\alpha$ with $\alpha \geq 0$ and B_1 is a unit ball in \mathbb{R}^N , then we have

$$\lambda^*(B_1, |x|^\alpha) = \frac{(2 + \alpha)(3N + \alpha - 4)}{9},$$

provided $N \geq 8$ and $0 \leq \alpha \leq \alpha^{**}(N) := \frac{4 - 6N + 3\sqrt{6}(N-2)}{4}$.

In Chapter 2, we also consider issues of uniqueness and multiplicity of solutions for $(S)_\lambda$ with $0 < \lambda \leq \lambda^*$. The bifurcation diagrams in Figure 2.1 of §2.1 show the complexity of the situation, even in the radially symmetric case. One can observe from Figure 2.1 that the number of branches –and of solutions– is closely connected to the space dimension, a fact that we analytically discuss in §2.4, by focussing on the very first branch of solutions considered to be “minimal” in the following way.

Definition 1.3.1. A solution $u_\lambda(x)$ of $(S)_\lambda$ is said to be minimal if for any other solution u of $(S)_\lambda$ we have $u_\lambda(x) \leq u(x)$ for all $x \in \Omega$.

We shall prove that for any $0 \leq \lambda < \lambda^*$, there exists a unique minimal solution u_λ of $(S)_\lambda$ such that $\mu_{1,\lambda}(u_\lambda) > 0$. Moreover, for each $x \in \Omega$, the function $\lambda \rightarrow u_\lambda(x)$ is strictly increasing and differentiable on $(0, \lambda^*)$.

On the other hand, one can introduce for any solution u of $(S)_\lambda$, the linearized operator at u defined by $L_{u,\lambda} = -\Delta - \frac{2\lambda f(x)}{(1-u)^3}$ and its eigenvalues $\{\mu_{k,\lambda}(u); k = 1, 2, \dots\}$. The first eigenvalue is then simple and is given by:

$$\mu_{1,\lambda}(u) = \inf \left\{ \langle L_{u,\lambda} \phi, \phi \rangle_{H_0^1(\Omega)}; \phi \in C_0^\infty(\Omega), \int_\Omega |\phi(x)|^2 dx = 1 \right\}.$$

Stable solutions (resp., *semi-stable solutions*) of $(S)_\lambda$ are those solutions u such that $\mu_{1,\lambda}(u) > 0$ (resp., $\mu_{1,\lambda}(u) \geq 0$). We note that there already exist in the literature many interesting results concerning the properties of the branch of semi-stable solutions for Dirichlet boundary value problems of the form $-\Delta u = \lambda h(u)$ where h is a regular nonlinearity (for example of the form e^u or $(1+u)^p$ for $p > 1$). See for example the seminal papers [20, 43, 44] and also [15] for a survey on the subject and an exhaustive list of related references. The singular situation was considered in a very general context in [48], and the analysis of Chapter 2 is completed to allow

for a general continuous permittivity profile $f(x) \geq 0$. Our main results in this direction are stated in Theorem 2.1.2, where fine properties of steady states –such as regularity, stability, uniqueness, multiplicity, energy estimates and comparison results– are shown to depend on the dimension of the ambient space and on the permittivity profile. More precisely, Theorem 2.1.2 gives that if $1 \leq N \leq 7$ then –by means of energy estimates– one has $\sup_{\lambda \in (0, \lambda^*)} \|u_\lambda\|_\infty < 1$ and consequently, $u^* = \lim_{\lambda \uparrow \lambda^*} u_\lambda$ exists in $C^{2,\alpha}(\bar{\Omega})$ with $0 < \alpha < 1$ and is a solution for $(S)_{\lambda^*}$ such that $\mu_{1,\lambda^*}(u^*) = 0$. In particular, u^* –often referred to as the extremal solution of problem $(S)_{\lambda^*}$ – is unique. On the other hand, if $N \geq 8$, $f(x) = |x|^\alpha$ with $0 \leq \alpha \leq \alpha^{**}(N) := \frac{4-6N+3\sqrt{6}(N-2)}{4}$ and Ω is the unit ball, then the extremal solution is necessarily $u^*(x) = 1 - |x|^{\frac{2+\alpha}{3}}$ and is therefore singular.

In general, the function u^* exists in any dimension, does solve $(S)_{\lambda^*}$ in a suitable weak sense, and is the unique solution in an appropriate class. The above result says that it is, however, a classical solution in dimensions $1 \leq N \leq 7$, and this will allow us to start another branch of non-minimal (unstable) solutions. Indeed, following ideas of Crandall-Rabinowitz [20], we show in §2.5 that, for $1 \leq N \leq 7$ and for λ close enough to λ^* , there exists a unique second branch U_λ of solutions for $(S)_\lambda$, bifurcating from u^* , with

$$\mu_{1,\lambda}(U_\lambda) < 0 \quad \text{while} \quad \mu_{2,\lambda}(U_\lambda) > 0. \quad (1.3.2)$$

In §2.6 we present some numerical evidences for various conjectures relating to the case where permittivity profile $f(x) = |x|^\alpha$ is defined in a unit ball. The bifurcation diagrams show four possible regimes –at least if the domain is a ball:

- A.** There is exactly one branch of solution for $0 < \lambda < \lambda^*$. This regime occurs when $N \geq 8$, and if $0 \leq \alpha \leq \alpha^{**}(N) := \frac{4-6N+3\sqrt{6}(N-2)}{4}$. The results of this section actually show that in this range, the first branch of solutions “disappears” at λ^* which happens to be equal to $\lambda_*(\alpha, N) = \frac{(2+\alpha)(3N+\alpha-4)}{9}$.
- B.** There exists an infinite number of branches of solutions. This regime occurs when
- $N = 1$ and $\alpha \geq \alpha^* := -\frac{1}{2} + \frac{1}{2}\sqrt{27/2}$.
 - $2 \leq N \leq 7$ and $\alpha \geq 0$;
 - $N \geq 8$ and $\alpha > \alpha^{**}(N) := \frac{4-6N+3\sqrt{6}(N-2)}{4}$.

In this case, $\lambda_*(\alpha, N) < \lambda^*$ and the multiplicity becomes arbitrarily large as λ approaches –from either side– $\lambda_*(\alpha, N)$ at which there is a touchdown solution u (i.e., $\|u\|_\infty = 1$).

- C.** There exists a finite number of branches of solutions. In this case, we have again that $\lambda_*(\alpha, N) < \lambda^*$, but now the branch approaches the value 1 monotonically, and the number of solutions increase but remains finite as λ approaches $\lambda_*(\alpha, N)$. This regime occurs when $N = 1$ and $1 < \alpha \leq \alpha^* := -\frac{1}{2} + \frac{1}{2}\sqrt{27/2}$.
- D.** There exist exactly two branches of solutions for $0 < \lambda < \lambda^*$ and one solution for $\lambda = \lambda^*$. The bifurcation diagram vanishes when it returns to $\lambda = 0$. This regime occurs when $N = 1$ and $0 \leq \alpha \leq 1$.

The main results of Chapter 3 are available in [22]. Note from Chapter 2 that the compactness of minimal branch solutions of $(S)_\lambda$ holds in $1 \leq N \leq 7$ for any profile $f(x)$. In §3.3 we extend such compactness to higher dimension $N \geq 8$, provided that Ω is a unit ball and $f(x) = |x|^\alpha$ satisfies $\alpha > \alpha^{**}(N) := \frac{4-6N+3\sqrt{6}(N-2)}{4}$. Analytically, this provides a clear distinction between the case where the permittivity profile $f(x)$ is bounded away from zero, and where it is allowed to vanish somewhere. Once the compactness of minimal branch solutions for $(S)_\lambda$ holds, then the standard Crandall-Rabinowitz theory [20] implies the existence of a second solution U_λ of $(S)_\lambda$ on the deleted left neighborhood of λ^* , where U_λ satisfies

$$\mu_{1,\lambda}(U_\lambda) < 0 \quad \text{while} \quad \mu_{2,\lambda}(U_\lambda) > 0. \quad (1.3.3)$$

In §3.2 using truncation we shall provide the mountain pass variational characterization of such branch U_λ .

In Chapter 3, we are also interested in continuing the second branch till the second bifurcation point, by means of the implicit function theorem. Suppose $2 \leq N \leq 7$ and $f \in C(\bar{\Omega})$ satisfies

$$f(x) = \left(\prod_{i=1}^k |x - p_i|^{\alpha_i} \right) g(x), \quad g(x) \geq C > 0 \text{ in } \Omega \quad (1.3.4)$$

for some points $p_i \in \Omega$ and exponents $\alpha_i \geq 0$. Let $(\lambda_n)_n$ be a sequence such that $\lambda_n \rightarrow \lambda \in [0, \lambda^*]$ and let u_n be an associated solution of $(S)_{\lambda_n}$ such that

$$\mu_{2,n} := \mu_{2,\lambda_n}(u_n) \geq 0. \quad (1.3.5)$$

Then in §3.4 we shall use blow-up analysis of elliptic PDE to prove the compactness of u_n . We expect that such a result should be true for radial solutions on the unit ball for $N \geq 8$, $\alpha > \alpha_N$, and $f \in C(\bar{\Omega})$ as in (3.3.1). As far as we know, there are no compactness results of this type in the case of regular nonlinearities, marking a substantial difference with the singular situation.

We define the second bifurcation point in the following way for $(S)_\lambda$:

$$\begin{aligned} \lambda_2^* &= \inf \{ \beta > 0 : \exists \text{ a curve } V_\lambda \in C([\beta, \lambda^*]; C^2(\Omega)) \text{ of solutions for } (S)_\lambda \\ &\text{s.t. } \mu_{2,\lambda}(V_\lambda) \geq 0, V_\lambda \equiv U_\lambda \forall \lambda \in (\lambda^* - \delta, \lambda^*) \}. \end{aligned}$$

Assume $f \in C(\bar{\Omega})$ to be of the form (1.3.4). Then for $2 \leq N \leq 7$ we shall prove in §3.5 that $\lambda_2^* \in (0, \lambda^*)$ and for any $\lambda \in (\lambda_2^*, \lambda^*)$ there exist at least two solutions u_λ and V_λ for $(S)_\lambda$, so that

$$\mu_{1,\lambda}(V_\lambda) < 0 \quad \text{while} \quad \mu_{2,\lambda}(V_\lambda) \geq 0.$$

In particular, for $\lambda = \lambda_2^*$, there exists a second solution, namely $V^* := \lim_{\lambda \downarrow \lambda_2^*} V_\lambda$ so that

$$\mu_{1,\lambda_2^*}(V^*) < 0 \quad \text{and} \quad \mu_{2,\lambda_2^*}(V^*) = 0.$$

We note that the second branch cannot approach the value $\lambda = 0$ as illustrated by the bifurcation diagram in Figure 3.1.

Now let V_λ , $\lambda \in (\beta, \lambda^*)$ be one of the curves appearing in the definition of λ_2^* . By (1.3.3), we have that $L_{V_\lambda, \lambda}$ is invertible for $\lambda \in (\lambda^* - \delta, \lambda^*)$ and, as long as it remains invertible, we

can use the Implicit Function Theorem to find V_λ as the unique smooth extension of the curve U_λ (in principle U_λ exists only for λ close to λ^*). We now define λ^{**} in the following way

$$\lambda^{**} = \inf\{\beta > 0 : \forall \lambda \in (\beta, \lambda^*) \exists V_\lambda \text{ solution of } (S)_\lambda \text{ so that } \mu_{2,\lambda}(V_\lambda) > 0, V_\lambda \equiv U_\lambda \text{ for } \lambda \in (\lambda^* - \delta, \lambda^*)\}.$$

Then, $\lambda_2^* \leq \lambda^{**}$ and there exists a smooth curve V_λ for $\lambda \in (\lambda^{**}, \lambda^*)$ so that V_λ is the unique maximal extension of the curve U_λ . This is what the second branch is supposed to be. If now $\lambda_2^* < \lambda^{**}$, then for $\lambda \in (\lambda_2^*, \lambda^{**})$ there is no longer uniqueness for the extension and the “second branch” is defined only as one of potentially many continuous extensions of U_λ .

In dimension 1, we have a stronger but somewhat different compactness result. Recall that $\mu_{k,\lambda_n}(u_n)$ is the k -th eigenvalue of L_{u_n,λ_n} counted with their multiplicity. Let I be a bounded interval in \mathbb{R} and $f \in C^1(\bar{I})$ be such that $f \geq C > 0$ in I . Suppose $(u_n)_n$ is a solution sequence for $(S)_{\lambda_n}$ on I , where $\lambda_n \rightarrow \lambda \in (0, \lambda^*)$. Assume for any $n \in \mathbb{N}$ and k large enough, we have $\mu_{k,n} := \mu_{k,\lambda_n}(u_n) \geq 0$. Then in §3.6 we shall prove the compactness of u_n . Note that the multiplicity result in dimension $2 \leq N \leq 7$ holds also in dimension 1 for any $\lambda \in (\lambda_2^*, \lambda^*)$.

Part II: Dynamic Deflection and Touchdown Behavior

The second part of this thesis is devoted to the dynamic deflection and touchdown behavior of (1.2.30). When $f(x) \equiv 1$, there already exist some results for touchdown (quenching) behavior of (1.2.30) since 1980s, see [38, 39, 46] and references therein. However, since the profile $f(x)$ is assumed to be varying and vanish somewhere for MEMS models, the dynamic behavior of (1.2.30) turns out to be a more rich source of interesting mathematical phenomena. So far the dynamic behavior of (1.2.30) with varying profile has been investigated in [26, 30–32].

Based on [30, 32], in Chapter 4 we focus on the dynamic problem of (1.2.30) in the form

$$\frac{\partial u}{\partial t} - \Delta u = \frac{\lambda f(x)}{(1-u)^2} \quad \text{for } x \in \Omega, \quad (1.3.6a)$$

$$u(x, t) = 0 \quad \text{for } x \in \partial\Omega, \quad u(x, 0) = 0 \quad \text{for } x \in \Omega. \quad (1.3.6b)$$

Recall that a point $x_0 \in \bar{\Omega}$ is said to be a *touchdown point* for a solution $u(x, t)$ of (1.3.6), if for some $T \in (0, +\infty]$, we have $\lim_{t_n \rightarrow T} u(x_0, t_n) = 1$. T is then said to be a –finite or infinite– touchdown time. For each such solution, we define its corresponding –possibly infinite– “first touchdown time”:

$$T_\lambda(\Omega, f, u) = \inf \left\{ t \in (0, +\infty]; \sup_{x \in \Omega} u(x, t) = 1 \right\}.$$

In §4.2, we analyze the relationship between the applied voltage λ , the permittivity profile f , and the solution u of (1.3.6). More precisely, for λ^* defined as in (1.3.1), we show in §§4.2.1 & 4.2.3 that if $\lambda \leq \lambda^*$, then the unique dynamic solution of (1.3.6) must globally converge to its unique minimal steady-state; while we shall prove in §4.2.2 that if $\lambda > \lambda^*$, then the unique dynamic solution of (1.3.6) must touchdown at finite time. Note that in the case where the unique minimal steady-state of (1.3.6) at $\lambda = \lambda^*$ is singular, which can happen if $N \geq 8$, above analysis shows the possibility of touchdown at infinite time.

In §4.3 we first compute global convergence or touchdown behavior of (1.3.6) for different applied voltage λ , and we then prove rigorously the following surprising fact exhibited by the

numerical simulations: the permittivity profile f cannot vanish in any isolated set of finite-time touchdown points.

§4.4 is focussed on the analysis and estimate of finite touchdown time, which often translates into useful information concerning the speed of the operation for many MEMS devices such as RF switches or micro-valves.

In §4.5 we discuss touchdown profiles by the method of asymptotic analysis, and our purpose is to look insights into the refined touchdown rate. §4.6 is devoted to the pull-in distance of MEMS devices, referred to as the maximum stable deflection of the elastic membrane before touchdown occurs. We provide numerical results for pull-in distance with some explicit examples, from which one can observe that both larger pull-in distance and pull-in voltage can be achieved by properly tailoring the permittivity profile. Some interesting phenomena are also observed there.

The purpose of Chapter 5 is to discuss the refined touchdown behavior of (5.1.1) (*i.e.*, (1.2.30)) at finite touchdown time. In §5.2 we shall derive some a priori estimates of touchdown profiles under the assumption that touchdown set of u is a compact subset of Ω . Note that whether the compactness of touchdown set holds for any $f(x)$ satisfying (5.1.2) is a quite challenging problem. In §5.2 we first prove that the compactness of touchdown set holds for the case where the domain Ω is convex and $f(x)$ satisfies the additional condition

$$\frac{\partial f}{\partial \nu} \leq 0 \quad \text{on} \quad \Omega_\delta^c := \{x \in \Omega : \text{dist}(x, \partial\Omega) \leq \delta\} \text{ for some } \delta > 0. \quad (1.3.7)$$

where ν is the outward unit norm vector to $\partial\Omega$. Whether the assumption (1.3.7) can be removed is still open. Under the compactness assumption of touchdown set, in §5.2.1 we establish the lower bound estimate of touchdown profiles and we also prove an interesting phenomenon: finite-time touchdown point of u is not the zero point of $f(x)$, see Theorem 5.1.1. In §5.2.2 we estimate the derivatives of touchdown solution u , see Lemma 5.2.4; and as a byproduct, an integral estimate is also given in Theorem 5.2.5 of §5.2.2.

Motivated by Theorem 5.1.1, the key point of studying touchdown profiles is a similarity variable transformation of (5.1.1). For the touchdown solution $u = u(x, t)$ of (5.1.1) at finite time T , we use the associated similarity variables

$$y = \frac{x - a}{\sqrt{T - t}}, \quad s = -\log(T - t), \quad u(x, t) = (T - t)^{\frac{1}{3}} w_a(y, s), \quad (1.3.8)$$

where a is any interior point of Ω . Then $w_a(y, s)$ is defined in $W_a := \{(y, s) : a + ye^{-s/2} \in \Omega, s > s' = -\log T\}$, and it solves

$$\rho(w_a)_s - \nabla \cdot (\rho \nabla w_a) - \frac{1}{3} \rho w_a + \frac{\lambda \rho f(a + ye^{-\frac{s}{2}})}{w_a^2} = 0,$$

where $\rho(y) = e^{-|y|^2/4}$. Here $w_a(y, s)$ is always strictly positive in W_a . The slice of W_a at a given time s^1 is denoted by $\Omega_a(s^1) := W_a \cap \{s = s^1\} = e^{s^1/2}(\Omega - a)$. Then for any interior point a of Ω , there exists $s_0 = s_0(a) > 0$ such that $B_s := \{y : |y| < s\} \subset \Omega_a(s)$ for $s \geq s_0$. We introduce the frozen energy functional

$$E_s[w_a](s) = \frac{1}{2} \int_{B_s} \rho |\nabla w_a|^2 dy - \frac{1}{6} \int_{B_s} \rho w_a^2 dy - \int_{B_s} \frac{\lambda \rho f(a)}{w_a} dy. \quad (1.3.9)$$

By estimating the energy $E_s[w_a](s)$ in B_s , in §5.2.3 we shall prove the upper bound estimate of w_a , see Theorem 5.2.10.

Applying certain a priori estimates of §5.2, we establish refined touchdown profiles in §5.3, using self-similarity methods and center manifold analysis. We note that for $N \geq 2$, we are only able to apply Theorem 5.3.5 to study the refined touchdown profiles for special touchdown points –such as $x = 0$ in the radial case– and the situation is widely open for more general cases.

Adapting various analytical and numerical techniques, we focus in §5.4 on the set of touchdown points. In §5.4.1 we discuss the radially symmetric case of (5.1.1), and we prove there that suppose $f(r) = f(|x|)$ satisfies (5.1.2) and $f'(r) \leq 0$ in a bounded ball $B_R(0) \subset \mathbb{R}^N$ with $N \geq 1$, then $r = 0$ is the unique touchdown point of u , which is the maximum value point of $f(r) = f(|x|)$, see Theorem 5.1.4 and Remark 5.1.1.

For the one dimensional case, Theorem 5.1.4 already implies that touchdown points must be unique when the permittivity profile $f(x)$ is uniform. In §5.4.2 we further discuss the one dimensional case of (5.1.1) for varying profile $f(x)$, where numerical simulations show that the touchdown set may consist of a discrete set or a finite compact subsets of the domain.

Finally, a summary of this thesis is given in Chapter 6.

Chapter 2

Pull-In Voltage and Steady-States

2.1 Introduction

In this Chapter we study pull-in voltage and stationary deflection of the elastic membrane satisfying (1.2.30), such that our discussion is centered on the following elliptic problem

$$\begin{cases} -\Delta u = \frac{\lambda f(x)}{(1-u)^2} & \text{in } \Omega, \\ 0 < u < 1 & \text{in } \Omega, \\ u = 0 & \text{on } \partial\Omega, \end{cases} \quad (S)_\lambda$$

where $\lambda > 0$ characterizes the applied voltage, while nonnegative $f(x)$ describes the varying permittivity profile of the elastic membrane shown in Figure 1.1. We focus on the stable and semi-stable stationary deflections of the membrane, while the unstable case is considered in Chapter 3, and the dynamic case in Chapters 4 and 5. Throughout this Chapter and unless mentioned otherwise, solutions for $(S)_\lambda$ are taken in the classical sense. The permittivity profile $f(x)$ will be allowed to vanish somewhere, and will be assumed to satisfy

$$\begin{aligned} f &\in C^\alpha(\bar{\Omega}) \text{ for some } \alpha \in (0, 1], 0 \leq f \leq 1 \text{ and} \\ f &> 0 \text{ on a subset of } \Omega \text{ of positive measure.} \end{aligned} \quad (2.1.1)$$

This Chapter is organized as follows. In §2.2 we mainly show the existence of a specific pull-in voltage in the sense

$$\lambda^*(\Omega, f) = \sup\{\lambda > 0 \mid (S)_\lambda \text{ possesses at least one solution}\},$$

and we also study its dependence on the size and shape of the domain, as well as on the permittivity profile. These monotonicity properties will help us establish in §2.3 new lower and upper bound estimates on the pull-in voltage. We shall write $|\Omega|$ for the volume of a domain Ω in R^N and $P(\Omega) := \int_{\partial\Omega} ds$ for its “perimeter”, with ω_N referring to the volume of the unit ball $B_1(0)$ in R^N . We denote by μ_Ω the first eigenvalue of $-\Delta$ on $H_0^1(\Omega)$ and by ϕ_Ω the corresponding positive eigenfunction normalized with $\int_\Omega \phi_\Omega dx = 1$.

Theorem 2.1.1. *Assume f is a function satisfying (2.1.1) on a bounded domain Ω in \mathbb{R}^N , then there exists a finite pull-in voltage $\lambda^* := \lambda^*(\Omega, f) > 0$ such that*

1. *If $0 \leq \lambda < \lambda^*$, there exists at least one solution for $(S)_\lambda$.*
2. *If $\lambda > \lambda^*$, there is no solution for $(S)_\lambda$.*

3. The following bounds on λ^* hold for any bounded domain Ω :

$$\underline{\lambda} := \max \left\{ \frac{8N}{27}, \frac{6N-8}{9} \right\} \frac{1}{\sup_{\Omega} f} \left(\frac{\omega_N}{|\Omega|} \right)^{\frac{2}{N}} \leq \lambda^*(\Omega), \quad (2.1.2a)$$

$$\min \left\{ \bar{\lambda}_1 := \frac{4\mu_{\Omega}}{27 \inf_{x \in \Omega} f(x)}, \bar{\lambda}_2 := \frac{\mu_{\Omega}}{3 \int_{\Omega} f \phi_{\Omega} dx} \right\} \geq \lambda^*(\Omega). \quad (2.1.2b)$$

4. If Ω is a strictly star-shaped domain, that is if $x \cdot \nu(x) \geq a > 0$ for all $x \in \partial\Omega$, where $\nu(x)$ is the unit outer normal at $x \in \partial\Omega$, and if $f \equiv 1$, then

$$\lambda^*(\Omega) \leq \bar{\lambda}_3 = \frac{(N+2)^2 P(\Omega)}{8aN|\Omega|}. \quad (2.1.3)$$

In particular, if $\Omega = B_1(0) \subset \mathbb{R}^N$ then we have the bound

$$\lambda^*(B_1(0)) \leq \frac{(N+2)^2}{8}.$$

5. If $f(x) \equiv |x|^{\alpha}$ with $\alpha \geq 0$ and Ω is a ball of radius R , then we have

$$\lambda^*(B_R, |x|^{\alpha}) \geq \lambda_c(\alpha) := \max \left\{ \frac{4(2+\alpha)(N+\alpha)}{27}, \frac{(2+\alpha)(3N+\alpha-4)}{9} \right\} R^{-(2+\alpha)}. \quad (2.1.4)$$

Moreover, if $N \geq 8$ and $0 \leq \alpha \leq \alpha^{**}(N) := \frac{4-6N+3\sqrt{6(N-2)}}{4}$, we have

$$\lambda^*(B_1, |x|^{\alpha}) = \frac{(2+\alpha)(3N+\alpha-4)}{9}. \quad (2.1.5)$$

In §2.3.3 we give some numerical estimates on λ^* to compare them with the analytic bounds given in Theorem 1.1 above. Note that the upper bound $\bar{\lambda}_1$ is relevant only when f is bounded away from 0, while the upper bound $\bar{\lambda}_2$ is valid for all permittivity profiles. However, the order between these two upper bounds can vary in general. For example, in the case of exponential permittivity profiles of the form $f(x) = e^{\alpha(|x|^2-1)}$ on the unit disc, one can see that $\bar{\lambda}_1$ is a better upper bound than $\bar{\lambda}_2$ for small α , while the reverse holds true for larger values of α . The lower bounds in (2.1.2) and (2.1.4) can be improved in small dimensions, but they are optimal—at least for the ball—in dimension larger than 8.

We also consider issues of uniqueness and multiplicity of solutions for $(S)_{\lambda}$ with $0 < \lambda \leq \lambda^*$. The bifurcation diagrams in Figure 2.1 show the complexity of the situation, even in the radially symmetric case. One can see that the number of branches—and of solutions—is closely connected to the space dimension, a fact that we establish analytically in §4, by focussing on the very first branch of solutions considered to be “minimal” in the following way.

Definition 2.1.1. A solution $u_{\lambda}(x)$ of $(S)_{\lambda}$ is said to be minimal if for any other solution u of $(S)_{\lambda}$ we have $u_{\lambda}(x) \leq u(x)$ for all $x \in \Omega$.

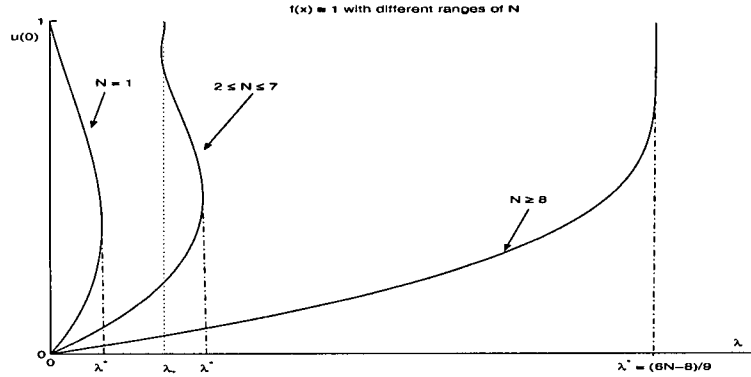


Figure 2.1: Plots of $u(0)$ versus λ for the constant permittivity profile $f(x) \equiv 1$ defined in the unit ball $B_1(0) \subset \mathbb{R}^N$ with different ranges of N . In the case of $N \geq 8$, we have $\lambda^* = (6N-8)/9$.

One can also consider for any solution u of $(S)_\lambda$, the linearized operator at u defined by $L_{u,\lambda} = -\Delta - \frac{2\lambda f(x)}{(1-u)^3}$ and its eigenvalues $\{\mu_{k,\lambda}(u); k = 1, 2, \dots\}$. The first eigenvalue is then simple and is given by

$$\mu_{1,\lambda}(u) = \inf \left\{ \langle L_{u,\lambda} \phi, \phi \rangle_{H_0^1(\Omega)}; \phi \in C_0^\infty(\Omega), \int_{\Omega} |\phi(x)|^2 dx = 1 \right\}.$$

Stable solutions (resp., semi-stable solutions) of $(S)_\lambda$ are those solutions u such that $\mu_{1,\lambda}(u) > 0$ (resp., $\mu_{1,\lambda}(u) \geq 0$). Our main results in this direction can be stated as follows.

Theorem 2.1.2. Assume f is a function satisfying (2.1.1) on a bounded domain Ω in \mathbb{R}^N , and consider $\lambda^* := \lambda^*(\Omega, f)$ as defined in Theorem 2.1.1. Then the following hold:

1. For any $0 \leq \lambda < \lambda^*$, there exists a unique minimal solution u_λ of $(S)_\lambda$ such that $\mu_{1,\lambda}(u_\lambda) > 0$. Moreover, for each $x \in \Omega$, the function $\lambda \rightarrow u_\lambda(x)$ is strictly increasing and differentiable on $(0, \lambda^*)$.
2. If $1 \leq N \leq 7$ then –by means of energy estimates– one has $\sup_{\lambda \in (0, \lambda^*)} \|u_\lambda\|_\infty < 1$ and consequently, $u^* = \lim_{\lambda \uparrow \lambda^*} u_\lambda$ exists in $C^{2,\alpha}(\bar{\Omega})$ with $0 < \alpha < 1$ and is a solution for $(S)_{\lambda^*}$ such that $\mu_{1,\lambda^*}(u^*) = 0$. In particular, u^* –often referred to as the extremal solution of problem $(S)_{\lambda^*}$ – is unique.
3. On the other hand, if $N \geq 8$, $f(x) = |x|^\alpha$ with $0 \leq \alpha \leq \alpha^{**}(N) := \frac{4-6N+3\sqrt{6(N-2)}}{4}$ and Ω is the unit ball, then the extremal solution is necessarily $u^*(x) = 1 - |x|^{\frac{2+\alpha}{3}}$ and is therefore singular.

We note that, in general, the function u^* exists in any dimension, does solve $(S)_{\lambda^*}$ in a suitable weak sense, and is the unique solution in an appropriate class. The above theorem says that it is, however, a classical solution in dimensions $1 \leq N \leq 7$, and this will allow us to start another branch of non-minimal (unstable) solutions. Indeed, we show in §2.5 –following ideas

of Crandall-Rabinowitz [20]– that, for $1 \leq N \leq 7$, and for λ close enough to λ^* , there exists a unique second branch U_λ of solutions for $(S)_\lambda$, bifurcating from u^* , with

$$\mu_{1,\lambda}(U_\lambda) < 0 \quad \text{while} \quad \mu_{2,\lambda}(U_\lambda) > 0. \quad (2.1.6)$$

In Chapter 3, we shall provide a variational (mountain pass) characterization of these unstable solutions and more importantly, we establish –under the same dimension restriction as above– a compactness result along the second branch of unstable solutions leading to a –nonzero– second bifurcation point.

Issues of uniqueness, multiplicity and other qualitative properties of the solutions for $(S)_\lambda$ are still far from being well understood, even in the radially symmetric case which we consider in §2.6. Some of the classical work of Joseph-Lundgren [43] and many that followed can be adapted to this situation when the permittivity profile is constant. However, the case of a power-law permittivity profile $f(x) = |x|^\alpha$ defined in a unit ball already presents a much richer situation. In §2.6 we present some numerical evidence for various conjectures relating to this case, some of which will be tackled in Chapter 3. A detailed and involved analysis of compactness along the unstable branches will be discussed there, as well as some information about the second bifurcation point.

2.2 The pull-in voltage λ^*

In this section, we first establish the existence and some monotonicity properties for the pull-in voltage λ^* , which is defined as

$$\lambda^*(\Omega, f) = \sup\{\lambda > 0 \mid (S)_\lambda \text{ possesses at least one solution}\}. \quad (2.2.1)$$

In other words, λ^* is called pull-in voltage if there exist uncollapsed states for $0 < \lambda < \lambda^*$ while there are none for $\lambda > \lambda^*$. We then study how $\lambda^*(\Omega, f)$ varies with the domain Ω , the dimension N and the permittivity profile f .

2.2.1 Existence of the pull-in voltage

For any bounded domain Γ in \mathbb{R}^N , we denote by μ_Γ the first eigenvalue of $-\Delta$ on $H_0^1(\Gamma)$ and by ψ_Γ the corresponding positive eigenfunction normalized with $\sup_{x \in \Gamma} \psi_\Gamma = 1$. We also associate with any domain Γ in \mathbb{R}^N the following parameter:

$$\nu_\Omega = \sup \left\{ \mu_\Gamma H(\inf_\Omega \psi_\Gamma); \Gamma \text{ domain of } \mathbb{R}^N, \Gamma \supset \bar{\Omega} \right\}, \quad (2.2.2)$$

where H is the function $H(t) = \frac{t(t+1+2\sqrt{t})}{(t+1+\sqrt{t})^3}$.

Theorem 2.2.1. *Assume f is a function satisfying (2.1.1) on a bounded domain Ω in \mathbb{R}^N , then there exists a finite pull-in voltage $\lambda^* := \lambda^*(\Omega, f) > 0$ such that*

1. *if $\lambda < \lambda^*$, there exists at least one solution for $(S)_\lambda$;*
2. *if $\lambda > \lambda^*$, there is no solution for $(S)_\lambda$.*

Moreover, we have the lower bound

$$\lambda^*(\Omega, f) \geq \frac{\nu_\Omega}{\sup_{x \in \Omega} f(x)}. \quad (2.2.3)$$

Proof: We need to show that $(S)_\lambda$ has at least one solution when $\lambda < \nu_\Omega (\sup_\Omega f(x))^{-1}$. Indeed, it is clear that $u \equiv 0$ is a subsolution of $(S)_\lambda$ for all $\lambda > 0$. To construct a supersolution of $(S)_\lambda$, we consider a bounded domain $\Gamma \supset \bar{\Omega}$ with smooth boundary, and let $(\mu_\Gamma, \psi_\Gamma)$ be its first eigenpair normalized in such a way that

$$\sup_{x \in \Gamma} \psi_\Gamma(x) = 1 \text{ and } \inf_{x \in \Omega} \psi_\Gamma(x) := s_1 > 0.$$

We construct a supersolution in the form $\psi = A\psi_\Gamma$ where A is a scalar to be chosen later. First, we must have $A\psi_\Gamma \geq 0$ on $\partial\Omega$ and $0 < 1 - A\psi_\Gamma < 1$ in Ω , which requires that $0 < A < 1$. We also require

$$-\Delta\psi - \frac{\lambda f(x)}{(1 - A\psi)^2} \geq 0 \quad \text{in } \Omega, \quad (2.2.4)$$

which can be satisfied as long as:

$$\mu_\Gamma A \psi_\Gamma \geq \frac{\lambda \sup_\Omega f(x)}{(1 - A \psi_\Gamma)^2} \quad \text{in } \Omega, \quad (2.2.5)$$

or

$$\lambda \sup_\Omega f(x) < \beta(A, \Gamma) := \mu_\Gamma \inf \{g(sA); s \in [s_1(\Gamma), 1]\}, \quad (2.2.6)$$

where $g(s) = s(1 - s)^2$. In other words, $\lambda^* \sup_\Omega f(x) \geq \sup\{\beta(A, \Gamma); 0 < a < 1, \Gamma \supset \bar{\Omega}\}$, and therefore it remains to show that

$$\nu_\Omega = \sup \{\beta(A, \Gamma); 0 < a < 1, \Gamma \supset \bar{\Omega}\}. \quad (2.2.7)$$

For that, we note first that

$$\inf_{s \in [s_1, 1]} g(As) = \min \{g(As_1), g(A)\}.$$

We also have that $g(As_1) \leq g(A)$ if and only if $A^2(s_1^3 - 1) - 2A(s_1^2 - 1) + (s_1 - 1) \leq 0$ which happens if and only if $A^2(s_1^2 + s_1 + 1) - 2A(s_1 + 1) + 1 \geq 0$ or if and only if either $A \leq A_-$ or $A \geq A_+$ where

$$A_+ = \frac{s_1 + 1 + \sqrt{s_1}}{s_1^2 + 1 + s_1} = \frac{1}{s_1 + 1 - \sqrt{s_1}}, \quad A_- = \frac{s_1 + 1 - \sqrt{s_1}}{s_1^2 + 1 + s_1} = \frac{1}{s_1 + 1 + \sqrt{s_1}}.$$

Since $A_- < 1 < A_+$, we get that

$$G(A) = \inf_{s \in [s_1, 1]} g(As) = \begin{cases} g(As_1) & \text{if } 0 \leq A \leq A_-, \\ g(A) & \text{if } A_- \leq A \leq 1. \end{cases} \quad (2.2.8)$$

We now have that $\frac{dG}{dA} = g'(As_1)s_1 \geq 0$ for all $0 \leq A \leq A_-$. And since $A_- \geq \frac{1}{3}$, we have $\frac{dG}{dA} = g'(A) \leq 0$ for all $A_- \leq A \leq 1$. It follows that

$$\begin{aligned} \sup_{0 < a < 1} \inf_{s \in [s_1, 1]} g(As) &= \sup_{0 < a < 1} G(A) = G(A_-) = g(A_-) \\ &= \frac{1}{s_1 + 1 + \sqrt{s_1}} \left(1 - \frac{1}{s_1 + 1 + \sqrt{s_1}}\right)^2 \\ &= \frac{s_1(s_1 + 1 + 2\sqrt{s_1})}{(s_1 + 1 + \sqrt{s_1})^3} \\ &= H(\inf_{\Omega} \psi_{\Gamma}), \end{aligned}$$

which proves our lower estimate.

Now that we know that $\lambda^* > 0$, pick $\lambda \in (0, \lambda^*)$ and use the definition of λ^* to find a $\bar{\lambda} \in (\lambda, \lambda^*)$ such that $(S)_{\bar{\lambda}}$ has a solution $u_{\bar{\lambda}}$,

$$-\Delta u_{\bar{\lambda}} = \frac{\bar{\lambda}f(x)}{(1-u_{\bar{\lambda}})^2}, \quad x \in \Omega; \quad u_{\bar{\lambda}} = 0, \quad x \in \partial\Omega,$$

and in particular $-\Delta u_{\bar{\lambda}} \geq \frac{\lambda f(x)}{(1-u_{\bar{\lambda}})^2}$ for $x \in \Omega$ which then implies that $u_{\bar{\lambda}}$ is a supersolution of $(S)_{\lambda}$. Since $u \equiv 0$ is a subsolution of $(S)_{\lambda}$, then we can conclude again that there is a solution u_{λ} of $(S)_{\lambda}$ for every $\lambda \in (0, \lambda^*)$.

It is also easy to show that λ^* is finite, since if $(S)_{\lambda}$ has at least one solution $0 < u < 1$, then, by integrating against the first (positive) eigenfunction ψ_{Ω} , we get

$$+\infty > \mu_{\Omega} \geq \mu_{\Omega} \int_{\Omega} u \psi_{\Omega} = - \int_{\Omega} u \Delta \psi_{\Omega} = - \int_{\Omega} \psi_{\Omega} \Delta u = \lambda \int_{\Omega} \frac{\psi_{\Omega} f}{(1-u)^2} dx \geq \lambda \int_{\Omega} \psi_{\Omega} f dx \quad (2.2.9)$$

and therefore $\lambda^* < +\infty$. The definition of λ^* implies that there is no solution of $(S)_{\lambda}$ for any $\lambda > \lambda^*$. \blacksquare

2.2.2 Monotonicity results for the pull-in voltage

In this subsection, we give a more precise characterization of λ^* , namely as the endpoint for the branch of minimal solutions. This will allow us to establish various monotonicity properties for λ^* that will help in the estimates given in the next subsections. First we give a recursive scheme for the construction of minimal solutions.

Theorem 2.2.2. *Assume f is a function satisfying (2.1.1) on a bounded domain Ω in \mathbb{R}^N , then for any $0 < \lambda < \lambda^*(\Omega, f)$ there exists a unique minimal positive solution u_{λ} for $(S)_{\lambda}$. It is obtained as the limit of the sequence $\{u_n(\lambda; x)\}$ constructed recursively as follows: $u_0 \equiv 0$ in Ω and, for each $n \geq 1$,*

$$\begin{aligned} -\Delta u_n &= \frac{\lambda f(x)}{(1-u_{n-1})^2}, \quad x \in \Omega; \\ 0 \leq u_n < 1, \quad x \in \Omega; \quad u_n &= 0, \quad x \in \partial\Omega. \end{aligned} \quad (2.2.10)$$

Proof: Let u be any positive solution for $(S)_\lambda$, and consider the sequence $\{u_n(\lambda; x)\}$ defined in (2.2.10). Clearly $u(x) > u_0 \equiv 0$ in Ω , and whenever $u(x) \geq u_{n-1}$ in Ω , then

$$\begin{aligned} -\Delta(u - u_n) &= \lambda f(x) \left[\frac{1}{(1-u)^2} - \frac{1}{(1-u_{n-1})^2} \right] \geq 0, \quad x \in \Omega, \\ u - u_n &= 0, \quad x \in \partial\Omega. \end{aligned}$$

The maximum principle and an immediate induction yield that $1 > u(x) \geq u_n$ in Ω for all $n \geq 0$. In a similar way, the maximum principle implies that the sequence $\{u_n(\lambda; x)\}$ is monotone increasing. Therefore, $\{u_n(\lambda; x)\}$ converges uniformly to a positive solution $u_\lambda(x)$, satisfying $u(x) \geq u_\lambda(x)$ in Ω , which is a minimal positive solution of $(S)_\lambda$. It is also clear that u_λ is unique in this class of solutions. ■

Remark 2.2.1. Let $g(x, \xi, \Omega)$ be the Green's function of the Laplace operator, with $g(x, \xi, \Omega) = 0$ on $\partial\Omega$. Then the iteration in (2.2.10) can be replaced by $u_0 \equiv 0$ in Ω , and for each $n \geq 1$,

$$\begin{aligned} u_n(\lambda; x) &= \lambda \int_{\Omega} \frac{f(\xi)g(x, \xi, \Omega)}{(1 - u_{n-1}(\lambda; \xi))^2} d\xi, \quad x \in \Omega; \\ u_n(\lambda; x) &= 0, \quad x \in \partial\Omega. \end{aligned} \quad (2.2.11)$$

The same reasoning as above yields that $\lim_{n \rightarrow \infty} u_n(\lambda; x) = u_\lambda(x)$ for all $x \in \Omega$.

The above construction of solutions yields the following monotonicity result for the pull-in voltage.

Proposition 2.2.3. *If $\Omega_1 \subset \Omega_2$ and if f is a function satisfying (2.1.1) on Ω_2 , then $\lambda^*(\Omega_1) \geq \lambda^*(\Omega_2)$ and the corresponding minimal solutions satisfy $u_{\Omega_1}(\lambda, x) \leq u_{\Omega_2}(\lambda, x)$ on Ω_1 for every $0 < \lambda < \lambda^*(\Omega_2)$.*

Proof: Again the method of sub/supersolutions immediately yields that $\lambda^*(\Omega_1) \geq \lambda^*(\Omega_2)$. Now consider, for $i = 1, 2$, the sequences $\{u_n(\lambda, x, \Omega_i)\}$ on Ω_i defined by (2.2.11) where $g(x, \xi, \Omega_i)$ are the corresponding Green's functions on Ω_i . Since $\Omega_1 \subset \Omega_2$, we have that $g(x, \xi, \Omega_1) \leq g(x, \xi, \Omega_2)$ on Ω_1 . Hence, it follows that

$$u_1(\lambda, x, \Omega_2) = \lambda \int_{\Omega_2} f(\xi)g(x, \xi, \Omega_2)d\xi \geq \lambda \int_{\Omega_1} f(\xi)g(x, \xi, \Omega_1)d\xi = u_1(\lambda, x, \Omega_1)$$

on Ω_1 . By induction we conclude that $u_n(\lambda, x, \Omega_2) \geq u_n(\lambda, x, \Omega_1)$ on Ω_1 for all n . On the other hand, since $u_n(\lambda, x, \Omega_2) \leq u_{n+1}(\lambda, x, \Omega_2)$ on Ω_2 for n , we get that $u_n(\lambda, x, \Omega_1) \leq u_{\Omega_2}(\lambda, x)$ on Ω_1 , and we are done. ■

We also note the following easy comparison results, and we omit the details.

Corollary 2.2.4. *Suppose $f_1, f_2 : \Omega \rightarrow R$ are two functions satisfying (2.1.1) such that $f_1(x) \leq f_2(x)$ on Ω , then $\lambda^*(\Omega, f_1) \geq \lambda^*(\Omega, f_2)$, and for $0 < \lambda < \lambda^*(\Omega, f_2)$ we have $u_1(\lambda, x) \leq u_2(\lambda, x)$ on Ω , where $u_1(\lambda, x)$ (resp., $u_2(\lambda, x)$) are the unique minimal positive solution of*

$$-\Delta u = \frac{\lambda f_1(x)}{(1-u)^2} \quad (\text{resp., } -\Delta u = \frac{\lambda f_2(x)}{(1-u)^2}) \quad \text{on } \Omega \text{ and } u = 0 \text{ on } \partial\Omega.$$

Moreover, if $f_2(x) > f_1(x)$ on a subset of positive measure, then $u_1(\lambda, x) < u_2(\lambda, x)$ for all $x \in \Omega$.

We shall also need the following result which is adapted from [6] (Theorem 4.10) where it is proved for regular nonlinearities.

Proposition 2.2.5. *For any bounded domain Γ in \mathbb{R}^N and any function f satisfying (2.1.1) on Γ , we have*

$$\lambda^*(\Gamma, f) \geq \lambda^*(B_R, f^*)$$

where $B_R = B_R(0)$ is the Euclidean ball in \mathbb{R}^N with radius $R > 0$ and with volume $|B_R| = |\Gamma|$, and where f^* is the Schwarz symmetrization of f .

Proof: For any bounded $\Gamma \subset \mathbb{R}^N$, define its symmetrized domain $\Gamma^* = B_R$ to be the ball $\{x : |x| < R\}$ with $|\Gamma| = |B_R|$. If u is a real-valued function on Γ , we define its symmetrized function $u^* : \Gamma^* = B_R \rightarrow \mathbb{R}$ by $u^*(x) = \sup\{\mu : x \in B_R(\mu)\}$ where $B_R(\mu)$ is the symmetrization of the superlevel set $\Gamma(\mu) = \{x \in \Omega : \mu \leq u(x)\}$ (i.e., $B_R(\mu) = \Gamma(\mu)^*$). If h and g are continuous functions on Γ , then the following inequality holds (See Lemma 2.4 of [6])

$$\int_{\Gamma} h g dx \leq \int_{B_R} h^* g^* dx. \quad (2.2.12)$$

As in Theorem 4.10 of [6], we consider for any $\lambda \in (0, \lambda^*(B_R))$ the minimal sequence $\{u_n\}$ for (S_{λ}) in Γ as defined in (2.2.10), and let $\{v_n\}$ be the minimal sequence for the corresponding Schwarz symmetrized problem:

$$-\Delta v = \frac{\lambda f^*(x)}{(1-v)^2} \quad x \in B_R, \quad (2.2.13a)$$

$$v = 0 \quad x \in \partial B_R \quad (2.2.13b)$$

with $0 < v < 1$ on $B_R = \Gamma^*$. Since $\lambda \in (0, \lambda^*(B_R))$, we can consider the corresponding minimal solution v_{λ} for (2.2.13b). As in Theorem 2.2.2 we have $0 \leq v_n \leq v_{\lambda} < 1$ on B_R for all $n \geq 1$. We shall show that $\{u_n\}$ also satisfies $0 \leq u_n^* \leq v_{\lambda} < 1$ on B_R for all $n \geq 1$.

We now write $\tilde{f}(a = \omega_N |x|^N)$ for $f^*(x)$, and $\tilde{u}_n(a = \omega_N |x|^N)$ for $u_n^*(x)$. Applying (2.2.12) and the argument for (4.9) in [6], we obtain that $\tilde{u}_0 = \tilde{v}_0 = 0$ in $(0, R)$, and for each $n \geq 1$,

$$\frac{d\tilde{u}_n}{da} + \frac{\lambda}{q(a)} \int_0^a \frac{\tilde{f}}{(1-\tilde{u}_{n-1})^2} dr \geq 0 \quad \text{in } (0, R), \quad (2.2.14)$$

and

$$\frac{d\tilde{v}_n}{da} + \frac{\lambda}{q(a)} \int_0^a \frac{\tilde{f}}{(1-\tilde{v}_{n-1})^2} dr = 0 \quad \text{in } (0, R) \quad (2.2.15)$$

with $q(a) = [N\omega_N^{1/N} a^{(N-1)/N}]^2 > 0$. We claim that for any $n \geq 1$, we have

$$\tilde{u}_n(a) \leq \tilde{v}_n(a) \quad a \in (0, R). \quad (2.2.16)$$

In fact, for $n = 1$ we have $d\tilde{u}_1/da \geq d\tilde{v}_1/da$, and integration yields that

$$-\tilde{u}_1(a) = \tilde{u}_1(R) - \tilde{u}_1(a) \geq \tilde{v}_1(R) - \tilde{v}_1(a) = -\tilde{v}_1(a),$$

and hence $\tilde{u}_1(a) \leq \tilde{v}_1(a)$ on $[0, R]$. (2.2.16) is now proved by induction. Suppose it holds for $n \leq k-1$, then one gets from (2.2.14) and (2.2.15) that $d\tilde{u}_k/da \geq d\tilde{v}_k/da$, which establishes (2.2.16) for all $n \geq 1$.

Therefore, the minimal sequence $\{u_n(x)\}$ on Γ is bounded by $\max_{x \in B_R} v_\lambda(x) < 1$, and again as in the proof of Theorem 2.2.2, there exists a minimal solution u_λ for $(S)_\lambda$ on Γ . This means $\lambda^*(\Gamma, f) \geq \lambda^*(B_R, f^*)$. \blacksquare

2.3 Estimates for the pull-in voltage

In this section, analytically and numerically we shall discuss estimates of pull-in voltage λ^* . For that we shall write $|\Omega|$ for the volume of a domain Ω in \mathbb{R}^N and $P(\Omega) := \int_{\partial\Omega} dS$ for its “perimeter”, with ω_N referring to the volume of the unit ball $B_1(0)$ in \mathbb{R}^N . We denote by μ_Ω the first eigenvalue of $-\Delta$ on $H_0^1(\Omega)$ and by ϕ_Ω the corresponding positive eigenfunction normalized with $\int_\Omega \phi_\Omega dx = 1$.

2.3.1 Lower bounds for λ^*

While the lower bound in (2.2.3) is useful to prove existence, it is not easy to compute. The following proposition gives more computationally accessible lower estimates for λ^* .

Proposition 2.3.1. *Assume f is a function satisfying (2.1.1) on a bounded domain Ω in \mathbb{R}^N , then we have the following lower bound:*

$$\lambda^*(\Omega, f) \geq \max \left\{ \frac{8N}{27}, \frac{6N-8}{9} \right\} \frac{1}{\sup_\Omega f} \left(\frac{\omega_N}{|\Omega|} \right)^{\frac{2}{N}}. \quad (2.3.1)$$

Moreover, if $f(x) \equiv |x|^\alpha$ with $\alpha \geq 0$ and Ω is a ball of radius R , then we have

$$\lambda^*(B_R, |x|^\alpha) \geq \max \left\{ \frac{4(2+\alpha)(N+\alpha)}{27}, \frac{(2+\alpha)(3N+\alpha-4)}{9} \right\} R^{-(2+\alpha)}. \quad (2.3.2)$$

Finally, if $N \geq 8$ and $0 \leq \alpha \leq \alpha^{**}(N) := \frac{4-6N+3\sqrt{6(N-2)}}{4}$, we have

$$\lambda^*(B_1, |x|^\alpha) = \frac{(2+\alpha)(3N+\alpha-4)}{9}. \quad (2.3.3)$$

Proof: Setting $R = \left(\frac{|\Omega|}{\omega_N} \right)^{\frac{1}{N}}$, it suffices—in view of Proposition 2.2.5—and since $\sup_{B_R} f^* = \sup_\Omega f$, to show that

$$\lambda^*(B_R, f^*) \geq \max \left\{ \frac{8N}{27R^2 \sup_\Omega f^*}, \frac{6N-8}{9R^2 \sup_\Omega f^*} \right\} \quad (2.3.4)$$

for the case where $\Omega = B_R$. In fact, the function $w(x) = \frac{1}{3} \left(1 - \frac{|x|^2}{R^2} \right)$ satisfies on B_R

$$\begin{aligned} -\Delta w &= \frac{2N}{3R^2} = \frac{2N(1-\frac{1}{3})^2}{3R^2} \frac{1}{(1-\frac{1}{3})^2} \\ &\geq \frac{8N}{27R^2 \sup_\Omega f} \frac{f(x)}{[1-\frac{1}{3}(1-\frac{|x|^2}{R^2})]^2} \\ &= \frac{8N}{27R^2 \sup_\Omega f} \frac{f(x)}{(1-w)^2}. \end{aligned}$$

So for $\lambda \leq \frac{8N}{27R^2 \sup_{\Omega} f}$, w is a supersolution of $(S)_{\lambda}$ in B_R . Since on the other hand $w_0 \equiv 0$ is a subsolution of $(S)_{\lambda}$ and $w_0 \leq w$ in B_R , then there exists a solution of $(S)_{\lambda}$ in B_R which proves a part of (2.3.4).

A similar computation applied to the function $v(x) = 1 - \left(\frac{|x|}{R}\right)^{\frac{2}{3}}$ shows that v is also a supersolution as long as $\lambda \leq \frac{6N-8}{9R^2 \sup_{\Omega} f}$.

In order to prove (2.3.2), it suffices to note that $w(x) = \frac{1}{3}\left(1 - \frac{|x|^{2+\alpha}}{R^{2+\alpha}}\right)$ is a supersolution for $(S)_{\lambda}$ on B_R provided $\lambda \leq \frac{4(2+\alpha)(N+\alpha)}{27R^{2+\alpha}}$, and that $v(x) = 1 - \left(\frac{|x|}{R}\right)^{\frac{2+\alpha}{3}}$ is a supersolution for $(S)_{\lambda}$ on B_R , provided $\lambda \leq \frac{(2+\alpha)(3N+\alpha-4)}{9R^{2+\alpha}}$.

In order to complete the proof of Proposition 2.3.1, we need to establish that the function $u^*(x) = 1 - |x|^{\frac{2+\alpha}{3}}$ is the extremal function as long as $N \geq 8$ and $0 \leq \alpha \leq \alpha^{**}(N) = \frac{4-6N+3\sqrt{6}(N-2)}{4}$. This will then yield that for such dimensions and these values of α , the voltage $\lambda = \frac{(2+\alpha)(3N+\alpha-4)}{9}$ is exactly the pull-in voltage λ^* .

First, it is easy to check that u^* is a $H_0^1(\Omega)$ -weak solution of $(S)_{\lambda^*}$. Since $\|u^*\|_{\infty} = 1$, and by the characterization of Theorem 2.5.1 below, we need only to prove that

$$\int_{\Omega} |\nabla \phi|^2 \geq \int_{\Omega} \frac{2\lambda |x|^{\alpha}}{(1-u^*)^3} \phi^2 \quad \forall \phi \in H_0^1(\Omega). \quad (2.3.5)$$

However, Hardy's inequality gives for $N \geq 2$:

$$\int_{B_1} |\nabla \phi|^2 \geq \frac{(N-2)^2}{4} \int_{B_1} \frac{\phi^2}{|x|^2}$$

for any $\phi \in H_0^1(B_1)$, which means that (2.3.5) holds whenever $2\lambda^* \leq \frac{(N-2)^2}{4}$ or, equivalently, if $N \geq 8$ and $0 \leq \alpha \leq \alpha^{**} = \frac{4-6N+3\sqrt{6}(N-2)}{4}$. \blacksquare

Remark 2.3.1. The above lower bounds can be improved at least in low dimensions. First note from (2.3.2) that if $N > \frac{12+\alpha}{5}$, then $\lambda_2 = \frac{(2+\alpha)(3N+\alpha-4)}{9}$ is the better lower bound and is actually sharp on the ball as soon as $N \geq 8$ and $\alpha \leq \alpha^{**}$. For lower dimensions, the best lower bounds are more complicated even when one considers supersolutions of the form $v(x) = a\left(1 - \left(\frac{|x|}{R}\right)^k\right)$ and optimize $\lambda(a, k, R)$ over a and k . For example, in the case where $\alpha = 0$, $N = 2$ and $R = 1$, one can see that a better lower bound can be obtained via the supersolution $v(x) = \frac{1}{2.4}(1 - |x|^{1.6})$.

2.3.2 Upper bounds for λ^*

We note that (2.2.9) already yields a finite upper bound for λ^* . However, Pohozaev-type arguments can be used to establish better and more computable upper bounds. For a general domain Ω , the following upper bounds on $\lambda^*(\Omega)$ were established in [50] and [32], respectively.

Proposition 2.3.2. (1) Assume f is a function satisfying (2.1.1) on a bounded domain Ω in \mathbb{R}^N such that $\inf_{\Omega} f > 0$, then

$$\lambda^*(\Omega, f) \leq \bar{\lambda}_1 \equiv \frac{4\mu_{\Omega}}{27} (\inf_{\Omega} f)^{-1}. \quad (2.3.6)$$

(2) If we only suppose that $f > 0$ on a set of positive measure, then

$$\lambda^*(\Omega, f) \leq \bar{\lambda}_2 \equiv \frac{\mu_\Omega}{3} \left(\int_\Omega f \phi_\Omega dx \right)^{-1}. \quad (2.3.7)$$

Proof: (1). We multiply the equation $(S)_\lambda$ by ϕ_Ω , integrate the resulting equation over Ω , and use Green's identity to obtain

$$\int_\Omega \left(-\mu_\Omega u + \frac{\lambda f(x)}{(1-u)^2} \right) \phi_\Omega dx = 0. \quad (2.3.8)$$

Since $C := \inf_\Omega f > 0$ and $\phi_\Omega > 0$, the equality in (2.3.8) is impossible when

$$-\mu_\Omega u + \frac{\lambda C}{(1-u)^2} > 0, \quad \text{for all } x \in \Omega. \quad (2.3.9)$$

A simple calculation using (2.3.9) shows that (2.3.9) holds when $\lambda > \bar{\lambda}_1$, where $\bar{\lambda}_1$ is given in (2.3.6). This completes the proof of Proposition 2.3.2(1).

As shown below, the bound (2.3.6) on λ^* is rather good when applied to the constant permittivity profile $f(x) \equiv 1$. However, this bound is useless when the minimum of $f(x)$ on Ω is zero, and cannot be used to estimate λ^* for the power-law permittivity profile $f(x) = |x|^\alpha$ with $\alpha > 0$. Therefore, it is desirable to obtain a bound on λ^* that depends more on the global properties of f . Such a bound was established in [32] and here is a sketch of its proof.

(2). Multiply now $(S)_\lambda$ by $\phi_\Omega(1-u)^2$, and integrate the resulting equation over Ω to get

$$\int_\Omega \lambda f \phi_\Omega dx = \int_\Omega \phi_\Omega (1-u)^2 \Delta u dx. \quad (2.3.10)$$

Using the identity $\nabla \cdot (Hg) = g \nabla \cdot H + H \cdot \nabla g$ for any smooth scalar field g and vector field H , together with the Divergence theorem, we calculate

$$\int_\Omega \lambda f \phi_\Omega dx = \int_{\partial\Omega} (1-u)^2 \phi_\Omega \nabla u \cdot \nu dS + \int_\Omega \nabla u \cdot \nabla [\phi_\Omega (1-u)^2] dx, \quad (2.3.11)$$

where ν is the unit outward normal to $\partial\Omega$. Since $\phi_\Omega = 0$ on $\partial\Omega$, the first term on the right-hand side of (2.3.11) vanishes. By calculating the second term on the right-hand side of (2.3.11) we get:

$$\int_\Omega \lambda f \phi_\Omega dx = - \int_\Omega 2(1-u) \phi_\Omega |\nabla u|^2 dx + \int_\Omega (1-u)^2 \nabla u \cdot \nabla \phi_\Omega dx \quad (2.3.12a)$$

$$\leq - \int_\Omega \frac{1}{3} \nabla \phi_\Omega \cdot \nabla [(1-u)^3] dx. \quad (2.3.12b)$$

The right-hand side of (2.3.12b) is evaluated explicitly by

$$\int_\Omega \lambda f \phi_\Omega dx \leq -\frac{1}{3} \int_{\partial\Omega} (1-u)^3 \nabla \phi_\Omega \cdot \nu dS - \frac{\mu_\Omega}{3} \int_\Omega (1-u)^3 \phi_\Omega dx. \quad (2.3.13)$$

For $0 \leq u < 1$, the last term on the right-hand side of (2.3.13) is positive. Moreover, $u = 0$ on $\partial\Omega$ so that $\int_{\partial\Omega} \nabla \phi_\Omega \cdot \nu dS = -\mu_\Omega$ since $\int_\Omega \phi_\Omega dx = 1$. Therefore, if $(S)_\lambda$ has a solution, then (2.3.13) yields

$$\lambda \int_\Omega f \phi_\Omega dx \leq \frac{\mu_\Omega}{3}. \quad (2.3.14)$$

This proves that there is no solution for $\lambda > \bar{\lambda}_2$, which gives (2.3.7). ■

Remark 2.3.2. The above estimate is not sharp, at least in dimensions $1 \leq N \leq 7$, as one can show that there exists $1 > \alpha(\Omega, N) > 0$ such that

$$\lambda \leq \frac{\mu_\Omega}{3}(1 - \alpha(\Omega, N)) \left(\int_\Omega f \phi_\Omega dx \right)^{-1}. \quad (2.3.15)$$

Indeed, this follows from inequality (2.3.13) above and Theorem 2.4.5 below where it will be shown that in these dimensions, there exists $0 < C(\Omega, N) < 1$ independent of λ such that $\|u_\lambda\|_\infty \leq C(\Omega, N)$ for any minimal solution u_λ . It is now easy to see that $\alpha(\Omega, N)$ can be taken to be

$$\alpha(\Omega, N) := (1 - C(\Omega, N))^3 \int_\Omega \phi_\Omega dx.$$

We now consider problem $(S)_\lambda$ in the case where $\Omega \subset \mathbb{R}^N$ is a strictly star-shaped domain containing 0, meaning that Ω satisfies the additional property that there exists a positive constant a such that

$$x \cdot \nu \geq a > 0 \quad \text{for all } x \in \partial\Omega, \quad (2.3.16)$$

where ν is the unit outer normal to $\partial\Omega$.

Proposition 2.3.3. *Suppose $f \equiv 1$ and that the strictly star-shaped smooth domain $\Omega \subset \mathbb{R}^N$ satisfies (2.3.16). Then the pull-in voltage $\lambda^*(\Omega)$ satisfies:*

$$\lambda^*(\Omega) \leq \bar{\lambda}_3 = \frac{(N+2)^2 P(\Omega)}{8aN|\Omega|}. \quad (2.3.17)$$

where $|\Omega|$ is the volume and $P(\Omega)$ is the perimeter of Ω .

In particular, if Ω is the Euclidean unit ball in \mathbb{R}^N , then we have the bound

$$\lambda^*(B_1(0)) \leq \frac{(N+2)^2}{8}.$$

Proof: Recall Pohozaev's identity: If u is a solution of

$$\begin{aligned} \Delta u + \lambda g(u) &= 0 & \text{for } x \in \Omega, \\ u &= 0 & \text{for } x \in \partial\Omega, \end{aligned}$$

then

$$N\lambda \int_\Omega G(u) dx - \frac{N-2}{2}\lambda \int_\Omega u g(u) dx = \frac{1}{2} \int_{\partial\Omega} (x \cdot \nu) \left(\frac{\partial u}{\partial \nu} \right)^2 dS, \quad (2.3.18)$$

where $G(u) = \int_0^u g(s) ds$. Applying this with $g(u) = \frac{1}{(1-u)^2}$ and $G(u) = \frac{u}{1-u}$ yields

$$\begin{aligned} \frac{\lambda}{2} \int_\Omega \frac{u(N+2-2Nu)}{(1-u)^2} dx &= \frac{1}{2} \int_{\partial\Omega} (x \cdot \nu) \left(\frac{\partial u}{\partial \nu} \right)^2 dS \\ &\geq \frac{a}{2P(\Omega)} \left(\int_{\partial\Omega} \frac{\partial u}{\partial \nu} dS \right)^2 \\ &= \frac{a}{2P(\Omega)} \left(- \int_\Omega \Delta u dx \right)^2 \\ &= \frac{a\lambda^2}{2P(\Omega)} \left(\int_\Omega \frac{dx}{(1-u)^2} \right)^2, \end{aligned} \quad (2.3.19)$$

where we have used the Divergence Theorem and Hölder's inequality

$$\int_{\partial\Omega} \frac{\partial u}{\partial \nu} dS \leq \left(\int_{\partial\Omega} \left(-\frac{\partial u}{\partial \nu} \right)^2 dS \right)^{1/2} \left(\int_{\partial\Omega} dS \right)^{1/2}.$$

Since

$$\begin{aligned} \int_{\Omega} \frac{u(N+2-2Nu)}{(1-u)^2} dx &= \int_{\Omega} \left[-2N \left(u - \frac{N+2}{4N} \right)^2 + \frac{(N+2)^2}{8N} \right] \frac{1}{(1-u)^2} dx \\ &\leq \frac{(N+2)^2}{8N} \int_{\Omega} \frac{dx}{(1-u)^2}, \end{aligned}$$

we deduce from (2.3.19) that

$$\frac{(N+2)^2}{8N} \geq \frac{a\lambda}{P(\Omega)} \int_{\Omega} \frac{dx}{(1-u)^2} \geq \frac{a\lambda|\Omega|}{P(\Omega)},$$

which implies the upper bound (2.3.17) for λ^* .

Finally, for the special case where $\Omega = B_1(0) \subset \mathbb{R}^N$, we have $a = 1$ and $\frac{P(B_1(0))}{\omega_N} = N$ and hence the bound $\lambda^*(B_1(0)) \leq \bar{\lambda}_3 = \frac{(N+2)^2}{8}$. ■

2.3.3 Numerical estimates for λ^*

In this subsection, we apply numerical methods to discussing the bounds of λ^* . In the computations below we shall consider two choices for the domain Ω ,

$$\Omega : [-1/2, 1/2] \quad (\text{slab}); \quad \Omega : x^2 + y^2 \leq 1 \quad (\text{unit disk}). \quad (2.3.20)$$

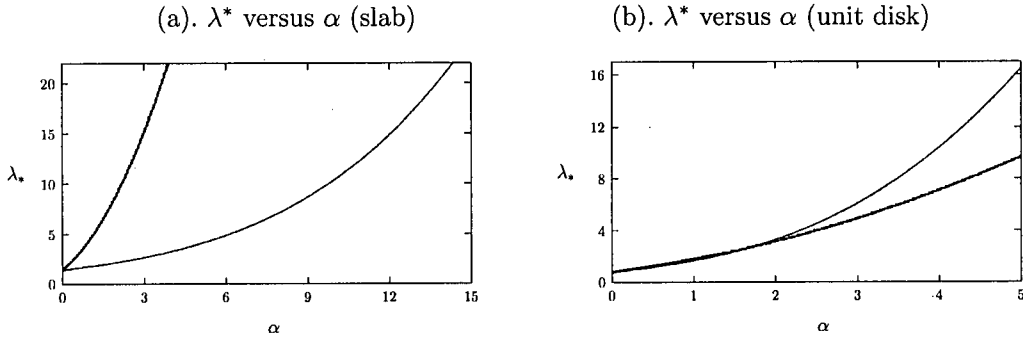


Figure 2.2: Plots of λ^* versus α for a power-law profile (heavy solid curve) and the exponential profile (solid curve). The left figure corresponds to the slab domain, while the right figure corresponds to the unit disk.

Exponential Profiles:

Ω	α	$\underline{\lambda}$	λ^*	$\bar{\lambda}_1$	$\bar{\lambda}_2$
slab	0	1.185	1.401	1.462	3.290
slab	1.0	1.185	1.733	1.878	4.023
slab	3.0	1.185	2.637	3.095	5.965
slab	6.0	1.185	4.848	6.553	10.50
unit disk	0	0.593	0.789	0.857	1.928
unit disk	0.5	0.593	1.153	1.413	2.706
unit disk	1.0	0.593	1.661	2.329	3.746
unit disk	3.0	0.593	6.091	17.21	11.86

Table 2.1: Numerical values for pull-in voltage λ^* with the bounds given in Theorem 2.1.1. Here the exponential permittivity profile is chosen as (2.3.21).

For the permittivity profile, following [32] we consider

$$\text{slab : } f(x) = |2x|^\alpha \quad (\text{power-law}); \quad f(x) = e^{\alpha(x^2-1/4)} \quad (\text{exponential}), \quad (2.3.21a)$$

$$\text{unit disk : } f(x) = |x|^\alpha \quad (\text{power-law}); \quad f(x) = e^{\alpha(|x|^2-1)} \quad (\text{exponential}), \quad (2.3.21b)$$

with $\alpha \geq 0$. To compute the bounds $\bar{\lambda}_1$ and $\bar{\lambda}_2$, we must calculate the first eigenpair μ_Ω and ϕ_Ω of $-\Delta$ on Ω , normalized by $\int_\Omega \phi_\Omega dx = 1$, for each of these domains. A simple calculation yields that

$$\mu_\Omega = \pi^2, \quad \phi_\Omega = \frac{\pi}{2} \sin \left[\pi \left(x + \frac{1}{2} \right) \right] \quad (\text{Slab}); \quad (2.3.22a)$$

$$\mu_\Omega = z_0^2 \approx 5.783, \quad \phi_\Omega = \frac{z_0}{J_1(z_0)} J_0(z_0|x|) \quad (\text{Unit Disk}). \quad (2.3.22b)$$

Here J_0 and J_1 are Bessel functions of the first kind, and $z_0 \approx 2.4048$ is the first zero of $J_0(z)$. The bounds $\bar{\lambda}_1$ and $\bar{\lambda}_2$ can be evaluated by substituting (2.3.22) into (2.1.2b). Notice that $\bar{\lambda}_2$ is, in general, determined only up to a numerical quadrature.

In Figure 2.2(a) we plot the saddle-node value λ^* versus α for the slab domain. A similar plot is shown in Figure 2.2(b) for the unit disk. The numerical computations are done using BVP solver COLSYS [2] to solve the boundary value problem $(S)_\lambda$ and Newton's method to determine the saddle-node point. Theorem 2.1.1 guarantees a finite pull-in voltage for any $\alpha > 0$, while λ^* is seen to increase rapidly with α . Therefore, by increasing α , or equivalently by increasing the spatial extent where $f(x) \ll 1$, one can increase the stable operating range of the MEMS capacitor. In Table 2.1 we give numerical results for λ^* , together with the bounds given by Theorem 2.1.1, in the case of exponential permittivity profiles, while Table 2.2 deals with power-law profiles. From Table 2.1, we observe that the bound $\bar{\lambda}_1$ for λ^* is better than $\bar{\lambda}_2$ for small values of α . However, for $\alpha \gg 1$, we can use Laplace's method on the integral defining $\bar{\lambda}_2$ to obtain for the exponential permittivity profile that

$$\bar{\lambda}_1 = \frac{4b_1^2}{27} e^{c_1\alpha}, \quad \bar{\lambda}_2 \sim c_2\alpha^2. \quad (2.3.23)$$

Power-Law Profiles:

Ω	α	$\lambda_c(\alpha)$	λ^*	$\bar{\lambda}_1$	$\bar{\lambda}_2$
slab	0	1.185	1.401	1.462	3.290
slab	1.0	3.556	4.388	∞	9.044
slab	3.0	11.851	15.189	∞	28.247
slab	6.0	33.185	43.087	∞	76.608
unit disk	0	0.593	0.789	0.857	1.928
unit disk	1.0	1.333	1.775	∞	3.019
unit disk	5.0	7.259	9.676	∞	15.82
unit disk	20	71.70	95.66	∞	161.54

Table 2.2: Numerical values for pull-in voltage λ^* with the bounds given in Theorem 2.1.1. Here the power-law permittivity profile is chosen as (2.3.21).

Here $b_1 = \pi^2$, $c_1 = 1/4$, $c_2 = 1/3$ for the slab domain, and $b_1 = z_0^2$, $c_1 = 1$, $c_2 = 4/3$ for the unit disk, where z_0 is the first zero of $J_0(z) = 0$. Therefore, for $\alpha \gg 1$, the bound $\bar{\lambda}_2$ is better than $\bar{\lambda}_1$. A similar calculation can be done for the power-law profile, see Table 2.2. For this case, it is clear that the lower bound $\lambda_c(\alpha)$ in (2.1.4) is better than $\underline{\lambda}$ in (2.1.2a), and the upper bound $\bar{\lambda}_1$ is undefined. However, by using Laplace's method, we readily obtain for $\alpha \gg 1$ that $\bar{\lambda}_2 \sim \alpha^2/3$ for the unit disk and $\bar{\lambda}_2 \sim 4\alpha^2/3$ for the slab domain.

Therefore, what is remarkable is that $\bar{\lambda}_1$ and $\bar{\lambda}_2$ are not comparable even when f is bounded away from 0 and that neither one of them provides the optimal value for λ^* . This leads us to conjecture that there should be a better estimate for λ^* , one involving the distribution of f in Ω , as opposed to the infimum or its average against the first eigenfunction ϕ_Ω .

2.4 The branch of minimal solutions

In the rest of this Chapter, we consider issues of uniqueness and multiplicity of solutions for $(S)_\lambda$ with $0 < \lambda \leq \lambda^*$. The bifurcation diagrams in Figure 2.1 show the complexity of the situation, even in the radially symmetric case. One can see that the number of branches—and of solutions—is closely connected to the space dimension. In this section, we focus on the very first branch of solutions considered to be “minimal”.

The branch of minimal solutions corresponds to the lowest branch in the bifurcation diagram, the one connecting the origin point $\lambda = 0$ to the first fold at $\lambda = \lambda^*$. To analyze further the properties of this branch, we consider for each solution u of $(S)_\lambda$, the operator

$$L_{u,\lambda} = -\Delta - \frac{2\lambda f}{(1-u)^3} \quad (2.4.1)$$

associated with the linearized problem around u . We denote by $\mu_1(\lambda, u)$ the smallest eigenvalue of $L_{u,\lambda}$, that is, the one corresponding to the following Dirichlet eigenvalue problem

$$-\Delta \phi - \frac{2\lambda f(x)}{(1-u)^3} \phi = \mu \phi \quad x \in \Omega, \quad \phi = 0 \quad x \in \partial\Omega. \quad (2.4.2a)$$

In other words,

$$\mu_1(\lambda, u) = \inf_{\phi \in H_0^1(\Omega)} \frac{\int_{\Omega} \{|\nabla \phi|^2 - 2\lambda f(1-u)^{-3} \phi^2\} dx}{\int_{\Omega} \phi^2 dx}.$$

A solution u for $(S)_{\lambda}$ is said to be *stable* (resp., *semi-stable*) if $\mu_1(\lambda, u) > 0$ (resp., $\mu_1(\lambda, u) \geq 0$).

2.4.1 Spectral properties of minimal solutions

We start with the following crucial lemma, which shows among other things that semi-stable solutions are necessarily minimal solutions.

Lemma 2.4.1. *Let f be a function satisfying (2.1.1) on a bounded domain Ω in \mathbb{R}^N , and let $\lambda^* := \lambda^*(\Omega, f)$ be as in Theorem (2.1.1). Suppose u is a positive solution of $(S)_{\lambda}$, and consider any -classical- supersolution v of $(S)_{\lambda}$, that is,*

$$-\Delta v \geq \frac{\lambda f(x)}{(1-v)^2} \quad x \in \Omega, \quad (2.4.3a)$$

$$0 \leq v(x) < 1 \quad x \in \Omega \quad (2.4.3b)$$

$$v = 0 \quad x \in \partial\Omega. \quad (2.4.3c)$$

If $\mu_1(\lambda, u) > 0$, then $v \geq u$ on Ω , and if $\mu_1(\lambda, u) = 0$, then $v = u$ on Ω .

Proof: For a given λ and $x \in \Omega$, use the fact that $f(x) \geq 0$ and that $t \rightarrow \frac{\lambda f(x)}{(1-t)^2}$ is convex on $(0, 1)$, to obtain

$$-\Delta(u + \tau(v - u)) - \frac{\lambda f(x)}{[1 - (u + \tau(v - u))]^2} \geq 0 \quad x \in \Omega, \quad (2.4.4)$$

for $\tau \in [0, 1]$. Note that (2.4.4) is an identity at $\tau = 0$, which means that the first derivative of the left-hand side for (2.4.4) with respect to τ is nonnegative at $\tau = 0$,

$$-\Delta(v - u) - \frac{2\lambda f(x)}{(1-u)^3}(v - u) \geq 0, \quad x \in \Omega, \quad (2.4.5a)$$

$$v - u = 0, \quad x \in \partial\Omega. \quad (2.4.5b)$$

Thus, the maximal principle implies that if $\mu_1(\lambda, u) > 0$, we have $v \geq u$ on Ω , while if $\mu_1(\lambda, u) = 0$, then Lemma 2.16 of [20] gives

$$-\Delta(v - u) - \frac{2\lambda f(x)}{(1-u)^3}(v - u) = 0 \quad x \in \Omega. \quad (2.4.6)$$

In the latter case the second derivative of the left-hand side for (2.4.4) with respect to τ is nonnegative at $\tau = 0$ again,

$$-\frac{6\lambda f(x)}{(1-u)^4}(v - u)^2 \geq 0 \quad x \in \Omega, \quad (2.4.7)$$

From (2.4.7) we deduce that $v \equiv u$ in $\Omega \setminus \Omega_0$, where

$$\Omega_0 = \{x \in \Omega : f(x) = 0 \text{ for } x \in \Omega\}. \quad (2.4.8)$$

On the other hand, (2.4.6) reduces to

$$-\Delta(v - u) = 0 \quad x \in \Omega_0; \quad v - u = 0 \quad x \in \partial\Omega_0,$$

which implies $v \equiv u$ on Ω_0 . Hence if $\mu_1(\lambda, u) = 0$ then $v \equiv u$ on Ω , which completes the proof of Lemma 2.4.1. \blacksquare

Theorem 2.4.2. *Assume f is a function satisfying (2.1.1) on a bounded domain Ω in \mathbb{R}^N , and consider the branch $\lambda \rightarrow u_\lambda$ of minimal solutions on $(0, \lambda^*)$. Then the following hold:*

1. *For each $x \in \Omega$, the function $\lambda \rightarrow u_\lambda(x)$ is differentiable and strictly increasing on $(0, \lambda^*)$.*
2. *For each $\lambda \in (0, \lambda^*)$, the minimal solution u_λ is stable and the function $\lambda \rightarrow \mu_{1,\lambda} := \mu_1(\lambda, u_\lambda)$ is decreasing on $(0, \lambda^*)$.*

Proof: Consider $\lambda_1 < \lambda_2 < \lambda^*$, their corresponding minimal positive solutions u_{λ_1} and u_{λ_2} and let u^* be a positive solution for $(S)_{\lambda_2}$. For the monotone increasing series $\{u_n(\lambda_1; x)\}$ defined in (2.2.10), we then have $u^* > u_0(\lambda_1; x) \equiv 0$, and if $u_{n-1}(\lambda_1; x) \leq u^*$ in Ω , then

$$\begin{aligned} -\Delta(u^* - u_n) &= f(x) \left[\frac{\lambda_2}{(1 - u^*)^2} - \frac{\lambda_1}{(1 - u_{n-1})^2} \right] \geq 0, \quad x \in \Omega \\ u^* - u_n &= 0, \quad x \in \partial\Omega. \end{aligned}$$

So we have $u_n(\lambda_1; x) \leq u^*$ in Ω . Therefore, $u_{\lambda_1} = \lim_{n \rightarrow \infty} u_n(\lambda_1; x) \leq u^*$ in Ω , and in particular $u_{\lambda_1} \leq u_{\lambda_2}$ in Ω . Therefore, $\frac{du_\lambda(x)}{d\lambda} \geq 0$ for all $x \in \Omega$.

That $\lambda \rightarrow \mu_{1,\lambda}$ is decreasing follows easily from the variational characterization of $\mu_{1,\lambda}$, the monotonicity of $\lambda \rightarrow u_\lambda$, as well as the monotonicity of $(1 - u)^{-3}$ with respect to u .

Now we define

$$\lambda^{**} = \sup \{ \lambda; u_\lambda \text{ is a stable solution for } (S)_\lambda \}.$$

It is clear that $\lambda^{**} \leq \lambda^*$, and to show the equality, it suffices to prove that there is no minimal solution for $(S)_\mu$ with $\mu > \lambda^{**}$. For that, suppose w is a minimal solution of $(S)_{\lambda^{**} + \delta}$ with $\delta > 0$, then we would have for $\lambda \leq \lambda^{**}$,

$$-\Delta w = \frac{(\lambda^{**} + \delta)f(x)}{(1 - w)^2} \geq \frac{\lambda f(x)}{(1 - w)^2} \quad x \in \Omega.$$

Since for $0 < \lambda < \lambda^{**}$ the minimal solutions u_λ are stable, it follows from Lemma 2.4.1 that $1 > w \geq u_\lambda$ for all $0 < \lambda < \lambda^{**}$. Consequently, $\underline{u} = \lim_{\lambda \nearrow \lambda^{**}} u_\lambda$ exists in $C^1(\Omega)$ and is a solution for $(S)_{\lambda^{**}}$. Now from the definition of λ^{**} , we necessarily have $\mu_{1,\lambda^{**}} = 0$, hence by again applying Lemma 2.4.1, we obtain that $w \equiv \underline{u}$ and $\delta = 0$ on Ω , which is a contradiction, and hence $\lambda^{**} = \lambda^*$.

Since each u_λ is stable, then by setting $F(\lambda, u_\lambda) := -\Delta - \frac{\lambda f}{(1 - u_\lambda)^2}$, we get that $F_{u_\lambda}(\lambda, u_\lambda)$ is invertible for $0 < \lambda < \lambda^*$. It then follows from the implicit function theorem that $u_\lambda(x)$ is differentiable with respect to λ .

Finally, by differentiating $(S)_\lambda$ with respect to λ , and since $\lambda \rightarrow u_\lambda(x)$ is non-decreasing, we get

$$\begin{aligned} -\Delta \frac{du_\lambda}{d\lambda} - \frac{2\lambda f(x)}{(1 - u_\lambda)^3} \frac{du_\lambda}{d\lambda} &= \frac{f(x)}{(1 - u_\lambda)^2} \geq 0, \quad x \in \Omega \\ \frac{du_\lambda}{d\lambda} &\geq 0, \quad x \in \partial\Omega. \end{aligned}$$

Applying the strong maximum principle, we conclude that $\frac{du_\lambda}{d\lambda} > 0$ on Ω for all $0 < \lambda < \lambda^*$, and the theorem is proved. \blacksquare

Remark 2.4.1. Lemma 3 of [20] yields $\mu_1(1, 0)$ as an upper bound for λ^{**} – at least in the case where $\inf_\Omega f > 0$ on Ω . Since $\lambda^{**} = \lambda^*$, this gives another upper bound for λ^* in our setting. It is worth noting that the upper bound in Theorem 2.1.1 gives a better estimate, since in the case where $f \equiv 1$, we have $\mu(1, 0) = \mu_\Omega/2$, while the estimate in Theorem 2.1.1 gives $\frac{4\mu_\Omega}{27}$ for an upper bound.

2.4.2 Energy estimates and regularity

We start with the following easy observations.

Lemma 2.4.3. *Let f be a function satisfying (2.1.1) on a bounded domain Ω in \mathbb{R}^N . Then,*

1. *Any (weak) solution u in $H_0^1(\Omega)$ of $(S)_\lambda$ then satisfies $\int_\Omega \frac{f}{(1-u)^2} dx < \infty$.*
2. *If $\inf_\Omega f > 0$ and $N \geq 3$, then any solution u such that $f/(1-u) \in L^{3N/2}(\Omega)$ is a classical solution.*

Proof: (1) Since $u \in H_0^1(\Omega)$ is a positive solution of $(S)_\lambda$, we have

$$\int_\Omega \frac{\lambda f}{(1-u)^2} - \int_\Omega \frac{\lambda f}{1-u} = \int_\Omega \frac{\lambda u f}{(1-u)^2} = \int_\Omega |\nabla u|^2 =: C < +\infty,$$

which implies that

$$\int_\Omega \frac{\lambda f}{(1-u)^2} \leq C + \int_\Omega \frac{\lambda f}{1-u} \leq C + \int_\Omega [C\varepsilon \frac{\lambda f}{(1-u)^2} + \frac{C}{\varepsilon} f] \leq C + C\varepsilon \int_\Omega \frac{\lambda f}{(1-u)^2}$$

with $\varepsilon > 0$. Therefore, by choosing $\varepsilon > 0$ small enough, we conclude that $\int_\Omega \frac{f}{(1-u)^2} < \infty$.

(2) Suppose u is a weak solution such that $\frac{f(x)}{(1-u)^3} \in L^p(\Omega)$, which means that $\frac{f(x)}{(1-u)^2} \in L^{3p/2}(\Omega)$. By Sobolev's theorem we can already deduce that $u \in C^{0,\alpha}(\Omega)$ with $\alpha = 2 - \frac{2N}{3p}$. To get more regularity, it suffices to show that $u < 1$ on Ω , but then if not we consider $x_0 \in \bar{\Omega}$ such that $u(x_0) = \|u\|_{C(\bar{\Omega})} = 1$, then we have

$$|1 - u(x)| = |u(x_0) - u(x)| \leq C|x_0 - x|^\alpha \quad \text{on } \bar{\Omega}.$$

This inequality shows that if $p \geq \frac{N}{2}$ then we have

$$\infty > \int_\Omega \left(\frac{f(x)}{(1-u)^3}\right)^p dx \geq C' \int_\Omega |x - x_0|^{-3p\alpha} dx = C' \int_\Omega |x - x_0|^{-N} dx = \infty,$$

a contradiction, which implies that we must have $\|u\|_{C(\bar{\Omega})} < 1$. \blacksquare

Note that the above argument cannot be applied to the case where $f(x) \geq 0$ vanishes on Ω , and therefore we have to use the iterative scheme outlined in the next theorem.

Theorem 2.4.4. *Let f be a function satisfying (2.1.1) on a bounded domain Ω in \mathbb{R}^N . Then for any constant $C > 0$ there exists $0 < K(C, N) < 1$ such that a positive weak solution u of $(S)_\lambda$ ($0 < \lambda < \lambda^*$) is a classical solution and $\|u\|_{C(\bar{\Omega})} \leq K(C, N)$ provided*

1. $N = 1$ and $\|\frac{f}{(1-u)^3}\|_{L^1(\Omega)} \leq C$,
2. $N \geq 2$ and $\|\frac{f}{(1-u)^3}\|_{L^{N/2}(\Omega)} \leq C$.

Proof: We prove this theorem by considering the following three cases separately:

(1) If $N = 1$, then for any $I > 0$ we write using the Sobolev inequality with constant $K(1) > 0$,

$$\begin{aligned}
 & K(1) \|(1-u)^{-1} - 1\|_{L^\infty}^2 \\
 & \leq \int_{\Omega} |\nabla[(1-u)^{-1} - 1]|^2 \\
 & = \frac{1}{3} \int_{\Omega} \nabla u \cdot \nabla[(1-u)^{-3} - 1] \\
 & = \frac{\lambda}{3} \int_{\Omega} f(1-u)^{-2}[(1-u)^{-3} - 1] \\
 & \leq CI + C \int_{\{(1-u)^{-3} \geq I\}} 8f(1-u)^{-2} \\
 & \quad + C \int_{\{(1-u)^{-3} \geq I\}} f[(1-u)^{-3} + 2(1-u)^{-2} + 4(1-u)^{-1}] [(1-u)^{-1} - 1]^2 \\
 & \leq CI + C + C \|(1-u)^{-1} - 1\|_{L^\infty(\{(1-u)^{-3} \geq I\})}^2 \int_{\{(1-u)^{-3} \geq I\}} \frac{f}{(1-u)^3} \\
 & \leq CI + C + C\varepsilon(I) \|(1-u)^{-1} - 1\|_{L^\infty}^2,
 \end{aligned} \tag{2.4.9}$$

with $\varepsilon(I) = \int_{\{(1-u)^{-3} \geq I\}} \frac{f}{(1-u)^3}$, where Lemma 2.4.3(1) is applied in the second inequality. From the assumption $f/(1-u)^3 \in L^1(\Omega)$, we have $\varepsilon(I) \rightarrow 0$ as $I \rightarrow \infty$. We now choose I such that $\varepsilon(I) \leq \frac{K(1)}{2C}$, so that the above estimates imply that $\|(1-u)^{-1} - 1\|_{L^\infty} < K(C)$. Standard regularity theory for elliptic problems now implies that $1/(1-u) \in C^{2,\alpha}(\Omega)$. Therefore, u is classical, and there exists a constant $K(C, N)$ which can be taken strictly less than 1 such that $\|u\|_{C(\bar{\Omega})} \leq K(C, N) < 1$.

(2) Assuming $N = 2$, we need to show that

$$(1-u)^{-1} \in L^p(\Omega) \text{ for any } p > 1. \tag{2.4.10}$$

Fix $p > 1$ and let us introduce $T_k u = \min\{u, 1-k\}$, the truncated function of u at level $1-k$, $0 < k < 1$. For k small, we take $(1 - T_k u)^{-1} - 1 \in H_0^1(\Omega)$ as a test function for $(S)_\lambda$:

$$\int_{\Omega} \frac{|\nabla T_k u|^2}{(1 - T_k u)^2} = \int_{\Omega} \frac{\lambda f(x)}{(1-u)^2} ((1 - T_k u)^{-1} - 1) \leq \int_{\Omega} \frac{\lambda f(x)}{|1-u|^3} \leq C < +\infty \tag{2.4.11}$$

Note that the classical consequence of the Moser-Trudinger inequality gives: there exists $C > 0$ so that

$$\int_{\Omega} e^{pv} \leq C \exp\left(\frac{p^2}{16\pi} \|v\|_{H_0^1(\Omega)}^2\right) \quad \forall v \in H_0^1(\Omega), \quad p > 1. \quad (2.4.12)$$

Since now $\log\left(\frac{1}{1-T_k u}\right) \in H_0^1(\Omega)$, (2.4.12) and (2.4.11) now yield that for any $p > 1$:

$$\int_{\Omega} (1 - T_k u)^{-p} \leq C_1 \exp\left(\frac{p^2}{16\pi} \int_{\Omega} |\nabla \log\left(\frac{1}{1-T_k u}\right)|^2\right) \leq C_2$$

where C_1, C_2 denote positive constants depending only on p and C . Taking the limit as $k \rightarrow 0$ and using that $u \leq 1$, we get the validity of (2.4.10).

(3) The case when $N > 2$ is more elaborate, and we first show that $(1-u)^{-1} \in L^q(\Omega)$ for all $q \in (1, \infty)$. Since $u \in H_0^1(\Omega)$ is a solution of $(S)_{\lambda}$, we already have $\int_{\Omega} \frac{f}{(1-u)^2} < C$. Now we proceed by iteration to show that if $\int_{\Omega} \frac{f}{(1-u)^{2+2\theta}} < C$ for some $\theta \geq 0$, then $\int_{\Omega} \frac{1}{(1-u)^{2^*(1+\theta)}} < C$ with $2^* = \frac{2N}{N-2}$.

Indeed, for any constant $\theta \geq 0$ and $\ell > 0$ we choose a test function $\phi = [(1-u)^{-3} - 1] \min\{(1-u)^{-2\theta}, \ell^2\}$. By applying this test function to both sides of $(S)_{\lambda}$, we have

$$\begin{aligned} & \lambda \int_{\Omega} f(1-u)^{-2} [(1-u)^{-3} - 1] \min\{(1-u)^{-2\theta}, \ell^2\} \\ &= \int_{\Omega} \nabla u \cdot \nabla [((1-u)^{-3} - 1) \min\{(1-u)^{-2\theta}, \ell^2\}] \\ &= 3 \int_{\Omega} |\nabla u|^2 (1-u)^{-4} \min\{(1-u)^{-2\theta}, \ell^2\} \\ &+ 2\theta \int_{\{(1-u)^{-\theta} \leq \ell\}} |\nabla u|^2 (1-u)^{-2\theta-1} [(1-u)^{-3} - 1]. \end{aligned} \quad (2.4.13)$$

We now suppose $\int_{\Omega} \frac{f}{(1-u)^{2+2\theta}} < C$. We then obtain from (2.4.13) and the fact that $\frac{1}{(1-u)^5} \leq C_I \frac{1}{(1-u)^3} \left(\frac{1}{1-u} - 1\right)^2$ whenever $(1-u)^{-3} \geq I > 1$ that:

$$\begin{aligned}
 & \int_{\Omega} |\nabla[(1-u)^{-1} - 1] \min\{(1-u)^{-\theta}, \ell\}|^2 \\
 & \leq 2 \int_{\Omega} |\nabla u|^2 (1-u)^{-4} \min\{(1-u)^{-2\theta}, \ell^2\} \\
 & \quad + 2\theta^2 \int_{\{(1-u)^{-\theta} \leq \ell\}} |\nabla u|^2 (1-u)^{-2\theta-2} [(1-u)^{-1} - 1]^2 \\
 & = 2 \int_{\Omega} |\nabla u|^2 (1-u)^{-4} \min\{(1-u)^{-2\theta}, \ell^2\} \\
 & \quad + 2\theta^2 \int_{\{(1-u)^{-\theta} \leq \ell\}} |\nabla u|^2 (1-u)^{-2\theta-1} \left[\frac{1}{(1-u)^3} + \frac{1}{1-u} - \frac{2}{(1-u)^2} \right] \\
 & \leq C\lambda \int_{\Omega} f(1-u)^{-2} [(1-u)^{-3} - 1] \min\{(1-u)^{-2\theta}, \ell^2\} \\
 & \leq C\lambda \int_{\Omega} f(1-u)^{-5} \min\{(1-u)^{-2\theta}, \ell^2\} \\
 & \leq CI + C \int_{\{(1-u)^{-3} \geq I\}} f(1-u)^{-5} \min\{(1-u)^{-2\theta}, \ell^2\} \\
 & \leq CI + C \int_{\{(1-u)^{-3} \geq I\}} f(1-u)^{-3} [(1-u)^{-1} - 1]^2 \min\{(1-u)^{-2\theta}, \ell^2\} \\
 & \leq CI + C \left[\int_{\{(1-u)^{-3} \geq I\}} \left(\frac{f}{(1-u)^3} \right)^{\frac{N}{2}} \right]^{\frac{2}{N}} \\
 & \quad \times \left[\int_{\{(1-u)^{-3} \geq I\}} \left([(1-u)^{-1} - 1] \min\{(1-u)^{-\theta}, \ell\} \right)^{\frac{2N}{N-2}} \right]^{\frac{N-2}{N}} \\
 & \leq CI + C\varepsilon(I) \int_{\Omega} |\nabla[(1-u)^{-1} - 1] \min\{(1-u)^{-\theta}, \ell\}|^2
 \end{aligned} \tag{2.4.14}$$

with

$$\varepsilon(I) = \left[\int_{\{(1-u)^{-3} \geq I\}} \left(\frac{f}{(1-u)^3} \right)^{\frac{N}{2}} \right]^{\frac{2}{N}}.$$

From the assumption $f/(1-u)^3 \in L^{\frac{N}{2}}(\Omega)$ we have $\varepsilon(I) \rightarrow 0$ as $I \rightarrow \infty$. We now choose I such that $\varepsilon(I) = \frac{1}{2C}$, and the above estimates imply that

$$\int_{\{(1-u)^{-\theta} \leq \ell\}} |\nabla[(1-u)^{-\theta-1} - (1-u)^{-\theta}]|^2 \leq CI,$$

where the bound is uniform with respect to ℓ . This estimate leads to

$$\begin{aligned} \frac{1}{(\theta+1)^2} \int_{\{(1-u)^{-\theta} \leq \ell\}} |\nabla[(1-u)^{-\theta-1}]|^2 &= \int_{\{(1-u)^{-\theta} \leq \ell\}} (1-u)^{-2\theta-4} |\nabla u|^2 \\ &\leq CI + C \int_{\{(1-u)^{-\theta} \leq \ell\}} (1-u)^{-2\theta-3} |\nabla u|^2 \\ &\leq CI + \int_{\{(1-u)^{-\theta} \leq \ell\}} [C\varepsilon(1-u)^{-2\theta-4} + C/\varepsilon] |\nabla u|^2 \\ &\leq CI + C/\varepsilon + C\varepsilon \int_{\{(1-u)^{-\theta} \leq \ell\}} (1-u)^{-2\theta-4} |\nabla u|^2 \end{aligned}$$

with $\varepsilon > 0$. This means that for $\varepsilon > 0$ sufficiently small

$$\int_{\{(1-u)^{-\theta} \leq \ell\}} |\nabla(1-u)^{-\theta-1}|^2 = \int_{\{(1-u)^{-\theta} \leq \ell\}} (\theta+1)^2 (1-u)^{-2\theta-4} |\nabla u|^2 < C.$$

Thus we can let $\ell \rightarrow \infty$ and we get that $(1-u)^{-\theta-1} \in H^1(\Omega) \hookrightarrow L^{2^*}(\Omega)$, which means that $\int_{\Omega} \frac{1}{(1-u)^{2^*(\theta+1)}} < C$.

By iterating the above argument for $\theta_i + 1 = \frac{N}{N-2}(\theta_{i-1} + 1)$ for $i \geq 1$ and starting with $\theta_0 = 0$, we find that $1/(1-u) \in L^q(\Omega)$ for all $q \in (1, \infty)$.

Standard regularity theory for elliptic problems applies again to give that $1/(1-u) \in C^{2,\alpha}(\Omega)$. Therefore, u is a classical solution and there exists a constant $0 < K(C, N) < 1$ such that $\|u\|_{C(\Omega)} \leq K(C, N) < 1$. This completes the proof of Theorem 2.4.4. \blacksquare

Theorem 2.4.5. *For any dimension $1 \leq N \leq 7$ there exists a constant $0 < C(N) < 1$ independent of λ such that for any $0 < \lambda < \lambda^*$ the minimal solution u_λ satisfies $\|u_\lambda\|_{C(\Omega)} \leq C(N)$.*

Consequently, $u^ = \lim_{\lambda \uparrow \lambda^*} u_\lambda$ exists in the topology of $C^{2,\alpha}(\bar{\Omega})$ with $0 < \alpha < 1$. It is the unique classical solution for $(S)_{\lambda^*}$ and satisfies $\mu_{1,\lambda^*}(u^*) = 0$.*

This result will follow from the following uniform energy estimate on the minimal solutions u_λ .

Proposition 2.4.6. *There exists a constant $C(p) > 0$ such that for each $\lambda \in (0, \lambda^*)$, the minimal solution u_λ satisfies $\|\frac{f}{(1-u_\lambda)^3}\|_{L^p(\Omega)} \leq C(p)$ as long as $p < 1 + \frac{4}{3} + 2\sqrt{\frac{2}{3}}$.*

Proof: Since minimal solutions are stable, we have

$$\lambda \int_{\Omega} \frac{2f(x)}{(1-u_\lambda)^3} w^2 dx \leq - \int_{\Omega} w \Delta w dx = \int_{\Omega} |\nabla w|^2 dx \quad (2.4.15)$$

for all $0 < \lambda < \lambda^*$ and nonnegative $w \in H_0^1(\bar{\Omega})$. Setting

$$w = (1-u_\lambda)^i - 1 > 0, \quad \text{where} \quad -2 - \sqrt{6} < i < 0, \quad (2.4.16)$$

then (2.4.15) becomes

$$i^2 \int_{\Omega} (1-u_\lambda)^{2i-2} |\nabla u_\lambda|^2 dx \geq \lambda \int_{\Omega} \frac{2[1 - (1-u_\lambda)^i]^2 f(x)}{(1-u_\lambda)^3} dx. \quad (2.4.17)$$

On the other hand, multiplying $(S)_\lambda$ by $\frac{i^2}{1-2i}[(1-u_\lambda)^{2i-1} - 1]$ and applying integration by parts yield that

$$i^2 \int_{\Omega} (1-u_\lambda)^{2i-2} |\nabla u_\lambda|^2 dx = \lambda \frac{i^2}{2i-1} \int_{\Omega} \frac{[1-(1-u_\lambda)^{2i-1}]f(x)}{(1-u_\lambda)^2} dx. \quad (2.4.18)$$

Hence (2.4.17) and (2.4.18) reduce to

$$\begin{aligned} & \frac{\lambda i^2}{2i-1} \int_{\Omega} \frac{f(x)}{(1-u_\lambda)^2} dx - 2\lambda \int_{\Omega} \frac{f(x)}{(1-u_\lambda)^3} dx + 4\lambda \int_{\Omega} \frac{f(x)}{(1-u_\lambda)^{3-i}} dx \\ & \geq \lambda \left(2 + \frac{i^2}{2i-1}\right) \int_{\Omega} \frac{f(x)}{(1-u_\lambda)^{3-2i}} dx. \end{aligned} \quad (2.4.19)$$

From the choice of i in (2.4.16) we have $2 + \frac{i^2}{2i-1} > 0$. So (2.4.19) implies that

$$\begin{aligned} \int_{\Omega} \frac{f(x)}{(1-u_\lambda)^{3-2i}} dx & \leq C \int_{\Omega} \frac{f(x)}{(1-u_\lambda)^{3-i}} dx \\ & \leq C \left(\int_{\Omega} \left| \frac{f^{\frac{3-i}{3-2i}}}{(1-u_\lambda)^{\frac{3-2i}{3-i}}} \right|^{\frac{3-2i}{3-i}} dx \right)^{\frac{3-i}{3-2i}} \cdot \left(\int_{\Omega} \left| f^{\frac{-i}{3-2i}} \right|^{\frac{3-2i}{-i}} dx \right)^{\frac{-i}{3-2i}} \\ & \leq C \left(\int_{\Omega} \frac{f(x)}{(1-u_\lambda)^{3-2i}} dx \right)^{\frac{3-i}{3-2i}}, \end{aligned} \quad (2.4.20)$$

where Hölder's inequality is applied. From the above we deduce that

$$\int_{\Omega} \frac{f(x)}{(1-u_\lambda)^{3-2i}} dx \leq C. \quad (2.4.21)$$

Further we have

$$\begin{aligned} \int_{\Omega} \left| \frac{f(x)}{(1-u_\lambda)^3} \right|^{\frac{3-2i}{3}} dx & = \int_{\Omega} f^{\frac{-2i}{3}} \cdot \frac{f}{(1-u_\lambda)^{3-2i}} dx \\ & \leq C \int_{\Omega} \frac{f}{(1-u_\lambda)^{3-2i}} dx \leq C. \end{aligned} \quad (2.4.22)$$

Therefore, we get that

$$\left\| \frac{f(x)}{(1-u_\lambda)^3} \right\|_{L^p} \leq C, \quad (2.4.23a)$$

where -in view of (2.4.16)-

$$p = \frac{3-2i}{3} \leq 1 + \frac{4}{3} + 2\sqrt{\frac{2}{3}}. \quad (2.4.23b)$$

■

Proof of Theorem 2.4.5: The existence of u^* as a classical solution follows from Proposition 2.4.6 and Theorem 2.4.4, as long as $\frac{N}{2} < 1 + \frac{4}{3} + 2\sqrt{\frac{2}{3}}$, which happens when $N \leq 7$.

Since $\mu_{1,\lambda} > 0$ on the minimal branch for any $\lambda < \lambda^*$, we have the limit $\mu_{1,\lambda^*} \geq 0$. If now $\mu_{1,\lambda^*} > 0$ the implicit function theorem could be applied to the operator $L_{u_{\lambda^*}, \lambda^*}$, and would allow the continuation of the minimal branch $\lambda \mapsto u_\lambda$ of classical solutions beyond λ^* , which is a contradiction, and hence $\mu_{1,\lambda^*} = 0$. The uniqueness in the class of classical solutions then follows from Lemma 2.4.1. ■

2.5 Uniqueness and multiplicity of solutions

The purpose of this section is to discuss uniqueness and multiplicity of solutions for $(S)_\lambda$.

2.5.1 Uniqueness of the solution at $\lambda = \lambda^*$

We first note that in view of the monotonicity in λ and the uniform boundedness of the first branch of solutions, the extremal function defined by $u^*(x) = \lim_{\lambda \uparrow \lambda^*} u_\lambda(x)$ always exists, and can always be considered as a solution for $(S)_{\lambda^*}$ in a generalized sense. Now if there exists $0 < C < 1$ such that $\|u_\lambda\|_{C(\bar{\Omega})} \leq C$ for each $\lambda < \lambda^*$ —just like in the case where $1 \leq N \leq 7$ —then we have seen in Theorem 2.4.5 that u^* is unique among the classical solutions. In the sequel, we tackle the important case when u^* is a weak solution (i.e., in $H_0^1(\Omega)$) of $(S)_{\lambda^*}$ but with the possibility that $\|u^*\|_\infty = 1$. Here and in the sequel, u will be called a $H_0^1(\Omega)$ -weak solution of $(S)_\lambda$ if $0 \leq u \leq 1$ a.e. while u solves $(S)_\lambda$ in the weak sense of $H_0^1(\Omega)$.

We shall borrow ideas from [10, 14], where the authors deal with the case of regular nonlinearities. However, unlike those papers where solutions are considered in a very weak sense, we consider here a more focussed and much simpler situation. We establish the following useful characterization of the extremal solution.

Theorem 2.5.1. *Assume f is a function satisfying (2.1.1) on a bounded domain Ω in \mathbb{R}^N . For $\lambda > 0$, consider $u \in H_0^1(\Omega)$ to be a weak solution of $(S)_\lambda$ (in the $H_0^1(\Omega)$ sense) such that $\|u\|_{L^\infty(\Omega)} = 1$. Then the following assertions are equivalent:*

1. $\mu_{1,\lambda} \geq 0$, that is u satisfies

$$\int_{\Omega} |\nabla \phi|^2 \geq \int_{\Omega} \frac{2\lambda f(x)}{(1-u)^3} \phi^2 \quad \forall \phi \in H_0^1(\Omega), \quad (2.5.1)$$

2. $\lambda = \lambda^*$ and $u = u^*$.

We need the following uniqueness result.

Proposition 2.5.2. *Assume f is a function satisfying (2.1.1) on a bounded domain Ω in \mathbb{R}^N . Let u_1, u_2 be two $H_0^1(\Omega)$ -weak solutions of $(S)_\lambda$ so that $\mu_{1,\lambda}(u_i) \geq 0$ for $i = 1, 2$. Then $u_1 = u_2$ almost everywhere in Ω .*

Proof: For any $\theta \in [0, 1]$ and $\phi \in H_0^1(\Omega)$, $\phi \geq 0$, we have that

$$\begin{aligned} I_{\theta,\phi} &:= \int_{\Omega} \nabla(\theta u_1 + (1-\theta)u_2) \nabla \phi - \int_{\Omega} \frac{\lambda f(x)}{(1-\theta u_1 - (1-\theta)u_2)^2} \phi \\ &= \lambda \int_{\Omega} f(x) \left(\frac{\theta}{(1-u_1)^2} + \frac{1-\theta}{(1-u_2)^2} - \frac{1}{(1-\theta u_1 - (1-\theta)u_2)^2} \right) \phi \geq 0 \end{aligned}$$

due to the convexity of $1/(1-u)^2$ with respect to u . Since $I_{0,\phi} = I_{1,\phi} = 0$, the derivative of $I_{\theta,\phi}$ at $\theta = 0, 1$ provides

$$\begin{aligned} \int_{\Omega} \nabla(u_1 - u_2) \nabla \phi - \int_{\Omega} \frac{2\lambda f(x)}{(1-u_2)^3} (u_1 - u_2) \phi &\geq 0, \\ \int_{\Omega} \nabla(u_1 - u_2) \nabla \phi - \int_{\Omega} \frac{2\lambda f(x)}{(1-u_1)^3} (u_1 - u_2) \phi &\leq 0 \end{aligned}$$

for any $\phi \in H_0^1(\Omega)$, $\phi \geq 0$. Testing the first inequality on $\phi = (u_1 - u_2)^-$ and the second one on $(u_1 - u_2)^+$, we get that

$$\begin{aligned} \int_{\Omega} \left[|\nabla(u_1 - u_2)^-|^2 - \frac{2\lambda f(x)}{(1 - u_2)^3} ((u_1 - u_2)^-)^2 \right] &\leq 0, \\ \int_{\Omega} \left[|\nabla(u_1 - u_2)^+|^2 - \frac{2\lambda f(x)}{(1 - u_1)^3} ((u_1 - u_2)^+)^2 \right] &\leq 0. \end{aligned}$$

Since $\mu_{1,\lambda}(u_1) \geq 0$, we have

- 1) either $\mu_{1,\lambda}(u_1) > 0$ and then $u_1 \leq u_2$ a.e.,
- 2) or $\mu_{1,\lambda}(u_1) = 0$, which then gives

$$\int_{\Omega} \nabla(u_1 - u_2) \nabla \bar{\phi} - \int_{\Omega} \frac{2\lambda f(x)}{(1 - u_1)^3} (u_1 - u_2) \bar{\phi} = 0 \quad (2.5.2)$$

where $\bar{\phi} = (u_1 - u_2)^+$. Since $I_{\theta, \bar{\phi}} \geq 0$ for any $\theta \in [0, 1]$ and $I_{1, \bar{\phi}} = \partial_{\theta} I_{1, \bar{\phi}} = 0$, we get that:

$$\partial_{\theta\theta}^2 I_{1, \bar{\phi}} = - \int_{\Omega} \frac{6\lambda f(x)}{(1 - u_1)^4} ((u_1 - u_2)^+)^3 \geq 0.$$

Let $Z_0 = \{x \in \Omega : f(x) = 0\}$. Clearly, $(u_1 - u_2)^+ = 0$ a.e. in $\Omega \setminus Z_0$ and, by (2.5.2) we get:

$$\int_{\Omega} |\nabla(u_1 - u_2)^+|^2 = 0.$$

Hence, $u_1 \leq u_2$ a.e. in Ω . The same argument applies to prove the reversed inequality: $u_2 \leq u_1$ a.e. in Ω . Therefore, $u_1 = u_2$ a.e. in Ω , and the proof is complete. \blacksquare

Since $\|u_{\lambda}\| < 1$ for any $\lambda \in (0, \lambda^*)$, we need—in order to prove Theorem 2.5.1—only to show that $(S)_{\lambda}$ does not have any $H_0^1(\Omega)$ -weak solution for $\lambda > \lambda^*$. By the definition of λ^* , this is already true for classical solutions. We shall now extend this property to the class of weak solutions by means of the following result.

Proposition 2.5.3. *If w is a $H_0^1(\Omega)$ -weak solution of $(S)_{\lambda}$, then for any $\varepsilon \in (0, 1)$ there exists a classic solution w_{ε} of $(S)_{\lambda(1-\varepsilon)}$.*

Proof: First we prove that for any $\psi \in C^2([0, 1])$ concave function so that $\psi(0) = 0$, we have that

$$\int_{\Omega} \nabla \psi(w) \nabla \varphi \geq \int_{\Omega} \frac{\lambda f}{(1 - w)^2} \psi(w) \varphi \quad (2.5.3)$$

for any $\varphi \in H_0^1(\Omega)$, $\varphi \geq 0$. Indeed, by concavity of ψ we get:

$$\begin{aligned} \int_{\Omega} \nabla \psi(w) \nabla \varphi &= \int_{\Omega} \dot{\psi}(w) \nabla w \nabla \varphi = \int_{\Omega} \nabla w \nabla (\psi(w) \varphi) - \int_{\Omega} \ddot{\psi}(w) \varphi |\nabla w|^2 \\ &\geq \int_{\Omega} \frac{\lambda f(x)}{(1 - w)^2} \psi(w) \varphi \end{aligned}$$

for any $\varphi \in C_0^{\infty}(\Omega)$, $\varphi \geq 0$. By density, we get (2.5.3).

Now let $\varepsilon \in (0, 1)$, and define

$$\psi_\varepsilon(w) := 1 - \left(\varepsilon + (1 - \varepsilon)(1 - w)^3 \right)^{\frac{1}{3}}, \quad 0 \leq w \leq 1.$$

Since $\psi_\varepsilon \in C^2([0, 1])$ is a concave function, $\psi_\varepsilon(0) = 0$ and

$$\dot{\psi}_\varepsilon(w) = (1 - \varepsilon) \frac{g(\psi_\varepsilon(w))}{g(w)}, \quad g(s) := (1 - s)^{-2},$$

by (2.5.3) we obtain that for any $\varphi \in H_0^1(\Omega)$, $\varphi \geq 0$:

$$\begin{aligned} \int_\Omega \nabla \psi_\varepsilon(w) \nabla \varphi &\geq \int_\Omega \frac{\lambda f(x)}{(1 - w)^2} \dot{\psi}_\varepsilon(w) \varphi = \lambda(1 - \varepsilon) \int_\Omega f(x) g(\psi_\varepsilon(w)) \varphi \\ &= \int_\Omega \frac{\lambda(1 - \varepsilon) f(x)}{(1 - \psi_\varepsilon(w))^2} \varphi. \end{aligned}$$

Hence, $\psi_\varepsilon(w)$ is a $H_0^1(\Omega)$ -weak supersolution of $(S)_{\lambda(1-\varepsilon)}$ so that $0 \leq \psi_\varepsilon(w) \leq 1 - \varepsilon^{\frac{1}{3}} < 1$. Since 0 is a subsolution for any $\lambda > 0$, we get the existence of a $H_0^1(\Omega)$ -weak solution w_ε of $(S)_{\lambda(1-\varepsilon)}$ so that $0 \leq w_\varepsilon \leq 1 - \varepsilon^{\frac{1}{3}}$. By standard elliptic regularity theory, w_ε is a classical solution of $(S)_{\lambda(1-\varepsilon)}$. \blacksquare

2.5.2 Uniqueness of low energy solutions for small voltage

In the following we focus on the uniqueness when λ is small enough. We first define nonminimal solutions for $(S)_\lambda$ as follows.

Definition 2.5.1. A solution $0 \leq u < 1$ is said to be a nonminimal positive solution of $(S)_\lambda$, if there exists another positive solution v of $(S)_\lambda$ and a point $x \in \Omega$ such that $u(x) > v(x)$.

Lemma 2.5.4. Suppose u is a nonminimal solution of $(S)_\lambda$ with $\lambda \in (0, \lambda^*)$. Then $\mu_1(\lambda, u) < 0$, and the function $w = u - u_\lambda$ is in the negative space of $L_{u,\lambda} = -\Delta - \frac{2\lambda f(x)}{(1-u)^3}$.

Proof: For a fixed $\lambda \in (0, \lambda^*)$, let u_λ be the minimal solution of $(S)_\lambda$. We have $w = u - u_\lambda \geq 0$ in Ω , and

$$-\Delta w - \frac{\lambda(2 - u - u_\lambda)f}{(1 - u)^2(1 - u_\lambda)^2} w = 0 \quad \text{in } \Omega.$$

Hence the strong maximum principle yields that $u_\lambda < u$ in Ω .

Let $\Omega_0 = \{x \in \Omega : f(x) = 0\}$ and $\Omega/\Omega_0 = \{x \in \Omega : f(x) > 0\}$. Direct calculations give that

$$\begin{aligned} &-\Delta(u - u_\lambda) - \frac{2\lambda f}{(1 - u)^3}(u - u_\lambda) \\ &= \lambda f \left[\frac{1}{(1 - u)^2} - \frac{1}{(1 - u_\lambda)^2} - \frac{2}{(1 - u)^3}(u - u_\lambda) \right] = \begin{cases} 0, & x \in \Omega_0; \\ < 0, & x \in \Omega/\Omega_0. \end{cases} \end{aligned} \quad (2.5.4)$$

From this we get

$$\langle L_{u,\lambda} w, w \rangle = \lambda \int_{\Omega/\Omega_0} f \left[\frac{1}{(1 - u)^2} - \frac{1}{(1 - u_\lambda)^2} - \frac{2}{(1 - u)^3}(u - u_\lambda) \right] (u - u_\lambda) < 0. \quad (2.5.5)$$

Now we are able to prove the following uniqueness result. ■

Theorem 2.5.5. *For every $M > 0$ there exists $0 < \lambda_1^*(M) < \lambda^*$ such that for $\lambda \in (0, \lambda_1^*(M))$ the equation $(S)_\lambda$ has a unique solution v satisfying*

1. $\| \frac{f}{(1-v)^3} \|_1 \leq M$ and the dimension $N = 1$,
2. $\| \frac{f}{(1-v)^3} \|_{1+\epsilon} \leq M$ for some $\epsilon > 0$ and $N = 2$,
3. $\| \frac{f}{(1-v)^3} \|_{N/2} \leq M$ and $N > 2$.

Proof: For any fixed $\lambda \in (0, \lambda^*)$, let u_λ be the minimal solution of $(S)_\lambda$, and suppose $(S)_\lambda$ has a nonminimal solution u . The preceding lemma then gives

$$\int_{\Omega} |\nabla(u - u_\lambda)|^2 dx < \int_{\Omega} \frac{2\lambda(u - u_\lambda)^2 f(x)}{(1 - u)^3} dx.$$

This implies in the case where $N > 2$ that

$$\begin{aligned} C(N) \left(\int_{\Omega} (u - u_\lambda)^{\frac{2N}{N-2}} dx \right)^{\frac{N-2}{N}} &< \lambda \int_{\Omega} \frac{2f(x)}{(1-u)^3} (u - u_\lambda)^2 dx \\ &\leq 2\lambda \left(\int_{\Omega} \left| \frac{f}{(1-u)^3} \right|^{\frac{N}{2}} dx \right)^{\frac{2}{N}} \left(\int_{\Omega} (u - u_\lambda)^{\frac{2N}{N-2}} dx \right)^{\frac{N-2}{N}} \\ &\leq 2\lambda M^{\frac{2}{N}} \left(\int_{\Omega} (u - u_\lambda)^{\frac{2N}{N-2}} dx \right)^{\frac{N-2}{N}}, \end{aligned}$$

which is a contradiction if $\lambda < \frac{C(N)}{2M^{\frac{2}{N}}}$ unless $u \equiv u_\lambda$. If $N = 1$, then we write

$$C(1) \| (u - u_\lambda) \|_{\infty}^2 < \lambda \int_{\Omega} \frac{2f(x)}{(1-u)^3} (u - u_\lambda)^2 dx \leq 2\lambda \| (u - u_\lambda) \|_{\infty}^2 \int_{\Omega} \frac{f}{(1-u)^3} dx,$$

and the proof follows. A similar proof holds for dimension $N = 2$. ■

Remark 2.5.1. The above gives uniqueness for small λ among all solutions that either stay away from 1 or those that approach it slowly. We do not know whether, if λ is small enough, any positive solution v of $(S)_\lambda$ satisfies $\int_{\Omega} (1-v)^{-\frac{3N}{2}} dx \leq M$ for some uniform bound M independent of λ . Numerical computations do show that we may have uniqueness for small λ —at least for radially symmetric solutions— as long as $N \geq 2$.

2.5.3 Second solutions around the bifurcation point

Our next result is quite standard.

Lemma 2.5.6. *Suppose there exists $0 < C < 1$ such that $\| u_\lambda \|_{C(\bar{\Omega})} \leq C$ for each $\lambda < \lambda^*$. Then there exists $\delta > 0$ such that the solutions of $(S)_\lambda$ near $(\lambda^*, u_{\lambda^*})$ form a curve $\rho(s) = \{(\bar{\lambda}(s), v(s)) : |s| < \delta\}$, and the pair $(\bar{\lambda}(s), v(s))$ satisfies*

$$\bar{\lambda}(0) = \lambda^*, \quad \bar{\lambda}'(0) = 0, \quad \bar{\lambda}''(0) < 0, \quad \text{and} \quad v(0) = u_{\lambda^*}, \quad v'(0)(x) > 0 \text{ in } \Omega. \quad (2.5.6)$$

In particular, if $1 \leq N \leq 7$, then for λ close enough to λ^* there exists a unique second branch U_λ of solutions for $(S)_\lambda$, bifurcating from u^* , such that

$$\mu_{1,\lambda}(U_\lambda) < 0 \quad \text{while} \quad \mu_{2,\lambda}(U_\lambda) > 0. \quad (2.5.7)$$

Proof: The proof is similar to a related result of Crandall and Rabinowitz (cf. [19, 20]), so we will be brief. First, the assumed upper bound on u_λ in C^1 and standard regularity theory show that if $f \in C(\bar{\Omega})$ then $\|u_\lambda\|_{C^{2,\alpha}(\bar{\Omega})} \leq C < 1$ for some $0 < \alpha < 1$ (while if $f \in L^\infty$, then $\|u_\lambda\|_{C^{1,\alpha}(\bar{\Omega})} \leq C < 1$). It follows that $\{(\lambda, u_\lambda)\}$ is precompact in the space $R \times C^{2,\alpha}$, and hence we have a limiting point $(\lambda^*, u_{\lambda^*})$ as desired. Since $\frac{\lambda^* f(x)}{(1-u_{\lambda^*})^2}$ is nonnegative, Theorem 3.2 of [19] characterizes the solution set of $(S)_\lambda$ near $(\lambda^*, u_{\lambda^*})$: $\bar{\lambda}(0) = \lambda^*$, $\bar{\lambda}'(0) = 0$, $v(0) = u_{\lambda^*}$ and $v'(0) > 0$ in Ω . The same computation as in Theorem 4.8 in [19] gives that $\bar{\lambda}''(0) < 0$. In particular, if $1 \leq N \leq 7$ then our Theorem 4.5 gives the compactness of $u^* = u_{\lambda^*}$, and the theory of Crandall and Rabinowitz in [20] then implies that, for λ close enough to λ^* , there exists a unique second branch U_λ of solutions for $(S)_\lambda$, bifurcating from u^* , such that $\mu_{1,\lambda}(U_\lambda) < 0$ while $\mu_{2,\lambda}(U_\lambda) > 0$. ■

Remark 2.5.2. A version of these results will be established variationally in next Chapter. Indeed, we shall give there a variational characterization for both the stable and unstable solutions u_λ, U_λ in the following sense: For $1 \leq N \leq 7$, there exists $\delta > 0$ such that for any $\lambda \in (\lambda^* - \delta, \lambda^*)$, the minimal solution u_λ is a local minimum for some regularized energy functional $J_{\epsilon,\lambda}$ on the space $H_0^1(\Omega)$, while the second solution U_λ is a mountain pass for the functional $J_{\epsilon,\lambda}$.

2.6 Radially symmetric case and power-law profiles

In this section, we discuss issues of uniqueness and multiplicity of solutions for $(S)_\lambda$ when Ω is a symmetric domain and when f is a radially symmetric permittivity profile. Here, one can again define the corresponding pull-in voltage $\lambda_r^*(\Omega, f)$ requiring the solutions to be radially symmetric, that is

$$\lambda_r^*(\Omega, f) = \sup \{ \lambda; (S)_\lambda \text{ has a radially symmetric solution} \}.$$

Proposition 2.6.1. *Let Ω be a symmetric domain and let f be a nonnegative bounded radially symmetric permittivity profile on Ω . Then the minimal solutions of $(S)_\lambda$ are necessarily radially symmetric and consequently $\lambda_r^*(\Omega, f) = \lambda^*(\Omega, f)$. Moreover, if Ω is a ball, then any radial solution of $(S)_\lambda$ attains its maximum at 0.*

Proof: It is clear that $\lambda_r^*(\Omega, f) \leq \lambda^*(\Omega, f)$, and the reverse will be proved if we establish that every minimal solution of $(S)_\lambda$ with $0 < \lambda < \lambda^*(\Omega, f)$ is radially symmetric. But this is a straightforward application of the recursive scheme defined in Theorem 2.2.2 which gives a radially symmetric function at each step and therefore the resulting limiting function—which is the minimal solution—is radially symmetric.

For any radially symmetric $u(r)$ of $(S)_\lambda$ defined in the ball of radius R , we have $u_r(0) = 0$ and

$$-u_{rr} - \frac{N-1}{r} u_r = \frac{\lambda f}{(1-u)^2} \quad \text{in } (0, R),$$

Multiplying by r^{N-1} , we get that $-\frac{d(r^{N-1}u_r)}{dr} = \frac{\lambda f r^{N-1}}{(1-u)^2} \geq 0$, and therefore $u_r < 0$ in $(0, R)$ since $u_r(0) = 0$. This shows that $u(r)$ attains its maximum at 0. ■

The bifurcation diagrams shown in the introduction actually reflect the radially symmetric situation, and our emphasis in this section is on whether there is a better chance to analyze mathematically the higher branches of solutions in this case. Now some of the classical work of Joseph-Lundgren [43] and many that followed can be adapted to this situation when the permittivity profile is constant. However, the case of a power-law permittivity profile $f(x) = |x|^\alpha$ defined in a unit ball already presents a much richer situation. We now present various analytical and numerical evidences for various conjectures relating to this case, some of which will be further discussed in Chapter 3.

Power-law permittivity profiles

Consider the domain Ω to be a unit ball $B_1(0) \subset \mathbb{R}^N$ ($N \geq 1$), and let $f(x) = |x|^\alpha$ ($\alpha \geq 0$). We analyze in this case the branches of radially symmetric solutions of $(S)_\lambda$ for $\lambda \in (0, \lambda^*]$. In this case, $(S)_\lambda$ reduces to

$$\begin{cases} -u_{rr} - \frac{N-1}{r}u_r = \frac{\lambda r^\alpha}{(1-u)^2}, & 0 < r \leq 1, \\ u'(0) = 0, \quad u(1) = 0. \end{cases} \quad (2.6.1)$$

Here $r = |x|$ and $0 < u = u(r) < 1$ for $0 < r < 1$.

Looking first for a solution of the form

$$u(r) = 1 - \beta w(P) \quad \text{with} \quad P = \gamma r,$$

where $\gamma, \beta > 0$, equation (2.6.1) implies that

$$\gamma^2 \beta (w'' + \frac{N-1}{P}w') = \frac{\lambda P^\alpha}{\beta^2 \gamma^\alpha} \frac{1}{w^2}.$$

We set $w(0) = 1$ and $\lambda = \gamma^{2+\alpha} \beta^3$. This yields the following initial value problem:

$$\begin{cases} w'' + \frac{N-1}{P}w' = \frac{P^\alpha}{w^2}, & P > 0, \\ w'(0) = 0, \quad w(0) = 1. \end{cases} \quad (2.6.2)$$

Since $u(1) = 0$ we have $\beta = 1/w(\gamma)$. Therefore, we conclude that

$$\begin{cases} u(0) = 1 - \frac{1}{w(\gamma)}, \\ \lambda = \frac{\gamma^{2+\alpha}}{w^3(\gamma)}, \end{cases} \quad (2.6.3)$$

where $w(\gamma)$ is a solution of (2.6.2).

As was done in [50], one can numerically integrate the initial value problem (2.6.2) and use the results to compute the complete bifurcation diagram for (2.6.1). We show such a computation of $u(0)$ versus λ defined in (2.6.3) for the slab domain ($N = 1$) in Figure 2.3. In

this case, one observes from the numerical results that when $N = 1$, and $0 \leq \alpha \leq 1$, there exist exactly two solutions for $(S)_\lambda$ whenever $\lambda \in (0, \lambda^*)$. On the other hand, the situation becomes more complex for $\alpha > 1$ as $u(0) \rightarrow 1$. This leads to the question of determining the asymptotic behavior of $w(P)$ as $P \rightarrow \infty$. Towards this end, we proceed as follows.

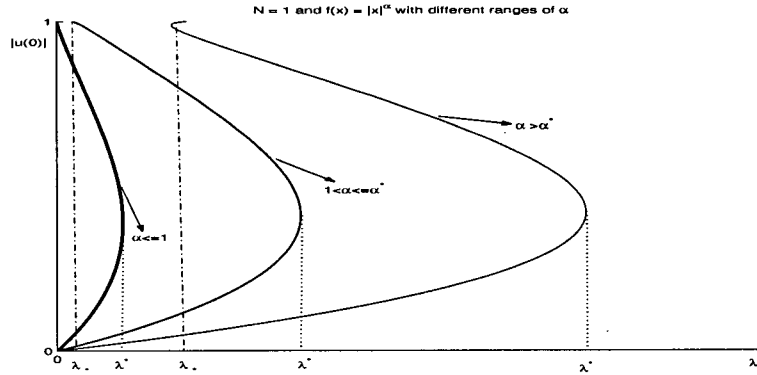


Figure 2.3: Plots of $u(0)$ versus λ for profile $f(x) = |x|^\alpha$ ($\alpha \geq 0$) defined in the slab domain ($N = 1$). The numerical experiments point to a constant $\alpha^* > 1$ (analytically given in (2.6.10)) such that the bifurcation diagrams are greatly different for different ranges of α : $0 \leq \alpha \leq 1$, $1 < \alpha \leq \alpha^*$ and $\alpha > \alpha^*$.

Setting $\eta = \log P$ and $w(P) = P^B V(\eta) > 0$ for some positive constant B , we obtain from (2.6.2) that

$$P^{B-2}V'' + (2B + N - 2)P^{B-2}V' + B(B + N - 2)P^{B-2}V = \frac{P^{\alpha-2B}}{V^2}. \quad (2.6.4)$$

Choosing $B - 2 = \alpha - 2B$ so that $B = (2 + \alpha)/3$, we get that

$$V'' + \frac{3N + 2\alpha - 2}{3}V' + \frac{(2 + \alpha)(3N + \alpha - 4)}{9}V = \frac{1}{V^2}. \quad (2.6.5)$$

We can already identify from this equation the following regimes.

Case 1. Assume that

$$N = 1 \text{ and } 0 \leq \alpha \leq 1. \quad (2.6.6)$$

In this case, there is no equilibrium point for (2.6.5), which means that the bifurcation diagram vanishes at $\lambda = 0$, from which one infers that in this case, there exist exactly two solutions for $\lambda \in (0, \lambda^*)$ and just one for $\lambda = \lambda^*$.

Case 2. N and α satisfy either one of the following conditions:

$$N = 1 \text{ and } \alpha > 1, \quad (2.6.7a)$$

$$N \geq 2. \quad (2.6.7b)$$

There exists then an equilibrium point V_e of (2.6.5) which must be positive and satisfies

$$V_e^3 = \frac{9}{(2+\alpha)(3N+\alpha-4)} > 0. \quad (2.6.8)$$

Linearizing around this equilibrium point by writing

$$V = V_e + Ce^{\sigma\eta}, \quad 0 < C \ll 1,$$

we obtain that

$$\sigma^2 + \frac{3N+2\alpha-2}{3}\sigma + \frac{(2+\alpha)(3N+\alpha-4)}{3} = 0.$$

This reduces to

$$\sigma_{\pm} = -\frac{3N+2\alpha-2}{6} \pm \frac{\sqrt{\Delta}}{6}, \quad (2.6.9a)$$

with

$$\Delta = -8\alpha^2 - (24N-16)\alpha + (9N^2 - 84N + 100). \quad (2.6.9b)$$

We note that $\sigma_{\pm} < 0$ whenever $\Delta \geq 0$. Now define

$$\alpha^* = -\frac{1}{2} + \frac{1}{2}\sqrt{\frac{27}{2}}, \quad \alpha^{**} = \frac{4-6N+3\sqrt{6}(N-2)}{4} \quad (N \geq 8). \quad (2.6.10)$$

Next, we discuss the ranges of N and α such that $\Delta \geq 0$ or $\Delta < 0$.

Case 2.A. N and α satisfy either one of the following:

$$N = 1 \quad \text{with} \quad 1 < \alpha \leq \alpha^*, \quad (2.6.11a)$$

$$N \geq 8 \quad \text{with} \quad 0 \leq \alpha \leq \alpha^{**}. \quad (2.6.11b)$$

In this case, we have $\Delta \geq 0$ and

$$V \sim \left(\frac{9}{(2+\alpha)(3N+\alpha-4)} \right)^{\frac{1}{3}} + C_1 e^{-\frac{3N+2\alpha-2-\sqrt{\Delta}}{6}\eta} + \dots, \quad \text{as } \eta \rightarrow +\infty.$$

Further, we conclude that

$$w \sim P^{\frac{2+\alpha}{3}} \left(\frac{9}{(2+\alpha)(3N+\alpha-4)} \right)^{\frac{1}{3}} + C_1 P^{-\frac{N-2+\sqrt{\Delta}}{2} + \frac{\sqrt{\Delta}}{6}} + \dots, \quad \text{as } P \rightarrow +\infty.$$

In both cases, the branch monotonically approaches the value 1 as $\eta \rightarrow +\infty$. Moreover, since $\lambda = \gamma^{2+\alpha}/w^3(\gamma)$, we have

$$\lambda \sim \lambda_* = \frac{(2+\alpha)(3N+\alpha-4)}{9} \quad \text{as } \gamma \rightarrow \infty, \quad (2.6.12)$$

which is another important critical threshold for the voltage.

In the case (2.6.11a) illustrated by Figure 2.3, we have $\lambda_* < \lambda^*$, and the number of solutions increase but remains finite as λ approaches λ_* . On the other hand, in the case of (2.6.11b)

illustrated by Figure 2.4, we have $\lambda_* = \lambda^*$, and there seems to be only one branch of solutions.

Case 2.B. N and α satisfy any one of the following three:

$$N = 1 \quad \text{with} \quad \alpha > \alpha^*, \quad (2.6.13a)$$

$$2 \leq N \leq 7 \quad \text{with} \quad \alpha \geq 0, \quad (2.6.13b)$$

$$N \geq 8 \quad \text{with} \quad \alpha > \alpha^{**}. \quad (2.6.13c)$$

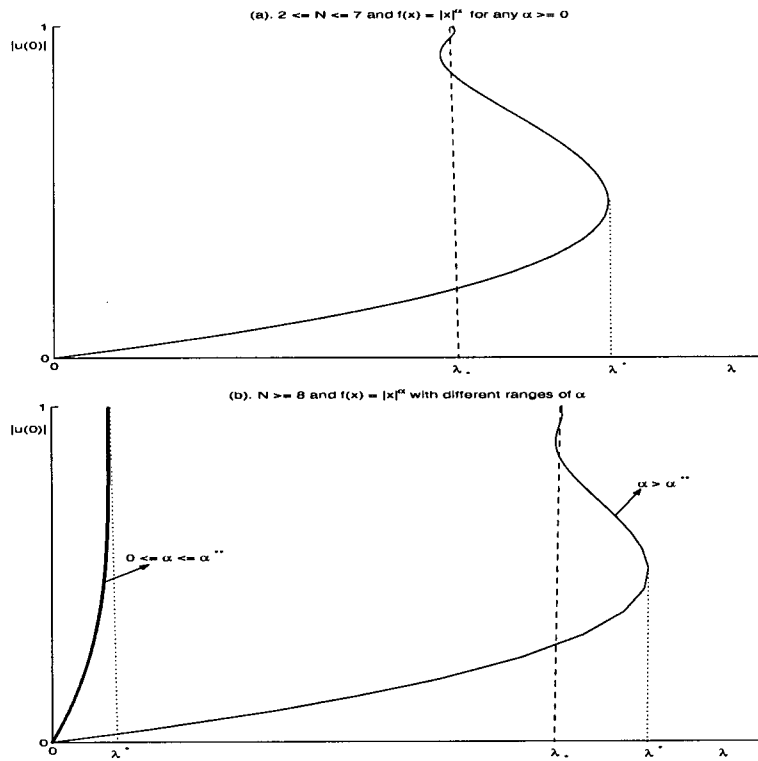


Figure 2.4: Top figure: Plots of $u(0)$ versus λ for $2 \leq N \leq 7$, where $u(0)$ oscillates around the value λ_* defined in (2.6.12) and u^* is regular. Bottom figure: Plots of $u(0)$ versus λ for $N \geq 8$: when $0 \leq \alpha \leq \alpha^{**}$, there exists a unique solution for $(S)_\lambda$ with $\lambda \in (0, \lambda^*)$ and u^* is singular; when $\alpha > \alpha^{**}$, $u(0)$ oscillates around the value λ_* defined in (2.6.12) and u^* is regular.

In this case, we have $\Delta < 0$ and

$$V \sim \left(\frac{9}{(2+\alpha)(3N+\alpha-4)} \right)^{\frac{1}{3}} + C_1 e^{-\frac{3N+2\alpha-2}{6}\eta} \cos\left(\frac{\sqrt{-\Delta}}{6}\eta + C_2\right) + \dots \quad \text{as } \eta \rightarrow +\infty.$$

We also have for $P \rightarrow +\infty$,

$$w \sim P^{\frac{2+\alpha}{3}} \left(\frac{9}{(2+\alpha)(3N+\alpha-4)} \right)^{\frac{1}{3}} + C_1 P^{-\frac{N-2}{2}} \cos\left(\frac{\sqrt{-\Delta}}{6} \log P + C_2\right) + \dots, \quad (2.6.14)$$

and from the fact that $\lambda = \gamma^{2+\alpha}/w^3(\gamma)$ we get again that

$$\lambda \sim \lambda_* = \frac{(2+\alpha)(3N+\alpha-4)}{9} \quad \text{as } \gamma \rightarrow \infty.$$

Note the oscillatory behavior of $w(P)$ in (2.6.14) for large P , which means that $u(0)$ is expected to oscillate around the value $\lambda_* = \frac{(2+\alpha)(3N+\alpha-4)}{9}$ as $P \rightarrow \infty$. The diagrams below point to the existence of a sequence $\{\lambda_i\}$ satisfying

$$\lambda_0 = 0, \quad \lambda_{2k} \nearrow \lambda_* \quad \text{as } k \rightarrow \infty;$$

$$\lambda_1 = \lambda^*, \quad \lambda_{2k-1} \searrow \lambda_* \quad \text{as } k \rightarrow \infty$$

and such that exactly $2k+1$ solutions for $(S)_\lambda$ exist when $\lambda \in (\lambda_{2k}, \lambda_{2k+2})$, while there are exactly $2k$ solutions when $\lambda \in (\lambda_{2k+1}, \lambda_{2k-1})$. Furthermore, $(S)_\lambda$ has infinitely multiple solutions at $\lambda = \lambda_*$.

The three cases (2.6.13a), (2.6.13b) and (2.6.13c) considered here for N and α are illustrated by the diagrams in Figure 2.3, Figure 2.4(a) and Figure 2.4(b), respectively.

We now conclude from above that the bifurcation diagrams show four possible regimes –at least if the domain is a ball:

A. There is exactly one branch of solution for $0 < \lambda < \lambda^*$. This regime occurs when $N \geq 8$, and if $0 \leq \alpha \leq \alpha^{**}(N) := \frac{4-6N+3\sqrt{6}(N-2)}{4}$. The results of this section actually show that in this range, the first branch of solutions “disappears” at λ^* which happens to be equal to $\lambda_*(\alpha, N) = \frac{(2+\alpha)(3N+\alpha-4)}{9}$.

B. There exists an infinite number of branches of solutions. This regime occurs when

- $N = 1$ and $\alpha \geq \alpha^* := -\frac{1}{2} + \frac{1}{2}\sqrt{27/2}$.
- $2 \leq N \leq 7$ and $\alpha \geq 0$;
- $N \geq 8$ and $\alpha > \alpha^{**}(N) := \frac{4-6N+3\sqrt{6}(N-2)}{4}$.

In this case, $\lambda_*(\alpha, N) < \lambda^*$ and the multiplicity becomes arbitrarily large as λ approaches –from either side– $\lambda_*(\alpha, N)$ at which there is a touchdown solution u (i.e., $\|u\|_\infty = 1$).

C. There exists a finite number of branches of solutions. In this case, we have again that $\lambda_*(\alpha, N) < \lambda^*$, but now the branch approaches the value 1 monotonically, and the number of solutions increase but remains finite as λ approaches $\lambda_*(\alpha, N)$. This regime occurs when $N = 1$ and $1 < \alpha \leq \alpha^* := -\frac{1}{2} + \frac{1}{2}\sqrt{27/2}$.

D. There exist exactly two branches of solutions for $0 < \lambda < \lambda^*$ and one solution for $\lambda = \lambda^*$. The bifurcation diagram vanishes when it returns to $\lambda = 0$. This regime occurs when $N = 1$ and $0 \leq \alpha \leq 1$.

Some of these questions will be considered in Chapter 3. A detailed and involved analysis of compactness along the unstable branches will be discussed there, as well as some information about the second bifurcation point.

Chapter 3

Compactness along Lower Branches

3.1 Introduction

In this Chapter we continue the analysis of the problem

$$\begin{cases} -\Delta u = \frac{\lambda f(x)}{(1-u)^2} & \text{in } \Omega, \\ 0 < u < 1 & \text{in } \Omega, \\ u = 0 & \text{on } \partial\Omega, \end{cases} \quad (S)_\lambda$$

where $\lambda > 0$ is a parameter, $\Omega \subset \mathbb{R}^N$ is a bounded smooth domain and f satisfies (2.1.1). Following the notations and terminology of Chapter 2, the solutions of $(S)_\lambda$ are considered to be in the classical sense, and the *minimal solution* u_λ of $(S)_\lambda$ is the classical solution of $(S)_\lambda$ satisfying $u_\lambda(x) \leq u(x)$ in Ω for any solution u of $(S)_\lambda$.

There already exist in the literature many interesting results concerning the properties of the branch of semi-stable solutions for Dirichlet boundary value problems of the form $-\Delta u = \lambda h(u)$ where h is a regular nonlinearity (for example of the form e^u or $(1+u)^p$ for $p > 1$). See for example the seminal papers [20, 43, 44] and also [15] for a survey on the subject and an exhaustive list of related references. The singular situation was considered in a very general context in [48], and this analysis is completed in Chapter 2 to allow for a general continuous permittivity profile $f(x) \geq 0$. Fine properties of steady states –such as regularity, stability, uniqueness, multiplicity, energy estimates and comparison results– are shown there to depend on the dimension of the ambient space and on the permittivity profile.

Now for any solution u of $(S)_\lambda$, one can introduce the linearized operator at u defined by:

$$L_{u,\lambda} = -\Delta - \frac{2\lambda f(x)}{(1-u)^3},$$

and its corresponding eigenvalues $\{\mu_{k,\lambda}(u); k = 1, 2, \dots\}$. Note that the first eigenvalue is simple and is given by:

$$\mu_{1,\lambda}(u) = \inf \left\{ \langle L_{u,\lambda} \phi, \phi \rangle_{H_0^1(\Omega)}; \phi \in C_0^\infty(\Omega), \int_\Omega |\phi(x)|^2 dx = 1 \right\}$$

with the infimum being attained at a first eigenfunction ϕ_1 , while the second eigenvalue is given by the formula:

$$\mu_{2,\lambda}(u) = \inf \left\{ \langle L_{u,\lambda} \phi, \phi \rangle_{H_0^1(\Omega)}; \phi \in C_0^\infty(\Omega), \int_\Omega |\phi(x)|^2 dx = 1, \int_\Omega \phi(x) \phi_1(x) dx = 0 \right\}.$$

This construction can then be iterated to obtain the k -th eigenvalue $\mu_{k,\lambda}(u)$ with the convention that eigenvalues are repeated according to their multiplicities.

The usual analysis of the minimal branch (composed of semi-stable solutions) is extended in Chapter 2 to cover the singular situation $(S)_\lambda$ above – best illustrated by the following bifurcation diagram– is obtained.

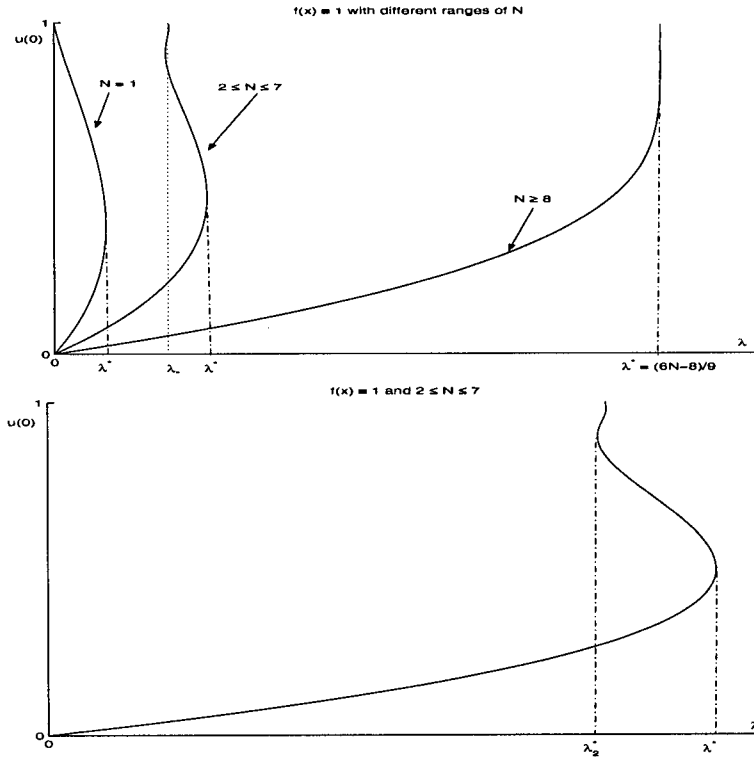


Figure 3.1: *Top figure: plots of $u(0)$ versus λ for the case where $f(x) \equiv 1$ is defined in the unit ball $B_1(0) \subset \mathbb{R}^N$ with different ranges of dimension N , where we have $\lambda^* = (6N - 8)/9$ for dimension $N \geq 8$. Bottom figure: plots of $u(0)$ versus λ for the case where $f(x) \equiv 1$ is defined in the unit ball $B_1(0) \subset \mathbb{R}^N$ with dimension $2 \leq N \leq 7$, where λ_1^* (resp. λ_2^*) is the first (resp. second) turning point.*

One can recognize from Chapter 2 a clear distinction –in techniques and in the available results– between the case where the permittivity profile f is bounded away from zero, and where it is allowed to vanish somewhere. A test case for the latter situation –that has generated much interest among both mathematicians and engineers– is when we have a power-law permittivity profile $f(x) = |x|^\alpha$ ($\alpha \geq 0$) on a ball. Our first goal of this Chapter is the study of the effect of power-like permittivity profiles $f(x) \simeq |x|^\alpha$ for the problem $(S)_\lambda$ on the unit ball $B = B_1(0)$. We extend Theorem 2.1.2 to higher dimensions:

Theorem 3.1.1. *Assume $N \geq 8$ and $\alpha > \alpha_N = \frac{3N-14-4\sqrt{6}}{4+2\sqrt{6}}$. Let $f \in C(\bar{B})$ be such that:*

$$f(x) = |x|^\alpha g(x), \quad g(x) \geq C > 0 \text{ in } B. \quad (3.1.1)$$

Let $(\lambda_n)_n$ be such that $\lambda_n \rightarrow \lambda \in [0, \lambda^*]$ and u_n be a solution of $(S)_{\lambda_n}$ so that $\mu_{1,n} := \mu_{1,\lambda_n}(u_n) \geq 0$. Then,

$$\sup_{n \in \mathbb{N}} \|u_n\|_\infty < 1.$$

In particular, the extremal solution $u^* = \lim_{\lambda \uparrow \lambda^*} u_\lambda$ is a solution of $(S)_{\lambda^*}$ satisfying $\mu_{1,\lambda^*}(u^*) = 0$.

As to non-minimal solutions, it is also shown in Chapter 2 –following ideas of Crandall-Rabinowitz [20]– that, for $1 \leq N \leq 7$, and for λ close enough to λ^* , there exists a unique second branch U_λ of solutions for $(S)_\lambda$, bifurcating from u^* , such that

$$\mu_{1,\lambda}(U_\lambda) < 0 \quad \text{while} \quad \mu_{2,\lambda}(U_\lambda) > 0. \quad (3.1.2)$$

For $N \geq 8$ and $\alpha > \alpha_N$, the same remains true for problem $(S)_\lambda$ on the unit ball with $f(x)$ as in (3.3.1) and U_λ is a radial function.

In the sequel, we try to provide a rigorous analysis for other features of the bifurcation diagram, in particular the second branch of unstable solutions, as well as the second bifurcation point. But first, and for the sake of completeness, we shall give a variational characterization for the unstable solution U_λ in the following sense:

Theorem 3.1.2. *Assume f is a non-negative function in $C(\bar{\Omega})$ where Ω is a bounded domain in \mathbb{R}^N . If $1 \leq N \leq 7$, then there exists $\delta > 0$ such that for any $\lambda \in (\lambda^* - \delta, \lambda^*)$, the second solution U_λ is a Mountain Pass solution for some regularized energy functional $J_{\varepsilon,\lambda}$ on the space $H_0^1(\Omega)$.*

Moreover, the same result is still true for $N \geq 8$ provided Ω is a ball, and $f(x)$ is as in (3.3.1) with $\alpha > \alpha_N$.

We are now interested in continuing the second branch till the second bifurcation point, by means of the implicit function theorem. For that, we have the following compactness result:

Theorem 3.1.3. *Assume $2 \leq N \leq 7$. Let $f \in C(\bar{\Omega})$ be such that:*

$$f(x) = \left(\prod_{i=1}^k |x - p_i|^{\alpha_i} \right) g(x), \quad g(x) \geq C > 0 \text{ in } \Omega, \quad (3.1.3)$$

for some points $p_i \in \Omega$ and exponents $\alpha_i \geq 0$. Let $(\lambda_n)_n$ be a sequence such that $\lambda_n \rightarrow \lambda \in [0, \lambda^]$ and let u_n be an associated solution such that*

$$\mu_{2,n} := \mu_{2,\lambda_n}(u_n) \geq 0. \quad (3.1.4)$$

Then, $\sup_{n \in \mathbb{N}} \|u_n\|_\infty < 1$. Moreover, if in addition $\mu_{1,n} := \mu_{1,\lambda_n}(u_n) < 0$, then necessarily $\lambda > 0$.

Let us remark that the case $\alpha_1 = \dots = \alpha_k = 0$ in (3.1.3) corresponds to a function $f(x)$ bounded away from zero. We also mention that Theorem 3.1.3 yields another proof –based on a blow-up argument– of the compactness result for minimal solutions established in Chapter 2 by means of some energy estimates, though under the more stringent assumption (3.1.3) on $f(x)$. We expect that the same result should be true for radial solutions on the unit ball for $N \geq 8$, $\alpha > \alpha_N$, and $f \in C(\bar{\Omega})$ as in (3.3.1).

As far as we know, there are no compactness results of this type in the case of regular nonlinearities, marking a substantial difference with the singular situation. Theorem 3.1.3 is based on a blow up argument and the knowledge of linear instability for solutions of a limit problem on \mathbb{R}^N , a result which is interesting in itself (see for example [16]) and which somehow explains the special role of dimension 7 and $\alpha = \alpha_N$ for this problem.

Theorem 3.1.4. *Assume that either $1 \leq N \leq 7$ and $\alpha \geq 0$ or that $N \geq 8$ and $\alpha > \alpha_N$. Let U be a solution of*

$$\begin{cases} \Delta U = \frac{|y|^\alpha}{U^2} & \text{in } \mathbb{R}^N, \\ U(y) \geq C > 0 & \text{in } \mathbb{R}^N. \end{cases} \quad (3.1.5)$$

Then, U is linearly unstable in the following sense:

$$\mu_1(U) = \inf \left\{ \int_{\mathbb{R}^N} (|\nabla \phi|^2 - \frac{2|y|^\alpha}{U^3} \phi^2) dx; \phi \in C_0^\infty(\mathbb{R}^N), \int_{\mathbb{R}^N} \phi^2 = 1 \right\} < 0. \quad (3.1.6)$$

Moreover, if $N \geq 8$ and $0 \leq \alpha \leq \alpha_N$, then there exists at least a solution U of (3.1.5) such that $\mu_1(U) \geq 0$, given by the limit as $\lambda \rightarrow \lambda^*$ of suitable rescaling of the minimal solution u_λ of $(S)_\lambda$ on the unit ball with $f(x) = |x|^\alpha$.

Theorem 3.1.4 is the main tool to control the blow up behavior of a possible non compact sequence of solutions. The usual asymptotic analysis for equations with Sobolev critical nonlinearity, based on some energy bounds (usually $L^{\frac{2N}{N-2}}(\Omega)$ -bounds), does not work in our context. In view of Chapter 2, a possible loss of compactness can be related to the $L^{\frac{3N}{2}}(\Omega)$ -norm along the sequence. Essentially, the blow up associated to a sequence u_n (in the sense of the blowing up of $(1 - u_n)^{-1}$) corresponds exactly to the blow up of the $L^{\frac{3N}{2}}(\Omega)$ -norm. We replace these energy bounds by some spectral information and, based on Theorem 3.1.4, we provide an estimate of the number of blow up points (counted with their "multiplicities") in terms of the Morse index along the sequence.

We now define the second bifurcation point in the following way for $(S)_\lambda$:

$$\begin{aligned} \lambda_2^* &= \inf \{ \beta > 0 : \exists \text{ a curve } V_\lambda \in C([\beta, \lambda^*]; C^2(\Omega)) \text{ of solutions for } (S)_\lambda \\ &\text{s.t. } \mu_{2,\lambda}(V_\lambda) \geq 0, V_\lambda \equiv U_\lambda \forall \lambda \in (\lambda^* - \delta, \lambda^*) \}. \end{aligned}$$

We then have the following multiplicity result.

Theorem 3.1.5. *Assume $f \in C(\bar{\Omega})$ to be of the form (3.1.3). Then, for $2 \leq N \leq 7$ we have that $\lambda_2^* \in (0, \lambda^*)$ and for any $\lambda \in (\lambda_2^*, \lambda^*)$ there exist at least two solutions u_λ and V_λ for $(S)_\lambda$, so that*

$$\mu_{1,\lambda}(V_\lambda) < 0 \quad \text{while} \quad \mu_{2,\lambda}(V_\lambda) \geq 0.$$

In particular, for $\lambda = \lambda_2^*$, there exists a second solution, namely $V^* := \lim_{\lambda \downarrow \lambda_2^*} V_\lambda$ so that

$$\mu_{1,\lambda_2^*}(V^*) < 0 \quad \text{and} \quad \mu_{2,\lambda_2^*}(V^*) = 0.$$

One can compare Theorem 3.1.5 with the multiplicity result of [1] for nonlinearities of the form $\lambda u^q + u^p$ ($0 < q < 1 < p$), where the authors show that for p subcritical, there exists a second

–Mountain Pass– solution for any $\lambda \in [0, \lambda^*)$. On the other hand, when p is critical, the second branch blows up as $\lambda \rightarrow 0$ (see also [4] for a related problem). We note that in our situation, the second branch cannot approach the value $\lambda = 0$ as illustrated by the bifurcation diagram above.

Now let V_λ , $\lambda \in (\beta, \lambda^*)$ be one of the curves appearing in the definition of λ_2^* . By (3.1.2), we have that $L_{V_\lambda, \lambda}$ is invertible for $\lambda \in (\lambda^* - \delta, \lambda^*)$ and, as long as it remains invertible, we can use the implicit function theorem to find V_λ as the unique smooth extension of the curve U_λ (in principle U_λ exists only for λ close to λ^*). We now define λ^{**} in the following way

$$\lambda^{**} = \inf\{\beta > 0 : \forall \lambda \in (\beta, \lambda^*) \exists V_\lambda \text{ solution of } (S)_\lambda \text{ so that } \mu_{2, \lambda}(V_\lambda) > 0, V_\lambda \equiv U_\lambda \text{ for } \lambda \in (\lambda^* - \delta, \lambda^*)\}.$$

Then, $\lambda_2^* \leq \lambda^{**}$ and there exists a smooth curve V_λ for $\lambda \in (\lambda^{**}, \lambda^*)$ so that V_λ is the unique maximal extension of the curve U_λ . This is what the second branch is supposed to be. If now $\lambda_2^* < \lambda^{**}$, then for $\lambda \in (\lambda_2^*, \lambda^{**})$ there is no longer uniqueness for the extension and the “second branch” is defined only as one of potentially many continuous extensions of U_λ .

It remains open the problem whether λ_2^* is the second turning point for the solution diagram of $(S)_\lambda$ or if the “second branch” simply disappears at $\lambda = \lambda_2^*$. Note that if the “second branch” does not disappear, then it can continue for λ less than λ_2^* but only along solutions whose first two eigenvalues are negative.

In dimension 1, we have a stronger but somewhat different compactness result. Recall that $\mu_{k, \lambda_n}(u_n)$ is the k -th eigenvalue of L_{u_n, λ_n} counted with their multiplicity.

Theorem 3.1.6. *Let I be a bounded interval in \mathbb{R} and $f \in C^1(\bar{I})$ be such that $f \geq C > 0$ in I . Let $(u_n)_n$ be a solution sequence for $(S)_{\lambda_n}$ on I , where $\lambda_n \rightarrow \lambda \in [0, \lambda^*]$. Assume that for any $n \in \mathbb{N}$ and k large enough, we have:*

$$\mu_{k, n} := \mu_{k, \lambda_n}(u_n) \geq 0. \tag{3.1.7}$$

If $\lambda > 0$, then again $\sup_{n \in \mathbb{N}} \|u_n\|_\infty < 1$ and compactness holds.

Even in dimension 1, we can still define λ_2^* but we don’t know when $\lambda_2^* = 0$ (this is indeed the case when $f(x) = 1$, see [56]) or when $\lambda_2^* > 0$. In the latter situation, there would exist a solution V^* for $(S)_{\lambda_2^*}$ which could be –in some cases– the second turning point. Let us remark that the multiplicity result of Theorem 3.1.5 holds also in dimension 1 for any $\lambda \in (\lambda_2^*, \lambda^*)$.

This Chapter is organized as follows. In §3.2 we provide the Mountain Pass variational characterization of U_λ for λ close to λ^* as stated in Theorem 3.1.2. The compactness result of Theorem 3.1.1 on the unit ball is proved in §3.3. §3.4 is concerned with the compactness of the second branch of $(S)_\lambda$ as stated in Theorem 3.1.3. In §3.5 we give the proof of the multiplicity result in Theorem 3.1.5. §3.6 deals with the dimension 1 of Theorem 3.1.6.

3.2 Mountain Pass solutions

This section is devoted to the variational characterization of the second solution U_λ of $(S)_\lambda$ for $\lambda \uparrow \lambda^*$ and in dimension $1 \leq N \leq 7$. Let us stress that the argument works also for problem $(S)_\lambda$ on the unit ball with $f(x)$ in the form (3.3.1) provided $N \geq 8$, $\alpha > \alpha_N$.

Since the nonlinearity $g(u) = \frac{1}{(1-u)^2}$ is singular at $u = 1$, we need to consider a regularized C^1 nonlinearity $g_\varepsilon(u)$, $0 < \varepsilon < 1$, of the following form:

$$g_\varepsilon(u) = \begin{cases} \frac{1}{(1-u)^2} & u \leq 1 - \varepsilon, \\ \frac{1}{\varepsilon^2} - \frac{2(1-\varepsilon)}{p\varepsilon^3} + \frac{2}{p\varepsilon^3(1-\varepsilon)^{p-1}}u^p & u \geq 1 - \varepsilon, \end{cases} \quad (3.2.1)$$

where $p > 1$ if $N = 1, 2$ and $1 < p < \frac{N+2}{N-2}$ if $3 \leq N \leq 7$. For $\lambda \in (0, \lambda^*)$, we study the regularized semilinear elliptic problem:

$$\begin{cases} -\Delta u = \lambda f(x)g_\varepsilon(u) & \text{in } \Omega, \\ u = 0 & \text{on } \partial\Omega. \end{cases} \quad (3.2.2)$$

From a variational viewpoint, the action functional associated to (3.2.2) is

$$J_{\varepsilon,\lambda}(u) = \frac{1}{2} \int_{\Omega} |\nabla u|^2 dx - \lambda \int_{\Omega} f(x)G_\varepsilon(u) dx, \quad u \in H_0^1(\Omega), \quad (3.2.3)$$

where $G_\varepsilon(u) = \int_{-\infty}^u g_\varepsilon(s) ds$.

In view of Theorem 2.4.5, we now fix $0 < \varepsilon < \frac{1-\|u^*\|_\infty}{2}$. For $\lambda \uparrow \lambda^*$, the minimal solution u_λ of $(S)_\lambda$ is still a solution of (3.2.2) so that $\mu_1(-\Delta - \lambda f(x)g'_\varepsilon(u_\lambda)) > 0$. The proof of existence of second solutions for (3.2.2) relies on the standard Mountain Pass Theorem [3]. For selfcontainedness, we include this theorem as follows:

Mountain Pass Theorem: Suppose C^1 functional $J_{\varepsilon,\lambda}(u)$ defines on a Banach space E satisfying (P.S.) conditions and

1. there exists a neighborhood U of u_λ in E and a constant $\sigma > 0$ such that $J_{\varepsilon,\lambda}(v_1) \geq J_{\varepsilon,\lambda}(u_\lambda) + \sigma$ for all $v_1 \in \partial U$;
2. $\exists v_2 \notin U$ such that $J_{\varepsilon,\lambda}(v_2) \leq J_{\varepsilon,\lambda}(u_\lambda)$.

Define

$$\Gamma = \left\{ \gamma \in C([0, 1], H) : \gamma(0) = u_\lambda, \quad \gamma(1) = v_2 \right\},$$

then

$$c_{\varepsilon,\lambda} = \inf_{\gamma \in \Gamma} \max_{0 \leq t \leq 1} \left\{ J_{\varepsilon,\lambda}(\gamma(t)) : t \in (0, 1) \right\}$$

is a critical value of $J_{\varepsilon,\lambda}$.

We next briefly sketch the proof of Theorem 3.1.2 as follows. First, we prove that u_λ is a local minimum for $J_{\varepsilon,\lambda}(u)$ for $\lambda \uparrow \lambda^*$. Then, by Mountain Pass Theorem, we show the existence of a second solution $U_{\varepsilon,\lambda}$ for (3.2.2). Using subcritical growth:

$$0 \leq g_\varepsilon(u) \leq C_\varepsilon(1 + |u|^p) \quad (3.2.4)$$

and applying the inequality:

$$\theta G_\varepsilon(u) \leq u g_\varepsilon(u) \quad \text{for } u \geq M_\varepsilon, \quad (3.2.5)$$

for some $C_\varepsilon, M_\varepsilon > 0$ large and $\theta = \frac{p+3}{2} > 2$, we obtain that $J_{\varepsilon,\lambda}$ satisfies the Palais-Smale condition and, by means of a bootstrap argument, we get the uniform convergence of $U_{\varepsilon,\lambda}$. On the other hand, a similar proof as in §2.4.1 shows that the convexity of $g_\varepsilon(u)$ ensures that problem (3.2.2) has the unique solution u^* at $\lambda = \lambda^*$, which then allows us to deduce that $U_{\varepsilon,\lambda} \rightarrow u^*$ in $C(\bar{\Omega})$ as $\lambda \uparrow \lambda^*$, and it implies $U_{\varepsilon,\lambda} \leq 1 - \varepsilon$. Therefore, $U_{\varepsilon,\lambda}$ is a second solution for $(S)_\lambda$ bifurcating from u^* . But since $U_{\varepsilon,\lambda}$ is a MP solution and since $(S)_\lambda$ has exactly two solutions (cf. Lemma 2.5.6) u_λ, U_λ for $\lambda \uparrow \lambda^*$, it finally yields that $U_{\varepsilon,\lambda} = U_\lambda$.

In order to complete the details for the proof of Theorem 3.1.2, we first need to show the following:

Lemma 3.2.1. *For $\lambda \uparrow \lambda^*$, the minimal solution u_λ of $(S)_\lambda$ is a local minimum of $J_{\varepsilon,\lambda}$ on $H_0^1(\Omega)$.*

Proof: First, we show that u_λ is a local minimum of $J_{\varepsilon,\lambda}$ in $C^1(\bar{\Omega})$. Indeed, since

$$\mu_{1,\lambda} := \mu_1(-\Delta - \lambda f(x)g'_\varepsilon(u_\lambda)) > 0,$$

we have the following inequality:

$$\int_\Omega |\nabla \phi|^2 dx - 2\lambda \int_\Omega \frac{f(x)}{(1-u_\lambda)^3} \phi^2 dx \geq \mu_{1,\lambda} \int_\Omega \phi^2 \quad (3.2.6)$$

for any $\phi \in H_0^1(\Omega)$, since $u_\lambda \leq 1 - \varepsilon$. Now, take any $\phi \in H_0^1(\Omega) \cap C^1(\bar{\Omega})$ such that $\|\phi\|_{C^1} \leq \delta_\lambda$. Since $u_\lambda \leq 1 - \frac{3}{2}\varepsilon$, if $\delta_\lambda \leq \frac{\varepsilon}{2}$, then $u_\lambda + \phi \leq 1 - \varepsilon$ and we have that:

$$\begin{aligned} & J_{\varepsilon,\lambda}(u_\lambda + \phi) - J_{\varepsilon,\lambda}(u_\lambda) \\ &= \frac{1}{2} \int_\Omega |\nabla \phi|^2 dx + \int_\Omega \nabla u_\lambda \cdot \nabla \phi dx - \lambda \int_\Omega f(x) \left(\frac{1}{1-u_\lambda-\phi} - \frac{1}{1-u_\lambda} \right) \\ &\geq \frac{\mu_{1,\lambda}}{2} \int_\Omega \phi^2 - \lambda \int_\Omega f(x) \left(\frac{1}{1-u_\lambda-\phi} - \frac{1}{1-u_\lambda} - \frac{\phi}{(1-u_\lambda)^2} - \frac{\phi^2}{(1-u_\lambda)^3} \right), \end{aligned} \quad (3.2.7)$$

where we have applied (3.2.6). Since now

$$\left| \frac{1}{1-u_\lambda-\phi} - \frac{1}{1-u_\lambda} - \frac{\phi}{(1-u_\lambda)^2} - \frac{\phi^2}{(1-u_\lambda)^3} \right| \leq C|\phi|^3$$

for some $C > 0$, (3.2.7) gives that

$$J_{\varepsilon,\lambda}(u_\lambda + \phi) - J_{\varepsilon,\lambda}(u_\lambda) \geq \left(\frac{\mu_{1,\lambda}}{2} - C\lambda \|f\|_\infty \delta_\lambda \right) \int_\Omega \phi^2 > 0$$

provided δ_λ is small enough. This proves that u_λ is a local minimum of $J_{\varepsilon,\lambda}$ in the C^1 topology. Since (3.2.4) is satisfied, we can then directly apply Theorem 1 in [12] to get that u_λ is a local minimum of $J_{\varepsilon,\lambda}$ in $H_0^1(\Omega)$. \blacksquare

Since now $f \neq 0$, fix some small ball $B_{2r} \subset \Omega$ of radius $2r$, $r > 0$, so that $\int_{B_r} f(x) dx > 0$. Take a cut-off function χ so that $\chi = 1$ on B_r and $\chi = 0$ outside B_{2r} . Let $w_\varepsilon = (1 - \varepsilon)\chi \in H_0^1(\Omega)$. We have that:

$$J_{\varepsilon,\lambda}(w_\varepsilon) \leq \frac{(1-\varepsilon)^2}{2} \int_\Omega |\nabla \chi|^2 dx - \frac{\lambda}{\varepsilon^2} \int_{B_r} f(x) \rightarrow -\infty$$

as $\varepsilon \rightarrow 0$, and uniformly for λ far away from zero. Since

$$J_{\varepsilon,\lambda}(u_\lambda) = \frac{1}{2} \int_{\Omega} |\nabla u_\lambda|^2 dx - \lambda \int_{\Omega} \frac{f(x)}{1-u_\lambda} dx \rightarrow \frac{1}{2} \int_{\Omega} |\nabla u^*|^2 dx - \lambda^* \int_{\Omega} \frac{f(x)}{1-u^*} dx$$

as $\lambda \rightarrow \lambda^*$, we can find that for $\varepsilon > 0$ small, the inequality

$$J_{\varepsilon,\lambda}(w_\varepsilon) < J_{\varepsilon,\lambda}(u_\lambda) \quad (3.2.8)$$

holds for any λ close to λ^* .

Fix now $\varepsilon > 0$ small enough so that (3.2.8) holds for λ close to λ^* , and define

$$c_{\varepsilon,\lambda} = \inf_{\gamma \in \Gamma} \max_{u \in \gamma} J_{\varepsilon,\lambda}(u),$$

where $\Gamma = \{\gamma : [0,1] \rightarrow H_0^1(\Omega); \gamma \text{ continuous and } \gamma(0) = u_\lambda, \gamma(1) = w_\varepsilon\}$. We can then use the Mountain Pass Theorem to get a solution $U_{\varepsilon,\lambda}$ of (3.2.2) for λ close to λ^* , provided the Palais-Smale condition holds at level c . We next prove this (PS)-condition in the following form:

Lemma 3.2.2. *Assume that $\{w_n\} \subset H_0^1(\Omega)$ satisfies*

$$J_{\varepsilon,\lambda_n}(w_n) \leq C, \quad J'_{\varepsilon,\lambda_n}(w_n) \rightarrow 0 \text{ in } H^{-1} \quad (3.2.9)$$

for $\lambda_n \rightarrow \lambda > 0$. Then the sequence $(w_n)_n$ is uniformly bounded in $H_0^1(\Omega)$ and therefore admits a convergent subsequence in $H_0^1(\Omega)$.

Proof: By (3.2.9) we have that:

$$\int_{\Omega} |\nabla w_n|^2 dx - \lambda_n \int_{\Omega} f(x) g_\varepsilon(w_n) w_n dx = o(\|w_n\|_{H_0^1})$$

as $n \rightarrow +\infty$ and then,

$$\begin{aligned} C &\geq \frac{1}{2} \int_{\Omega} |\nabla w_n|^2 dx - \lambda_n \int_{\Omega} f(x) G_\varepsilon(w_n) dx \\ &= \left(\frac{1}{2} - \frac{1}{\theta}\right) \int_{\Omega} |\nabla w_n|^2 dx + \lambda_n \int_{\Omega} f(x) \left(\frac{1}{\theta} w_n g_\varepsilon(w_n) - G_\varepsilon(w_n)\right) dx + o(\|w_n\|_{H_0^1}) \\ &\geq \left(\frac{1}{2} - \frac{1}{\theta}\right) \int_{\Omega} |\nabla w_n|^2 dx + o(\|w_n\|_{H_0^1}) - C_\varepsilon \\ &\quad + \lambda_n \int_{\{w_n \geq M_\varepsilon\}} f(x) \left(\frac{1}{\theta} w_n g_\varepsilon(w_n) - G_\varepsilon(w_n)\right) dx \\ &\geq \left(\frac{1}{2} - \frac{1}{\theta}\right) \int_{\Omega} |\nabla w_n|^2 dx + o(\|w_n\|_{H_0^1}) - C_\varepsilon \end{aligned}$$

in view of (3.2.5). Hence, $\sup_{n \in \mathbb{N}} \|w_n\|_{H_0^1} < +\infty$.

Since p is subcritical, the compactness of the embedding $H_0^1(\Omega) \hookrightarrow L^{p+1}(\Omega)$ provides that, up to a subsequence, $w_n \rightarrow w$ weakly in $H_0^1(\Omega)$ and strongly in $L^{p+1}(\Omega)$, for some $w \in H_0^1(\Omega)$. By (3.2.9) we get that $\int_{\Omega} |\nabla w|^2 = \lambda \int_{\Omega} f(x) g_\varepsilon(w) w$, and then, by (3.2.4), we deduce that

$$\begin{aligned} \int_{\Omega} |\nabla(w_n - w)|^2 &= \int_{\Omega} |\nabla w_n|^2 - \int_{\Omega} |\nabla w|^2 + o(1) \\ &= \lambda_n \int_{\Omega} f(x) g_\varepsilon(w_n) w_n - \lambda \int_{\Omega} f(x) g_\varepsilon(w) w + o(1) \rightarrow 0 \end{aligned}$$

as $n \rightarrow +\infty$. ■

Completion of Theorem 3.1.2: Consider for any $\lambda \in (\lambda^* - \delta, \lambda^*)$ the Mountain Pass solution $U_{\varepsilon, \lambda}$ of (3.2.2) at energy level $c_{\varepsilon, \lambda}$, where $\delta > 0$ is small enough. Since $c_{\varepsilon, \lambda} \leq c_{\varepsilon, \lambda^* - \delta}$ for any $\lambda \in (\lambda^* - \delta, \lambda^*)$, and applying again Lemma 3.2.2, we get that $\|U_{\varepsilon, \lambda}\|_{H_0^1} \leq C$, for any λ close to λ^* . Then, by (3.2.4) and elliptic regularity theory, we get that $U_{\varepsilon, \lambda}$ is uniformly bounded in $C^{2, \alpha}(\bar{\Omega})$ for $\lambda \uparrow \lambda^*$, for $\alpha \in (0, 1)$. Hence, we can extract a subsequence $U_{\varepsilon, \lambda_n}$, $\lambda_n \uparrow \lambda^*$, converging in $C^2(\bar{\Omega})$ to some function U^* , where U^* is a solution for problem (3.2.2) at $\lambda = \lambda^*$. Also u^* is a solution for (3.2.2) at $\lambda = \lambda^*$ so that $\mu_1(-\Delta - \lambda^* f(x) g'_\varepsilon(u^*)) = 0$. By convexity of $g_\varepsilon(u)$, similar to §2.4.1 it is classical to show that u^* is the unique solution of this equation and therefore $U^* = u^*$. Since along any convergent sequence of $U_{\varepsilon, \lambda}$ as $\lambda \uparrow \lambda^*$ the limit is always u^* , we get that $\lim_{\lambda \uparrow \lambda^*} U_{\varepsilon, \lambda} = u^*$ in $C^2(\bar{\Omega})$. Therefore, since $u^* \leq 1 - 2\varepsilon$, there exists $\delta > 0$ so that for any $\lambda \in (\lambda^* - \delta, \lambda^*)$ $U_{\varepsilon, \lambda} \leq u^* + \varepsilon \leq 1 - \varepsilon$ and hence, $U_{\varepsilon, \lambda}$ is a solution of $(S)_\lambda$. Since the Mountain Pass energy level $c_{\varepsilon, \lambda}$ satisfies $c_{\varepsilon, \lambda} > J_{\varepsilon, \lambda}(u_\lambda)$, we have that $U_{\varepsilon, \lambda} \neq u_\lambda$ and then $U_{\varepsilon, \lambda} = U_\lambda$ for any $\lambda \in (\lambda^* - \delta, \lambda^*)$. Note that by [20], we know that u_λ, U_λ are the only solutions of $(S)_\lambda$ as $\lambda \uparrow \lambda^*$. ■

Applying the compactness of Theorem 3.3.1 proved in next section, one can note that the argument of Theorem 3.1.2 works also for problem $(S)_\lambda$ on the unit ball with $f(x)$ in the form (3.3.1) provided $N \geq 8$, $\alpha > \alpha_N$. This leads to the following proposition for higher dimensional case.

Proposition 3.2.3. *Theorem 3.1.2 is still true for $N \geq 8$ provided Ω is a ball, and $f(x)$ is as in (3.3.1) with $\alpha > \alpha_N$.*

3.3 Minimal branch for power-law profiles

Our goal of this section is to study the effect of power-like permittivity profiles $f(x) \simeq |x|^\alpha$ on the problem $(S)_\lambda$ defined in the unit ball $B = B_1(0)$. The following main results of this section extend Theorem 2.1.2 to higher dimensions $N \geq 8$, which give Theorem 3.1.1 concerning the compactness of minimal branch.

Theorem 3.3.1. *Assume $N \geq 8$ and $\alpha > \alpha_N = \frac{3N-14-4\sqrt{6}}{4+2\sqrt{6}}$. Let $f \in C(\bar{B})$ be such that:*

$$f(x) = |x|^\alpha g(x), \quad g(x) \geq C > 0 \text{ in } B. \quad (3.3.1)$$

Let $(\lambda_n)_n$ be such that $\lambda_n \rightarrow \lambda \in [0, \lambda^*]$ and u_n be a solution of $(S)_{\lambda_n}$ so that $\mu_{1, n} := \mu_{1, \lambda_n}(u_n) \geq 0$. Then,

$$\sup_{n \in \mathbb{N}} \|u_n\|_\infty < 1.$$

In particular, the extremal solution $u^* = \lim_{\lambda \uparrow \lambda^*} u_\lambda$ is a solution of $(S)_{\lambda^*}$ such that $\mu_{1, \lambda^*}(u^*) = 0$.

Proof: Let B be the unit ball, and let $(\lambda_n)_n$ be such that $\lambda_n \rightarrow \lambda \in [0, \lambda^*]$ and u_n be a solution of $(S)_{\lambda_n}$ on B so that

$$\mu_{1, n} := \mu_{1, \lambda_n}(u_n) \geq 0. \quad (3.3.2)$$

By Proposition 2.5.2 u_n coincides with the minimal solution u_{λ_n} and, by some symmetrization arguments, it is shown in Proposition 2.6.1 that the minimal solution u_n is radial and achieves its absolute maximum only at zero.

Given a permittivity profile $f(x)$ as in (3.3.1), in order to get Theorem 3.3.1, we want to show:

$$\sup_{n \in \mathbb{N}} \|u_n\|_\infty < 1, \quad (3.3.3)$$

provided $N \geq 8$ and $\alpha > \alpha_N = \frac{3N-14-4\sqrt{6}}{4+2\sqrt{6}}$. In particular, since u_λ is non decreasing in λ and

$$\sup_{\lambda \in [0, \lambda^*)} \|u_\lambda\|_\infty < 1,$$

the extremal solution $u^* = \lim_{\lambda \uparrow \lambda^*} u_\lambda$ would be a solution of $(S)_{\lambda^*}$ so that $\mu_{1, \lambda^*}(u^*) \geq 0$. Property $\mu_{1, \lambda^*}(u^*) = 0$ must hold because otherwise, by implicit function theorem, we could find solutions of $(S)_\lambda$ for $\lambda > \lambda^*$, which contradicts the definition of λ^* .

In order to prove (3.3.3), let us argue by contradiction. Up to a subsequence, assume that $u_n(0) = \max_B u_n \rightarrow 1$ as $n \rightarrow +\infty$. Since $\lambda = 0$ implies $u_n \rightarrow 0$ in $C^2(\bar{B})$, we can assume that $\lambda_n \rightarrow \lambda > 0$. Let $\varepsilon_n := 1 - u_n(0) \rightarrow 0$ as $n \rightarrow +\infty$ and introduce the following rescaled function:

$$U_n(y) = \frac{1 - u_n(\varepsilon_n^{\frac{3}{2+\alpha}} \lambda_n^{-\frac{1}{2+\alpha}} y)}{\varepsilon_n}, \quad y \in B_n := B_{\varepsilon_n^{-\frac{3}{2+\alpha}} \lambda_n^{\frac{1}{2+\alpha}}}(0). \quad (3.3.4)$$

The function U_n satisfies:

$$\begin{cases} \Delta U_n = \frac{|y|^\alpha g(\varepsilon_n^{\frac{3}{2+\alpha}} \lambda_n^{-\frac{1}{2+\alpha}} y)}{U_n^2} & \text{in } B_n, \\ U_n(y) \geq U_n(0) = 1, \end{cases} \quad (3.3.5)$$

and $B_n \rightarrow \mathbb{R}^N$ as $n \rightarrow +\infty$. This would reduce to a contradiction between (3.3.2) and the following Proposition 3.3.2. \blacksquare

Proposition 3.3.2. *There exists a subsequence $\{U_n\}_n$ defined in (3.3.4) such that $U_n \rightarrow U$ in $C_{loc}^1(\mathbb{R}^N)$, where U is a solution of the problem*

$$\begin{cases} \Delta U = g(0) \frac{|y|^\alpha}{U^2} & \text{in } \mathbb{R}^N, \\ U(y) \geq U(0) = 1 & \text{in } \mathbb{R}^N. \end{cases} \quad (3.3.6)$$

Moreover, there exists $\phi_n \in C_0^\infty(B)$ such that:

$$\int_B (|\nabla \phi_n|^2 - \frac{2\lambda_n |x|^\alpha g(x)}{(1-u_n)^3} \phi_n^2) < 0.$$

The rest of this section is devoted to the proof of Proposition 3.3.2. First, we establish the following theorem, which characterizes the instability for solutions of a limit problem (3.3.7) on \mathbb{R}^N .

Theorem 3.3.3. *Assume either $1 \leq N \leq 7$ or $N \geq 8$ and $\alpha > \alpha_N$. Let U be a solution of the problem*

$$\begin{cases} \Delta U = \frac{|y|^\alpha}{U^2} & \text{in } \mathbb{R}^N, \\ U(y) \geq C > 0 & \text{in } \mathbb{R}^N. \end{cases} \quad (3.3.7)$$

Then,

$$\mu_1(U) = \inf \left\{ \int_{\mathbb{R}^N} (|\nabla \phi|^2 - \frac{2|y|^\alpha}{U^3} \phi^2); \phi \in C_0^\infty(\mathbb{R}^N) \text{ and } \int_{\mathbb{R}^N} \phi^2 = 1 \right\} < 0. \quad (3.3.8)$$

Moreover, if $N \geq 8$ and $0 \leq \alpha \leq \alpha_N$, then there exists at least one solution U of (3.3.7) satisfying $\mu_1(U) \geq 0$.

Proof: By contradiction, assume that

$$\mu_1(U) = \inf \left\{ \int_{\mathbb{R}^N} (|\nabla \phi|^2 - \frac{2|y|^\alpha}{U^3} \phi^2); \phi \in C_0^\infty(\mathbb{R}^N) \text{ and } \int_{\mathbb{R}^N} \phi^2 dx = 1 \right\} \geq 0.$$

By the density of $C_0^\infty(\mathbb{R}^N)$ in $D^{1,2}(\mathbb{R}^N)$, we have

$$\int |\nabla \phi|^2 \geq 2 \int \frac{|y|^\alpha}{U^3} \phi^2, \quad \forall \phi \in D^{1,2}(\mathbb{R}^N). \quad (3.3.9)$$

In particular, the test function $\phi = \frac{1}{(1+|y|^2)^{\frac{N-2+\delta}{4}}}$ $\in D^{1,2}(\mathbb{R}^N)$ applied in (3.3.9) gives that

$$\int \frac{|y|^\alpha}{(1+|y|^2)^{\frac{N-2}{2}+\delta} U^3} \leq C \int \frac{1}{(1+|y|^2)^{\frac{N}{2}+\delta}} < +\infty$$

for any $\delta > 0$. Therefore, we have

$$\begin{aligned} \int \frac{1}{(1+|y|^2)^{\frac{N-2-\alpha}{2}+\delta} U^3} &= \int_{B_1} \frac{(1+|y|^2)^{\frac{\alpha}{2}}}{(1+|y|^2)^{\frac{N-2}{2}+\delta} U^3} + \int_{B_1^c} \frac{(1+|y|^2)^{\frac{\alpha}{2}}}{(1+|y|^2)^{\frac{N-2}{2}+\delta} U^3} \\ &\leq C \int_{B_1} \frac{1}{U^3} + C \int_{B_1^c} \frac{|y|^\alpha}{(1+|y|^2)^{\frac{N-2}{2}+\delta} U^3} \\ &\leq C + C \int \frac{|y|^\alpha}{(1+|y|^2)^{\frac{N-2}{2}+\delta} U^3}, \end{aligned} \quad (3.3.10)$$

which gives

$$\int \frac{1}{(1+|y|^2)^{\frac{N-2-\alpha}{2}+\delta} U^3} \leq C + C \int \frac{1}{(1+|y|^2)^{\frac{N}{2}+\delta}} < +\infty. \quad (3.3.11)$$

Step 1. We want to show that (3.3.9) allows us to perform the following Moser-type iteration scheme: for any $0 < q < 4 + 2\sqrt{6}$ and β there holds

$$\int \frac{1}{(1+|y|^2)^{\beta-1-\frac{\alpha}{2}} U^{q+3}} \leq C_q \left(1 + \int \frac{1}{(1+|y|^2)^\beta U^q} \right) \quad (3.3.12)$$

(provided the second integral is finite).

Indeed, let $R > 0$ and consider a smooth radial cut-off function η so that: $0 \leq \eta \leq 1$, $\eta = 1$ in $B_R(0)$, $\eta = 0$ in $\mathbb{R}^N \setminus B_{2R}(0)$. Multiplying (3.3.7) by $\frac{\eta^2}{(1+|y|^2)^{\beta-1} U^{q+1}}$, $q > 0$, and

integrating by parts we get:

$$\begin{aligned}
 & \int \frac{|y|^\alpha \eta^2}{(1+|y|^2)^{\beta-1} U^{q+3}} \\
 &= \frac{4(q+1)}{q^2} \int \left| \nabla \left(\frac{\eta}{(1+|y|^2)^{\frac{\beta-1}{2}} U^{\frac{q}{2}}} \right) \right|^2 - \frac{4(q+1)}{q^2} \int \frac{1}{U^q} \left| \nabla \left(\frac{\eta}{(1+|y|^2)^{\frac{\beta-1}{2}}} \right) \right|^2 \\
 & \quad - \frac{q+2}{q^2} \int \nabla \left(\frac{1}{U^q} \right) \nabla \left(\frac{\eta^2}{(1+|y|^2)^{\beta-1}} \right) \\
 &= \frac{4(q+1)}{q^2} \int \left| \nabla \left(\frac{\eta}{(1+|y|^2)^{\frac{\beta-1}{2}} U^{\frac{q}{2}}} \right) \right|^2 - \frac{2}{q} \int \frac{1}{U^q} \left| \nabla \left(\frac{\eta}{(1+|y|^2)^{\frac{\beta-1}{2}}} \right) \right|^2 \\
 & \quad + \frac{2(q+2)}{q^2} \int \frac{1}{U^q} \frac{\eta}{(1+|y|^2)^{\frac{\beta-1}{2}}} \Delta \left(\frac{\eta}{(1+|y|^2)^{\frac{\beta-1}{2}}} \right),
 \end{aligned}$$

where the relation $\Delta(\psi)^2 = 2|\nabla\psi|^2 + 2\psi\Delta\psi$ is used in the second equality. Then, by (3.3.9) we deduce that

$$\begin{aligned}
 & (8q+8-q^2) \int \frac{|y|^\alpha \eta^2}{(1+|y|^2)^{\beta-1} U^{q+3}} \\
 & \leq C'_q \int \frac{1}{U^q} \left(\left| \nabla \left(\frac{\eta}{(1+|y|^2)^{\frac{\beta-1}{2}}} \right) \right|^2 + \frac{\eta}{(1+|y|^2)^{\frac{\beta-1}{2}}} \left| \Delta \left(\frac{\eta}{(1+|y|^2)^{\frac{\beta-1}{2}}} \right) \right| \right).
 \end{aligned}$$

Assuming $|\nabla\eta| \leq \frac{C}{R}$ and $|\Delta\eta| \leq \frac{C}{R^2}$, it is straightforward to see that:

$$\begin{aligned}
 & \left| \nabla \left(\frac{\eta}{(1+|y|^2)^{\frac{\beta-1}{2}}} \right) \right|^2 + \frac{\eta}{(1+|y|^2)^{\frac{\beta-1}{2}}} \left| \Delta \left(\frac{\eta}{(1+|y|^2)^{\frac{\beta-1}{2}}} \right) \right| \\
 & \leq C \left[\frac{1}{(1+|y|^2)^\beta} + \frac{1}{R^2(1+|y|^2)^{\beta-1}} \chi_{B_{2R}(0) \setminus B_R(0)} \right]
 \end{aligned}$$

for some constant C independent of R . Then,

$$(8q+8-q^2) \int \frac{|y|^\alpha \eta^2}{(1+|y|^2)^{\beta-1} U^{q+3}} \leq C''_q \int \frac{1}{(1+|y|^2)^\beta U^q}.$$

Let $q_+ = 4 + 2\sqrt{6}$. For any $0 < q < q_+$, we have $8q+8-q^2 > 0$ and therefore:

$$\int \frac{|y|^\alpha \eta^2}{(1+|y|^2)^{\beta-1} U^{q+3}} \leq C_q \int \frac{1}{(1+|y|^2)^\beta U^q},$$

where C_q does not depend on $R > 0$. Taking the limit as $R \rightarrow +\infty$, we get that:

$$\int \frac{|y|^\alpha}{(1+|y|^2)^{\beta-1} U^{q+3}} \leq C_q \int \frac{1}{(1+|y|^2)^\beta U^q},$$

and then, the validity of (3.3.12) easily follows from the same argument of (3.3.10).

Step 2. Let either $1 \leq N \leq 7$ or $N \geq 8$ and $\alpha > \alpha_N$. We want to show that

$$\int \frac{1}{(1+|y|^2)U^q} < +\infty \tag{3.3.13}$$

for some $0 < q < q_+ = 4 + 2\sqrt{6}$.

Indeed, set $\beta_0 = \frac{N-2-\alpha}{2} + \delta$, $\delta > 0$, and $q_0 = 3$. By (3.3.11) we get that

$$\int \frac{1}{(1+|y|^2)^{\beta_0} U^{q_0}} < +\infty.$$

Let $\beta_i = \beta_0 - i(1 + \frac{\alpha}{2})$ and $q_i = q_0 + 3i$, $i \in \mathbb{N}$. Since $q_0 < q_1 < q_+ = 4 + 2\sqrt{6} < q_2$, we can iterate (3.3.12) exactly two times to get that:

$$\int \frac{1}{(1+|y|^2)^{\beta_2} U^{q_2}} < +\infty \quad (3.3.14)$$

where $\beta_2 = \frac{N-6-3\alpha}{2} + \delta$, $q_2 = 9$.

Let $0 < q < q_+ = 4 + 2\sqrt{6} < 9$. By (3.3.14) and Hölder inequality we get that:

$$\begin{aligned} & \int \frac{1}{(1+|y|^2)U^q} \\ &= \int \frac{(1+|y|^2)^{\frac{q}{9}(\frac{6-N}{2}-\delta+\frac{3}{2}\alpha)}}{U^q} \cdot \frac{1}{(1+|y|^2)^{\frac{q}{9}(\frac{6-N}{2}-\delta+\frac{3}{2}\alpha)+1}} \\ &\leq \left(\int \frac{1}{(1+|y|^2)^{\beta_2} U^{q_2}} \right)^{\frac{q}{9}} \left(\int \frac{1}{(1+|y|^2)^{\frac{q}{9-q}(\frac{6-N}{2}-\delta+\frac{3}{2}\alpha)+\frac{9}{9-q}}} \right)^{\frac{9-q}{9}} < +\infty \end{aligned}$$

provided $-\frac{2q}{9-q}\beta_2 + \frac{18}{9-q} > N$ or equivalently

$$q > \frac{9N-18}{6-2\delta+3\alpha}. \quad (3.3.15)$$

To assure (3.3.15) for some $\delta > 0$ small and $q < q_+$ at the same time, it requires $\frac{3N-6}{2+\alpha} < q_+$ or equivalently

$$1 \leq N \leq 7 \quad \text{or} \quad N \geq 8, \quad \alpha > \alpha_N = \frac{3N-14-4\sqrt{6}}{4+2\sqrt{6}}.$$

Our assumptions then provide the existence of some $0 < q < q_+ = 4 + 2\sqrt{6}$ such that (3.3.13) holds.

Step 3. We are ready to obtain a contradiction. Let $0 < q < 4 + 2\sqrt{6}$ be such that (3.3.13) holds, and suppose η is the cut-off function of Step 1. Using equation (3.3.7) we compute:

$$\begin{aligned} & \int |\nabla(\frac{\eta}{U^{\frac{q}{2}}})|^2 - \int \frac{2|y|^\alpha}{U^3} (\frac{\eta}{U^{\frac{q}{2}}}) \\ &= \frac{q^2}{4} \int \frac{\eta^2 |\nabla U|^2}{U^{q+2}} + \int \frac{|\nabla \eta|^2}{U^q} + \frac{1}{2} \int \nabla(\eta^2) \nabla(\frac{1}{U^q}) - \int \frac{2|y|^\alpha \eta^2}{U^{q+3}} \\ &= -\frac{q^2}{4(q+1)} \int \nabla U \cdot \nabla(\frac{\eta^2}{U^{q+1}}) + \int \frac{|\nabla \eta|^2}{U^q} \\ &\quad + \frac{q+2}{4(q+1)} \int \nabla(\eta^2) \nabla(\frac{1}{U^q}) - \int \frac{2|y|^\alpha \eta^2}{U^{q+3}} \\ &= -\frac{8q+8-q^2}{4(q+1)} \int \frac{|y|^\alpha \eta^2}{U^{q+3}} + \int \frac{|\nabla \eta|^2}{U^q} - \frac{q+2}{4(q+1)} \int \frac{\Delta \eta^2}{U^q}. \end{aligned}$$

Since $0 < q < 4 + 2\sqrt{6}$, we have $8q + 8 - q^2 > 0$ and

$$\begin{aligned} & \int \left| \nabla \left(\frac{\eta}{U^{\frac{q}{2}}} \right) \right|^2 - \int \frac{2|y|^\alpha}{U^3} \left(\frac{\eta}{U^{\frac{q}{2}}} \right)^2 \\ & \leq -\frac{8q + 8 - q^2}{4(q+1)} \int_{B_1(0)} \frac{|y|^\alpha \eta^2}{U^{q+3}} + O\left(\frac{1}{R^2} \int_{B_{2R}(0) \setminus B_R(0)} \frac{1}{U^q} \right) \\ & \leq -\frac{8q + 8 - q^2}{4(q+1)} \int_{B_1(0)} \frac{|y|^\alpha \eta^2}{U^{q+3}} + O\left(\int_{|y| \geq R} \frac{1}{(1+|y|^2)U^q} \right). \end{aligned}$$

Since (3.3.13) implies: $\lim_{R \rightarrow +\infty} \int_{|y| \geq R} \frac{1}{(1+|y|^2)U^q} = 0$, we get that for R large

$$\begin{aligned} & \int \left| \nabla \left(\frac{\eta}{U^{q/2}} \right) \right|^2 - \int \frac{2|y|^\alpha}{U^3} \left(\frac{\eta}{U^{q/2}} \right)^2 \\ & \leq -\frac{8q + 8 - q^2}{4(q+1)} \int_{B_1(0)} \frac{|y|^\alpha}{U^{q+3}} + O\left(\int_{|y| \geq R} \frac{1}{(1+|y|^2)U^q} \right) < 0. \end{aligned}$$

A contradiction to (3.3.9). Hence, (3.3.8) holds and the proof of the first part of Theorem 3.3.3 is complete.

We now deal with the second part of Theorem 3.3.3. Consider the minimal solution u_n of $(S)_{\lambda_n}$ as $\lambda_n \rightarrow \lambda^*$ on the unit ball with $f(x) = |x|^\alpha$. Using the density of $C_0^\infty(\Omega)$ in $H_0^1(\Omega)$, Theorem 2.5.1 gives

$$\int_B \left(|\nabla \phi_n|^2 - \frac{2\lambda_n |x|^\alpha}{(1-u_n)^3} \phi_n^2 \right) dx \geq 0 \quad \forall \phi_n \in C_0^\infty(\Omega).$$

In view of the rescaled function (3.3.4), we now define

$$\phi_n(x) = \left(\varepsilon_n^{\frac{3}{2+\alpha}} \lambda_n^{-\frac{1}{2+\alpha}} \right)^{-\frac{N-2}{2}} \phi \left(\varepsilon_n^{-\frac{3}{2+\alpha}} \lambda_n^{\frac{1}{2+\alpha}} x \right).$$

Then we have

$$\begin{aligned} \int \left(|\nabla \phi|^2 - \frac{2|y|^\alpha}{U^3} \phi^2 \right) dy &= \lim_{n \rightarrow \infty} \int \left(|\nabla \phi_n|^2 - \frac{2|y|^\alpha}{U_n^3} \phi_n^2 \right) dy \\ &= \lim_{n \rightarrow \infty} \int_B \left(|\nabla \phi_n|^2 - \frac{2\lambda_n |x|^\alpha}{(1-u_n)^3} \phi_n^2 \right) dx \geq 0, \end{aligned}$$

since ϕ has compact support and $U_n \rightarrow U$ in $C_{\text{loc}}^1(\mathbb{R}^N)$. This completes the proof of Theorem 3.3.3. \blacksquare

Proof of Proposition 3.3.2: Let $R > 0$. For n large, decompose $U_n = U_n^1 + U_n^2$, where U_n^2 satisfies:

$$\begin{cases} \Delta U_n^2 = \Delta U_n & \text{in } B_R(0), \\ U_n^2 = 0 & \text{on } \partial B_R(0). \end{cases}$$

By (3.3.5) we get that on $B_R(0)$:

$$0 \leq \Delta U_n \leq R^\alpha \|g\|_\infty,$$

and standard elliptic regularity theory gives that U_n^2 is uniformly bounded in $C^{1,\beta}(B_R(0))$ for some $\beta \in (0, 1)$. Up to a subsequence, we get that $U_n^2 \rightarrow U^2$ in $C^1(B_R(0))$. Since $U_n^1 = U_n \geq 1$ on $\partial B_R(0)$, by harmonicity $U_n^1 \geq 1$ in $B_R(0)$ and then the Harnack inequality gives

$$\sup_{B_{R/2}(0)} U_n^1 \leq C_R \inf_{B_{R/2}(0)} U_n^1 \leq C_R U_n^1(0) = C_R(1 - U_n^2(0)) \leq C_R(1 + \sup_{n \in \mathbb{N}} |U_n^2(0)|) < \infty.$$

Hence, U_n^1 is uniformly bounded in $C^{1,\beta}(B_{R/4}(0))$ for some $\beta \in (0, 1)$. Up to a further subsequence, we get that $U_n^1 \rightarrow U^1$ in $C^1(B_{R/4}(0))$ and then, $U_n \rightarrow U^1 + U^2$ in $C^1(B_{R/4}(0))$ for any $R > 0$. By a diagonal process and up to a subsequence, we find that $U_n \rightarrow U$ in $C_{\text{loc}}^1(\mathbb{R}^N)$, where U is a solution of the equation (3.3.6).

If either $1 \leq N \leq 7$ or $N \geq 8$ and $\alpha > \alpha_N$, since $g(0) > 0$ Theorem 3.3.3 shows that $\mu_1(U) < 0$ and then, we find $\phi \in C_0^\infty(\mathbb{R}^N)$ so that:

$$\int (|\nabla \phi|^2 - 2g(0) \frac{|y|^\alpha}{U^3} \phi^2) < 0.$$

Defining now

$$\phi_n(x) = (\varepsilon_n^{\frac{3}{2+\alpha}} \lambda_n^{-\frac{1}{2+\alpha}})^{-\frac{N-2}{2}} \phi(\varepsilon_n^{-\frac{3}{2+\alpha}} \lambda_n^{\frac{1}{2+\alpha}} x),$$

then we have

$$\begin{aligned} \int_B (|\nabla \phi_n|^2 - \frac{2\lambda_n |x|^\alpha g(x)}{(1-u_n)^3} \phi_n^2) &= \int (|\nabla \phi|^2 - \frac{2|y|^\alpha}{U_n^3} g(\varepsilon_n^{\frac{3}{2+\alpha}} \lambda_n^{-\frac{1}{2+\alpha}} y) \phi^2) \\ &\rightarrow \int (|\nabla \phi|^2 - 2g(0) \frac{|y|^\alpha}{U^3} \phi^2) < 0 \end{aligned}$$

as $n \rightarrow +\infty$, since ϕ has compact support and $U_n \rightarrow U$ in $C_{\text{loc}}^1(\mathbb{R}^N)$. The proof of Proposition 3.3.2 is now complete. \blacksquare

3.4 Compactness along the second branch

In this section, we are interested in continuing the second branch till the second bifurcation point, by means of the implicit function theorem. Our main result of this section is the compactness of Theorem 3.1.3 for $2 \leq N \leq 7$.

In order to prove Theorem 3.1.3, we now assume that $f \in C(\bar{\Omega})$ is in the form (3.1.3), and let $(u_n)_n$ be a solution sequence for $(S)_{\lambda_n}$ where $\lambda_n \rightarrow \lambda \in [0, \lambda^*]$.

3.4.1 Blow-up analysis

Assume that the sequence $(u_n)_n$ is not compact, which means that up to passing to a subsequence, we may assume that $\max_{\Omega} u_n \rightarrow 1$ as $n \rightarrow \infty$. Let x_n be a maximum point of u_n in Ω (i.e., $u_n(x_n) = \max_{\Omega} u_n$) and set $\varepsilon_n = 1 - u_n(x_n)$. Let us assume that $x_n \rightarrow p$ as $n \rightarrow +\infty$. We have three different situations depending on the location of p and the rate of $|x_n - p|$:

- 1) blow up outside the zero set $\{p_1, \dots, p_k\}$ of $f(x)$, i.e. $p \notin \{p_1, \dots, p_k\}$;
- 2) "slow" blow up at some p_i in the zero set of $f(x)$, i.e. $x_n \rightarrow p_i$ and $\varepsilon_n^{-3} \lambda_n |x_n - p_i|^{\alpha+2} \rightarrow +\infty$ as $n \rightarrow +\infty$;

3) "fast" blow at some p_i in the zero set of $f(x)$, i.e. $x_n \rightarrow p_i$ and $\lim_{n \rightarrow +\infty} \sup(\varepsilon_n^{-3} \lambda_n |x_n - p_i|^{\alpha+2}) < +\infty$.

Accordingly, for $2 \leq N \leq 7$ we next discuss each one of these situations.

1st Case Assume that $p \notin \{p_1, \dots, p_k\}$. In general, we are not able to prove that a blow up point p is always far away from $\partial\Omega$, even though we suspect it to be true. However, the following weaker estimate is available and –as explained later– will be sufficient for our purposes.

Lemma 3.4.1. *Let h_n be a function on a smooth bounded domain A_n in \mathbb{R}^N . Let W_n be a solution of the problem*

$$\begin{cases} \Delta W_n = \frac{h_n(x)}{W_n^2} & \text{in } A_n, \\ W_n(y) \geq C > 0 & \text{in } A_n, \\ W_n(0) = 1, \end{cases} \quad (3.4.1)$$

for some $C > 0$. Assume that $\sup_{n \in \mathbb{N}} \|h_n\|_\infty < +\infty$ and $A_n \rightarrow T_\mu$ as $n \rightarrow +\infty$ for some $\mu \in (0, +\infty)$, where T_μ is a hyperspace so that $0 \in T_\mu$ and $\text{dist}(0, \partial T_\mu) = \mu$. Then for sufficiently large n , either

$$\inf_{\partial A_n \cap B_{2\mu}(0)} W_n \leq C \quad (3.4.2)$$

or

$$\inf_{\partial A_n \cap B_{2\mu}(0)} \partial_\nu W_n \leq 0, \quad (3.4.3)$$

where ν is the unit outward normal of A_n .

Proof: Assume that $\partial_\nu W_n > 0$ on $\partial A_n \cap B_{2\mu}(0)$. Let

$$G(x) = \begin{cases} -\frac{1}{2\pi} \log \frac{|x|}{2\mu} & \text{if } N = 2 \\ c_N \left(\frac{1}{|x|^{N-2}} - \frac{1}{(2\mu)^{N-2}} \right) & \text{if } N \geq 3 \end{cases}$$

be the Green function of the operator $-\Delta$ in $B_{2\mu}(0)$ with homogeneous Dirichlet boundary condition, where $c_N = \frac{1}{(N-2)|\partial B_1(0)|}$ and $|\cdot|$ stands for the Lebesgue measure.

Here and in the sequel, when there is no ambiguity on the domain, ν and dS will denote the unit outward normal and the boundary integration element of the corresponding domain. By the representation formula we have that:

$$\begin{aligned} W_n(0) = & - \int_{A_n \cap B_{2\mu}(0)} \Delta W_n(x) G(x) dx - \int_{\partial A_n \cap B_{2\mu}(0)} W_n(x) \partial_\nu G(x) dS \\ & + \int_{\partial A_n \cap B_{2\mu}(0)} \partial_\nu W_n(x) G(x) dS - \int_{\partial B_{2\mu}(0) \cap A_n} W_n(x) \partial_\nu G(x) dS. \end{aligned} \quad (3.4.4)$$

Note that on ∂T_μ we have

$$-\partial_\nu G(x) = \begin{cases} \frac{1}{2\pi} \frac{x}{|x|^2} \cdot \nu > 0 & \text{if } N = 2; \\ (N-2)c_N \frac{x}{|x|^N} \cdot \nu > 0 & \text{if } N \geq 3. \end{cases} \quad (3.4.5)$$

Since $\partial A_n \rightarrow \partial T_\mu$ as $n \rightarrow \infty$, it yields that for sufficiently large n ,

$$\partial_\nu G(x) \leq 0 \quad \text{on } \partial A_n \cap B_{2\mu}(0). \quad (3.4.6)$$

Hence, by (3.4.4), (3.4.6) and the assumptions on W_n , we then get for sufficiently large n ,

$$1 \geq - \int_{A_n \cap B_{2\mu}(0)} \frac{h_n(x)}{W_n^2(x)} G(x) dx - \left(\inf_{\partial A_n \cap B_{2\mu}(0)} W_n \right) \int_{\partial A_n \cap B_{2\mu}(0)} \partial_\nu G(x) dS,$$

since $G(x) \geq 0$ in $B_{2\mu}(0)$ and $\partial_\nu G(x) \leq 0$ on $\partial B_{2\mu}(0)$. On the other hand, we have

$$\left| \int_{A_n \cap B_{2\mu}(0)} \frac{h_n(x)}{W_n^2(x)} G(x) \right| \leq C,$$

and (3.4.5) also implies that for sufficiently large n ,

$$- \int_{\partial A_n \cap B_{2\mu}(0)} \partial_\nu G(x) d\sigma(x) \rightarrow - \int_{\partial T_\mu \cap B_{2\mu}(0)} \partial_\nu G(x) dS > 0.$$

Then for sufficiently large n , $1 \geq -C + C^{-1} \left(\inf_{\partial A_n \cap B_{2\mu}(0)} W_n \right)$ for some $C > 0$ large enough. Therefore, we conclude that for sufficiently large n , $\inf_{\partial A_n \cap B_{2\mu}(0)} W_n$ is bounded and the proof is complete. \blacksquare

We are now ready to completely discuss this first case. Introduce the following rescaled function:

$$U_n(y) = \frac{1 - u_n(\varepsilon_n^{\frac{3}{2}} \lambda_n^{-\frac{1}{2}} y + x_n)}{\varepsilon_n}, \quad y \in \Omega_n = \frac{\Omega - x_n}{\varepsilon_n^{\frac{3}{2}} \lambda_n^{-\frac{1}{2}}}, \quad (3.4.7)$$

then U_n satisfies

$$\begin{cases} \Delta U_n = \frac{f(\varepsilon_n^{\frac{3}{2}} \lambda_n^{-\frac{1}{2}} y + x_n)}{U_n^2} & \text{in } \Omega_n, \\ U_n(0) = 1 & \text{in } \Omega_n. \end{cases} \quad (3.4.8)$$

In addition, we have that $U_n \geq U_n(0) = 1$ as long as x_n is the maximum point of u_n in Ω .

We would like to prove the following:

Proposition 3.4.2. *Let $x_n \in \Omega$ and $\varepsilon_n := 1 - u_n(x_n)$, and assume*

$$x_n \rightarrow p \notin \{p_1, \dots, p_k\}, \quad \varepsilon_n^3 \lambda_n^{-1} \rightarrow 0 \quad \text{as } n \rightarrow +\infty. \quad (3.4.9)$$

Let U_n and Ω_n be defined as in (3.4.7) satisfying

$$U_n \geq C > 0 \quad \text{in } \Omega_n \cap B_{R_n}(0) \quad (3.4.10)$$

for some $R_n \rightarrow +\infty$ as $n \rightarrow +\infty$. Then, there exists a subsequence of $(U_n)_n$ such that $U_n \rightarrow U$ in $C_{loc}^1(\mathbb{R}^N)$, where U is a solution of the problem

$$\begin{cases} \Delta U = \frac{f(p)}{U^2} & \text{in } \mathbb{R}^N, \\ U(y) \geq C > 0 & \text{in } \mathbb{R}^N. \end{cases} \quad (3.4.11)$$

Moreover, there exists a function $\phi_n \in C_0^\infty(\Omega)$ such that

$$\int_{\Omega} (|\nabla \phi_n|^2 - \frac{2\lambda_n f(x)}{(1-u_n)^3} \phi_n^2) < 0, \quad (3.4.12)$$

and $\text{Supp } \phi_n \subset B_{M\varepsilon_n^{\frac{3}{2}}\lambda_n^{-\frac{1}{2}}}(x_n)$ for some $M > 0$.

Proof: We first claim that Lemma 3.4.1 provides us with a stronger estimate:

$$\varepsilon_n^3 \lambda_n^{-1} (\text{dist}(x_n, \partial\Omega))^{-2} \rightarrow 0 \quad \text{as } n \rightarrow +\infty. \quad (3.4.13)$$

Indeed, by contradiction and up to a subsequence, assume that $\varepsilon_n^3 \lambda_n^{-1} d_n^{-2} \rightarrow \delta > 0$ as $n \rightarrow +\infty$, where $d_n := \text{dist}(x_n, \partial\Omega)$. We get from (3.4.9) that $d_n \rightarrow 0$ as $n \rightarrow +\infty$. We introduce the following rescaling W_n :

$$W_n(y) = \frac{1 - u_n(d_n y + x_n)}{\varepsilon_n}, \quad y \in A_n = \frac{\Omega - x_n}{d_n}.$$

Since $d_n \rightarrow 0$, we get that $A_n \rightarrow T_\mu$ as $n \rightarrow +\infty$, where T_μ is a hyperspace containing 0 so that $\text{dist}(0, \partial T_\mu) = \mu$. The function W_n solves problem (3.4.1) with $h_n(y) = \frac{\lambda_n d_n^2}{\varepsilon_n^3} f(d_n y + x_n)$ and $C = W_n(0) = 1$. We have that:

$$\|h_n\|_\infty \leq \frac{\lambda_n d_n^2}{\varepsilon_n^3} \|f\|_\infty \leq \frac{2}{\delta} \|f\|_\infty$$

and $W_n = \frac{1}{\varepsilon_n} \rightarrow +\infty$ on ∂A_n as $n \rightarrow \infty$. By Lemma 3.4.1 we get that (3.4.3) must hold, a contradiction to Hopf Lemma applied to u_n . This gives the validity of (3.4.13).

(3.4.13) now implies that $\Omega_n \rightarrow \mathbb{R}^N$ as $n \rightarrow +\infty$. Arguing as in the proof of Proposition 3.3.2, we get that $U_n \rightarrow U$ in $C_{\text{loc}}^1(\mathbb{R}^N)$, where U is a solution of (3.4.11) by means of (3.4.8)-(3.4.10).

If $2 \leq N \leq 7$, since $f(p) > 0$ by Theorem 3.3.3 we get that $\mu_1(U) < 0$ and then, we find $\phi \in C_0^\infty(\mathbb{R}^N)$ so that:

$$\int (|\nabla \phi|^2 - \frac{2f(p)}{U^3} \phi^2) < 0.$$

Defining now $\phi_n(x) = (\varepsilon_n^{\frac{3}{2}} \lambda_n^{-\frac{1}{2}})^{-\frac{N-2}{2}} \phi(\varepsilon_n^{-\frac{3}{2}} \lambda_n^{\frac{1}{2}}(x - x_n))$, then we have

$$\begin{aligned} \int_{\Omega} (|\nabla \phi_n|^2 - \frac{2\lambda_n f(x)}{(1-u_n)^3} \phi_n^2) &= \int (|\nabla \phi|^2 - \frac{2f(\varepsilon_n^{\frac{3}{2}} \lambda_n^{-\frac{1}{2}} y + x_n)}{U_n^3} \phi^2) \\ &\rightarrow \int (|\nabla \phi|^2 - \frac{2f(p)}{U^3} \phi^2) < 0 \end{aligned}$$

as $n \rightarrow +\infty$, since ϕ has compact support and $U_n \rightarrow U$ in $C_{\text{loc}}^1(\mathbb{R})$. The proof of Proposition 3.4.2 is now complete. \blacksquare

2nd Case Assume that $x_n \rightarrow p_i$ and $\varepsilon_n^{-3} \lambda_n |x_n - p_i|^{\alpha_i+2} \rightarrow +\infty$ as $n \rightarrow +\infty$. For convenience, in the following we denote

$$\alpha := \alpha_i, \quad f_i(x) := \left(\prod_{j=1, j \neq i}^k |x - p_j|^{\alpha_j} \right) g(x), \quad (3.4.14)$$

and we rescale the function u_n in a different way:

$$U_n(y) = \frac{1 - u_n(\varepsilon_n^{\frac{3}{2}} \lambda_n^{-\frac{1}{2}} |x_n - p_i|^{-\frac{\alpha}{2}} y + x_n)}{\varepsilon_n}, \quad y \in \Omega_n = \frac{\Omega - x_n}{\varepsilon_n^{\frac{3}{2}} \lambda_n^{-\frac{1}{2}} |x_n - p_i|^{-\frac{\alpha}{2}}}. \quad (3.4.15)$$

In this situation, U_n satisfies:

$$\begin{cases} \Delta U_n = |\varepsilon_n^{\frac{3}{2}} \lambda_n^{-\frac{1}{2}} |x_n - p_i|^{-\frac{\alpha+2}{2}} y + \frac{x_n - p_i}{|x_n - p_i|} |^{\alpha} \frac{f_i(\varepsilon_n^{\frac{3}{2}} \lambda_n^{-\frac{1}{2}} |x_n - p_i|^{-\frac{\alpha}{2}} y + x_n)}{U_n^2} & \text{in } \Omega_n, \\ U_n(0) = 1 & \text{in } \Omega_n, \end{cases} \quad (3.4.16)$$

and we have the following

Proposition 3.4.3. *Let $x_n \in \Omega$ and $\varepsilon_n := 1 - u_n(x_n)$, and assume*

$$x_n \rightarrow p_i, \quad \varepsilon_n^{-3} \lambda_n |x_n - p_i|^{\alpha+2} \rightarrow +\infty \quad \text{as } n \rightarrow +\infty. \quad (3.4.17)$$

Let U_n and Ω_n be defined as in (3.4.15) satisfying (3.4.10). Then, up to a subsequence, $U_n \rightarrow U$ in $C_{loc}^1(\mathbb{R}^N)$, where U is a solution of the equation:

$$\begin{cases} \Delta U = \frac{f_i(p_i)}{U^2} & \text{in } \mathbb{R}^N, \\ U(y) \geq C > 0 & \text{in } \mathbb{R}^N. \end{cases} \quad (3.4.18)$$

Moreover, there holds (3.4.12) for some $\phi_n \in C_0^\infty(\Omega)$ such that

$$\text{Supp } \phi_n \subset B_{M \varepsilon_n^{\frac{3}{2}} \lambda_n^{-\frac{1}{2}} |x_n - p_i|^{-\frac{\alpha}{2}}}(x_n) \quad \text{for some } M > 0.$$

Proof: Similar to Proposition 3.4.2 we get from (3.4.17) that $\Omega_n \rightarrow \mathbb{R}^N$ as $n \rightarrow +\infty$. As before, $U_n \rightarrow U$ in $C_{loc}^1(\mathbb{R}^N)$ and U is a solution of (3.4.18) in view of (3.4.10) and (3.4.16)-(3.4.17). Since $2 \leq N \leq 7$ and $f_i(p_i) > 0$, Theorem 3.3.3 implies $\mu_1(U) < 0$ and the existence of some $\phi \in C_0^\infty(\mathbb{R}^N)$ so that:

$$\int (|\nabla \phi|^2 - \frac{2f_i(p_i)}{U^3} \phi^2) < 0.$$

Defining now $\phi_n(x) = (\varepsilon_n^{\frac{3}{2}} \lambda_n^{-\frac{1}{2}} |x_n - p_i|^{-\frac{\alpha}{2}})^{-\frac{N-2}{2}} \phi(\varepsilon_n^{-\frac{3}{2}} \lambda_n^{\frac{1}{2}} |x_n - p_i|^{\frac{\alpha}{2}} (x - x_n))$, then we have

$$\begin{aligned} & \int_{\Omega} (|\nabla \phi_n|^2 - \frac{2\lambda_n f(x)}{(1 - u_n)^3} \phi_n^2) \\ &= \int (|\nabla \phi|^2 - |\varepsilon_n^{\frac{3}{2}} \lambda_n^{-\frac{1}{2}} |x_n - p_i|^{-\frac{\alpha+2}{2}} y + \frac{x_n - p_i}{|x_n - p_i|} |^{\alpha} \frac{2f_i(\varepsilon_n^{\frac{3}{2}} \lambda_n^{-\frac{1}{2}} |x_n - p_i|^{-\frac{\alpha}{2}} y + x_n)}{U_n^3} \phi^2) \\ &\rightarrow \int (|\nabla \phi|^2 - \frac{2f_i(p_i)}{U^3} \phi^2) < 0 \end{aligned}$$

as $n \rightarrow +\infty$, which completes the proof of Proposition 3.4.3. ■

3rd Case Assume that $x_n \rightarrow p_i$ as $n \rightarrow +\infty$ and $\varepsilon_n^{-3}\lambda_n|x_n - p_i|^{\alpha_i+2} \leq C$. In the following we denote $\alpha := \alpha_i$, and we rescale the function u_n in a still different way:

$$U_n(y) = \frac{1 - u_n(\varepsilon_n^{\frac{3}{2+\alpha}} \lambda_n^{-\frac{1}{2+\alpha}} y + x_n)}{\varepsilon_n}, \quad y \in \Omega_n = \frac{\Omega - x_n}{\varepsilon_n^{\frac{3}{2+\alpha}} \lambda_n^{-\frac{1}{2+\alpha}}}. \quad (3.4.19)$$

Then U_n satisfies

$$\begin{cases} \Delta U_n = |y + \varepsilon_n^{-\frac{3}{2+\alpha}} \lambda_n^{\frac{1}{2+\alpha}} (x_n - p_i)|^\alpha \frac{f_i(\varepsilon_n^{\frac{3}{2+\alpha}} \lambda_n^{-\frac{1}{2+\alpha}} y + x_n)}{U_n^2} & \text{in } \Omega_n, \\ U_n(0) = 1 & \text{in } \Omega_n, \end{cases} \quad (3.4.20)$$

where f_i is defined in (3.4.14).

In this situation, the result we have is the following

Proposition 3.4.4. *Let $x_n \in \Omega$ and $\varepsilon_n := 1 - u_n(x_n)$, and assume*

$$\varepsilon_n^3 \lambda_n^{-1} \rightarrow 0, \quad x_n \rightarrow p_i, \quad \varepsilon_n^{-\frac{3}{\alpha+2}} \lambda_n^{\frac{1}{\alpha+2}} (x_n - p_i) \rightarrow y_0 \quad \text{as } n \rightarrow +\infty. \quad (3.4.21)$$

Let U_n and Ω_n be defined as in (3.4.19) satisfying either (3.4.10) or

$$U_n \geq C (\varepsilon_n^{-\frac{3}{\alpha+2}} \lambda_n^{\frac{1}{\alpha+2}} |x_n - p_i|)^{-\frac{\alpha}{3}} |y + \varepsilon_n^{-\frac{3}{\alpha+2}} \lambda_n^{\frac{1}{\alpha+2}} (x_n - p_i)|^{\frac{\alpha}{3}} \quad \text{in } \Omega_n \cap B_{R_n}(0) \quad (3.4.22)$$

for some $R_n \rightarrow +\infty$ as $n \rightarrow +\infty$ and $C > 0$. Then, up to a subsequence, $U_n \rightarrow U$ in $C_{loc}^1(\mathbb{R}^N)$ and U satisfies:

$$\begin{cases} \Delta U = |y + y_0|^\alpha \frac{f_i(p_i)}{U^2} & \text{in } \mathbb{R}^N, \\ U(y) \geq C > 0 & \text{in } \mathbb{R}^N. \end{cases} \quad (3.4.23)$$

Moreover, we have (3.4.12) for some function $\phi_n \in C_0^\infty(\Omega)$ such that

$$\text{Supp } \phi_n \subset B_{M\varepsilon_n^{\frac{3}{2+\alpha}} \lambda_n^{-\frac{1}{2+\alpha}}}(x_n) \quad \text{for some } M > 0.$$

Proof: By (3.4.21) we get again that $\Omega_n \rightarrow \mathbb{R}^N$ as $n \rightarrow +\infty$. If (3.4.10) holds, as before we have $U_n \rightarrow U$ in $C_{loc}^1(\mathbb{R}^N)$ and, by (3.4.10) and (3.4.20)-(3.4.21), U solves (3.4.23).

We need to discuss the non trivial case when we have the validity of (3.4.22). Arguing as in the proof of Proposition 3.3.2, fix $R > 2|y_0|$ and decompose $U_n = U_n^1 + U_n^2$, where U_n^2 satisfies:

$$\begin{cases} \Delta U_n^2 = \Delta U_n & \text{in } B_R(0), \\ U_n^2 = 0 & \text{on } \partial B_R(0). \end{cases}$$

By (3.4.20) and (3.4.22) we get that on $B_R(0)$:

$$\begin{aligned} 0 \leq \Delta U_n &= |y + \varepsilon_n^{-\frac{3}{2+\alpha}} \lambda_n^{\frac{1}{2+\alpha}} (x_n - p_i)|^\alpha \frac{f_i(\varepsilon_n^{\frac{3}{2+\alpha}} \lambda_n^{-\frac{1}{2+\alpha}} y + x_n)}{U_n^2} \\ &\leq C (\varepsilon_n^{-\frac{3}{\alpha+2}} \lambda_n^{\frac{1}{\alpha+2}} |x_n - p_i|)^{\frac{2\alpha}{3}} |y + \varepsilon_n^{-\frac{3}{2+\alpha}} \lambda_n^{\frac{1}{2+\alpha}} (x_n - p_i)|^{\frac{\alpha}{3}}. \end{aligned}$$

Since $\varepsilon_n^{-\frac{3}{\alpha+2}} \lambda_n^{\frac{1}{\alpha+2}}(x_n - p_i)$ is bounded, we get that $0 \leq \Delta U_n \leq C_R$ on $B_R(0)$ for n large, and then, standard elliptic regularity theory gives that U_n^2 is uniformly bounded in $C^{1,\beta}(B_R(0))$ for some $\beta \in (0, 1)$. Up to a subsequence, we get that $U_n^2 \rightarrow U^2$ in $C^1(B_R(0))$. Since by (3.4.22) $U_n^1 = U_n \geq C(R - 2|y_0|)^{\frac{\alpha}{3}} > 0$ on $\partial B_R(0)$, by harmonicity $U_n^1 \geq C_R$ in $B_R(0)$ and hence the Harnack inequality gives

$$\begin{aligned} \sup_{B_{R/2}(0)} U_n^1 &\leq C_R \inf_{B_{R/2}(0)} U_n^1 \leq C_R U_n^1(0) = C_R(1 - U_n^2(0)) \\ &\leq C_R(1 + \sup_{n \in \mathbb{N}} |U_n^2(0)|) < \infty. \end{aligned}$$

Therefore, U_n^1 is uniformly bounded in $C^{1,\beta}(B_{R/4}(0))$, $\beta \in (0, 1)$. Up to a further subsequence, we get that $U_n^1 \rightarrow U^1$ in $C^1(B_{R/4}(0))$ and then, $U_n \rightarrow U^1 + U^2$ in $C^1(B_{R/4}(0))$ for any $R > 0$. By a diagonal process and up to a subsequence, by (3.4.22) we find that $U_n \rightarrow U$ in $C_{\text{loc}}^1(\mathbb{R}^N)$, where $U \in C^1(\mathbb{R}^N) \cap C^2(\mathbb{R}^N \setminus \{-y_0\})$ is a solution of the equation

$$\begin{cases} \Delta U = |y + y_0|^\alpha \frac{f_i(p_i)}{U^2} & \text{in } \mathbb{R}^N \setminus \{-y_0\}, \\ U(y) \geq C|y + y_0|^{\frac{\alpha}{3}} & \text{in } \mathbb{R}^N, \end{cases}$$

for some $C > 0$. In order to prove that U is a solution of (3.4.23), we still need to prove that $U(-y_0) > 0$. Let B be some ball so that $-y_0 \in \partial B$ and assume by contradiction that $U(-y_0) = 0$. Since

$$-\Delta U + c(y)U = 0 \text{ in } B, \quad U \in C^2(B) \cap C(\bar{B}), \quad U(y) > U(-y_0) \text{ in } B,$$

and $c(y) = f_i(p_i) \frac{|y+y_0|^\alpha}{U^3} \geq 0$ is a bounded function, Hopf Lemma shows that $\partial_\nu U(-y_0) < 0$, where ν is the unit outward normal of B at $-y_0$. Hence, U becomes negative in a neighborhood of $-y_0$, in contradiction with the positivity of U . Hence, $U(-y_0) > 0$ and U satisfies (3.4.23).

Since $2 \leq N \leq 7$ and $f_i(p_i) > 0$, Theorem 3.3.3 implies $\mu_1(U) < 0$ and the existence of some $\phi \in C_0^\infty(\mathbb{R}^N)$ so that:

$$\int (|\nabla \phi|^2 - |y + y_0|^\alpha \frac{2f_i(p_i)}{U^3} \phi^2) < 0.$$

Let $\phi_n(x) = (\varepsilon_n^{\frac{3}{2+\alpha}} \lambda_n^{-\frac{1}{2+\alpha}})^{-\frac{N-2}{2}} \phi(\varepsilon_n^{-\frac{3}{2+\alpha}} \lambda_n^{\frac{1}{2+\alpha}}(x - x_n))$, then it reduces to

$$\begin{aligned} &\int_{\Omega} (|\nabla \phi_n|^2 - \frac{2\lambda_n f(x)}{(1-u_n)^3} \phi_n^2) \\ &= \int (|\nabla \phi|^2 - |y + \varepsilon_n^{-\frac{3}{2+\alpha}} \lambda_n^{\frac{1}{2+\alpha}}(x_n - p_i)|^\alpha \frac{2f_i(\varepsilon_n^{\frac{3}{2+\alpha}} \lambda_n^{-\frac{1}{2+\alpha}} y + x_n)}{U_n^3} \phi^2) \\ &\rightarrow \int (|\nabla \phi|^2 - |y + y_0|^\alpha \frac{2f_i(p_i)}{U^3} \phi^2) < 0 \end{aligned}$$

as $n \rightarrow +\infty$, and Proposition 3.4.4 is established. ■

3.4.2 Spectral confinement

Let us now assume the validity of (3.1.4), namely $\mu_{2,n} := \mu_{2,\lambda_n}(u_n) \geq 0$ for any $n \in \mathbb{N}$. This information will play a crucial role in controlling the number k of “blow up points” (for $(1 - u_n)^{-1}$) in terms of the spectral information on u_n . Indeed, roughly speaking, we can estimate k with the number of negative eigenvalues of L_{u_n,λ_n} (with multiplicities). In particular, assumption (3.1.4) implies that “blow up” can occur only along the sequence x_n of maximum points of u_n in Ω .

Proposition 3.4.5. *Assume $2 \leq N \leq 7$, and suppose $f \in C(\bar{\Omega})$ is as in (3.1.3). Let $\lambda_n \rightarrow \lambda \in [0, \lambda^*]$ and u_n be an associated solution. Assume that $u_n(x_n) = \max_{\Omega} u_n \rightarrow 1$ as $n \rightarrow +\infty$. Then, there exist constants $C > 0$ and $N_0 \in \mathbb{N}$ such that*

$$(1 - u_n(x)) \geq C \lambda_n^{\frac{1}{3}} d(x)^{\frac{\alpha}{3}} |x - x_n|^{\frac{2}{3}}, \quad \forall x \in \Omega, \quad n \geq N_0, \quad (3.4.24)$$

where $d(x)^{\frac{\alpha}{3}} = \min\{|x - p_i|^{\frac{\alpha}{3}} : i = 1, \dots, k\}$ is the distance function from the zero set $\{p_1, \dots, p_k\}$ of $f(x)$.

Proof: Let $\varepsilon_n = 1 - u_n(x_n)$. Then, $\varepsilon_n \rightarrow 0$ as $n \rightarrow +\infty$ and, even more precisely:

$$\varepsilon_n^2 \lambda_n^{-1} \rightarrow 0 \quad \text{as } n \rightarrow +\infty. \quad (3.4.25)$$

Indeed, otherwise we would have along some subsequence:

$$0 \leq \frac{\lambda_n f(x)}{(1 - u_n)^2} \leq \frac{\lambda_n}{\varepsilon_n^2} \|f\|_{\infty} \leq C, \quad \lambda_n \rightarrow 0 \text{ as } n \rightarrow +\infty.$$

But if the right hand side of $(S)_{\lambda_n}$ is uniformly bounded, then elliptic regularity theory implies that u_n is uniformly bounded in $C^{1,\beta}(\bar{\Omega})$ for some $\beta \in (0, 1)$. Hence, up to a further subsequence, $u_n \rightarrow u$ in $C^1(\bar{\Omega})$, where u is a harmonic function such that $u = 0$ on $\partial\Omega$, and hence $u \equiv 0$ on Ω . On the other hand, $\varepsilon_n \rightarrow 0$ implies that $\max_{\Omega} u = 1$, a contradiction.

By (3.4.25) we get that $\varepsilon_n^3 \lambda_n^{-1} \rightarrow 0$ as $n \rightarrow +\infty$, as needed in (3.4.9) and (3.4.21) for Propositions 3.4.2 and 3.4.4, respectively. Now, depending on the case corresponding to the blow up sequence x_n , we can apply one among Propositions 3.4.2 and 3.4.4 to obtaining the existence of a function $\phi_n \in C_0^{\infty}(\Omega)$ such that (3.4.12) holds, together with a specific control on $\text{Supp } \phi_n$.

By contradiction, assume now that (3.4.24) is false: up to a subsequence, then there exists a sequence $y_n \in \Omega$ such that

$$\begin{aligned} & \lambda_n^{-\frac{1}{3}} d(y_n)^{-\frac{\alpha}{3}} |y_n - x_n|^{-\frac{2}{3}} (1 - u_n(y_n)) \\ &= \lambda_n^{-\frac{1}{3}} \min_{x \in \Omega} \left(d(x)^{-\frac{\alpha}{3}} |x - x_n|^{-\frac{2}{3}} (1 - u_n(x)) \right) \rightarrow 0 \quad \text{as } n \rightarrow +\infty. \end{aligned} \quad (3.4.26)$$

Then, $\mu_n := 1 - u_n(y_n) \rightarrow 0$ as $n \rightarrow \infty$ and (3.4.26) can be rewritten as:

$$\frac{\mu_n^{\frac{3}{2}} \lambda_n^{-\frac{1}{2}}}{|x_n - y_n| d(y_n)^{\frac{\alpha}{2}}} \rightarrow 0 \quad \text{as } n \rightarrow +\infty. \quad (3.4.27)$$

We now want to explain the meaning of the crucial choice (3.4.26). Let β_n be a sequence of positive numbers so that

$$R_n := \beta_n^{-\frac{1}{2}} \min\{d(y_n)^{\frac{1}{2}}, |x_n - y_n|^{\frac{1}{2}}\} \rightarrow +\infty \quad \text{as } n \rightarrow +\infty. \quad (3.4.28)$$

Let us introduce the following rescaled function:

$$\hat{U}_n(y) = \frac{1 - u_n(\beta_n y + y_n)}{\mu_n}, \quad y \in \hat{\Omega}_n = \frac{\Omega - y_n}{\beta_n}.$$

Formula (3.4.26) implies:

$$\begin{aligned} \mu_n &= d(y_n)^{\frac{\alpha}{3}} |y_n - x_n|^{\frac{2}{3}} \min_{x \in \Omega} \left(d(x)^{-\frac{\alpha}{3}} |x - x_n|^{-\frac{2}{3}} (1 - u_n(x)) \right) \\ &\leq \mu_n d(y_n)^{\frac{\alpha}{3}} |y_n - x_n|^{\frac{2}{3}} d(\beta_n y + y_n)^{-\frac{\alpha}{3}} |\beta_n y + y_n - x_n|^{-\frac{2}{3}} \hat{U}_n(y). \end{aligned}$$

Since

$$\frac{d(\beta_n y + y_n)}{d(y_n)} = \min\left\{ \left| \frac{y_n - p_i}{d(y_n)} + \frac{\beta_n}{d(y_n)} y \right| : i = 1, \dots, k \right\} \geq 1 - \frac{\beta_n}{d(y_n)} |y|$$

in view of $|y_n - p_i| \geq d(y_n)$, by (3.4.28) we get that:

$$\hat{U}_n(y) \geq \left(1 - \frac{\beta_n R_n}{d(y_n)}\right)^{\frac{\alpha}{3}} \left(1 - \frac{\beta_n R_n}{|x_n - y_n|}\right)^{\frac{2}{3}} \geq \left(\frac{1}{2}\right)^{\frac{2+\alpha}{3}}$$

for any $y \in \hat{\Omega}_n \cap B_{R_n}(0)$. Hence, whenever (3.4.28) holds, we get the validity of (3.4.10) for the rescaled function \hat{U}_n at y_n with respect to β_n .

We need to discuss all the possible types of blow up at y_n .

1st Case Assume that $y_n \rightarrow q \notin \{p_1, \dots, p_k\}$. By (3.4.27) we get that $\mu_n^3 \lambda_n^{-1} \rightarrow 0$ as $n \rightarrow +\infty$. Since $d(y_n) \geq C > 0$, let $\beta_n = \mu_n^{\frac{3}{2}} \lambda_n^{-\frac{1}{2}}$ and, by (3.4.27) we get that (3.4.28) holds. Associated to y_n, μ_n , define $\hat{U}_n, \hat{\Omega}_n$ as in (3.4.7). We have from above that (3.4.10) holds by the validity of (3.4.28) for our choice of β_n . Hence, Proposition 3.4.2 applied to \hat{U}_n gives the existence of $\psi_n \in C_0^\infty(\Omega)$ such that (3.4.12) holds and $\text{Supp } \psi_n \subset B_{M \mu_n^{\frac{3}{2}} \lambda_n^{-\frac{1}{2}}}(y_n)$ for some $M > 0$.

In the worst case $x_n \rightarrow q$, given U_n be as in (3.4.7) associated to x_n, ε_n , we get by scaling that for $x = \varepsilon_n^{\frac{3}{2}} \lambda_n^{-\frac{1}{2}} y + x_n$,

$$\begin{aligned} &\lambda_n^{-\frac{1}{3}} \left(d(x)^{-\frac{\alpha}{3}} |x - x_n|^{-\frac{2}{3}} (1 - u_n(x)) \right) \\ &\geq C \lambda_n^{-\frac{1}{3}} \left(|x - x_n|^{-\frac{2}{3}} (1 - u_n(x)) \right) = C |y|^{-\frac{2}{3}} U_n(y) \geq C_R > 0 \end{aligned}$$

uniformly in n and $y \in B_R(0)$ for any $R > 0$. Then,

$$\frac{\varepsilon_n^{\frac{3}{2}} \lambda_n^{-\frac{1}{2}}}{|x_n - y_n|} \rightarrow 0 \quad \text{as } n \rightarrow +\infty.$$

Hence, in this situation ϕ_n and ψ_n have disjoint compact supports and obviously, it remains true when $x_n \rightarrow p \neq q$. Hence, $\mu_{2,n} < 0$ in contradiction with (3.1.4).

2nd Case Assume that $y_n \rightarrow p_i$ in a "slow" way:

$$\mu_n^{-3} \lambda_n |y_n - p_i|^{\alpha+2} \rightarrow +\infty \quad \text{as } n \rightarrow +\infty.$$

Let now $\beta_n = \mu_n^{\frac{3}{2}} \lambda_n^{-\frac{1}{2}} |y_n - p_i|^{-\frac{\alpha}{2}}$. Since $d(y_n) = |y_n - p_i|$ in this situation, we get that:

$$\frac{d(y_n)}{\beta_n} = \mu_n^{-\frac{3}{2}} \lambda_n^{\frac{1}{2}} |y_n - p_i|^{\frac{\alpha+2}{2}} \rightarrow +\infty,$$

and (3.4.27) exactly gives

$$\frac{|x_n - y_n|}{\beta_n} = \frac{|x_n - y_n|}{\mu_n^{\frac{3}{2}} \lambda_n^{-\frac{1}{2}} |y_n - p_i|^{-\frac{\alpha}{2}}} \rightarrow +\infty \quad (3.4.29)$$

as $n \rightarrow +\infty$. Hence, (3.4.28) holds. Associated to μ_n, y_n , define now $\hat{U}_n, \hat{\Omega}_n$ according to (3.4.15). Since (3.4.10) follows by (3.4.28), Proposition 3.4.3 for \hat{U}_n gives some $\psi_n \in C_0^\infty(\Omega)$ such that (3.4.12) holds and $\text{Supp } \psi_n \subset B_{M\mu_n^{\frac{3}{2}} \lambda_n^{-\frac{1}{2}} |y_n - p_i|^{-\frac{\alpha}{2}}}(y_n)$ for some $M > 0$. If $x_n \rightarrow p \neq p_i$, then clearly ϕ_n, ψ_n have disjoint compact supports leading to $\mu_{2,n} < 0$ in contradiction with (3.1.4). If also $x_n \rightarrow p_i$, we can easily show by scaling that:

1) if $\varepsilon_n^{-3} \lambda_n |x_n - p_i|^{\alpha+2} \rightarrow +\infty$ as $n \rightarrow +\infty$, given U_n be as in (3.4.15) associated to x_n, ε_n , we get that for $x = \varepsilon_n^{\frac{3}{2}} \lambda_n^{-\frac{1}{2}} |x_n - p_i|^{-\frac{\alpha}{2}} y + x_n$,

$$\begin{aligned} & \lambda_n^{-\frac{1}{3}} (d(x)^{-\frac{\alpha}{3}} |x - x_n|^{-\frac{2}{3}} (1 - u_n(x))) \\ &= |y|^{-\frac{2}{3}} U_n(y) |\varepsilon_n^{\frac{3}{2}} \lambda_n^{-\frac{1}{2}} |x_n - p_i|^{-\frac{\alpha+2}{2}} y + \frac{x_n - p_i}{|x_n - p_i|} |^{-\frac{\alpha}{3}} \geq C_R > 0 \end{aligned}$$

uniformly in n and $y \in B_R(0)$ for any $R > 0$. Then,

$$\frac{\varepsilon_n^{\frac{3}{2}} \lambda_n^{-\frac{1}{2}} |x_n - p_i|^{-\frac{\alpha}{2}}}{|x_n - y_n|} \rightarrow 0 \quad \text{as } n \rightarrow +\infty,$$

and hence, by (3.4.29) ϕ_n and ψ_n have disjoint compact supports leading to $\mu_{2,n} < 0$, which contradicts (3.1.4).

2) if $\varepsilon_n^{-3} \lambda_n |x_n - p_i|^{\alpha+2} \leq C$ as $n \rightarrow +\infty$, given U_n be as in (3.4.19) associated to x_n, ε_n , we get that for $x = \varepsilon_n^{\frac{3}{2+\alpha}} \lambda_n^{-\frac{1}{2+\alpha}} y + x_n$,

$$\begin{aligned} \lambda_n^{-\frac{1}{3}} (d(x)^{-\frac{\alpha}{3}} |x - x_n|^{-\frac{2}{3}} (1 - u_n(x))) &= |y|^{-\frac{2}{3}} U_n(y) |y + \varepsilon_n^{-\frac{3}{2+\alpha}} \lambda_n^{\frac{1}{2+\alpha}} (x_n - p_i)|^{-\frac{\alpha}{3}} \\ &\geq D_R |y|^{-\frac{2}{3}} U_n(y) \geq C_R > 0 \end{aligned}$$

uniformly in n and $y \in B_R(0)$ for any $R > 0$. Then,

$$\frac{\varepsilon_n^{\frac{3}{2+\alpha}} \lambda_n^{-\frac{1}{2+\alpha}}}{|x_n - y_n|} \rightarrow 0 \quad \text{as } n \rightarrow +\infty,$$

and hence, by (3.4.29) ϕ_n and ψ_n have disjoint compact supports leading to a contradiction.

3rd Case Assume that $y_n \rightarrow p_i$ in a "fast" way:

$$\mu_n^{-3} \lambda_n |y_n - p_i|^{\alpha+2} \leq C.$$

Since $d(y_n) = |y_n - p_i|$, by (3.4.27) we get that

$$\frac{|y_n - p_i|}{|x_n - y_n|} = \frac{\mu_n^{\frac{3}{2}} \lambda_n^{-\frac{1}{2}}}{|x_n - y_n| |y_n - p_i|^{\frac{\alpha}{2}}} (\mu_n^{-3} \lambda_n |y_n - p_i|^{\alpha+2})^{\frac{1}{2}} \rightarrow 0 \quad \text{as } n \rightarrow +\infty, \quad (3.4.30)$$

and then for n large

$$\frac{|x_n - p_i|}{|y_n - p_i|} \geq \frac{|x_n - y_n|}{|y_n - p_i|} - 1 \geq 1, \quad \frac{|x_n - p_i|}{|x_n - y_n|} \geq 1 - \frac{|y_n - p_i|}{|x_n - y_n|} \geq \frac{1}{2}. \quad (3.4.31)$$

Since $\varepsilon_n \leq \mu_n$, (3.4.27) and (3.4.31) give that

$$\begin{aligned} & \varepsilon_n^{-3} \lambda_n |x_n - p_i|^{\alpha+2} \\ & \geq \left(\frac{\mu_n^{\frac{3}{2}} \lambda_n^{-\frac{1}{2}}}{|x_n - y_n| |y_n - p_i|^{\frac{\alpha}{2}}} \right)^{-2} \left(\frac{|x_n - p_i|}{|x_n - y_n|^{\frac{2}{\alpha+2}} |y_n - p_i|^{\frac{\alpha}{\alpha+2}}} \right)^{\alpha+2} \\ & \geq C \left(\frac{\mu_n^{\frac{3}{2}} \lambda_n^{-\frac{1}{2}}}{|x_n - y_n| d(y_n)^{\frac{\alpha}{2}}} \right)^{-2} \rightarrow +\infty \quad \text{as } n \rightarrow +\infty. \end{aligned} \quad (3.4.32)$$

The meaning of (3.4.32) is the following: once y_n provides a fast blowing up sequence at p_i , then no other fast blow up at p_i can occur as (3.4.32) states for x_n .

Let $\beta_n = \mu_n^{\frac{3}{2+\alpha}} \lambda_n^{-\frac{1}{2+\alpha}}$. By (3.4.27) and (3.4.30) we get that

$$\begin{aligned} \frac{\beta_n}{|x_n - y_n|} &= \mu_n^{\frac{3}{2+\alpha}} \lambda_n^{-\frac{1}{2+\alpha}} |x_n - y_n|^{-1} \\ &= \left(\frac{\mu_n^{\frac{3}{2}} \lambda_n^{-\frac{1}{2}}}{|x_n - y_n| d(y_n)^{\frac{\alpha}{2}}} \right)^{\frac{2}{2+\alpha}} \left(\frac{|y_n - p_i|}{|x_n - y_n|} \right)^{\frac{\alpha}{2+\alpha}} \rightarrow 0 \quad \text{as } n \rightarrow +\infty. \end{aligned} \quad (3.4.33)$$

However, since u_n blows up fast at p_i along y_n , we have $\beta_n^{-1} d(y_n) \leq C$ and then, (3.4.28) does not hold. Letting as before

$$\hat{U}_n(y) = \frac{1 - u_n(\beta_n y + y_n)}{\mu_n}, \quad y \in \hat{\Omega}_n = \frac{\Omega - y_n}{\beta_n},$$

we need to refine the analysis before in order to get some estimate for \hat{U}_n even when only (3.4.33) does hold. Formula (3.4.26) gives that:

$$\begin{aligned} \hat{U}_n(y) &\geq |y_n - p_i|^{-\frac{\alpha}{3}} |y_n - x_n|^{-\frac{2}{3}} |\beta_n y + y_n - p_i|^{\frac{\alpha}{3}} |\beta_n y + y_n - x_n|^{\frac{2}{3}} \\ &= \left(\mu_n^{-\frac{3}{2+\alpha}} \lambda_n^{\frac{1}{2+\alpha}} |y_n - p_i| \right)^{-\frac{\alpha}{3}} \left| \frac{\beta_n}{|x_n - y_n|} y + \frac{y_n - x_n}{|x_n - y_n|} \right|^{\frac{2}{3}} \\ &\quad \cdot \left| y + \mu_n^{-\frac{3}{2+\alpha}} \lambda_n^{\frac{1}{2+\alpha}} (y_n - p_i) \right|^{\frac{\alpha}{3}} \\ &\geq C \left(\mu_n^{-\frac{3}{2+\alpha}} \lambda_n^{\frac{1}{2+\alpha}} |y_n - p_i| \right)^{-\frac{\alpha}{3}} \left| y + \mu_n^{-\frac{3}{2+\alpha}} \lambda_n^{\frac{1}{2+\alpha}} (y_n - p_i) \right|^{\frac{\alpha}{3}} \end{aligned} \quad (3.4.34)$$

for $|y| \leq R_n = \left(\frac{|x_n - y_n|}{\beta_n}\right)^{\frac{1}{2}}$, and $R_n \rightarrow +\infty$ as $n \rightarrow +\infty$ by (3.4.33). Since (3.4.34) implies that (3.4.22) holds for μ_n, y_n, \tilde{U}_n , Proposition 3.4.4 provides some $\psi_n \in C_0^\infty(\Omega)$ such that (3.4.12) holds and $\text{Supp } \psi_n \subset B_{M\mu_n^{\frac{3}{2+\alpha}}\lambda_n^{-\frac{1}{2+\alpha}}}(y_n)$ for some $M > 0$.

Since y_n cannot lie in any ball centered at x_n and radius of order of the scale parameter $(\varepsilon_n^{\frac{3}{2}}\lambda_n^{-\frac{1}{2}}$ or $\varepsilon_n^{\frac{3}{2}}\lambda_n^{-\frac{1}{2}}|x_n - p_i|^{-\frac{\alpha}{2}}$), we get from (3.4.33) that ϕ_n and ψ_n have disjoint compact supports leading to $\mu_{2,n} < 0$, a contradiction to (3.1.4). This completes the proof of Proposition 3.4.5. \blacksquare

3.4.3 Compactness issues

We are now in position to give the proof of Theorem 3.1.3. Assume $2 \leq N \leq 7$, and let $f \in C(\bar{\Omega})$ be as in (3.1.3). Let $(\lambda_n)_n$ be a sequence such that $\lambda_n \rightarrow \lambda \in [0, \lambda^*]$ and let u_n be an associated solution such that (3.1.4) holds, namely

$$\mu_{2,n} := \mu_{2,\lambda_n}(u_n) \geq 0.$$

The essential ingredient will be the estimate of Proposition 3.4.5 combined with the uniqueness result of Proposition 2.5.2.

Proof of Theorem 3.1.3: Let x_n be the maximum point of u_n in Ω and, up to a subsequence, assume by contradiction that $u_n(x_n) = \max_{\Omega} u_n(x) \rightarrow 1$ as $n \rightarrow \infty$. Then Proposition 3.4.5 gives that for some $C > 0$ and $N_0 \in \mathbb{N}$ large,

$$u_n(x) \leq 1 - C\lambda_n^{\frac{1}{3}}d(x)^{\frac{\alpha}{3}}|x - x_n|^{\frac{2}{3}}$$

for any $x \in \Omega$ and $n \geq N_0$, where $d(x)^{\frac{\alpha}{3}} = \min\{|x - p_i|^{\frac{\alpha}{3}} : i = 1, \dots, k\}$ stands for the distance function from the zero set of $f(x)$. Thus, we have that:

$$0 \leq \frac{\lambda_n f(x)}{(1 - u_n)^2} \leq C \frac{f(x)}{d(x)^{\frac{2\alpha}{3}} |x - x_n|^{\frac{4}{3}}} \quad (3.4.35)$$

for any $x \in \Omega$ and $n \geq N_0$. Since by (3.1.3)

$$\left| \frac{f(x)}{d(x)^{\frac{2\alpha}{3}}} \right| \leq |x - p_i|^{\frac{\alpha}{3}} \|f_i\|_\infty \leq C$$

for x close to p_i , f_i as in (3.4.14), we get that $\frac{f(x)}{d(x)^{\frac{2\alpha}{3}}}$ is a bounded function on Ω and then, (3.4.35) gives that $\lambda_n f(x)/(1 - u_n)^2$ is uniformly bounded in $L^s(\Omega)$, for any $1 < s < \frac{3N}{4}$. Standard elliptic regularity theory now implies that u_n is uniformly bounded in $W^{2,s}(\Omega)$. By Sobolev's imbedding theorem, u_n is uniformly bounded in $C^{0,\beta}(\bar{\Omega})$ for any $0 < \beta < 2/3$. Up to a subsequence, we get that $u_n \rightarrow u_0$ weakly in $H_0^1(\Omega)$ and strongly in $C^{0,\beta}(\bar{\Omega})$, $0 < \beta < 2/3$, where u_0 is a Hölderian function solving weakly in $H_0^1(\Omega)$ the equation:

$$\begin{cases} -\Delta u_0 = \frac{\lambda f(x)}{(1 - u_0)^2} & \text{in } \Omega, \\ 0 \leq u_0 \leq 1 & \text{in } \Omega, \\ u_0 = 0 & \text{on } \partial\Omega. \end{cases} \quad (3.4.36)$$

Moreover, by uniform convergence

$$\max_{\Omega} u_0 = \lim_{n \rightarrow +\infty} \max_{\Omega} u_n = 1$$

and, in particular $u_0 > 0$ in Ω . Clearly, $\lambda > 0$ since any weak harmonic function in $H_0^1(\Omega)$ is identically zero. To reach a contradiction, we shall first show that $\mu_{1,\lambda}(u_0) \geq 0$ and then deduce from the uniqueness, stated in Proposition 2.5.2, of the semi-stable solution u_λ that $u_0 = u_\lambda$. But $\max_{\Omega} u_\lambda < 1$ for any $\lambda \in [0, \lambda^*]$, contradicting $\max_{\Omega} u_0 = 1$. Hence, the claimed compactness must hold.

In addition to (3.1.4), assume now that $\mu_{1,n} < 0$, then $\lambda > 0$. Indeed, if $\lambda_n \rightarrow 0$, then by compactness and standard regularity theory, we get that $u_n \rightarrow u_0$ in $C^2(\bar{\Omega})$, where u_0 is a harmonic function so that $u_0 = 0$ on $\partial\Omega$. Then, $u_0 = 0$ and $u_n \rightarrow 0$ in $C^2(\bar{\Omega})$. But the only branch of solutions for $(S)_\lambda$ bifurcating from 0 for λ small is the branch of minimal solutions u_λ and then, $u_n = u_{\lambda_n}$ for n large contradicting $\mu_{1,n} < 0$.

In order to complete the proof, we need only to show that

$$\mu_{1,\lambda}(u_0) = \inf \left\{ \int_{\Omega} (|\nabla \phi|^2 - \frac{2\lambda f(x)}{(1-u_0)^3} \phi^2); \phi \in C_0^\infty(\Omega) \text{ and } \int_{\Omega} \phi^2 = 1 \right\} \geq 0. \quad (3.4.37)$$

Indeed, first Propositions 3.4.2 ~ 3.4.4 imply the existence of a function $\phi_n \in C_0^\infty(\Omega)$ so that

$$\int_{\Omega} (|\nabla \phi_n|^2 - \frac{2\lambda_n f(x)}{(1-u_n)^3} \phi_n^2) < 0. \quad (3.4.38)$$

Moreover, $\text{Supp } \phi_n \subset B_{r_n}(x_n)$ and $r_n \rightarrow 0$ as $n \rightarrow +\infty$. Up to a subsequence, assume that $x_n \rightarrow p \in \bar{\Omega}$ as $n \rightarrow +\infty$.

By contradiction, if (3.4.37) were false, then there exist $\phi_0 \in C_0^\infty(\Omega)$ such that

$$\int_{\Omega} (|\nabla \phi_0|^2 - \frac{2\lambda f(x)}{(1-u_0)^3} \phi_0^2) < 0. \quad (3.4.39)$$

We will replace ϕ_0 with a truncated function ϕ_δ with $\delta > 0$ small enough, so that (3.4.39) is still true while $\phi_\delta = 0$ in $B_{\delta^2}(p) \cap \Omega$. In this way, ϕ_n and ϕ_δ would have disjoint compact supports in contradiction to $\mu_{2,n} \geq 0$.

Let $\delta > 0$ and set $\phi_\delta = \chi_\delta \phi_0$, where χ_δ is a cut-off function defined as:

$$\chi_\delta(x) = \begin{cases} 0 & |x-p| \leq \delta^2, \\ 2 - \frac{\log|x-p|}{\log\delta} & \delta^2 \leq |x-p| \leq \delta, \\ 1 & |x-p| \geq \delta. \end{cases}$$

By Lebesgue's theorem, we have:

$$\int_{\Omega} \frac{2\lambda f(x)}{(1-u_0)^3} \phi_\delta^2 \rightarrow \int_{\Omega} \frac{2\lambda f(x)}{(1-u_0)^3} \phi_0^2 \quad \text{as } \delta \rightarrow 0. \quad (3.4.40)$$

For the gradient term, we have the expansion:

$$\int_{\Omega} |\nabla \phi_\delta|^2 = \int_{\Omega} \phi_0^2 |\nabla \chi_\delta|^2 + \int_{\Omega} \chi_\delta^2 |\nabla \phi_0|^2 + 2 \int_{\Omega} \chi_\delta \phi_0 \nabla \chi_\delta \nabla \phi_0.$$

The following estimates hold:

$$0 \leq \int_{\Omega} \phi_{\delta}^2 |\nabla \chi_{\delta}|^2 \leq \|\phi_0\|_{\infty}^2 \int_{\delta^2 \leq |x-p| \leq \delta} \frac{1}{|x-p|^2 \log^2 \delta} \leq \frac{C}{\log \frac{1}{\delta}}$$

and

$$|2 \int_{\Omega} \chi_{\delta} \phi_0 \nabla \chi_{\delta} \nabla \phi_0| \leq \frac{2\|\phi_0\|_{\infty} \|\nabla \phi_0\|_{\infty}}{\log \frac{1}{\delta}} \int_{B_1(0)} \frac{1}{|x|},$$

which provide

$$\int_{\Omega} |\nabla \phi_{\delta}|^2 \rightarrow \int_{\Omega} |\nabla \phi_0|^2 \quad \text{as } \delta \rightarrow 0. \quad (3.4.41)$$

Combining (3.4.39)-(3.4.41), we get that

$$\int_{\Omega} (|\nabla \phi_{\delta}|^2 - \frac{2\lambda f(x)}{(1-u_0)^3} \phi_{\delta}^2) < 0$$

for $\delta > 0$ sufficiently small. This completes the proof of (3.4.37) and therefore, Theorem 3.1.3 is completely established. \blacksquare

3.5 The second bifurcation point

In this section, we discuss the second bifurcation point for $(S)_{\lambda}$ in the sense

$$\lambda_2^* = \inf \{ \beta > 0 : \exists \text{ a curve } V_{\lambda} \in C([\beta, \lambda^*]; C^2(\Omega)) \text{ of solutions for } (S)_{\lambda} \text{ such that } \mu_{2,\lambda}(V_{\lambda}) \geq 0, V_{\lambda} \equiv U_{\lambda} \forall \lambda \in (\lambda^* - \delta, \lambda^*) \},$$

where U_{λ} and δ are as in Theorem 3.1.2, and we prove the multiplicity result of Theorem 3.1.5.

Proof of Theorem 3.1.5: For any $\lambda \in (\lambda_2^*, \lambda^*)$, the definition of λ_2^* gives that there exists a solution V_{λ} such that:

$$\mu_{1,\lambda} := \mu_{1,\lambda}(V_{\lambda}) < 0 \quad \forall \lambda \in (\lambda_2^*, \lambda^*). \quad (3.5.1)$$

In particular, $V_{\lambda} \neq u_{\lambda}$ provides a second solution different from the minimal one.

Clearly (3.5.1) is true because first $\mu_{1,\lambda} < 0$ for λ close to λ^* . Moreover, if $\mu_{1,\lambda} = 0$ for some $\lambda \in (\lambda_2^*, \lambda^*)$, then by Proposition 2.5.2 $V_{\lambda} = u_{\lambda}$ contradicting the fact that $\mu_{1,\lambda}(u_{\lambda}) > 0$ for any $0 < \lambda < \lambda^*$.

Since the definition of λ_2^* gives $\mu_{2,\lambda}(V_{\lambda}) \geq 0$ for any $\lambda \in (\lambda_2^*, \lambda^*)$, we can take a sequence $\lambda_n \downarrow \lambda_2^*$ and apply Theorem 3.1.3 that $\lambda_2^* = \lim_{n \rightarrow +\infty} \lambda_n > 0$, $\sup_{n \in \mathbb{N}} \|V_{\lambda_n}\|_{\infty} < 1$. By elliptic regularity theory, up to a subsequence $V_{\lambda_n} \rightarrow V^*$ in $C^2(\bar{\Omega})$, where V^* is a solution for $(S)_{\lambda_2^*}$. As before, $\mu_{1,\lambda_2^*}(V^*) < 0$ and by continuity $\mu_{2,\lambda_2^*}(V^*) \geq 0$.

Suppose $\mu_{2,\lambda_2^*}(V^*) > 0$, let us fix some $\varepsilon > 0$ so small that $0 \leq V^* \leq 1 - 2\varepsilon$ and consider the truncated nonlinearity $g_{\varepsilon}(u)$ as in (3.2.1). Clearly, V^* is a solution of (3.2.2) at $\lambda = \lambda_2^*$ so that $-\Delta - \lambda_2^* f(x) g'_{\varepsilon}(V^*)$ has no zero eigenvalues, since $\mu_{1,\lambda_2^*}(V^*) < 0$ and $\mu_{2,\lambda_2^*}(V^*) > 0$. Namely, V^* solves $N(\lambda_2^*, V^*) = 0$, where N is a map from $\mathbb{R} \times C^{2,\alpha}(\bar{\Omega})$ into $C^{2,\alpha}(\bar{\Omega})$, $\alpha \in (0, 1)$, defined as:

$$N : (\lambda, V) \longrightarrow V + \Delta^{-1}(\lambda f(x) g_{\varepsilon}(V)).$$

Moreover,

$$\partial_V N(\lambda_2^*, V^*) = \text{Id} + \Delta^{-1} \left(\frac{2\lambda_2^* f(x)}{(1 - V^*)^3} \right)$$

is an invertible map since $-\Delta - \lambda_2^* f(x) g'_\varepsilon(V^*)$ has no zero eigenvalues. The implicit function theorem gives the existence of a curve W_λ , $\lambda \in (\lambda_2^* - \delta, \lambda_2^* + \delta)$, of solution for (3.2.2) so that $\lim_{\lambda \rightarrow \lambda_2^*} W_\lambda = V^*$ in $C^{2,\alpha}(\bar{\Omega})$. Up to take δ smaller, this convergence implies that $\mu_{2,\lambda}(W_\lambda) > 0$ and $W_\lambda \leq 1 - \varepsilon$ for any $\lambda \in (\lambda_2^* - \delta, \lambda_2^* + \delta)$. Hence, W_λ is a solution of $(S)_\lambda$ so that $\mu_{2,\lambda}(W_\lambda) > 0$, contradicting the definition of λ_2^* . Therefore, $\mu_{2,\lambda_2^*}(V^*) = 0$, which completes the proof of Theorem 3.1.5. \blacksquare

3.6 The one dimensional problem

In this section, we discuss the compactness of solutions for $(S)_\lambda$ in one dimensional case. Recall that $\mu_{k,\lambda_n}(u_n)$ is the k -th eigenvalue of L_{u_n,λ_n} counted with their multiplicity.

Proof of Theorem 3.1.6: Let $I = (a, b)$ be a bounded interval in \mathbb{R} . Assume $f \in C^1(\bar{I})$ so that $f \geq C > 0$ in I . We study solutions u_n of $(S)_{\lambda_n}$ in the form

$$\begin{cases} -\ddot{u}_n = \frac{\lambda_n f(x)}{(1 - u_n)^2} & \text{in } I, \\ 0 < u_n < 1 & \text{in } I, \\ u_n(a) = u_n(b) = 0. \end{cases} \quad (3.6.1)$$

Assume that u_n satisfy (3.1.7) and $\lambda_n \rightarrow \lambda \in (0, \lambda^*]$. Let $x_n \in I$ be a maximum point: $u_n(x_n) = \max_I u_n$. If $(u_n)_n$ is not compact, then up to a subsequence, we may assume that $u_n(x_n) \rightarrow 1$ with $x_n \rightarrow x_0 \in \bar{I}$ as $n \rightarrow +\infty$. Away from x_0 , u_n is uniformly far away from 1. Otherwise, by the maximum principle we would have $u_n \rightarrow 1$ on an interval of positive measure, and then $\mu_{k,\lambda_n}(u_n) < 0$ for any k and n large, a contradiction.

Assume, for example, that $a \leq x_0 < b$. By elliptic regularity theory, $\dot{u}_n(x)$ is uniformly bounded for x far away from x_0 . Letting $\varepsilon > 0$, we multiply (3.6.1) by \dot{u}_n and integrate on $(x_n, x_0 + \varepsilon)$:

$$\begin{aligned} \dot{u}_n^2(x_n) - \dot{u}_n^2(x_0 + \varepsilon) &= \int_{x_n}^{x_0 + \varepsilon} \frac{2\lambda_n f(s) \dot{u}_n(s)}{(1 - u_n(s))^2} ds \\ &= \frac{2\lambda_n f(x_0 + \varepsilon)}{1 - u_n(x_0 + \varepsilon)} - \frac{2\lambda_n f(x_n)}{1 - u_n(x_n)} - \int_{x_n}^{x_0 + \varepsilon} \frac{2\lambda_n \dot{f}(s)}{1 - u_n(s)} ds. \end{aligned}$$

Then, for n large:

$$\begin{aligned} \dot{u}_n^2(x_n) + \frac{C\lambda}{1 - u_n(x_n)} &\leq \dot{u}_n^2(x_0 + \varepsilon) + 2\lambda_n \frac{f(x_0 + \varepsilon)}{1 - u_n(x_0 + \varepsilon)} - 2\lambda_n \int_{x_n}^{x_0 + \varepsilon} \frac{\dot{f}(s)}{1 - u_n(s)} ds \\ &\leq C_\varepsilon + 4\lambda \|\dot{f}\|_\infty \frac{x_0 + \varepsilon - x_n}{1 - u_n(x_n)} \end{aligned}$$

since $u_n(x_n)$ is the maximum value of u_n in I . Choosing $\varepsilon > 0$ sufficiently small, we get that for any n large: $\frac{1}{1 - u_n(x_n)} \leq C_\varepsilon$, contradicting $u_n(x_n) \rightarrow 1$ as $n \rightarrow +\infty$. \blacksquare

Chapter 4

Dynamic Deflection

4.1 Introduction

The rest of this thesis is devoted to the dynamic deflection of the elastic membrane satisfying (1.2.30). Throughout this Chapter and unless mentioned otherwise, for convenience we study dynamic solutions of (1.2.30) in the form

$$\frac{\partial u}{\partial t} - \Delta u = \frac{\lambda f(x)}{(1-u)^2} \quad \text{for } x \in \Omega, \quad (4.1.1a)$$

$$u(x, t) = 0 \quad \text{for } x \in \partial\Omega, \quad u(x, 0) = 0 \quad \text{for } x \in \Omega, \quad (4.1.1b)$$

where nonnegative $f \in C^\alpha(\bar{\Omega})$ for some $\alpha \in (0, 1]$ describes the permittivity profile of the elastic membrane shown in Figure 1.1, while $\lambda > 0$ characterizes the applied voltage, see §1.3.2.

In this Chapter we deal with issues of global convergence, finite and infinite time “touchdown”, and touchdown profiles as well as pull-in distance. Recall that a point $x_0 \in \bar{\Omega}$ is said to be a *touchdown point* for a solution $u(x, t)$ of (4.1.1), if for some $T \in (0, +\infty]$, we have $\lim_{t_n \rightarrow T} u(x_0, t_n) = 1$. T is then said to be a –finite or infinite– touchdown time. For each such solution, we define its corresponding –possibly infinite– “first touchdown time”:

$$T_\lambda(\Omega, f, u) = \inf \left\{ t \in (0, +\infty]; \sup_{x \in \Omega} u(x, t) = 1 \right\}.$$

We first analyze the relationship between the applied voltage λ , the permittivity profile f , and the dynamic deflection of the elastic membrane. It is already known that solutions corresponding to large voltages λ necessarily touchdown in finite time (see [32]). The following theorem proved in §4.2 completes the picture.

Theorem 4.1.1. *Suppose $\lambda^* := \lambda^*(\Omega, f)$ is the pull-in voltage defined in Theorem 2.1.1, then the following hold:*

1. *If $\lambda \leq \lambda^*$, then there exists a unique solution $u(x, t)$ for (4.1.1) which globally converges as $t \rightarrow +\infty$, monotonically and pointwise to its unique minimal steady-state.*
2. *If $\lambda > \lambda^*$ and $\inf_\Omega f > 0$, then the unique solution $u(x, t)$ of (4.1.1) must touchdown at a finite time.*

This “touchdown” phenomenon is referred to sometimes as *quenching*. Note that in the case where the unique minimal steady-state of (4.1.1) at $\lambda = \lambda^*$ is non-regular – which can happen if $N \geq 8$ – the above result means that the corresponding dynamic solution must touchdown but that quenching occurs here in infinite time.

In §4.3 we shall establish that –an isolated– touchdown cannot occur at a point in Ω where the permittivity profile is zero, a fact that was observed numerically and conjectured to hold in [32]. More precisely, we prove the following.

Theorem 4.1.2. *Suppose $u(x, t)$ is a touchdown solution of (4.1.1) at a finite time T , then $u_t > 0$ for all $0 < t < T$. Furthermore,*

1. *The permittivity profile f cannot vanish on an isolated set of touchdown points in Ω .*
2. *On the other hand, zeroes of the permittivity profile can be locations of touchdown in infinite time.*

In §4.4 we shall provide upper and lower estimates for finite touchdown times. Uniqueness considerations lead to a first touchdown time $T_\lambda(\Omega, f)$ that only depends on the domain Ω and on the profile f . These touchdown times translate into useful information concerning the speed of the operation for many MEMS devices, such as Radio Frequency (RF) switches and microvalves. Estimates (4.1.4) and (4.1.5) below were already established in [32] for large λ . Considering that $\lambda^* < \min\{\bar{\lambda}_1, \bar{\lambda}_2\}$, the estimate (4.1.3) below gives an upper bound on the first touchdown time as soon as we exceed the pull-in voltage λ^* .

Theorem 4.1.3. *Suppose f is a non-negative continuous function on a bounded domain Ω , and let $T_\lambda(\Omega, f)$ be the first –possibly infinite– touchdown time corresponding to a voltage λ .*

1. *The following lower estimate then holds for any $\lambda > 0$:*

$$\frac{1}{3\lambda \sup_{x \in \Omega} f(x)} \leq T_\lambda(\Omega, f). \quad (4.1.2)$$

2. *If $\inf_{x \in \Omega} f(x) > 0$, then the following upper estimate holds for any $\lambda > \lambda^*$:*

$$T_\lambda(\Omega, f) \leq T_{0,\lambda}(\Omega, f) := \frac{8(\lambda + \lambda^*)^2}{3 \inf_{x \in \Omega} f(x) (\lambda - \lambda^*)^2 (\lambda + 3\lambda^*)} \left[1 + \left(\frac{\lambda + 3\lambda^*}{2\lambda + 2\lambda^*} \right)^{1/2} \right]. \quad (4.1.3)$$

3. *If $\inf_{x \in \Omega} f(x) > 0$, and $\lambda > \bar{\lambda}_1 := \frac{4\mu_\Omega}{27 \inf_{x \in \Omega} f(x)}$, then*

$$T_\lambda(\Omega, f) \leq T_{1,\lambda}(\Omega, f) := \int_0^1 \left[\frac{\lambda \inf_{x \in \Omega} f(x)}{(1-s)^2} - \mu_\Omega s \right]^{-1} ds. \quad (4.1.4)$$

4. *If $\lambda > \bar{\lambda}_2 := \frac{\mu_\Omega}{3 \int_\Omega f \phi_\Omega dx}$, then*

$$T_\lambda(\Omega, f) \leq T_{2,\lambda}(\Omega, f) := -\frac{1}{\mu_\Omega} \log \left[1 - \frac{\mu_\Omega}{3\lambda} \left(\int_\Omega f \phi_\Omega dx \right)^{-1} \right]. \quad (4.1.5)$$

Here μ_Ω and ϕ_Ω are the first eigenpair of $-\Delta$ on $H_0^1(\Omega)$ with normalized $\int_\Omega \phi_\Omega dx = 1$.

Note that the upper bounds $T_{0,\lambda}$ and $T_{1,\lambda}$ are relevant only when f is bounded away from 0, while the upper bound $T_{2,\lambda}$ is valid for all permittivity profiles provided of course that $\lambda > \bar{\lambda}_2$.

In §4.5 we discuss touchdown profiles by the method of asymptotic analysis, and our purpose is to provide some information on the refined touchdown rate discussed in next Chapter.

§4.6 is devoted to the pull-in distance of MEMS devices, referred to as the maximum stable deflection of the elastic membrane before touchdown occurs. We provide numerical results for pull-in distance with some explicit examples, from which one can observe that both larger pull-in distance and pull-in voltage can be achieved by properly tailoring the permittivity profile.

4.2 Global convergence or touchdown

In this section, we analyze the relationship between the applied voltage λ , the permittivity profile f , and the dynamic deflection u of (4.1.1). We first prove in §4.2.1 global convergence in the case $\lambda < \lambda^*$. In §4.2.2 we study finite-time touchdown for the case $\lambda > \lambda^*$. Finally we discuss the case $\lambda = \lambda^*$ in §4.2.3.

First, we note the following uniqueness result.

Lemma 4.2.1. *Suppose u_1 and u_2 are solutions of (4.1.1) on the interval $[0, T]$ such that $\|u_i\|_{L^\infty(\bar{\Omega} \times [0, T])} < 1$ for $i = 1, 2$, then $u_1 \equiv u_2$.*

Proof: Indeed, the difference $U = u_1 - u_2$ then satisfies

$$U_t - \Delta U = \alpha U \quad \text{in } \Omega \quad (4.2.1)$$

with initial data $U(x, 0) = 0$ and zero boundary condition. Here

$$\alpha(x, t) = \frac{\lambda(2 - u_1 - u_2)f(x)}{(1 - u_1)^2(1 - u_2)^2}.$$

The assumption on u_1, u_2 implies that $\alpha(x, t) \in L^\infty(\bar{\Omega} \times [0, T])$. We now fix $T_1 \in [0, T]$ and consider the solution ϕ of the problem

$$\begin{cases} \phi_t + \Delta \phi + \alpha \phi = 0 & x \in \Omega, 0 < t < T_1, \\ \phi(x, T_1) = \theta(x) \in C_0(\Omega), \\ \phi(x, t) = 0 & x \in \partial\Omega, \end{cases} \quad (4.2.2)$$

The standard linear theory (cf. Theorem 8.1 of [47]) gives that the solution of (4.2.2) is unique and bounded. Now multiplying (4.2.1) by ϕ , and integrating it on $\Omega \times [0, T_1]$, together with (4.2.2), yield that

$$\int_{\Omega} U(x, T_1)\theta(x)dx = 0$$

for arbitrary T_1 and $\theta(x)$, which implies that $U \equiv 0$, and we are done. \blacksquare

4.2.1 Global convergence when $\lambda < \lambda^*$

Theorem 4.2.2. *Suppose $\lambda^* := \lambda^*(\Omega, f)$ is the pull-in voltage defined in Theorem 2.1.1, then for $\lambda < \lambda^*$ there exists a unique global solution $u(x, t)$ for (4.1.1) which monotonically converges as $t \rightarrow +\infty$ to the unique minimal solution $u_\lambda(x)$ of $(S)_\lambda$.*

Proof: This is standard and follows from the maximum principle combined with the existence of regular minimal steady-state solutions at this range of λ . Indeed, fix $0 < \lambda < \lambda^*$, and use Theorem 2.1.2 to obtain the existence of a unique minimal solution $u_\lambda(x)$ of $(S)_\lambda$. It is clear that the pair $\tilde{u} \equiv 0$ and $\hat{u} = u_\lambda(x)$ are sub- and super-solutions of (4.1.1) for all $t > 0$. This implies that the unique global solution $u(x, t)$ of (4.1.1) satisfies $1 > u_\lambda(x) \geq u(x, t) \geq 0$ in $\Omega \times (0, \infty)$.

By differentiating in time and setting $v = u_t$, we get for any fixed $t_0 > 0$

$$v_t = \Delta v + \frac{2\lambda f(x)}{(1 - u)^3}v \quad x \in \Omega, 0 < t < t_0, \quad (4.2.3a)$$

$$v(x, t) = 0 \quad x \in \partial\Omega, \quad v(x, 0) \geq 0 \quad x \in \Omega. \quad (4.2.3b)$$

Here $\frac{2\lambda f(x)}{(1-u)^3}$ is a locally bounded non-negative function, and by the strong maximum principle, we get that $u_t = v > 0$ for $(x, t) \in \Omega \times (0, t_0)$ or $u_t \equiv 0$. The second case is impossible because otherwise $u(x, t) \equiv u_\lambda(x)$ for any $t > 0$. It follows that $u_t > 0$ holds for all $(x, t) \in \Omega \times (0, \infty)$, and since $u(x, t)$ is bounded, this monotonicity property implies that the unique global solution $u(x, t)$ converges to some function $u_s(x)$ as $t \rightarrow \infty$. Hence, $1 > u_\lambda(x) \geq u_s(x) > 0$ in Ω .

Next we claim that the limit $u_s(x)$ is a solution of $(S)_\lambda$. Indeed, consider a solution u_1 of the linear stationary boundary problem

$$-\Delta u_1 = \frac{\lambda f(x)}{(1-u_s)^2} \quad x \in \Omega, \quad u_1 = 0 \quad x \in \partial\Omega. \quad (4.2.4)$$

Let $w(x, t) = u(x, t) - u_1(x)$, then w satisfies

$$w_t - \Delta w = \lambda f(x) \left[\frac{1}{(1-u)^2} - \frac{1}{(1-u_s)^2} \right], \quad (x, t) \in \Omega \times (0, T); \quad (4.2.5a)$$

$$w(x, t) = 0 \quad x \in \partial\Omega \times (0, T); \quad w(x, 0) = -u_1(x) \quad x \in \Omega. \quad (4.2.5b)$$

Since the right side of (4.2.5a) converges to zero in $L^2(\Omega)$ as $t \rightarrow \infty$, a standard eigenfunction expansion implies that the solution w of (4.2.5) also converges to zero in $L^2(\Omega)$ as $t \rightarrow \infty$. This shows that $u(x, t) \rightarrow u_1(x)$ in $L^2(\Omega)$ as $t \rightarrow \infty$. But since $u(x, t) \rightarrow u_s(x)$ pointwise in Ω as $t \rightarrow \infty$, we deduce that $u_1(x) \equiv u_s(x)$ in $L^2(\Omega)$, which implies that $u_s(x)$ is also a solution for $(S)_\lambda$. The minimal property of $u_\lambda(x)$ then yields that $u_\lambda(x) \equiv u_s(x)$ on Ω , which follows that for every $x \in \Omega$, we have $u(x, t) \uparrow u_\lambda(x)$ as $t \rightarrow \infty$. ■

4.2.2 Touchdown at finite time when $\lambda > \lambda^*$

Recall from Theorem 2.1.1 that there is no solution for $(S)_\lambda$ as soon as $\lambda > \lambda^*$. Since the solution $u(x, t)$ of (4.1.1) –whenever it exists– is strictly increasing in time t (see preceding theorem), then there must be $T \leq \infty$ such that $u(x, t)$ reaches 1 at some point of $\bar{\Omega}$ as $t \rightarrow T^-$. Otherwise, a proof similar to Theorem 4.2.2 would imply that $u(x, t)$ would converge to its steady-state which is then the unique minimal solution u_λ of $(S)_\lambda$, contrary to the hypothesis that $\lambda > \lambda^*$. Therefore for this case, it only remains to know whether the touchdown time is finite or infinite. This is exactly what we prove in the following.

Theorem 4.2.3. *Suppose $\lambda^* := \lambda^*(\Omega, f)$ is the pull-in voltage defined in Theorem 2.1.1. If $\inf_{x \in \Omega} f(x) > 0$, then for $\lambda > \lambda^*$ there exists a finite time $T_\lambda(\Omega, f)$ at which the unique solution $u(x, t)$ of (4.1.1) must touchdown. Moreover, we have the bound*

$$T_\lambda(\Omega, f) \leq T_{0,\lambda} := \frac{8(\lambda + \lambda^*)^2}{3 \inf_{x \in \Omega} f(x) (\lambda - \lambda^*)^2 (\lambda + 3\lambda^*)} \left[1 + \left(\frac{\lambda + 3\lambda^*}{2\lambda + 2\lambda^*} \right)^{1/2} \right]. \quad (4.2.6)$$

We start by transforming the problem from a touchdown situation (i.e. quenching) into a blow-up problem where a concavity method can be used. For that, we set $V = 1/(1-u)$ which

reduces (1.1) to the following parabolic problem

$$V_t = \Delta V - \frac{2|\nabla V|^2}{V} + \lambda f(x)V^4 \quad \text{for } x \in \Omega, \quad (4.2.7a)$$

$$V(x, t) = 1 \quad \text{for } x \in \partial\Omega, \quad (4.2.7b)$$

$$V(x, 0) = 1 \quad \text{for } x \in \Omega. \quad (4.2.7c)$$

This transformation implies that when $\lambda > \lambda^*$, the solution of (4.2.7) must blow up (in finite or infinite time) and that there is no solution for the corresponding stationary equation:

$$\Delta V - \frac{2|\nabla V|^2}{V} + \lambda f(x)V^4 = 0, \quad x \in \Omega; \quad V = 1, \quad x \in \partial\Omega. \quad (4.2.8)$$

Therefore, proving finite touchdown time of u for (1.1) is equivalent to showing finite blow-up time of the solution V for (4.2.7).

For the proof, we shall first analyze the following auxiliary parabolic equation

$$v_t = \Delta v - \frac{2|\nabla v|^2}{v} + \lambda a^2 t^2 f(x)v^4 \quad \text{for } x \in \Omega, \quad (4.2.9a)$$

$$v = 1 \quad \text{for } x \in \partial\Omega, \quad (4.2.9b)$$

$$v(x, 0) = 1 \quad \text{for } x \in \Omega, \quad (4.2.9c)$$

where $a > 0$ is a given constant.

Lemma 4.2.4. *Suppose v is a solution of (4.2.9) up to a finite time \bar{T} , then $(\frac{v_t}{v^4})_t \geq 0$ for all $t < \bar{T}$.*

Proof: Dividing (4.2.9a) by v^4 , we obtain

$$\frac{v_t}{v^4} = \frac{\Delta v}{v^4} - \frac{2|\nabla v|^2}{v^5} + \lambda a^2 t^2 f(x).$$

Setting $w = v^{-3}$, then direct calculations show that

$$w_t - \Delta w + \frac{2|\nabla w|^2}{3w} + 3\lambda a^2 t^2 f(x) = 0. \quad (4.2.10)$$

Differentiate (4.2.10) twice with respect to t , we obtain

$$\begin{aligned} \left(\frac{|\nabla w|^2}{w}\right)_{tt} &= \left(\frac{2\nabla w \nabla w_t}{w} - \frac{|\nabla w|^2 w_t}{w^2}\right)_t \\ &= \frac{2\nabla w \nabla w_{tt}}{w} + \frac{2|\nabla w_t|^2}{w} - \frac{4\nabla w \nabla w_t w_t}{w^2} - \frac{|\nabla w|^2 w_{tt}}{w^2} + \frac{2|\nabla w|^2 w_t^2}{w^3}, \end{aligned}$$

which means that the function

$$z = w_{tt} = -3\left(\frac{v_t}{v^4}\right)_t \quad (4.2.11)$$

satisfies

$$\begin{aligned} L(z) &:= z_t - \Delta z + \frac{4\nabla w}{3w} \nabla z - \frac{2|\nabla w|^2}{3w^2} z \\ &= -6\lambda a^2 f(x) - \frac{2}{3} \left[\frac{2|\nabla w_t|^2}{w} + \frac{2|\nabla w|^2 w_t^2}{w^3} - \frac{4\nabla w \nabla w_t w_t}{w^2} \right] \\ &\leq -6\lambda a^2 f(x), \end{aligned}$$

after an application of Cauchy-Schwarz inequality. Hence we have

$$L(z) \leq -6\lambda a^2 f(x) \leq 0. \quad (4.2.12)$$

Now from (4.2.9) and the definition of z , we have $z(x, 0) = 0$ and $z = 0$ on $\partial\Omega$. Since the coefficients of L remain bounded as long as v is bounded, we conclude that $z(x, t) \leq 0$ holds for all $t < \bar{T}$. This completes the proof of Lemma 4.2.4. ■

Proof of Theorem 4.2.3: Let $\lambda > \lambda^*$, and set $\lambda' = \lambda - \lambda^* > 0$, $\delta = \inf_{x \in \Omega} f(x) > 0$, and

$$a_0 = \frac{3\delta\lambda'(4\lambda^* + \lambda')}{4(2\lambda^* + \lambda')} \left[1 - \left(\frac{4\lambda^* + \lambda'}{2(2\lambda^* + \lambda')} \right)^{1/2} \right], \quad (4.2.13a)$$

and

$$T_{0,\lambda} = \frac{1}{a_0} = \frac{8(\lambda + \lambda^*)^2}{3\delta(\lambda - \lambda^*)^2(\lambda + 3\lambda^*)} \left[1 + \left(\frac{\lambda + 3\lambda^*}{2\lambda + 2\lambda^*} \right)^{1/2} \right] < +\infty. \quad (4.2.13b)$$

Consider now a solution v of (4.2.9) corresponding to $\lambda = \lambda^* + \lambda'$ and a_0 as defined in (4.2.13a). We first establish the following

Claim: There exists $x_0 \in \Omega$ such that $v(x_0, t) \rightarrow \infty$ as $t \nearrow T_{0,\lambda}$.

Indeed, let $t_0 = \frac{1}{a_0} \left[\frac{4\lambda^* + \lambda'}{2(2\lambda^* + \lambda')} \right]^{1/2}$ in such a way that

$$t_0 < T_{0,\lambda} \quad \text{and} \quad a_0^2 t_0^2 (\lambda^* + \frac{\lambda'}{2}) = \lambda^* + \frac{\lambda'}{4}.$$

We claim that there exists $x_0 \in \Omega$ such that

$$\Delta v(x_0, t_0) - \frac{2|\nabla v(x_0, t_0)|^2}{v(x_0, t_0)} + (\lambda^* + \frac{\lambda'}{4})f(x_0)|v(x_0, t_0)|^4 > 0. \quad (4.2.14)$$

Essentially, otherwise we get that for all $x \in \Omega$

$$\Delta v(x, t_0) - \frac{2|\nabla v(x, t_0)|^2}{v(x, t_0)} + (\lambda^* + \frac{\lambda'}{4})f(x)|v(x, t_0)|^4 \leq 0. \quad (4.2.15)$$

Since $v(x, t_0) \geq 1$ on Ω and hence on Ω , this means that the function $\bar{v}(x) = v(x, t_0)$ is a supersolution for the equation

$$\Delta V - \frac{2|\nabla V|^2}{V} + \lambda f(x)V^4 = 0, \quad x \in \Omega; \quad V = 1, \quad x \in \partial\Omega. \quad (4.2.16)$$

Since $\bar{v} \equiv 1$ is obviously a subsolution of (4.2.16), it follows that the latter has a solution which contradicts the fact that $\lambda = \lambda^* + \frac{\lambda'}{4} > \lambda^*(f, \Omega)$. Hence, assertion (4.2.14) is verified.

On the other hand, we do get from (4.2.9) that for $t = t_0$ and every $x \in \Omega$,

$$v_t = \Delta v - \frac{2|\nabla v|^2}{v} + (\lambda^* + \frac{\lambda'}{4})f(x)v^4 + \frac{\lambda'}{2}a_0^2 t_0^2 f(x)v^4. \quad (4.2.17)$$

We then deduce from (4.2.17) and (4.2.14) that at the point (x_0, t_0) , we have

$$\frac{v_t}{v^4} \geq \frac{\lambda'}{2}a_0^2 t_0^2 f(x_0) > 0.$$

Applying Lemma 4.2.4, we then get for all (x_0, t) , $t_0 \leq t < T_{0,\lambda}$ that:

$$\frac{v_t}{v^4} \geq \frac{\lambda'}{2} a_0^2 t_0^2 f(x_0) > 0. \quad (4.2.18)$$

Integrating (4.2.18) with respect to t in $(t_0, T_{0,\lambda})$, we obtain since $f(x_0) \geq \delta$ that:

$$\frac{1}{3} (1 - v^{-3}(x_0, T_{0,\lambda})) \geq \frac{\lambda'}{2} a_0^2 t_0^2 f(x_0) (T_{0,\lambda} - t_0) \geq \frac{\lambda'}{2} a_0^2 t_0^2 \delta (T_{0,\lambda} - t_0) = \frac{1}{3}.$$

It follows that $v(x_0, t) \rightarrow \infty$ as $t \nearrow T_{0,\lambda}$, and the claim is proved.

To complete the proof of Theorem 4.2.3, we note that since $a_0^2 t^2 \leq 1$ for all $t \leq T_{0,\lambda}$, we get from (4.2.9) that

$$v_t \leq \Delta v - \frac{2|\nabla v|^2}{v} + \lambda f(x) v^4, \quad (x, t) \in \Omega \times (0, T_{0,\lambda}).$$

Setting $w = V - v$, where V is the solution of (4.2.7), then w satisfies

$$w_t - \Delta w - \frac{2\nabla(V+v)}{V} \nabla w + \left[\lambda(V^2 + v^2)(V+v)f(x) + \frac{2|\nabla v|^2}{Vv} \right] w \geq 0, \quad (x, t) \in \Omega \times (0, T_{0,\lambda}).$$

Here the coefficients of ∇w and w are bounded functions as long as V and v are both bounded. It is also clear that $w = 0$ on $\partial\Omega$ and $w(x, 0) = 0$. Applying the maximum principle, we reduce that $w \geq 0$ and thus $V \geq v$. Consequently, V must also blow up at some finite time $T \leq T_{0,\lambda}$, which means that u must touchdown at some finite time prior to $T_{0,\lambda}$. ■

Remark 4.2.1. A slightly revised proof of Theorem 4.2.3 can be essentially adopted to prove finite-time touchdown for the case where $\lambda > \lambda^*$ and $f(x) > 0$ is almost everywhere on Ω . The extension to more general nonnegative profile $f(x)$ is now in progress.

4.2.3 Global convergence or touchdown in infinite time for $\lambda = \lambda^*$

In order to complete the proof of Theorem 4.1.1, the rest is to discuss the dynamic behavior of (4.1.1) at $\lambda = \lambda^*$. For this critical case, there exists a unique steady-state w^* of (4.1.1) obtained as a pointwise limit of the minimal solution u_λ as $\lambda \uparrow \lambda^*$. If w^* is regular (i.e. if it is a classical solution such as in the case when $N \leq 7$) a similar proof as in the case where $\lambda < \lambda^*$, yields the existence of a unique solution $u^*(x, t)$ which globally converges to the unique steady-state w^* as $t \rightarrow \infty$. On the other hand, if w^* is a non-regular steady-state, i.e. if $\|w^*\|_\infty = 1$, the situation is complicated as we shall still prove global convergence to the extremal solution, which then amounts to a touchdown in infinite time.

Throughout this subsection, we shall consider the unique solution $0 \leq u^* = u^*(x, t) < 1$ for the problem

$$u_t^* - \Delta u^* = \frac{\lambda^* f(x)}{(1 - u^*)^2} \quad \text{for } (x, t) \in \Omega \times [0, t^*), \quad (4.2.19a)$$

$$u^*(x, t) = 0 \quad \text{for } x \in \partial\Omega \times [0, t^*), \quad (4.2.19b)$$

$$u^*(x, 0) = 0 \quad \text{for } x \in \Omega, \quad (4.2.19c)$$

where t^* is the maximal time for existence. We shall use techniques developed in [10] to establish the following

Theorem 4.2.5. *If w^* is a non-regular minimal steady-state of (4.2.19), then there exists a unique global solution u^* of (4.2.19) such that $u^*(x, t) \leq w^*(x)$ for all $t < \infty$, while $u^*(x, t) \rightarrow w^*(x)$ as $t \rightarrow \infty$. In particular, $\lim_{t \rightarrow +\infty} \|u^*(x, t)\|_\infty = 1$.*

The proof of Theorem 4.2.5 needs to use the following lemma.

Lemma 4.2.6. *Consider the function $\delta(x) := \text{dist}(x, \partial\Omega)$, then for any $0 < T < \infty$, there exists $\varepsilon_1 = \varepsilon_1(T)$ such that for $0 < \varepsilon \leq \varepsilon_1$ the solution Z^ε of the problem*

$$\begin{aligned} Z_t - \Delta Z &= -\varepsilon f(x) & \text{in } \Omega \times (0, \infty), \\ Z(x, t) &= 0 & \text{on } \partial\Omega \times (0, \infty), \\ Z(x, 0) &= \delta(x) & \text{in } \Omega \end{aligned}$$

satisfies $Z^\varepsilon \geq 0$ on $[0, T] \times \bar{\Omega}$.

Proof: Let $(T(t))_{t \geq 0}$ be the heat semigroup with Dirichlet boundary condition, and consider the solution ξ_0 of

$$-\Delta \xi_0 = 1 \quad \text{in } \Omega; \quad \xi_0 = 0 \quad \text{on } \partial\Omega.$$

then we have

$$\xi_0 = T(t)\xi_0 + \int_0^t T(s)1_\Omega ds$$

for all $t \geq 0$. Since $T(t)\xi_0 \geq 0$, it follows that

$$\int_0^t T(s)1_\Omega ds \leq \xi_0 \leq C\delta \quad \text{for all } t \geq 0. \quad (4.2.20)$$

On the other hand, we have

$$Z^\varepsilon(t) = T(t)\delta - \varepsilon f \int_0^t T(s)1_\Omega ds,$$

and so we have $Z^\varepsilon(t) \geq T(t)\delta - \varepsilon C\delta$. Consider now $c_0, c_1 > 0$ such that $c_0\phi_1 \leq \delta \leq c_1\phi_1$, where ϕ_1 is the first eigenfunction of $-\Delta$ in $H_0^1(\Omega)$, associated to the eigenvalue μ_1 . We have

$$T(t)\delta \geq c_0 T(t)\phi_1 = c_0 e^{-\mu_1 t} \phi_1 \geq \frac{c_0}{c_1} e^{-\mu_1 t} \delta.$$

Therefore, we have $Z^\varepsilon(t) \geq (\frac{c_0}{c_1} e^{-\mu_1 t} - C\varepsilon)\delta$. And hence it follows that $Z^\varepsilon(t) \geq 0$ on $[0, T]$ provided $\varepsilon \leq \frac{c_0}{c_1 C} e^{-\mu_1 T}$. ■

Proof of Theorem 4.2.5: We proceed in four steps.

Claim 1. We have that $u^*(x, t) \leq w^*(x)$ for all $(x, t) \in \Omega \times [0, t^*]$. Indeed, fix any $T < t^*$ and let ξ be the solution of the backward heat equation:

$$\begin{aligned} \xi_t - \Delta \xi &= h(x, t) & \text{in } \Omega \times (0, T), \\ \xi|_{\partial\Omega} &= 0, & \xi(T) = 0, \end{aligned}$$

where $h(x, t) \geq 0$ is in $\Omega \times (0, T)$. Multiplying (4.2.19) by ξ and integrating on $\Omega \times (0, T)$ we find that

$$\int_0^T \int_{\Omega} u^* h \, dx dt = \int_0^T \int_{\Omega} \frac{\lambda^* \xi f(x)}{(1 - u^*)^2} \, dx dt.$$

On the other hand,

$$-\int_0^T \int_{\Omega} w^* \xi_t \, dx dt = \int_{\Omega} w^* \xi(0) \, dx \quad \text{and} \quad -\int_0^T \int_{\Omega} w^* \Delta \xi \, dx dt = \int_0^T \int_{\Omega} \frac{\lambda^* \xi f(x)}{(1 - w^*)^2} \, dx dt.$$

Therefore, we have

$$\begin{aligned} \int_0^T \int_{\Omega} (u^* - w^*) h \, dx dt &\leq \int_{\Omega} w^* \xi(0) \, dx + \int_0^T \int_{\Omega} (u^* - w^*) h \, dx dt \\ &= \int_0^T \int_{\Omega} \left(\frac{1}{(1 - u^*)^2} - \frac{1}{(1 - w^*)^2} \right) \lambda^* \xi f(x) \, dx dt \\ &\leq C \int_0^T \int_{\{u^* \geq w^*\}} \left(\frac{1}{(1 - u^*)^2} - \frac{1}{(1 - w^*)^2} \right) \xi \, dx dt \\ &\leq C \int_0^T \int_{\Omega} (u^* - w^*)^+ \xi \, dx dt, \end{aligned}$$

since $\|u^*\|_{\infty} < 1$ for $t \in [0, T)$. Therefore, we have

$$\int_0^T \int_{\Omega} (u^* - w^*) h \, dx dt \leq C \left(\int_0^T \int_{\Omega} [(u^* - w^*)^+]^2 \, dx dt \right)^{1/2} \left(\int_0^T \int_{\Omega} \xi^2 \, dx dt \right)^{1/2}.$$

On the other hand, $\xi(x, t) = \int_t^T T(s - t) h(x, s) \, ds$, where $T(t)$ is the heat semigroup with Dirichlet boundary condition, and hence

$$\|\xi(x, t)\|_{L^2}^2 \leq \left(\int_t^T \|h(x, s)\|_{L^2} \, ds \right)^2 \leq (T - t) \int_{\Omega} h^2 \, dx dt.$$

Therefore,

$$\int_0^T \int_{\Omega} \xi^2 \, dx dt \leq \frac{T^2}{2} \int_0^T \int_{\Omega} h^2 \, dx dt,$$

and so,

$$\int_0^T \int_{\Omega} (u^* - w^*) h \, dx dt \leq \frac{CT}{\sqrt{2}} \left(\int_0^T \int_{\Omega} [(u^* - w^*)^+]^2 \, dx dt \right)^{1/2} \left(\int_0^T \int_{\Omega} h^2 \, dx dt \right)^{1/2}.$$

Letting h converge to $(u^* - w^*)^+$ in L^2 , and since $u^* - w^* \in L^1(\Omega)$ we have

$$\int_0^T \int_{\Omega} [(u^* - w^*)^+]^2 \, dx dt \leq \frac{CT}{\sqrt{2}} \int_0^T \int_{\Omega} [(u^* - w^*)^+]^2 \, dx dt,$$

which gives that $u^* \leq w^*$ provided $C^2 T^2 < 2$, and our first claim follows.

Claim 2. There exist $0 < \tau_1 < t^*$, and $C_0, c_0 > 0$ such that for all $x \in \Omega$

$$u^*(x, \tau_1) \leq \min\{C_0\delta(x); w^*(x) - c_0\delta(x)\}. \quad (4.2.21)$$

Fix $0 < \tau < t^*$ sufficiently small, and let v be the solution of

$$v_t - \Delta v = \frac{\lambda^* f(x)}{(1-v)^2} \quad \text{for } (x, t) \in \Omega \times [0, \bar{T}), \quad (4.2.22a)$$

$$v(x, t) = 0 \quad \text{for } x \in \partial\Omega \times [0, \bar{T}), \quad (4.2.22b)$$

$$v(x, 0) = v_0 = u^*(x, \tau) \quad \text{for } x \in \Omega, \quad (4.2.22c)$$

where $[0, \bar{T})$ is the maximal interval of existence for v . Similarly to Claim 1, we can show that $0 \leq v \leq w^*$. Choose now $K > 1$ sufficiently large such that the path $z(x, t) := u^*(x, t) + \frac{1}{K}T(t)v_0$ satisfies $\|z(x, t)\|_\infty \leq 1$ for $0 \leq t < \bar{T}$. We then have

$$\begin{aligned} z_t - \Delta z &= \frac{\lambda^* f(x)}{(1-u^*)^2} \leq \frac{\lambda^* f(x)}{(1-z)^2} && \text{in } \Omega \times (0, \bar{T}), \\ z(x, t) &= 0 && \text{on } \partial\Omega \times (0, \bar{T}), \\ z(x, 0) &= \frac{v_0(x)}{K} && \text{in } \Omega, \end{aligned}$$

and the maximum principle gives that $z \leq v$. Consider now a function $\gamma : [0, \infty) \rightarrow R$ such that $\gamma(t) > 0$ and

$$T(t)v_0 \geq K\gamma(t)\delta \text{ on } \Omega. \quad (4.2.23)$$

We then get

$$u^* \leq v - \frac{1}{K}T(t)v_0 \leq w^* - \frac{1}{K}T(t)v_0 \leq w^* - \gamma(t)\delta \quad \text{for } 0 \leq t < \bar{T}. \quad (4.2.24)$$

On the other hand, for any $0 \leq t \leq T < t^*$, u^* is bounded by some constant $M < 1$ on $\bar{\Omega} \times [0, T]$ such that

$$u^* \leq MT(t)1_\Omega + \frac{C}{(1-M)^2} \int_0^t T(s)1_\Omega ds.$$

Consider now a function $C : [0, \infty) \rightarrow R$ such that $T(t)1_\Omega \leq C(t)\delta$ for $t \geq 0$, which means that

$$u^* \leq MC(t)\delta + C(M)C\delta$$

for any $0 \leq t \leq T$, where (4.2.20) is applied. This combined with (4.2.24) conclude the proof of Claim (4.2.21).

Claim 3. For $0 < \varepsilon < 1$ there exists w_ε satisfying $\|w_\varepsilon\|_\infty < 1$ and

$$\int_\Omega \nabla w_\varepsilon \nabla \varphi \geq \int_\Omega \left(\frac{1}{(1-w_\varepsilon)^2} - \varepsilon \right) \lambda^* \varphi f(x) \quad (4.2.25)$$

for all $\varphi \in H_0^1(\Omega)$ with $\varphi \geq 0$ on Ω . Moreover, there exists $0 < \varepsilon_1 \leq 1$ such that for $0 < \varepsilon < \varepsilon_1$, we also have

$$0 \leq w_\varepsilon(x) - \frac{c_0}{2}\delta(x) \quad \text{for } x \in \Omega \quad (4.2.26)$$

c_0 being as in (4.2.21).

To prove (4.2.25), we set

$$g(w^*) = \frac{1}{(1-w^*)^2}, \quad h(w^*) = \int_0^{w^*} \frac{ds}{g(s)}, \quad 0 \leq w^* < 1. \quad (4.2.27)$$

For any $\varepsilon \in (0, 1)$ we also set

$$\tilde{g}(w^*) = \frac{1}{(1-w^*)^2} - \varepsilon, \quad \tilde{h}(w^*) = \int_0^{w^*} \frac{ds}{\tilde{g}(s)}, \quad 0 \leq w^* < 1, \quad (4.2.28)$$

and $\phi_\varepsilon(w^*) := \tilde{h}^{-1}(h(w^*))$. It is easy to check that $\phi_\varepsilon(0) = 0$ and $0 \leq \phi_\varepsilon(s) < s$ for $s \geq 0$, and ϕ_ε is increasing and concave with

$$\phi'_\varepsilon(s) = \frac{g(\phi_\varepsilon(s)) - \varepsilon}{g(s)} > 0.$$

Setting $w_\varepsilon = \phi_\varepsilon(w^*)$, we have for any $\varphi \in H_0^1(\Omega)$ with $\varphi \geq 0$ on Ω ,

$$\begin{aligned} \int_\Omega \nabla w_\varepsilon \nabla \varphi &= \int_\Omega \phi'_\varepsilon(w^*) \nabla w^* \nabla \varphi = \int_\Omega \nabla w^* \nabla (\phi'_\varepsilon(w^*) \varphi) - \int_\Omega \phi''_\varepsilon(w^*) \varphi |\nabla w^*|^2 \\ &\geq \int_\Omega \frac{\lambda^* f(x)}{(1-w^*)^2} \phi'_\varepsilon(w^*) \varphi = \int_\Omega \left(\frac{1}{(1-w_\varepsilon)^2} - \varepsilon \right) \lambda^* \varphi f(x), \end{aligned}$$

which gives (4.2.25) for any $\varepsilon \in (0, \varepsilon_0)$.

In order to prove (4.2.26), we set

$$\eta(x) = \min\{w^*(x), (C_0 + c_0)\delta(x)\} \quad \text{and} \quad \eta_\varepsilon = \phi_\varepsilon \circ \eta,$$

where $\phi_\varepsilon(\cdot)$ is defined above, and C_0 and c_0 are as in (4.2.21). Since $\eta \leq w^*$ and ϕ_ε is increasing, we have $\eta_\varepsilon \leq \phi_\varepsilon(w^*) = w_\varepsilon$. Applying (4.2.21) we get that

$$0 \leq \eta(x) - c_0\delta(x) \quad \text{on} \quad \Omega. \quad (4.2.29)$$

We also note that $\eta_\varepsilon = \phi_\varepsilon(\eta) \leq \eta \leq M$ with $M = (C_0 + c_0)\delta(x)$, and $\phi'_\varepsilon(s) \rightarrow 1$ as $\varepsilon \rightarrow 0$ uniformly in $[0, 1]$. Therefore, for some $\theta \in (0, 1)$ we have

$$\begin{aligned} \eta - \eta_\varepsilon &= \eta - (\phi_\varepsilon(\eta) - \phi_\varepsilon(0)) = \eta(1 - \phi'_\varepsilon(\theta\eta)) \leq \eta \sup_{\{0 \leq s \leq 1\}} (1 - \phi'_\varepsilon(s)) \\ &\leq (C_0 + c_0)\delta \sup_{\{0 \leq s \leq 1\}} (1 - \phi'_\varepsilon(s)) \leq \frac{c_0}{2}\delta \end{aligned}$$

provided ε small enough, which gives

$$\eta \leq \eta_\varepsilon + \frac{c_0}{2}\delta. \quad (4.2.30)$$

We now conclude from (4.2.29) and (4.2.30) that

$$0 \leq \eta - c_0\delta \leq \eta_\varepsilon - \frac{c_0}{2}\delta \leq w_\varepsilon - \frac{c_0}{2}\delta$$

for small $\varepsilon > 0$, and (4.2.26) is therefore proved.

To complete the proof of Theorem 4.2.5, we assume that $t^* < \infty$ and we shall work towards a contradiction. In view of Claim 3), we let $\varepsilon > 0$ be small enough so that $0 \leq w_\varepsilon - \frac{c_0}{2}\delta$. Use Lemma 4.2.6 and choose $K > 2$ large enough such that the solution Z of the problem

$$\begin{aligned} Z_t - \Delta Z &= -\varepsilon \lambda^* f(x) && \text{in } \Omega \times (0, t^*), \\ Z(x, t) &= 0 && \text{on } \partial\Omega \times (0, t^*), \\ Z(x, 0) &= \frac{c_0}{K}\delta && \text{in } \Omega \end{aligned}$$

satisfies $0 \leq Z < 1 - u^*$ on $\bar{\Omega} \times (0, t^*)$. Let v be the solution of

$$\begin{aligned} v_t - \Delta v &= \left(\frac{1}{(1-|v|)^2} - \varepsilon \right) \lambda^* f(x) && \text{in } \Omega \times (0, s^*), \\ v(x, t) &= 0 && \text{on } \partial\Omega \times (0, s^*), \\ v(x, 0) &= w_\varepsilon && \text{in } \Omega, \end{aligned}$$

where $[0, s^*)$ is the maximal interval of existence for v . Setting $z(x, t) = Z(x, t) + u^*(x, t)$ for $0 \leq t < t^*$, we then have $0 \leq u^* \leq z < 1$ and

$$\begin{aligned} z_t - \Delta z &= \left(\frac{1}{(1-u^*)^2} - \varepsilon \right) \lambda^* f(x) \leq \left(\frac{1}{(1-z)^2} - \varepsilon \right) \lambda^* f(x) && \text{in } \Omega \times (0, t^*), \\ z(x, t) &= 0 && \text{on } \partial\Omega \times (0, t^*), \\ z(x, 0) &= \frac{c_0}{K}\delta(x) \leq w_\varepsilon(x) && \text{in } \Omega. \end{aligned}$$

Now the maximum principle gives that $z \leq v$ on $\Omega \times (0, \min\{s^*, t^*\})$, and in particular we have $0 \leq v$ on $\Omega \times (0, \min\{s^*, t^*\})$. Furthermore, the maximum principle and (4.2.25) also yield that $v \leq w_\varepsilon$. Since $\|w_\varepsilon\|_\infty < 1$ we necessarily have $t^* < s^* = \infty$. Therefore, $u^* \leq z \leq v \leq w_\varepsilon$ on $[0, t^*)$, which implies that $\|u^*\|_\infty < 1$ at $t = t^*$, which contradicts to our initial assumption that u^* is not a regular solution. ■

4.3 Location of touchdown points

In this section, we first present a couple of numerical simulations for different domains, different permittivity profiles, and various values of λ , by applying an implicit Crank-Nicholson scheme (see [32] for details) on (4.1.1). For the connection with the involved figures below, we discuss (4.1.1) in the form of

$$\frac{\partial u}{\partial t} - \Delta u = -\frac{\lambda f(x)}{(1+u)^2} \quad \text{for } x \in \Omega, \quad (4.3.1a)$$

$$u(x, t) = 0 \quad \text{for } x \in \partial\Omega; \quad u(x, 0) = 0 \quad \text{for } x \in \Omega, \quad (4.3.1b)$$

with the following two choices for the domain Ω

$$\Omega : [-1/2, 1/2] \quad (\text{slab}); \quad \Omega : x^2 + y^2 \leq 1 \quad (\text{unit disk}). \quad (4.3.2)$$

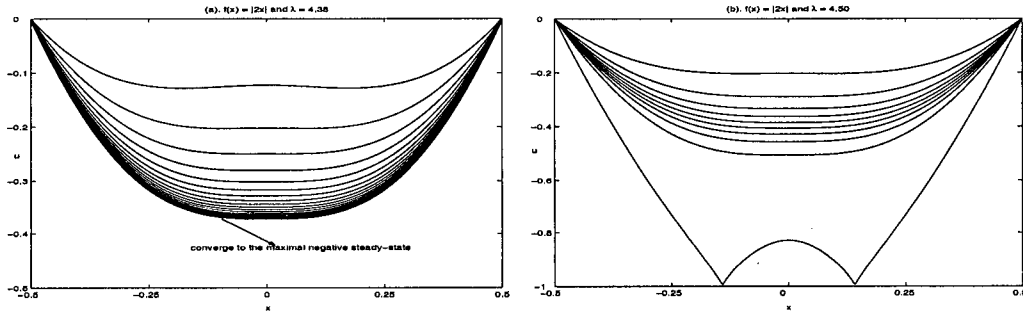


Figure 4.1: *Left Figure: u versus x for $\lambda = 4.38$. Right Figure: u versus x for $\lambda = 4.50$. Here we consider (4.3.1) with $f(x) = |2x|$ in the slab domain.*

Simulation 1: We consider $f(x) = |2x|$ for a permittivity profile in the slab domain $-1/2 \leq x \leq 1/2$. Here the number of the meshpoints is chosen as $N = 2000$ for the plots u versus x at different times. Figure 4.1(a) shows, for $\lambda = 4.38$, a typical sequence of solutions u for (4.3.1) approaching to the maximal negative steady-state. In Figure 4.1(b) we take $\lambda = 4.50$ and plot u versus x at different times $t = 0, 0.1880, 0.3760, 0.5639, 0.7519, 0.9399, 1.1279, 1.3159, 1.5039, 1.6918, 1.879818$, and a touchdown behavior is observed at two different nonzero points $x = \pm 0.14132$. These numerical results and Remark 4.2.1 point to a pull-in voltage $4.38 \leq \lambda^* < 4.50$.

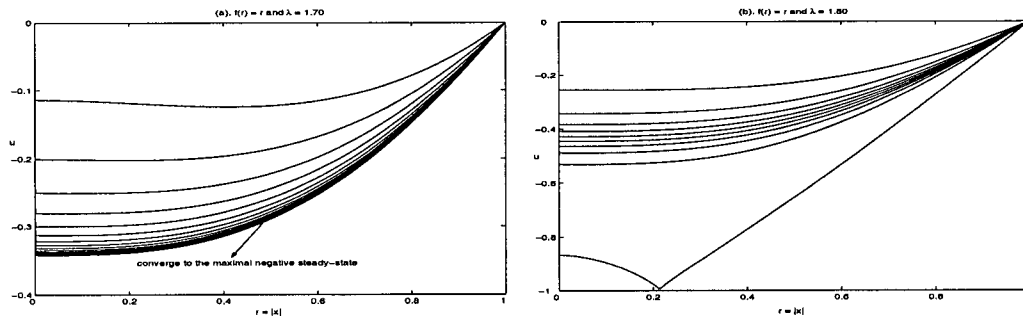


Figure 4.2: *Left Figure: u versus r for $\lambda = 1.70$. Right Figure: u versus r for $\lambda = 1.80$. Here we consider (4.3.1) with $f(r) = r$ in the unit disk domain.*

Simulation 2: Here we consider $f(r) = r$ for a permittivity profile in the unit disk domain. The number of meshpoints is again chosen to be $N = 2000$ for the plots u versus r at different times. Figure 4.2(a) shows how for $\lambda = 1.70$, a typical sequence of solutions u for (4.3.1) approach to the maximal negative steady-state. In Figure 4.2(b) we take $\lambda = 1.80$ and plot u versus r at different times $t = 0, 0.4475, 0.8950, 1.3426, 1.7901, 2.2376, 2.6851, 3.1326, 3.5802, 4.0277, 4.4751942$, and a touchdown behavior is observed at the nonzero points $r = 0.21361$. Again these numerical results point to a pull-in voltage $1.70 \leq \lambda^* < 1.80$.

One can observe from above that touchdown points at finite time are not the zero points of the varying permittivity profile f , a fact firstly observed and conjectured in [32]. The main purpose of this section is to analyze this phenomena.

Theorem 4.3.1. *Suppose $u(x, t)$ is a touchdown solution of (4.1.1) at a finite time T , then we have*

1. *The permittivity profile f cannot vanish on an isolated set of touchdown points in Ω .*
2. *On the other hand, zeroes of the permittivity profile can be locations of touchdown in infinite time.*

Note that Theorem 4.3.1 holds for any bounded domain. The proof of Theorem 4.3.1 is based on the following Harnack-type estimate.

Lemma 4.3.2. *For any compact subset K of Ω and any $m > 0$, there exists a constant $C = C(K, m) > 0$ such that $\sup_{x \in K} |u(x)| \leq C < 1$ whenever u satisfies*

$$\Delta u \geq \frac{m}{(1-u)^2} \quad x \in \Omega; \quad 0 \leq u < 1 \quad x \in \Omega. \quad (4.3.3)$$

Proof: Setting $v = 1/(1-u)$, then (4.3.3) gives that v satisfies

$$\frac{\Delta v}{v^2} - \frac{2|\nabla v|^2}{v^3} \geq mv^2 \quad \text{in } \Omega,$$

which means that v is a subsolution of the “linear” equation $\Delta v = 0$ in Ω . In order to apply the Harnack inequality on v , we need to show that for balls $B_r \subset \Omega$, we have that $v \in L^3(B_r)$ with an L^3 -norm that only depends on m and the radius r .

Without loss of generality, we may assume $0 \in K \subset \bar{\Omega}$. Let $B_r = B_r(0) \subset K$ be the ball centered at $x = 0$ and radius r . For $0 < r_1 < r_2 \leq 4r_1$, let $\eta(x) \in C_0^\infty(B_{r_2})$ be such that $\eta \equiv 1$ in B_{r_1} , $0 \leq \eta \leq 1$ in $B_{r_2} \setminus B_{r_1}$ and $|\nabla \eta| \leq 2/(r_2 - r_1)$. Multiplying (4.3.3) by $\phi^2/(1-u)$, where $\phi = \eta^\alpha$ and $\alpha \geq 1$ is to be determined later, and integrating by parts we have

$$\int_{B_{r_2}} \frac{m\phi^2}{(1-u)^3} \leq \int_{B_{r_2}} \frac{\phi^2 \Delta u}{1-u} = - \int_{B_{r_2}} \frac{\phi^2 |\nabla u|^2}{(1-u)^2} - \int_{B_{r_2}} \frac{2\phi \nabla \phi \cdot \nabla u}{1-u}. \quad (4.3.4)$$

From the fact,

$$\int_{B_{r_2}} \frac{2\phi \nabla \phi \cdot \nabla u}{1-u} \leq \int_{B_{r_2}} \phi^2 |\nabla u|^2 + 4 \int_{B_{r_2}} \frac{|\nabla \phi|^2}{(1-u)^2} \leq \int_{B_{r_2}} \frac{\phi^2 |\nabla u|^2}{(1-u)^2} + 4 \int_{B_{r_2}} \frac{|\nabla \phi|^2}{(1-u)^2},$$

(4.3.4) gives that

$$\int_{B_{r_2}} \frac{m\phi^2}{(1-u)^3} \leq 4 \int_{B_{r_2}} \frac{|\nabla \phi|^2}{(1-u)^2}.$$

Now choose $\phi = \eta^{2\beta}$ with $\beta = \frac{3}{2}$. Then Hölder’s inequality implies that

$$m \int_{B_{r_2}} \frac{\eta^{4\beta}}{(1-u)^3} \leq 16\beta^2 \left[\int_{B_{r_2}} |\nabla \eta|^{4\beta} \right]^{\frac{1}{2\beta}} \left[\int_{B_{r_2}} \frac{\eta^{4\beta}}{(1-u)^3} \right]^{\frac{2\beta-1}{2\beta}}.$$

This shows that

$$\int_{B_{r_1}} \frac{1}{(1-u)^3} \leq \int_{B_{r_2}} \frac{\eta^{4\beta}}{(1-u)^3} < C(m, r_1). \quad (4.3.5)$$

By virtue of the one-sided Harnack inequality, we have

$$\left\| \frac{1}{1-u} \right\|_{L^\infty(B_{\frac{r_1}{2}})} = \|v\|_{L^\infty(B_{\frac{r_1}{2}})} \leq C(r_1) \|v\|_{L^3(B_{r_1})} < C(r_1, m).$$

The rest follows from a standard compactness argument. ■

Proof of Theorem 4.3.1: Set $v = u_t$, then we have for any $t_1 < T$ that

$$v_t = \Delta v + \frac{2\lambda f(x)}{(1-u)^3} v \quad (x, t) \in \Omega \times (0, t_1); \quad (4.3.6a)$$

$$v(x, t) = 0 \quad (x, t) \in \partial\Omega \times (0, t_1); \quad v(x, 0) \geq 0 \quad x \in \Omega. \quad (4.3.6b)$$

Note that the term $\frac{2\lambda f}{(1-u)^3}$ is locally bounded in $\Omega \times (0, t_1)$, so that by the strong maximum principle, we may conclude

$$u_t = v > 0 \text{ for } (x, t) \in \Omega \times (0, t_1) \quad (4.3.7)$$

and therefore, $u_t > 0$ holds for all $(x, t) \in \Omega \times (0, T)$. Since K is an isolated set of touchdown points, there exists an open set U such that $K \subset U \subset \bar{U} \subset \Omega$ with no touchdown points in $\bar{U} \setminus K$. Consider now $0 < t_0 < T$ such that $\inf_{x \in \bar{U}} u_t(x, t_0) = C_1 > 0$. We claim that there exists $\varepsilon > 0$ such that

$$J^\varepsilon(x, t) = u_t - \frac{\varepsilon}{(1-u)^2} \geq 0 \quad \text{for all } (x, t) \in U \times (t_0, T), \quad (4.3.8)$$

Indeed, there exists $C_2 > 0$ such that $u_t(x, T) \geq C_2 > 0$ on U , and since ∂U has no touchdown points, there exists $\varepsilon > 0$ such that $J^\varepsilon \geq 0$ on the parabolic boundary of $U \times (t_0, T)$. Also, direct calculations imply that

$$J_t^\varepsilon - \Delta J^\varepsilon = \frac{2\lambda f}{(1-u)^3} J^\varepsilon + \frac{6\varepsilon |\nabla u|^2}{(1-u)^4} \geq \frac{2\lambda f}{(1-u)^3} J^\varepsilon.$$

Since $\frac{\varepsilon}{(1-u)^2}$ is locally bounded on $U \times (t_0, T)$, we can apply the maximum principle to obtaining (4.3.8).

If now $\inf_{x \in K} f(x) = 0$, then we may combine (4.3.8) and (4.1.1), to deduce that for a small neighborhood $B \subset U$ of some point $x_0 \in K$ where $f(x) \leq \varepsilon/2$, we have

$$\Delta u \geq \frac{\varepsilon}{2} \frac{1}{(1-u)^2} \quad \text{for } (x, t) \in B \times (t_0, T).$$

In view of Lemma 4.3.2, this contradicts the assumption that x_0 is a touchdown point.

For the second part, recall from Theorem 2.1.2 that the unique extremal solution for the stationary problem on the ball in the case $N \geq 8$ and for a permittivity profile $f(x) = |x|^\alpha$, is $u^*(x) = 1 - |x|^{\frac{2+\alpha}{3}}$ as long as α is small enough. Theorem 4.1.1 then implies that the origin 0 is a touchdown point of the solution even though it is also a root for the permittivity profile

(i.e., $f(0) = 0$). This complements the statement of Theorem 4.3.1 above. In other words, zero points of f in Ω cannot be on the isolated set of touchdown points in finite time (which occur when $\lambda > \lambda^*$) but can very well be touchdown points in infinite time of (4.1.1), which can only happen when $\lambda = \lambda^*$. The proof of Theorem 4.3.1 fails for touchdowns in infinite time, simply because the maximum principle cannot be applied in the infinite cylinder $\Omega \times (0, \infty)$. ■

4.4 Estimates for finite touchdown times

In this section we give comparison results and explicit estimates on finite touchdown times of dynamic deflections $u = u(x, t)$. This often translates into useful information concerning the speed of the operation for many MEMS devices such as RF switches or micro-valves.

4.4.1 Comparison results for finite touchdown time

We start by comparing the effect on finite touchdown time of two different but comparable permittivity profiles $f(x)$, at a given voltage λ .

Theorem 4.4.1. *Suppose $u_1 = u_1(x, t)$ (resp., $u_2 = u_2(x, t)$) is a touchdown solution for (4.1.1) associated to a fixed voltage λ and permittivity profiles f_1 (resp., f_2) with a corresponding finite touchdown time $T_\lambda(\Omega, f_1)$ (resp., $T_\lambda(\Omega, f_2)$). If $f_1(x) \geq f_2(x)$ on Ω and if $f_1(x) > f_2(x)$ on a set of positive measure, then necessarily $T_\lambda(\Omega, f_1) < T_\lambda(\Omega, f_2)$.*

Proof: By making a change of variable $v = 1 - u$, we can assume to be working with solutions of the following equation:

$$\frac{\partial v}{\partial t} - \Delta v = -\frac{\lambda f(x)}{v^2} \quad \text{for } x \in \Omega, \quad (4.4.1a)$$

$$v(x, t) = 1 \quad \text{for } x \in \partial\Omega, \quad (4.4.1b)$$

$$v(x, 0) = 1 \quad \text{for } x \in \Omega, \quad (4.4.1c)$$

where f is either f_1 or f_2 . Suppose now that $T_\lambda(\Omega, f_1) > T_\lambda(\Omega, f_2)$ and let $\Omega_0 \subset \Omega$ be the set of touchdown points of u_2 at finite time $T_\lambda(\Omega, f_2)$. Setting $w = u_2 - u_1$, we get that

$$w_t - \Delta w - \frac{\lambda(f_2 u_1 + f_1 u_2)}{u_1^2 u_2^2} w = \frac{\lambda(f_1 - f_2)}{u_1 u_2} \geq 0 \quad (x, t) \in \Omega \times (0, T_\lambda(\Omega, f_2)). \quad (4.4.2)$$

Since $w = 0$ at $t = 0$ as well as on $\partial\Omega \times (0, T_\lambda(\Omega, f_2))$, we get from the maximum principle that w cannot attain a negative minimum in $\Omega \times (0, T_\lambda(\Omega, f_2))$, and therefore $w \geq 0$ in $\Omega \times (0, T_\lambda(\Omega, f_2))$. Since $u_2 \rightarrow 0$ in Ω_0 as $t \rightarrow T_\lambda(\Omega, f_2)$, and since our assumption is that $T_\lambda(\Omega, f_1) > T_\lambda(\Omega, f_2)$, we then have $u_1 > 0$ in Ω_0 as $t \rightarrow T_\lambda(\Omega, f_2)$. Therefore, $w < 0$ in Ω_0 as $t \rightarrow T_\lambda(\Omega, f_2)$, which is a contradiction and therefore $T_\lambda(\Omega, f_1) \leq T_\lambda(\Omega, f_2)$.

To prove the strict inequality, we note that the above proof shows that $w \geq 0$ in $\Omega \times (0, T_\lambda(\Omega, f_2))$, which once combined with (4.4.2) gives that

$$w_t - \Delta w \geq 0, \quad \text{in } \Omega \times (t_1, T_\lambda(\Omega, f_2)),$$

where $t_1 > 0$ is chosen so that $w(x, t_1) \neq 0$ in Ω . Now we compare w with the solution z of

$$z_t - \Delta z = 0 \quad \text{in } \Omega \times (t_1, T_\lambda(\Omega, f_2))$$

subject to $z(x, t_1) = w(x, t_1)$ and $z(x, t) = 0$ on $\partial\Omega \times (t_1, T_\lambda(\Omega, f_2))$. Clearly, $w \geq z$ in $\Omega \times (t_1, T_\lambda(\Omega, f_2))$. On the other hand, for any $t_0 > t_1$ we have $z > 0$ in $\Omega \times (t_0, T_\lambda(\Omega, f_2))$. Consequently, $w > 0$ which means that $u_2 > u_1$ in $\Omega \times (t_0, T_\lambda(\Omega, f_2))$ and therefore $T_\lambda(\Omega, f_1) < T_\lambda(\Omega, f_2)$. ■

The second comparison result deals with different applied voltages but identical permittivity profiles.

Theorem 4.4.2. *Suppose $u_1 = u_1(x, t)$ (resp., $u_2 = u_2(x, t)$) is a solution for (4.1.1) associated to a voltage λ_1 (resp., λ_2) and which has a finite touchdown time $T_{\lambda_1}(\Omega, f)$ (resp., $T_{\lambda_2}(\Omega, f)$). If $\lambda_1 > \lambda_2$ then necessarily $T_{\lambda_1}(\Omega, f) < T_{\lambda_2}(\Omega, f)$.*

Proof: It is similar to the proof of Theorem 4.4.1, except that for $w = u_2 - u_1$, (4.4.2) is replaced by

$$w_t - \Delta w - \frac{\lambda_1(u_1 + u_2)f}{u_1^2 u_2^2} w = \frac{(\lambda_1 - \lambda_2)f}{u_2^2} \geq 0 \quad (x, t) \in \Omega \times (0, T).$$

The details are left for the interested reader. ■

Remark 4.4.1. A reasoning similar to the one found in Proposition 2.5 of [29], gives some information on the dependence on the shape of the domain. Indeed, for any bounded domain Γ in \mathbb{R}^N and any non-negative continuous function f on Γ , we have

$$\lambda^*(\Gamma, f) \geq \lambda^*(B_R, f^*) \text{ and } T_\lambda(\Gamma, f) \geq T_\lambda(B_R, f^*),$$

where $B_R = B_R(0)$ is the Euclidean ball in \mathbb{R}^N with radius $R > 0$ and with volume $|B_R| = |\Gamma|$, where f^* is the Schwarz symmetrization of f .

We now present numerical results comparing finite touchdown times in a slab domain.

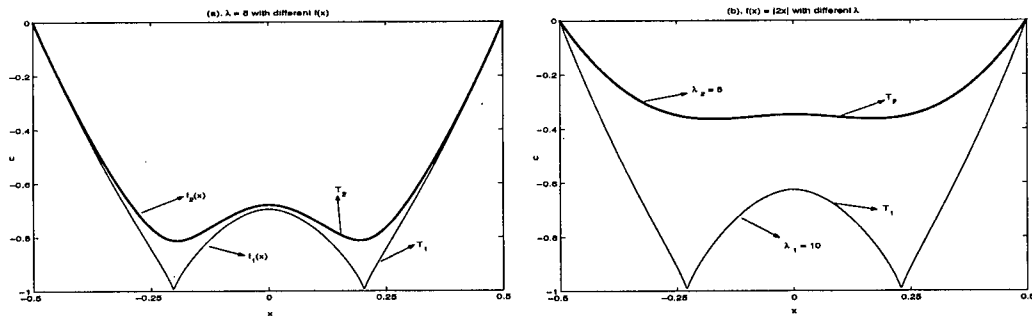


Figure 4.3: Left Figure: plots of u versus x for different $f(x)$ at $\lambda = 8$ and $t = 0.185736$. Right Figure: plots of u versus x for different λ with $f(x) = |2x|$ and $t = 0.1254864$.

Figure 4.3(a): Dependence on the dielectric permittivity profiles f

We consider (4.3.1) for the cases where

$$f_1(x) = |2x| \quad \text{and} \quad f_2(x) = \begin{cases} |2x| & \text{if } |x| \leq \frac{1}{8}, \\ 1/4 + 2 \sin(|x| - 1/8) & \text{otherwise.} \end{cases} \quad (4.4.3)$$

Using $N = 1000$ meshpoints, we plot u versus x with $\lambda = 8$ at the time $t = 0.185736$ in Figure 4.3(a). The numerical results show that the finite touchdown time $T_\lambda(\Omega, f_1)$ for the case $f_1(x)$ and $T_\lambda(\Omega, f_2)$ for the case $f_2(x)$ are 0.185736 and 0.186688, respectively.

Figure 4.3(b): Dependence on the applied voltage λ

Using $N = 1000$ meshpoints and the profile $f(x) = |2x|$, we plot u of (4.3.1) versus x with different values of λ at the time $t = 0.1254864$. The numerical results show that finite touchdown time $T_{\lambda_1}(\Omega, f)$ for applied voltage $\lambda_1 = 10$ and $T_{\lambda_2}(\Omega, f)$ for applied voltage $\lambda_2 = 8$ are 0.1254864 and 0.185736, respectively.

4.4.2 Explicit bounds on touchdown times

We now establish claims 1), 3) and 4) in Theorem 1.3 of the introduction. Note that here $\bar{\lambda}_1 \geq \lambda^*$ and $\bar{\lambda}_2 \geq \lambda^*$ are as in Theorem 2.1.1.

Proposition 4.4.3. Suppose f is a non-negative continuous function on a bounded domain Ω , and let u be a solution of (4.1.1) corresponding to a voltage λ . Then,

1. For any $\lambda > 0$, we have $T_\lambda(\Omega, f) \geq T_* := \frac{1}{3\lambda \sup_{x \in \Omega} f(x)}$.
2. If $\inf_\Omega f > 0$, and if $\lambda > \bar{\lambda}_1 := \frac{4\mu_\Omega}{27 \inf_{x \in \Omega} f(x)}$, then

$$T_\lambda(\Omega, f) \leq T_{1,\lambda} := \int_0^1 \left[\frac{\lambda \inf_{x \in \Omega} f(x)}{(1-s)^2} - \mu_\Omega s \right]^{-1} ds. \tag{4.4.4}$$

3. If $f > 0$ on a set of positive measure, and if $\lambda > \bar{\lambda}_2 := \frac{\mu_\Omega}{3 \int_\Omega f \phi_\Omega dx}$, then

$$T_\lambda(\Omega, f) \leq T_{2,\lambda} := -\frac{1}{\mu_\Omega} \log \left[1 - \frac{\mu_\Omega}{3\lambda} \left(\int_\Omega f \phi_\Omega dx \right)^{-1} \right]. \tag{4.4.5}$$

Here μ_Ω and ϕ_Ω are the first eigenpair of $-\Delta$ on $H_0^1(\Omega)$ with normalized $\int_\Omega \phi_\Omega dx = 1$.

Proof: 1) Consider the initial value problem:

$$\begin{aligned} \frac{d\eta(t)}{dt} &= \frac{\lambda M}{(1-\eta(t))^2}, \\ \eta(0) &= 0, \end{aligned} \tag{4.4.6}$$

where $M = \sup_{x \in \Omega} f(x)$. From (4.4.6) one has $\frac{1}{\lambda M} \int_0^{\eta(t)} (1-s)^2 ds = t$. If T_* is the time where $\lim_{t \rightarrow T_*} \eta(t) = 1$, then we have $T_* = \frac{1}{\lambda M} \int_0^1 (1-s)^2 ds = \frac{1}{3\lambda M}$. Obviously, $\eta(t)$ is now a super-function of $u(x, t)$ near touchdown, and thus we have

$$T \geq T_* = \frac{1}{3\lambda M} = \frac{1}{3\lambda \sup_{x \in \Omega} f(x)},$$

which completes the proof of 1).

The following analytic upper bounds of finite touchdown time T were established in Theorem 3.1 and 3.2 of [32].

2) Without loss of generality we assume that $\phi_\Omega > 0$ in Ω . Multiplying (4.1.1a) by ϕ_Ω , and integrating over the domain, we obtain

$$\frac{d}{dt} \int_{\Omega} \phi_\Omega u \, dx = \int_{\Omega} \phi_\Omega \Delta u \, dx + \int_{\Omega} \frac{\lambda \phi_\Omega f(x)}{(1-u)^2} \, dx. \quad (4.4.7)$$

Using Green's theorem, together with the lower bound C_0 of f , we get

$$\frac{d}{dt} \int_{\Omega} \phi_\Omega u \, dx \geq -\mu_\Omega \int_{\Omega} \phi_\Omega u \, dx + \lambda C_0 \int_{\Omega} \frac{\phi_\Omega}{(1-u)^2} \, dx. \quad (4.4.8)$$

Next, we define an energy-like variable $E(t)$ by $E(t) = \int_{\Omega} \phi_\Omega u \, dx$ so that

$$E(t) = \int_{\Omega} \phi_\Omega u \, dx \leq \sup_{\Omega} u \int_{\Omega} \phi_\Omega \, dx = \sup_{\Omega} u. \quad (4.4.9)$$

Moreover, $E(0) = 0$ since $u = 0$ at $t = 0$. Then, using Jensen's inequality on the second term on the right-hand side of (4.4.8), we obtain

$$\frac{dE}{dt} + \mu_\Omega E \geq \frac{\lambda C_0}{(1-E)^2}, \quad E(0) = 0. \quad (4.4.10)$$

We then compare $E(t)$ with the solution $F(t)$ of

$$\frac{dF}{dt} + \mu_\Omega F = \frac{\lambda C_0}{(1-F)^2}, \quad F(0) = 0. \quad (4.4.11)$$

Standard comparison principles yield that $E(t) \geq F(t)$ on their domains of existence. Therefore,

$$\sup_{\Omega} u \geq E(t) \geq F(t). \quad (4.4.12)$$

Next, we separate variables in (4.4.11) to determine t in terms of F . The touchdown time \bar{T}_1 for F is obtained by setting $F = 1$ in the resulting formula. In this way, we get

$$\bar{T}_1 \equiv \int_0^1 \left[\frac{\lambda C_0}{(1-s)^2} - \mu_\Omega s \right]^{-1} ds. \quad (4.4.13)$$

The touchdown time \bar{T}_1 is finite when the integral in (4.4.13) converges. A simple calculation shows that this occurs when $\lambda > \bar{\lambda}_1 \equiv \frac{4\mu_\Omega}{27C_0}$. Hence if \bar{T}_1 is finite, then (4.4.12) implies that the touchdown time T of (4.1.1) must also be finite. Therefore, when $\lambda > \bar{\lambda}_1 = \frac{4\mu_\Omega}{27C_0}$, we have that T satisfies

$$T \leq \bar{T}_1 \equiv \int_0^1 \left[\frac{\lambda C_0}{(1-s)^2} - \mu_\Omega s \right]^{-1} ds. \quad (4.4.14)$$

(3) Multiply now (4.1.1a) by $\phi_\Omega(1-u)^2$, and integrate the resulting equation over Ω to get

$$\frac{d}{dt} \int_{\Omega} \frac{\phi_\Omega}{3} (1-u)^3 \, dx = - \int_{\Omega} \phi_\Omega (1-u)^2 \Delta u \, dx - \int_{\Omega} \lambda f \phi_\Omega \, dx. \quad (4.4.15)$$

We calculate the first term on the right-hand side of (4.4.15) to get

$$\frac{d}{dt} \int_{\Omega} \frac{\phi_{\Omega}}{3} (1-u)^3 dx \quad (4.4.16a)$$

$$= \int_{\Omega} \nabla u \cdot \nabla [\phi_{\Omega} (1-u)^2] dx + \int_{\partial\Omega} (1-u)^2 \phi_{\Omega} \nabla u \cdot \hat{n} dS - \int_{\Omega} \lambda f \phi_{\Omega} dx \quad (4.4.16b)$$

$$= - \int_{\Omega} 2(1-u) \phi_{\Omega} |\nabla u|^2 dx - \int_{\Omega} \frac{1}{3} \nabla \phi_{\Omega} \cdot \nabla [(1-u)^3] dx - \int_{\Omega} \lambda f \phi_{\Omega} dx \quad (4.4.16c)$$

$$\leq - \frac{1}{3} \int_{\partial\Omega} \nabla \phi_{\Omega} \cdot \nu dS - \frac{\mu_{\Omega}}{3} \int_{\Omega} (1-u)^3 \phi_{\Omega} dx - \int_{\Omega} \lambda f \phi_{\Omega} dx, \quad (4.4.16d)$$

where ν is the unit outward normal to $\partial\Omega$. Since $\int_{\partial\Omega} \nabla \phi_{\Omega} \cdot \nu dS = -\mu_{\Omega}$, we further estimate from (4.4.16d) that

$$\frac{dE}{dt} + \mu_{\Omega} E \leq R, \quad R \equiv \frac{\mu_{\Omega}}{3} - \lambda \int_{\Omega} f \phi_{\Omega} dx, \quad (4.4.17)$$

where $E(t)$ is defined by

$$E(t) \equiv \frac{1}{3} \int_{\Omega} \phi_{\Omega} (1-u)^3 dx, \quad E(0) = \frac{1}{3}. \quad (4.4.18)$$

Next, we compare $E(t)$ with the solution $F(t)$ of

$$\frac{dF}{dt} + \mu_{\Omega} F = R, \quad F(0) = \frac{1}{3}. \quad (4.4.19)$$

Again, comparison principles and the definition of E yield

$$\frac{1}{3} \inf_{\Omega} (1-u)^3 \leq E(t) \leq F(t). \quad (4.4.20)$$

For $\lambda > \bar{\lambda}_2$ we have that $R < 0$ in (4.4.17) and (4.4.19). For $R < 0$, we have that $F = 0$ at some finite time $t = \bar{T}_2$. From (4.4.20), this implies that $E = 0$ at finite time. Thus, u has touchdown at some finite-time $T < \bar{T}_2$. By calculating \bar{T}_2 explicitly, and by using (4.4.20), the touchdown time T for (4.1.1) is found to satisfy

$$T \leq \bar{T}_2 \equiv -\frac{1}{\mu_{\Omega}} \log \left[1 - \frac{\mu_{\Omega}}{3\lambda} \left(\int_{\Omega} f \phi_{\Omega} dx \right)^{-1} \right]. \quad (4.4.21)$$

■

Remark 4.4.2. It follows from the above that if $\lambda > \max \{ \bar{\lambda}_1, \bar{\lambda}_2 \}$, then

$$T \leq \min \{ T_{0,\lambda}, T_{1,\lambda}, T_{2,\lambda} \}. \quad (4.4.22)$$

where $T_{0,\lambda}$ is given by Theorem 4.2.3. We note that the three estimates on the touchdown times are not comparable. Indeed, it is clear that $T_{0,\lambda}$ is the better estimate when $\lambda^* < \lambda < \min \{ \bar{\lambda}_1, \bar{\lambda}_2 \}$ since $T_{1,\lambda}$ and $T_{2,\lambda}$ are not finite. On the other hand, our numerical simulations show that $T_{0,\lambda}$ can be much worse than the others, for $\lambda > \max \{ \bar{\lambda}_1, \bar{\lambda}_2 \}$.

Here are now some numerical estimates of touchdown times for several choices of the domain Ω given by (4.3.2) and the exponential profile $f(x)$ satisfying

$$\text{(slab) : } f(x) = e^{\alpha(x^2-1/4)} \quad \text{(exponential),} \quad (4.4.23a)$$

$$\text{(unit disk) : } f(x) = e^{\alpha(|x|^2-1)} \quad \text{(exponential),} \quad (4.4.23b)$$

where $\alpha \geq 0$.

[htb]

Ω	α	T_*	T	$T_{0,\lambda}$	$T_{1,\lambda}$	$T_{2,\lambda}$
slab	0	1/60	0.01668	0.2555	0.0175	0.01825
slab	1.0	1/60	0.02096	≤ 0.3383	0.0229	0.02275
slab	3.0	1/60	0.03239	≤ 0.6121	0.0395	0.03588
slab	6.0	1/60	0.06312	≤ 1.7033	0.0973	0.07544
unit disk	0	1/60	0.01667	0.2420	0.0172	0.01745
unit disk	0.5	1/60	0.02241	≤ 0.4103	0.0289	0.02507
unit disk	1.0	1/60	0.02927	≤ 0.7123	0.0492	0.03579
unit disk	3.0	1/60	0.09563	≤ 8.9847	1.1614	0.15544

Table 4.1: Computations for finite touchdown time T with the bounds T_* , $T_{0,\lambda}$, $T_{1,\lambda}$ and $T_{2,\lambda}$ given in Proposition 4.4.3. Here the applied voltage $\lambda = 20$ and the profile is chosen as (4.4.23).

[htb]

Ω	$T(\lambda = 5)$	$T(\lambda = 10)$	$T(\lambda = 15)$	$(\lambda = 20)$
slab	0.07495	0.03403	0.02239	0.01668
unit disk	0.06699	0.03342	0.02235	0.01667

Table 4.2: Numerical values for finite touchdown time T at different applied voltages $\lambda = 5, 10, 15$ and 20 , respectively. Here the constant permittivity profile $f(x) \equiv 1$ is chosen.

In Table 2.1 of §2.2 we give numerical results for the saddle-node value λ^* with the bounds $\underline{\lambda}$, $\bar{\lambda}_1$ and $\bar{\lambda}_2$ given in Theorem 2.1.1, for the exponential permittivity profile chosen as (4.4.23). Following the numerical results of Table 2.1 of §2.2, here we can compute in Table 4.1 the values of finite touchdown time T at $\lambda = 20$, with the bounds T_* , $T_{0,\lambda}$, $T_{1,\lambda}$ and $T_{2,\lambda}$ given in Theorem 4.2.3 and Proposition 4.4.3. Using the meshpoints $N = 800$ we compute finite touchdown time T with error less than 0.00001. The numerical results in Table 4.1 show that the bounds $T_{1,\lambda}$ and $T_{2,\lambda}$ for T are much better than $T_{0,\lambda}$. Further the bound $T_{1,\lambda}$ is better than $T_{2,\lambda}$ for smaller values of α , and however the bound $T_{2,\lambda}$ is better than $T_{1,\lambda}$ for larger values of α . In fact, for $\alpha \gg 1$ and λ large enough we can deduce from (2.3.23) that

$$T_{1,\lambda} \sim \frac{1}{3\lambda} e^{d_1 \alpha}, \quad T_{2,\lambda} \sim \frac{d_2}{\lambda} \alpha^2.$$

Here $d_1 = 1/4$, $d_2 = 1/3\pi^2$ for the slab domain, and $d_1 = 1$, $d_2 = 4/3z_0^2$ for the unit disk, where z_0 is the first zero of $J_0(z) = 0$. Therefore, for $\alpha \gg 1$ and fixed λ large enough, the bound $T_{2,\lambda}$

is better than $T_{1,\lambda}$. Table 4.1 also shows that for fixed applied voltage λ , the touchdown time is seen to increase once α is increased or equivalently the spatial extent where $f(x) \ll 1$ is increased. However, Theorem 4.4.2 tells us that for fixed permittivity profile f , by increasing the applied voltage λ within the available power supply, the touchdown time can be decreased and consequently the operating speed of MEMS devices can be improved. In Table 4.2 we give numerical values for finite touchdown time T with error less than 0.00001, at different applied voltages $\lambda = 5, 10, 15$ and 20 , respectively. Here the constant permittivity profile $f(x) \equiv 1$ is chosen and the meshpoints $N = 800$ again.

4.5 Asymptotic analysis of touchdown profiles

In this section, we discuss touchdown profiles by the method of asymptotic analysis, which provide some information on the refined touchdown rate studied in next Chapter.

4.5.1 Touchdown profile: $f(x) \equiv 1$

We first construct a local expansion of the solution near the touchdown time and touchdown location by adapting the method of [45] used for blow-up behavior. In the analysis of this subsection we assume that $f(x) \equiv 1$ and touchdown occurs at $x = 0$ and $t = T$. In the absence of diffusion, the time-dependent behavior of (4.1.1) is given by $u_t = \lambda(1 - u)^{-2}$. Integrating this differential equation and setting $u(T) = 1$, we get $(1 - u)^3 = -3\lambda(t - T)$. This solution motivates the introduction of a new variable $v(x, t)$ defined in terms of $u(x, t)$ by

$$v = \frac{1}{3\lambda}(1 - u)^3. \quad (4.5.1)$$

A simple calculation shows that (4.1.1) transforms exactly to the following problem for v :

$$v_t = \Delta v - \frac{2}{3v}|\nabla v|^2 - 1, \quad x \in \Omega, \quad (4.5.2a)$$

$$v = \frac{1}{3\lambda}, \quad x \in \partial\Omega; \quad v = \frac{1}{3\lambda}, \quad t = 0. \quad (4.5.2b)$$

Notice that $u = 1$ maps to $v = 0$. We will find a formal power series solution to (4.5.2a) near $v = 0$.

As in [45] we look for a locally radially symmetric solution to (4.5.2) in the form

$$v(x, t) = v_0(t) + \frac{r^2}{2!}v_2(t) + \frac{r^4}{4!}v_4(t) + \dots, \quad (4.5.3)$$

where $r = |x|$. We then substitute (4.5.3) into (4.5.2a) and collect coefficients in r . In this way, we obtain the following coupled ordinary differential equations for v_0 and v_2 :

$$v_0' = -1 + Nv_2, \quad v_2' = -\frac{4}{3v_0}v_2^2 + \frac{(N+2)}{3}v_4. \quad (4.5.4)$$

We are interested in the solution to this system for which $v_0(T) = 0$, with $v_0' < 0$ and $v_2 > 0$ for $T - t > 0$ with $T - t \ll 1$. The system (4.5.4) has a closure problem in that v_2 depends

on v_4 . However, we will assume that $v_4 \ll v_2^2/v_0$ near the singularity. With this assumption, (4.5.4) reduces to

$$v_0' = -1 + Nv_2, \quad v_2' = -\frac{4}{3v_0}v_2^2. \quad (4.5.5)$$

We now solve the system (4.5.5) asymptotically as $t \rightarrow T^-$ in a similar manner as was done in [45]. We first assume that $Nv_2 \ll 1$ near $t = T$. This leads to $v_0 \sim T - t$, and the following differential equation for v_2 :

$$v_2' \sim \frac{-4}{3(T-t)}v_2^2, \quad \text{as } t \rightarrow T^-. \quad (4.5.6)$$

By integrating (4.5.6), we obtain that

$$v_2 \sim -\frac{3}{4[\log(T-t)]} + \frac{B_0}{[\log(T-t)]^2} + \dots, \quad \text{as } t \rightarrow T^-, \quad (4.5.7)$$

for some unknown constant B_0 . From (4.5.7), we observe that the consistency condition that $Nv_2 \ll 1$ as $t \rightarrow T^-$ is indeed satisfied. Substituting (4.5.7) into the equation (4.5.5) for v_0 , we obtain for $t \rightarrow T^-$ that

$$v_0' = -1 + N\left(-\frac{3}{4[\log(T-t)]} + \frac{B_0}{[\log(T-t)]^2} + \dots\right). \quad (4.5.8)$$

Using the method of dominant balance, we look for a solution to (4.5.8) as $t \rightarrow T^-$ in the form

$$v_0 \sim (T-t) + (T-t)\left[\frac{C_0}{[\log(T-t)]} + \frac{C_1}{[\log(T-t)]^2} + \dots\right], \quad (4.5.9)$$

for some C_0 and C_1 to be found. A simple calculation yields that

$$v_0 \sim (T-t) + \frac{-3N(T-t)}{4|\log(T-t)|} + \frac{-N(B_0 - 3/4)(T-t)}{|\log(T-t)|^2} + \dots, \quad \text{as } t \rightarrow T^-. \quad (4.5.10)$$

The local form for v near touchdown is $v \sim v_0 + r^2v_0/2$. Using the leading term in v_2 from (4.5.7) and the first two terms in v_0 from (4.5.10), we obtain the local form

$$v \sim (T-t)\left[1 - \frac{3N}{4|\log(T-t)|} + \frac{3r^2}{8(T-t)|\log(T-t)|} + \dots\right], \quad (4.5.11)$$

for $r \ll 1$ and $t - T \ll 1$. Finally, using the nonlinear mapping (4.5.1) relating u and v , we conclude that

$$u \sim 1 - \left[3\lambda(T-t)\right]^{1/3} \left(1 - \frac{3N}{4|\log(T-t)|} + \frac{3r^2}{8(T-t)|\log(T-t)|} + \dots\right)^{1/3}. \quad (4.5.12)$$

We note, as in [45], that if we use the local behavior $v \sim (T-t) + 3r^2/[8|\log(T-t)|]$, we get that

$$\frac{|\nabla v|^2}{v} \sim \left[\frac{2}{3}|\log(T-t)| + \frac{16(T-t)|\log(T-t)|^2}{9r^2}\right]^{-1}. \quad (4.5.13)$$

Hence, the term $|\nabla v|^2/v$ in (4.5.2a) is bounded for any r , even as $t \rightarrow T^-$. This allows us to use a simple finite-difference scheme to compute numerical solutions to (4.5.2). With this observation, we now perform a few numerical experiments on the transformed problem (4.5.2). For the slab domain, we define v_j^m for $j = 1, \dots, N+2$ to be the discrete approximation to $v(m\Delta t, -1/2 + (j-1)h)$, where $h = 1/(N+1)$ and Δt are the spatial and temporal mesh sizes, respectively. A second order accurate in space, and first order accurate in time, discretization of (4.5.2) is

$$v_j^{m+1} = v_j^m + \Delta t \left(\frac{(v_{j+1}^m - 2v_j^m + v_{j-1}^m)}{h^2} - 1 - \frac{(v_{j+1}^m - v_{j-1}^m)^2}{6v_j^m h^2} \right), \quad j = 2, \dots, N+1, \quad (4.5.14)$$

with $v_1^m = v_{N+2}^m = (3\lambda)^{-1}$ for $m \geq 0$. The initial condition is $v_j^0 = (3\lambda)^{-1}$ for $j = 1, \dots, N+2$. The time-step Δt is chosen to satisfy $\Delta t < h^2/4$ for the stability of the discrete scheme. Using this argument, one can compute numerical results of dynamic deflection u , see Figures 4.1-4.3 of this Chapter.

4.5.2 Touchdown profile: variable permittivity

In this subsection we obtain some formal asymptotic results for touchdown behavior associated with a spatially variable permittivity profile in a slab domain. Suppose u is a touchdown solution of (4.1.1) at finite time T , and let $x = x_0$ be a touchdown point of u . With the transformation

$$v = \frac{1}{3\lambda}(1-u)^3, \quad (4.5.15)$$

the problem (4.1.1) for u in the slab domain transforms exactly to

$$v_t = v_{xx} - \frac{2}{3v}v_x^2 - f(x), \quad -1/2 < x < 1/2, \quad (4.5.16a)$$

$$v = \frac{1}{3\lambda}, \quad x = \pm 1/2; \quad v = \frac{1}{3\lambda}, \quad t = 0, \quad (4.5.16b)$$

where $f(x)$ is the permittivity profile.

In order to discuss the touchdown profile of u near (x_0, T) , we use the formal power series method of §4.5.1 to locally construct a power series solution to (4.5.16) near touchdown point x_0 and touchdown time T . For this purpose, we look for a touchdown profile for (4.5.16), near $x = x_0$, in the form

$$v(x, t) = v_0(t) + \frac{(x-x_0)^2}{2!}v_2(t) + \frac{(x-x_0)^3}{3!}v_3(t) + \frac{(x-x_0)^4}{4!}v_4(t) + \dots \quad (4.5.17)$$

In order for v to be a touchdown profile, it is clear that we must require that

$$\lim_{t \rightarrow T^-} v_0 = 0, \quad v_0 > 0, \quad \text{for } t < T; \quad v_2 > 0, \quad \text{for } t - T \ll 1. \quad (4.5.18)$$

We first discuss the case where $f(x)$ is analytic at $x = x_0$ with $f(x_0) > 0$. Therefore, for $x - x_0 \ll 1$, $f(x)$ has the convergent power series expansion

$$f(x) = f_0 + f_0'(x-x_0) + \frac{f_0''(x-x_0)^2}{2} + \dots, \quad (4.5.19)$$

where $f_0 \equiv f(x_0)$, $f'_0 \equiv f'(x_0)$, and $f''_0 \equiv f''(x_0)$. Substituting (4.5.17) and (4.5.19) into (4.5.16), we equate powers of $x - x_0$ to obtain

$$v'_0 = -f_0 + v_2, \quad (4.5.20a)$$

$$v'_2 = -\frac{4v_2^2}{3v_0} + v_4 - f''_0, \quad (4.5.20b)$$

$$v_3 = f'_0. \quad (4.5.20c)$$

We now assume that $v_2 \ll 1$ and $v_4 \ll 1$ as $t \rightarrow T^-$. This yields that $v_0 \sim f_0(T - t)$, and

$$v'_2 \sim -\frac{4v_2^2}{3f_0(T - t)} - f''_0. \quad (4.5.21)$$

For $t \rightarrow T^-$, we obtain from a simple dominant balance argument that

$$v_2 \sim -\frac{3f_0}{4[\log(T - t)]} + \dots, \quad \text{as } t \rightarrow T^-. \quad (4.5.22)$$

Substituting (4.5.22) into (4.5.20a), and integrating, we obtain that

$$v_0 \sim f_0(T - t) + \frac{-3f_0(T - t)}{4|\log(T - t)|} + \dots, \quad \text{as } t \rightarrow T^-. \quad (4.5.23)$$

Next, we substitute (4.5.22), (4.5.23) and (4.5.20c) into (4.5.17), to obtain the local touchdown behavior

$$v \sim f_0(T - t) \left[1 - \frac{3}{4|\log(T - t)|} + \frac{3(x - x_0)^2}{8(T - t)|\log(T - t)|} + \frac{f'_0(x - x_0)^3}{6f_0(T - t)} + \dots \right], \quad (4.5.24)$$

for $(x - x_0) \ll 1$ and $t - T \ll 1$. Finally, using the nonlinear mapping (4.5.15) relating u and v , we conclude that

$$u \sim 1 - \left[3f_0\lambda(T - t) \right]^{1/3} \left(1 - \frac{3}{4|\log(T - t)|} + \frac{3(x - x_0)^2}{8(T - t)|\log(T - t)|} + \frac{f'_0(x - x_0)^3}{6f_0(T - t)} + \dots \right)^{1/3}. \quad (4.5.25)$$

Here $f_0 \equiv f(x_0)$ and $f'_0 \equiv f'(x_0)$.

In the following, we exclude the possibility of $f(x_0) = 0$ by using a formal power series analysis. We discuss the case where $f(x)$ is analytic at $x = x_0$, with $f(x_0) = 0$ and $f'(x_0) = 0$, so that $f(x) = f_0(x - x_0)^2 + O((x - x_0)^3)$ as $x \rightarrow x_0$ with $f_0 > 0$. We then look for a power series solution to (4.5.16) as in (4.5.17). In place of (4.5.20) for v_3 , we get $v_3 = 0$, and

$$v'_0 = v_2, \quad v'_2 = -\frac{4v_2^2}{3v_0} + v_4 - 2f_0. \quad (4.5.26)$$

Assuming that $v_4 \ll 1$ as before, we can combine the equations in (4.5.26) to get

$$v''_0 = -\frac{4(v'_0)^2}{3v_0} - 2f_0. \quad (4.5.27)$$

By solving (4.5.27) with $v_0(T) = 0$, we obtain the exact solution

$$v_0 = -\frac{3f_0}{11}(T-t)^2 < 0, \quad v_2 = \frac{6f_0}{11}(T-t). \quad (4.5.28)$$

Since the criteria (4.5.18) are not satisfied, the form (4.5.28) does not represent a touchdown profile centered at $x = x_0$. Therefore, the above asymptotical analysis also shows that the point $x = x_0$ satisfying $f(x_0) = 0$ is not a touchdown point of u .

4.6 Pull-in distance

One of the primary goals in the design of MEMS devices is to maximize the pull-in distance over a certain allowable voltage range that is set by the power supply. Here pull-in distance refers to as the maximum stable deflection of the elastic membrane before touchdown occurs. In this section, we provide numerical results of pull-in distance with some explicit examples, from which one can observe that both larger pull-in distance and pull-in voltage can be achieved by properly tailoring the permittivity profile.

Following from [32], we focus on the dynamic solution u satisfying

$$\frac{\partial u}{\partial t} - \Delta u = -\frac{\lambda f(x)}{(1+u)^2} \quad \text{for } x \in \Omega, \quad (4.6.1a)$$

$$u(x, t) = 0 \quad \text{for } x \in \partial\Omega; \quad u(x, 0) = 0 \quad \text{for } x \in \Omega, \quad (4.6.1b)$$

One can apply Theorem 4.1.1 that for $\lambda \leq \lambda^*$, the dynamic solution $u(x, t)$ of (4.6.1) globally converges to its unique maximal negative steady-state $u_\lambda(x)$. On the other hand, Theorem 2.1.2 implies that the unique maximal negative steady-state $u_\lambda(x)$ is strictly increasing in λ . Therefore, we can deduce that pull-in distance of (4.6.1) is achieved exactly at $\lambda = \lambda^*$. Since the space dimension N of MEMS devices is 1 or 2, Theorems 2.1.2 & 4.1.1 give that the pull-in distance \mathcal{D} of MEMS devices exactly satisfies

$$\mathcal{D} := \lim_{t \rightarrow \infty} \|u^*(x, t)\|_{L^\infty(\Omega)} = \|u^*(x)\|_{L^\infty(\Omega)} \leq C(N) < 1, \quad N = 1, 2, \quad (4.6.2)$$

where $u^*(x, t)$ is the unique global solution of (4.6.1) at $\lambda = \lambda^*$, and while $u^*(x)$ is the unique extremal steady-state of (4.6.1).

In order to understand the relationship between pull-in distance \mathcal{D} and permittivity profile $f(x)$, we first consider the steady-state of (4.6.1) satisfying

$$\begin{cases} \Delta u = \frac{\lambda f(x)}{(1+u)^2} & \text{in } \Omega, \\ -1 < u < 0 & \text{in } \Omega, \\ u = 0 & \text{on } \partial\Omega, \end{cases} \quad (4.6.3)$$

where the domain Ω is considered to be a slab or an unit disk defined by (4.3.2). Here we still choose the following permittivity profile $f(x)$ as before:

$$\text{slab : } f(x) = |2x|^\alpha \quad (\text{power-law}); \quad f(x) = e^{\alpha(x^2-1/4)} \quad (\text{exponential}), \quad (4.6.4a)$$

$$\text{unit disk : } f(x) = |x|^\alpha \quad (\text{power-law}); \quad f(x) = e^{\alpha(|x|^2-1)} \quad (\text{exponential}), \quad (4.6.4b)$$

(a). Exponential Profiles:			(b). Power-Law Profiles:		
Ω	α	λ^*	Ω	α	λ^*
slab	0	1.401	slab	0	1.401
slab	3	2.637	slab	1	4.388
slab	6	4.848	slab	3	15.189
slab	10	10.40	slab	6	43.087
unit disk	0	0.789	unit disk	0	0.789
unit disk	3	6.096	unit disk	1	1.775
unit disk	4.8	15.114	unit disk	5	9.676
unit disk	5.6	20.942	unit disk	20	95.66

Table 4.3: Numerical values for pull-in voltage λ^* : Table (a) corresponds to exponential profiles, while Table (b) corresponds to power-law profiles.

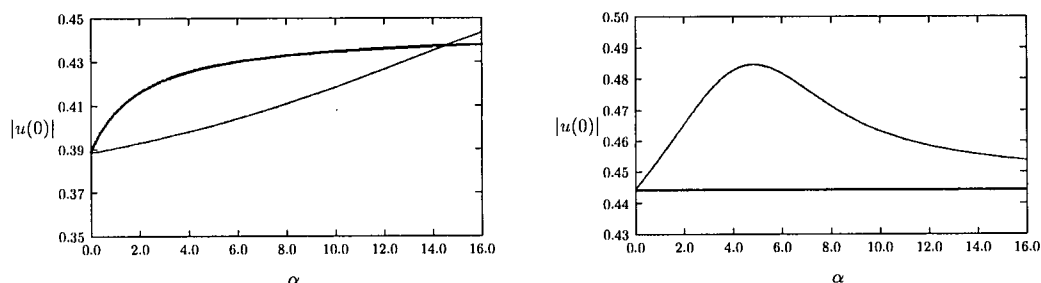


Figure 4.4: Plots of the pull-in distance $|u(0)| = |u^*(0)|$ versus α for the power-law profile (heavy solid curve) and the exponential profile (solid curve). Left figure: the slab domain. Right figure: the unit disk.

with $\alpha \geq 0$. For above choices of domain Ω and profile $f(x)$, since the extremal solution $u^*(x)$ of (4.6.3) is unique, Lemma 2.6.1 shows that $u^*(x)$ must be radially symmetric. Therefore, the pull-in distance \mathcal{D} of (4.6.3) satisfies $\mathcal{D} = |u^*(0)|$.

As in §2.2, using Newton's method and COLSYS [2] to solve the boundary value problem (4.6.3), we first numerically calculate λ^* of (4.6.3) as the saddle-node point. We give numerical values of λ^* in Table 4.3(a) for exponential profiles and in Table 4.3(b) for power-law profiles, respectively. For the slab domain, in Figure 4.4(a) we plot $\mathcal{D} = |u(0)| = |u^*(0)|$ versus α for both the power-law and the exponential conductivity profile $f(x)$ in the slab domain, which show that the pull-in distance \mathcal{D} can be increased by increasing the value of α (and hence by increasing the range of $f(x) \ll 1$). A similar plot of $\mathcal{D} = |u(0)| = |u^*(0)|$ versus α is shown in Figure 4.4(b) for the unit disk. For the power-law profile in the unit disk we observe that $|u(0)| \approx 0.444$ for any $\alpha > 0$. Therefore, rather curiously, the power-law profile does not increase the pull-in distance for the unit disk. For the exponential profile we observe from Figure 4.4(b) that the pull-in distance is not a monotonic function of α . The maximum value occurs at $\alpha \approx 4.8$ where $\lambda^* \approx 15.11$ (see Figure 2.1(b)) and $\mathcal{D} = |u(0)| = 0.485$. For $\alpha = 0$,

we have $\lambda^* \approx 0.789$ and $|u(0)| = 0.444$. Therefore, since λ^* is proportional to V^2 (cf. §1.1.2) we conclude that the exponential permittivity profile for the unit disk can increase the pull-in distance by roughly 9% if the voltage is increased by roughly a factor of four.

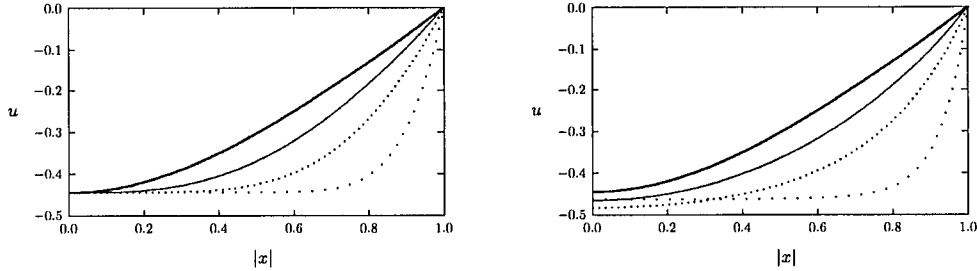


Figure 4.5: *Left figure: plots of u versus $|x|$ at $\lambda = \lambda^*$ for $\alpha = 0$, $\alpha = 1$, $\alpha = 3$, and $\alpha = 10$, in the unit disk for the power-law profile. Right figure: plots of u versus $|x|$ at $\lambda = \lambda^*$ for $\alpha = 0$, $\alpha = 2$, $\alpha = 4$, and $\alpha = 10$, in the unit disk for the exponential profile. In both figures the solution develops a boundary-layer structure near $|x| = 1$ as α is increased.*

For the unit disk, in Figure 4.5(a) we plot u versus $|x|$ at $\lambda = \lambda^*$ with four values of α for the power-law profile. Notice that $u(0)$ is the same for each of these values of α . A similar plot is shown in Figure 4.5(b) for the exponential permittivity profile. From these figures, we observe that u has a boundary-layer structure when $\alpha \gg 1$. In this limit, $f(x) \ll 1$ except in a narrow zone near the boundary of the domain. For $\alpha \gg 1$ the pull-in distance $\mathcal{D} = |u(0)|$ also reaches some limiting value (see Figure 4.4 & 4.5). For the slab domain with an exponential permittivity profile, we remark that the limiting asymptotic behavior of $|u(0)|$ for $\alpha \gg 1$ is beyond the range shown in Figure 4.4(a).

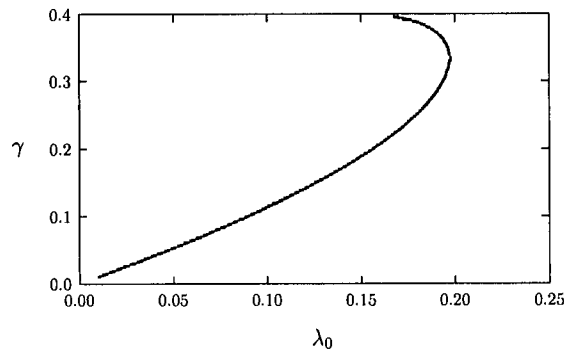


Figure 4.6: *Bifurcation diagram of $w'(0) = -\gamma$ versus λ_0 from the numerical solution of (4.6.6).*

For $\alpha \gg 1$, we now use a boundary-layer analysis to determine a scaling law of λ^* for both types of permittivity profiles and for either a slab domain or the unit disk. We illustrate the

analysis for a power-law permittivity profile in the unit disk. For $\alpha \gg 1$, there is an outer region defined by $0 \leq r \ll 1 - O(\alpha^{-1})$, and an inner region where $r - 1 = O(1/\alpha)$. In the outer region, where $\lambda r^\alpha \ll 1$, (4.6.3) reduces asymptotically to $\Delta u = 0$. Therefore, the leading-order outer solution is a constant $u = A$. In the inner region, we introduce new variables w and ρ by

$$w(\rho) = u(1 - \rho/\alpha), \quad \rho = \alpha(1 - r). \quad (4.6.5)$$

Substituting (4.6.5) into (4.6.3) with $f(r) = r^\alpha$, using the limiting behavior $(1 - \rho/\alpha)^\alpha \rightarrow e^{-\rho}$ as $\alpha \rightarrow \infty$, and defining $\lambda = \alpha^2 \lambda_0$, we obtain the leading-order boundary-layer problem

$$w'' = \frac{\lambda_0 e^{-\rho}}{(1+w)^2}, \quad 0 \leq \rho < \infty; \quad w(0) = 0, \quad w'(\infty) = 0, \quad \lambda = \alpha^2 \lambda_0. \quad (4.6.6)$$

In terms of the solution to (4.6.6), the leading-order outer solution is $u = A = w(\infty)$.

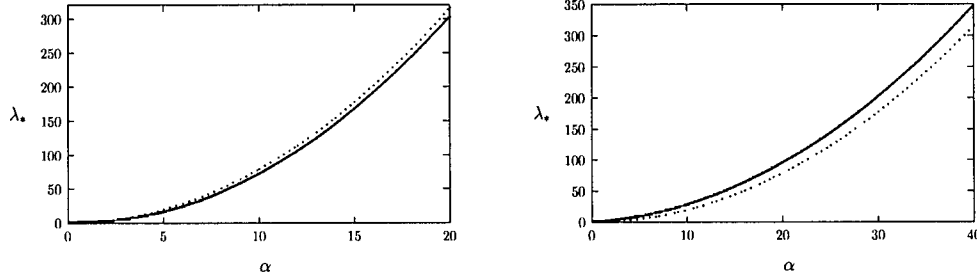


Figure 4.7: Comparison of numerically computed λ^* (heavy solid curve) with the asymptotic result (dotted curve) from (4.6.7) for the unit disk. Left figure: the exponential profile. Right figure: the power-law profile.

We define γ by $w'(0) = -\gamma$ for $\gamma > 0$, and we solve (4.6.6) numerically using COLSYS [2] to determine $\lambda_0 = \lambda_0(\gamma)$. In Figure 4.6 we plot $\lambda_0(\gamma)$ and show that this curve has a saddle-node point at $\lambda_0 = \lambda_0^* \equiv 0.1973$. At this value, we compute $w(\infty) \approx 0.445$, which sets the limiting membrane deflection for $\alpha \gg 1$. Therefore, (4.6.6) shows that for $\alpha \gg 1$, the saddle-node value has the scaling law behavior $\lambda^* \sim 0.1973\alpha^2$ for a power-law profile in the unit disk. A similar boundary-layer analysis can be done to determine the scaling law of λ^* when $\alpha \gg 1$ for other cases. In each case we can relate λ^* to the saddle-node value of the boundary-layer problem (4.6.6). In this way, for $\alpha \gg 1$, we obtain

$$\lambda^* \sim 4(0.1973)\alpha^2, \quad \bar{\lambda}_2 \sim \frac{4\alpha^2}{3}, \quad (\text{power-law, slab}), (\text{exponential, unit disk}), \quad (4.6.7a)$$

$$\lambda^* \sim (0.1973)\alpha^2, \quad \bar{\lambda}_2 \sim \frac{\alpha^2}{3}, \quad (\text{power-law, unit disk}), (\text{exponential, slab}), \quad (4.6.7b)$$

Notice that $\bar{\lambda}_2 = O(\alpha^2)$, with a factor that is about 5/3 times as large as the multiplier of α^2 in the asymptotic formula for λ^* . In Figure 4.7, we compare the computed λ^* as a saddle-node point with the asymptotic result of λ^* from (4.6.7).

Next we present a few of numerical results for pull-in distance of dynamic problem (4.3.1) by applying the implicit Crank-Nicholson scheme again. Here we always consider the domain and the profile defined by (4.3.2) and (4.6.4), respectively. We choose the meshpoints $N = 4000$ and the applied voltage $\lambda = \lambda^*$ given in Table 4.3:

Figure 4.8: Case of exponential profiles

We consider pull-in distance of (4.3.1) for exponential profiles in the slab or unit disk domain. In Figure 4.8(a) we plot u versus x at the time $t = 80$ in the slab domain, with $\alpha = 0$ (solid line), $\alpha = 3$ (dashed line), $\alpha = 6$ (dotted line) and $\alpha = 10$ (dash-dot line), respectively. This figure and Figure 4.4(a) show that pull-in distance is increasing in α . In Figure 4.8(b) we plot u versus $|x|$ at the time $t = 80$ in the unit disk domain, with $\alpha = 0$ (dash-dot line), $\alpha = 3$ (dashed line), $\alpha = 4.8$ (dotted line) and $\alpha = 5.6$ (solid line), respectively. In this figure we observe that the solution develops a boundary-layer structure near the boundary of the domain as α is increased, and pull-in distance is not a monotonic function of α . Actually from Figure 4.4(b) we know that pull-in distance is first increasing and then decreasing in α . The maximum value of pull-in distance occurs at $\alpha \approx 4.8$ and $\lambda^* \approx 15.114$.

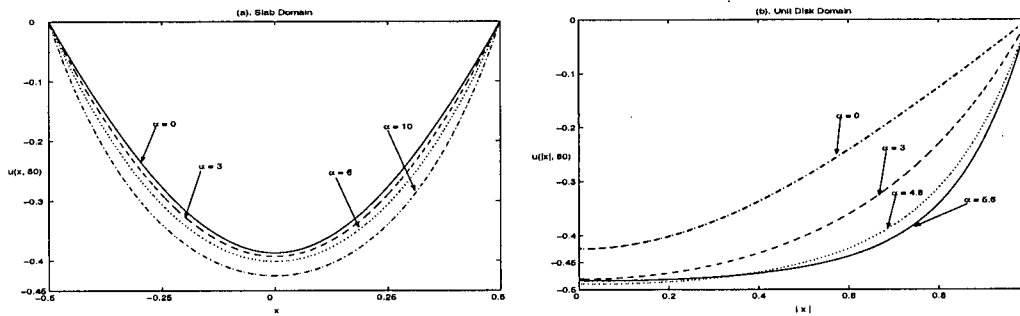


Figure 4.8: Left figure: plots of u versus x at $\lambda = \lambda^*$ in the slab domain. Right figure: plots of u versus $|x|$ at $\lambda = \lambda^*$ in the unit disk domain.

Figure 4.9: Case of power-law profiles

We consider pull-in distance of the membrane for power-law profiles in the slab or unit disk domain. In Figure 4.9(a) we plot u versus x at the time $t = 80$ in the slab domain, with $\alpha = 0$ (solid line), $\alpha = 1$ (dashed line), $\alpha = 3$ (dash-dot line) and $\alpha = 6$ (dotted line), respectively. This figure and Figure 4.4(a) show that pull-in distance is increasing in α . In Figure 4.9(b) we plot u versus $|x|$ at the time $t = 80$ in the unit disk domain, with $\alpha = 0$ (dotted line), $\alpha = 1$ (dash-dot line), $\alpha = 5$ (dashed line) and $\alpha = 20$ (solid line), respectively. For the power-law profiles in the unit disk domain, we observe that pull-in distance is a constant for any $\alpha \geq 0$. Therefore, with Figure 4.4(b), it is rather curious that power-law profile does not change pull-in distance in the unit disk domain. In both figures, the solution develops a boundary-layer structure near the boundary of the domain as α in increased.

Since one of the primary goals of MEMS design is to maximize the pull-in distance over a certain allowable voltage range that is set by the power supply, it would be interesting to

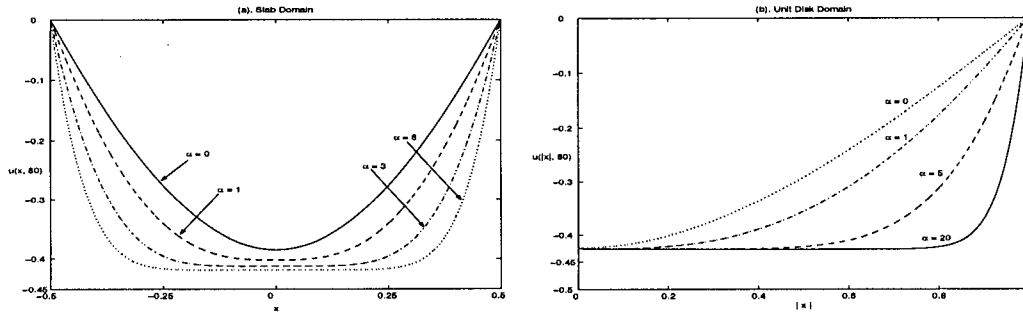


Figure 4.9: *Left figure: plots of u versus x at $\lambda = \lambda^*$ in the slab domain. Right figure: plots of u versus $|x|$ at $\lambda = \lambda^*$ in the unit disk domain.*

formulate an optimization problem that computes a dielectric permittivity $f(x)$ that maximizes the pull-in distance for a prescribed range of the saddle-node threshold λ^* .

Chapter 5

Refined Touchdown Behavior

5.1 Introduction

In this Chapter, we continue the study of dynamic solutions of (1.2.30) in the form

$$u_t - \Delta u = -\frac{\lambda f(x)}{u^2} \quad \text{for } x \in \Omega, \quad (5.1.1a)$$

$$u(x, t) = 1 \quad \text{for } x \in \partial\Omega, \quad (5.1.1b)$$

$$u(x, 0) = 1 \quad \text{for } x \in \Omega, \quad (5.1.1c)$$

where the permittivity profile $f(x)$ is allowed to vanish somewhere, and will be assumed to satisfy

$$\begin{aligned} f &\in C^\alpha(\bar{\Omega}) \text{ for some } \alpha \in (0, 1], 0 \leq f \leq 1 \text{ and} \\ f &> 0 \text{ on a subset of } \Omega \text{ of positive measure.} \end{aligned} \quad (5.1.2)$$

We focus on the case where a unique solution u of (5.1.1) must touchdown at finite time $T = T(\lambda, \Omega, f)$ in the sense

Definition 5.1.1. *A solution $u(x, t)$ of (5.1.1) is said to touchdown at finite time $T = T(\lambda, \Omega, f)$ if the minimum value of u reaches 0 at the time $T < \infty$.*

We shall give a refined description of finite-time touchdown behavior for u satisfying (5.1.1), including some touchdown estimates, touchdown rates, as well as some information on the properties of touchdown set –such as compactness, location and shape.

This Chapter is organized as follows. The purpose of §5.2 is mainly to derive some a priori estimates of touchdown profiles under the assumption that touchdown set of u is a compact subset of Ω . In §5.2.1, we establish the following lower bound estimate of touchdown profiles.

Theorem 5.1.1. *Assume f satisfies (5.1.2) on a bounded domain Ω , and suppose u is a touchdown solution of (5.1.1) at finite time T . If touchdown set of u is a compact subset of Ω , then*

1. any point $a \in \bar{\Omega}$ satisfying $f(a) = 0$ is not a touchdown point for $u(x, t)$;
2. there exists a bounded positive constant M such that

$$M(T - t)^{\frac{1}{3}} \leq u(x, t) \quad \text{in } \Omega \times (0, T). \quad (5.1.3)$$

Note that whether the compactness of touchdown set holds for any $f(x)$ satisfying (5.1.2) is a quite challenging problem. We shall prove in Proposition 5.2.1 of §5.2 that the compactness of

touchdown set holds for the case where the domain Ω is convex and $f(x)$ satisfies the additional condition

$$\frac{\partial f}{\partial \nu} \leq 0 \quad \text{on } \Omega_\delta^c := \{x \in \Omega : \text{dist}(x, \partial\Omega) \leq \delta\} \text{ for some } \delta > 0. \quad (5.1.4)$$

Here ν is the outward unit norm vector to $\partial\Omega$. On the other hand, when $f(x)$ does not satisfy (5.1.4), the compactness of touchdown set is numerically observed, see Chapter 4 or §5.4. Therefore, it is our conjecture that under the convexity of Ω , the compactness of touchdown set may hold for any $f(x)$ satisfying (5.1.2). In §5.2.2 we estimate the derivatives of touchdown solution u , see Lemma 5.2.4; and as a byproduct, an integral estimate is also given in §5.2.2, see Theorem 5.2.5.

Motivated by Theorem 5.1.1, the key point of studying touchdown profiles is a similarity variable transformation of (5.1.1). For the touchdown solution $u = u(x, t)$ of (5.1.1) at finite time T , we use the associated similarity variables

$$y = \frac{x - a}{\sqrt{T - t}}, \quad s = -\log(T - t), \quad u(x, t) = (T - t)^{\frac{1}{3}} w_a(y, s), \quad (5.1.5)$$

where a is any interior point of Ω . Then $w_a(y, s)$ is defined in $W_a := \{(y, s) : a + ye^{-s/2} \in \Omega, s > s' = -\log T\}$, and it solves

$$\rho(w_a)_s - \nabla \cdot (\rho \nabla w_a) - \frac{1}{3} \rho w_a + \frac{\lambda \rho f(a + ye^{-\frac{s}{2}})}{w_a^2} = 0,$$

where $\rho(y) = e^{-|y|^2/4}$. Here $w_a(y, s)$ is always strictly positive in W_a . The slice of W_a at a given time s^1 is denoted by $\Omega_a(s^1) := W_a \cap \{s = s^1\} = e^{s^1/2}(\Omega - a)$. Then for any interior point a of Ω , there exists $s_0 = s_0(a) > 0$ such that $B_s := \{y : |y| < s\} \subset \Omega_a(s)$ for $s \geq s_0$. We now introduce the frozen energy functional

$$E_s[w_a](s) = \frac{1}{2} \int_{B_s} \rho |\nabla w_a|^2 dy - \frac{1}{6} \int_{B_s} \rho w_a^2 dy - \int_{B_s} \frac{\lambda \rho f(a)}{w_a} dy. \quad (5.1.6)$$

By estimating the energy $E_s[w_a](s)$ in B_s , one can establish the following upper bound estimate.

Theorem 5.1.2. *Assume f satisfies (5.1.2) on a bounded domain Ω in \mathbb{R}^N , suppose u is a touchdown solution of (5.1.1) at finite time T and $w_a(y, s)$ is defined by (5.1.5). Assume touchdown set of u is a compact subset of Ω . If $w_a(y, s) \rightarrow \infty$ as $s \rightarrow \infty$ uniformly for $|y| \leq C$, where C is any positive constant, then a is not a touchdown point for u .*

Based on a prior estimates of §5.2, we shall establish refined touchdown profiles in §5.3, where self-similar method and center manifold analysis will be applied. Here is the statement of refined touchdown profiles:

Theorem 5.1.3. *Assume f satisfies (5.1.2) on a bounded domain Ω in \mathbb{R}^N , and suppose u is a touchdown solution of (5.1.1) at finite time T . Assume touchdown set of u is a compact subset of Ω , then,*

1. *If $N = 1$ and $x = a$ is a touchdown point of u , then we have*

$$\lim_{t \rightarrow T^-} u(x, t)(T - t)^{-\frac{1}{3}} \equiv (3\lambda f(a))^{\frac{1}{3}} \quad (5.1.7)$$

uniformly on $|x - a| \leq C\sqrt{T - t}$ for any bounded constant C . Moreover, when $t \rightarrow T^-$,

$$u \sim [3\lambda f(a)(T - t)]^{1/3} \left(1 - \frac{1}{4|\log(T - t)|} + \frac{|x - a|^2}{8(T - t)|\log(T - t)|} + \dots \right), \quad N = 1. \quad (5.1.8)$$

2. If $\Omega = B_R(0) \subset \mathbb{R}^N$ is a bounded ball with $N \geq 2$, and $f(r) = f(|x|)$ is radially symmetric. Suppose $r = 0$ is a touchdown point of u , then we have

$$\lim_{t \rightarrow T^-} u(r, t)(T - t)^{-\frac{1}{3}} \equiv (3\lambda f(0))^{\frac{1}{3}} \quad (5.1.9)$$

uniformly on $r \leq C\sqrt{T - t}$ for any bounded constant C . Moreover, when $t \rightarrow T^-$,

$$u \sim [3\lambda f(0)(T - t)]^{1/3} \left(1 - \frac{1}{2|\log(T - t)|} + \frac{r^2}{4(T - t)|\log(T - t)|} + \dots \right), \quad N = 2. \quad (5.1.10)$$

Note that the uniqueness of solutions for (5.1.1) gives the radial symmetry of u in Theorem 5.1.3(2). When dimension $N \geq 2$, it should remark from Theorem 5.1.3(2) that we are only able to discuss the refined touchdown profiles for special touchdown point $x = 0$ in the radial situation, and it seems unknown for the general case.

Adapting various analytical and numerical techniques, §5.4 will be focused on the set of touchdown points. This may provide useful information on the design of MEMS devices. In §5.4.1 we discuss the radially symmetric case of (5.1.1) as follows:

Theorem 5.1.4. Assume $f(r) = f(|x|)$ satisfies (5.1.2) and $f'(r) \leq 0$ in a bounded ball $B_R(0) \subset \mathbb{R}^N$ with $N \geq 1$, and suppose u is a touchdown solution of (5.1.1) at finite time T . Then, $r = 0$ is the unique touchdown point of u .

Remark 5.1.1. Assume $f(r) = f(|x|)$ satisfies (5.1.2) and $f'(r) \leq 0$ in a bounded ball $B_R(0) \subset \mathbb{R}^N$ with $N \geq 1$. Together with Proposition 5.2.1 below, Theorems 5.1.1 and 5.1.4 show an interesting phenomenon: finite-time touchdown point is not the zero point of $f(x)$, but the maximum value point of $f(x)$.

Remark 5.1.2. Numerical simulations in §5.4.1 show that the assumption $f'(r) \leq 0$ in Theorem 5.1.4 is sufficient, but not necessary. This gives that Theorem 5.1.3(2) does hold for a larger class of profiles $f(r) = f(|x|)$.

For one dimensional case, Theorem 5.1.4 already implies that touchdown points must be unique when permittivity profile $f(x)$ is uniform. In §5.4.2 we further discuss one dimensional case of (5.1.1) for varying profile $f(x)$, where numerical simulations show that touchdown points may be composed of finite points or finite compact subsets of the domain.

5.2 A priori estimates of touchdown behavior

Under the assumption that touchdown set of u is a compact subset of Ω , in this section we study some a priori estimates of touchdown behavior, and establish the claims in Theorems 5.1.1 and 5.1.2. In §5.2.1 we establish a lower bound estimate, from which we complete the proof of

Theorem 5.1.1. Using the lower bound estimate, in §5.2.2 we shall prove some estimates for the derivatives of touchdown solution u , and an integration estimate will be also obtained as a byproduct. In §5.2.3 we shall study the upper bound estimate by energy methods, which gives Theorem 5.1.2.

We first prove the following compactness result for a large class of profiles $f(x)$ satisfying (5.1.2) and

$$\frac{\partial f}{\partial \nu} \leq 0 \quad \text{on } \Omega_\delta^c := \{x \in \Omega : \text{dist}(x, \partial\Omega) \leq \delta\} \text{ for some } \delta > 0. \quad (5.2.1)$$

Proposition 5.2.1. *Assume f satisfies (5.1.2) and (5.2.1) on a bounded convex domain Ω , and suppose u is a touchdown solution of (5.1.1) at finite time T . Then, the set of touchdown points for u is a compact subset of Ω .*

Proof: We prove Proposition 5.2.1 by adapting moving plane method from Theorem 3.3 in [27], where it is used to deal with blow-up problems. Take any point $y_0 \in \partial\Omega$, and assume for simplicity that $y_0 = 0$ and that the half space $\{x_1 > 0\}$ ($x = (x_1, x')$) is tangent to Ω at y_0 . Let $\Omega_\alpha^+ = \Omega \cap \{x_1 > \alpha\}$ where $\alpha < 0$ and $|\alpha|$ is small, and also define $\Omega_\alpha^- = \{(x_1, x') : (2\alpha - x_1, x') \in \Omega_\alpha^+\}$, the reflection of Ω_α^+ with respect to the plane $\{x_1 = \alpha\}$, where $x' = (x_2, \dots, x_N)$.

Consider the function

$$w(x, t) = u(2\alpha - x_1, x', t) - u(x_1, x', t)$$

for $x \in \Omega_\alpha^-$, then w satisfies

$$w_t - \Delta w = \frac{\lambda(u(x_1, x', t) + u(2\alpha - x_1, x', t))f(x)}{u^2(x_1, x', t)u^2(2\alpha - x_1, x', t)}w.$$

It is clear that $w = 0$ on $\{x_1 = \alpha\}$. Since $u(x, t) = 1$ along $\partial\Omega$ and since the maximum principle gives $u_t < 0$ for $0 < t < T$, we may choose a small $t_0 > 0$ such that

$$\frac{\partial u(x, t_0)}{\partial \nu} > 0 \quad \text{along } \partial\Omega, \quad (5.2.2)$$

where ν is the outward unit norm vector to $\partial\Omega$. Then for sufficiently small $|\alpha|$, (5.2.2) implies that $w(x, t_0) \geq 0$ in Ω_α^- and also $w = 1 - u(x_1, x', t) > 0$ on $(\partial\Omega_\alpha^- \cap \{x_1 < \alpha\}) \times (t_0, T)$. Applying the maximal principle we now conclude that $w > 0$ in $\Omega_\alpha^- \times (t_0, T)$ and $\frac{\partial w}{\partial x_1} = -2\frac{\partial u}{\partial x_1} < 0$ on $\{x_1 = \alpha\}$. Since α is arbitrary, it follows by varying α that

$$\frac{\partial u}{\partial x_1} > 0, \quad (x, t) \in \Omega_{\alpha_0}^+ \times (t_0, T) \quad (5.2.3)$$

provided $|\alpha_0| = |\alpha_0(t_0)| > 0$ is sufficiently small.

Fix $0 < |\alpha_0| \leq \delta$, where δ is as in (5.2.1), we now consider the function

$$J = u_{x_1} - \varepsilon_1(x_1 - \alpha_0) \quad \text{in } \Omega_{\alpha_0}^+ \times (t_0, T),$$

where $\varepsilon_1 = \varepsilon_1(\alpha_0, t_0) > 0$ is a constant to be determined later. The direct calculations show that

$$J_t - \Delta J = \frac{2\lambda f}{u^3}u_{x_1} - \frac{\lambda f_{x_1}}{u^2} = \frac{2\lambda f}{u^3}u_{x_1} - \frac{\lambda}{u^2} \frac{\partial f}{\partial \nu} \frac{\partial \nu}{\partial x_1} \geq 0 \quad \text{in } \Omega_{\alpha_0}^+ \times (t_0, T) \quad (5.2.4)$$

due to (5.2.1). Therefore, J can not attain negative minimum in $\Omega_{\alpha_0}^+ \times (t_0, T)$. Next, $J > 0$ on $\{x_1 = \alpha_0\}$ by (5.2.3). Since (5.2.2) gives $\frac{\partial u(x, t_0)}{\partial x_1} \geq C > 0$ along $(\partial\Omega_{\alpha_0}^+ \cap \partial\Omega)$ for some $C > 0$, we have $J > 0$ on $\{t = t_0\}$ provided $\varepsilon_1 = \varepsilon_1(\alpha_0, t_0) > 0$ is sufficiently small. We now claim that for small $\varepsilon_1 > 0$,

$$J > 0 \quad \text{on} \quad (\partial\Omega_{\alpha_0}^+ \cap \partial\Omega) \times (t_0, T). \quad (5.2.5)$$

To prove (5.2.5), we compare the solution $U := 1 - u$ satisfying

$$\begin{aligned} U_t - \Delta U &= \frac{\lambda f(x)}{(1-U)^2} \quad (x, t) \in \Omega \times (t_0, T), \\ U(x, t_0) &= 1 - u(x, t_0); \quad U(x, t) = 0 \quad x \in \partial\Omega \end{aligned}$$

with the solution v of the heat equation

$$v_t = \Delta v, \quad (x, t) \in \Omega \times (t_0, T),$$

where $0 \leq v(x, t_0) = U(x, t_0) < 1$ and $v = 0$ on $\partial\Omega$. Then we have $U \geq v$ in $\Omega \times (t_0, T)$. Consequently,

$$\frac{\partial U}{\partial \nu} \leq \frac{\partial v}{\partial \nu} \leq -C_0 < 0 \quad \text{on} \quad (\partial\Omega_{\alpha_0}^+ \cap \partial\Omega) \times (t_0, T),$$

and hence $\frac{\partial u}{\partial \nu} \geq C_0 > 0$ on $(\partial\Omega_{\alpha_0}^+ \cap \partial\Omega) \times (t_0, T)$. It then follows that $J \geq C_0 \frac{\partial \nu}{\partial x_1} - \varepsilon_1(x_1 - \alpha_0) > 0$ provided $\varepsilon_1 = \varepsilon_1(\alpha_0, t_0)$ is small enough, which gives (5.2.5).

The maximum principle now yields that there exists $\varepsilon_1 = \varepsilon_1(\alpha_0, t_0) > 0$ so small that $J \geq 0$ in $\Omega_{\alpha_0}^+ \times (t_0, T)$, i.e.,

$$u_{x_1} \geq \varepsilon_1(x_1 - \alpha_0), \quad (5.2.6)$$

if $x' = 0$ and $\alpha_0 \leq x_1 < 0$. Integrating (5.2.6) with respect to x_1 on $[\alpha_0, y_1]$, where $\alpha_0 < y_1 < 0$, yields that

$$u(y_1, 0, t) - u(\alpha_0, 0, t) \geq \frac{\varepsilon_1}{2} |y_1 - \alpha_0|^2.$$

It follows that

$$\underline{\lim}_{t \rightarrow T^-} u(0, t) = \underline{\lim}_{t \rightarrow T^-} \lim_{y_1 \rightarrow 0^-} u(y_1, 0, t) \geq \varepsilon_1 \alpha_0^2 / 2 > 0,$$

which shows that $y_0 = 0$ can not be a touchdown point of $u(x, t)$.

The proof of (5.2.3) can be slightly modified to show that $\frac{\partial u}{\partial \nu} > 0$ in $\Omega_{\alpha_0}^+ \times (t_0, T)$ for any direction ν close enough to the x_1 -direction. Together with (5.2.1), this enables us to deduce that any point in $\{x' = 0, \alpha_0 < x_1 < 0\}$ can not be a touchdown point. Since above proof shows that α_0 can be chosen independently of initial point y_0 on $\partial\Omega$, by varying y_0 along $\partial\Omega$ we deduce that there is an Ω -Neighborhood Ω' of $\partial\Omega$ such that each point $x \in \Omega'$ can not be a touchdown point. This completes the proof of Proposition 5.2.1. \blacksquare

Remark 5.2.1. When $f(x)$ does not satisfy (5.2.1), the compactness of touchdown set is numerically observed, see numerical simulations in Chapter 4 or in §5.4 of the present paper. Therefore, it is our conjecture that under the convexity of Ω , the compactness of touchdown set may hold for any $f(x)$ satisfying (5.1.2).

5.2.1 Lower bound estimate

Define for $\eta > 0$,

$$\Omega_\eta := \{x \in \Omega : \text{dist}(x, \partial\Omega) > \eta\}, \quad \Omega_\eta^c := \{x \in \Omega : \text{dist}(x, \partial\Omega) \leq \eta\}. \quad (5.2.7)$$

Since touchdown set of u is assumed to be a compact subset of Ω , in the rest of this section we may choose a small $\eta > 0$ such that any touchdown point of u must lie in Ω_η . Our first aim of this subsection is to prove that any point $x_0 \in \bar{\Omega}_\eta$ satisfying $f(x_0) = 0$ can not be a touchdown point of u at finite time T , which then leads to the following proposition.

Proposition 5.2.2. *Assume f satisfies (5.1.2) on a bounded domain Ω , and suppose $u(x, t)$ is a touchdown solution of (5.1.1) at finite time T . If touchdown set of u is a compact subset of Ω , then any point $x_0 \in \bar{\Omega}$ satisfying $f(x_0) = 0$ cannot be a touchdown point of $u(x, t)$.*

Proof: Since touchdown set of u is assumed to be a compact subset of Ω , it now suffices to discuss the point x_0 lying in the interior domain Ω_η for some small $\eta > 0$, such that there is no touchdown point on Ω_η^c .

For any $t_1 < T$, we first recall that the maximum principle gives $u_t < 0$ for all $(x, t) \in \Omega \times (0, t_1)$. Further, the boundary point lemma shows that the outward normal derivative of $v = u_t$ on $\partial\Omega$ is positive for $t > 0$. This implies that for taking small $0 < t_0 < T$, there exists a positive constant $C = C(t_0, \eta)$ such that $u_t(x, t_0) \leq -C < 0$ for all $x \in \bar{\Omega}_\eta$. For any $0 < t_0 < t_1 < T$, we next claim that there exists $\varepsilon = \varepsilon(t_0, t_1, \eta) > 0$ such that

$$J^\varepsilon(x, t) = u_t + \frac{\varepsilon}{u^2} \leq 0 \quad \text{for all } (x, t) \in \Omega_\eta \times (t_0, t_1). \quad (5.2.8)$$

Indeed, it is now clear that there exists $C_\eta = C_\eta(t_0, t_1, \eta) > 0$ such that $u_t(x, t) \leq -C_\eta$ on the parabolic boundary of $\Omega_\eta \times (t_0, t_1)$. And further, we can choose $\varepsilon = \varepsilon(t_0, t_1, \eta) > 0$ so small that $J^\varepsilon \leq 0$ on the parabolic boundary of $\Omega_\eta \times (t_0, t_1)$, due to the local boundedness of $\frac{1}{u^2}$ on $\partial\Omega_\eta \times (t_0, t_1)$. Also, direct calculations imply that

$$J_t^\varepsilon - \Delta J^\varepsilon = \frac{2\lambda f}{u^3} J^\varepsilon - \frac{6\varepsilon|\nabla u|^2}{u^4} \leq \frac{2\lambda f}{u^3} J^\varepsilon.$$

Now (5.2.8) follows again from the maximum principle.

Combining (5.2.8) and (5.1.1) we deduce that for a small neighborhood B of x_0 where $\lambda f(x) \leq \varepsilon/2$ is in $B \subset \bar{\Omega}_\eta$, we have for $v := 1 - u$,

$$\Delta v \geq \frac{\varepsilon}{2} \frac{1}{(1-v)^2}, \quad (x, t) \in B \times (t_0, t_1).$$

Now Proposition 5.2.2 is a direct result of Lemma 4.3.2, since $t_1 < T$ is arbitrary. ■

Proof of Theorem 5.1.1: In view of Proposition 5.2.2, it now needs only to prove the lower bound estimate (5.1.3).

Given any small $\eta > 0$, applying the same argument used for (5.2.8) yields that for any $0 < t_0 < t_1 < T$, there exists $\varepsilon = \varepsilon(t_0, t_1, \eta) > 0$ such that

$$u_t \leq -\frac{\varepsilon}{u^2} \quad \text{in } \Omega_\eta \times (t_0, t_1).$$

This inequality shows that $u_t \rightarrow -\infty$ as u touchdown, and there exists $M > 0$ such that

$$M_1(T-t)^{\frac{1}{3}} \leq u(x, t) \quad \text{in } \Omega_\eta \times (0, T) \quad (5.2.9)$$

due to the arbitrary of t_0 and t_1 , where M_1 depends only on λ , f and η . Furthermore, one can obtain (5.1.3) because of the boundedness of u on Ω_η^c , and the theorem is proved. \blacksquare

5.2.2 Gradient estimates

As a preliminary of next section, it is now important to know a priori estimates for the derivatives of touchdown solution u , which are the contents of this subsection. Following the analysis in [27], our first lemma is about the derivatives of first order without the compactness assumption of touchdown set.

Lemma 5.2.3. *Assume f satisfies (5.1.2) on a bounded convex domain Ω , and suppose u is a touchdown solution of (5.1.1) at finite time T . Then for any $0 < t_0 < T$, there exists a bounded constant $C > 0$ such that*

$$\frac{1}{2}|\nabla u|^2 \leq \frac{C}{\underline{u}} - \frac{C}{u} \quad \text{in } \Omega \times (0, t_0), \quad (5.2.10)$$

where $\underline{u} = \underline{u}(t_0) = \min_{x \in \Omega} u(x, t_0)$, and C depends only on λ , f and Ω .

Proof: Fix any $0 < t_0 < T$ and treat $\underline{u}(t_0)$ as a fixed constant. Let $w = u - \underline{u}$, then w satisfies

$$\begin{aligned} w_t - \Delta w &= -\frac{\lambda f(x)}{(w + \underline{u})^2} & \text{in } \Omega \times (0, t_0), \\ w &= 1 - \underline{u} & \text{in } \partial\Omega \times (0, t_0), \\ w(x, 0) &= 1 - \underline{u} & \text{in } \Omega. \end{aligned}$$

We introduce the function

$$P = \frac{1}{2}|\nabla w|^2 + \frac{C}{w + \underline{u}} - \frac{C}{\underline{u}}, \quad (5.2.11)$$

where the bounded constant $C \geq 2\lambda \sup_{x \in \bar{\Omega}} f$ will be determined later. Then we have

$$\begin{aligned} P_t - \Delta P &= \frac{C\lambda f(x)}{(w + \underline{u})^4} - \frac{\lambda \nabla f(x) \nabla w}{(w + \underline{u})^2} + \frac{2(\lambda f(x) - C)|\nabla w|^2}{(w + \underline{u})^3} - \sum_{i,j=1}^N w_{ij}^2 \\ &\leq \frac{\lambda C \sup_{x \in \bar{\Omega}} f}{(w + \underline{u})^4} + \frac{-2\lambda |\nabla w|^2 \sup_{x \in \bar{\Omega}} f + \lambda |\nabla w| \sup_{x \in \bar{\Omega}} |\nabla f|}{(w + \underline{u})^3} - \sum_{i,j=1}^N w_{ij}^2 \\ &\leq \frac{\lambda(C \sup_{x \in \bar{\Omega}} f + C_1)}{(w + \underline{u})^4} - \sum_{i,j=1}^N w_{ij}^2, \end{aligned} \quad (5.2.12)$$

where $C_1 := \frac{(\sup_{x \in \bar{\Omega}} |\nabla f|)^2}{8 \sup_{x \in \bar{\Omega}} f} \geq 0$ is bounded. Since (5.2.11) gives

$$\sum_{i=1}^N \left(P_i + \frac{C}{(w + \underline{u})^2} w_i \right)^2 = \sum_{i,j=1}^N (w_j w_{ij})^2 \leq |\nabla w|^2 \sum_{i,j=1}^N w_{ij}^2, \quad (5.2.13)$$

we now take

$$C := \max \left\{ 2\lambda \sup_{x \in \bar{\Omega}} f, \frac{\lambda \sup_{x \in \bar{\Omega}} f + \lambda \sqrt{(\sup_{x \in \bar{\Omega}} f)^2 + 4C_1}}{2} \right\} \geq 2\lambda \sup_{x \in \bar{\Omega}} f$$

so that $C^2 \geq \lambda(C \sup_{x \in \bar{\Omega}} f + C_1)$, where C clearly depends only on λ , f and Ω . From the choice of C , a combination of (5.2.12) and (5.2.13) gives that

$$P_t - \Delta P \leq \vec{b} \cdot \nabla P,$$

where $\vec{b} = -|\nabla w|^{-2}(\nabla P + \frac{2C\nabla w}{(w+\underline{u})^2})$ is a locally bounded when $\nabla w \neq 0$. Therefore, P can only attain positive maximum either at the point where $\nabla w = 0$, or on the parabolic boundary of $\Omega \times (0, t_0)$. But when $\nabla w = 0$, we have $P \leq 0$.

On the initial boundary, $P = \frac{C}{1+\underline{u}} - \frac{C}{\underline{u}} < 0$. Let (y, s) be any point on $\partial\Omega \times (0, t_0)$, if we can prove that

$$\frac{\partial P}{\partial \nu} \leq 0 \quad \text{at } (y, s), \quad (5.2.14)$$

it then follows from the maximum principle that $P \leq 0$ in $\Omega \times (0, t_0)$. And therefore, the assertion (5.2.10) is reduced from (5.2.11) together with $w = u - \underline{u}$.

To prove (5.2.14), we recall the fact that since $w = \text{const.}$ on $\partial\Omega$ (for $t = s$), we have

$$\Delta w = w_{\nu\nu} + (N-1)\kappa w_{\nu} \quad \text{at } (y, s),$$

where κ is the non-negative mean curvature of $\partial\Omega$ at y . It then follows that

$$\begin{aligned} \frac{\partial P}{\partial \nu} &= w_{\nu} w_{\nu\nu} - \frac{C w_{\nu}}{(w+\underline{u})^2} \leq w_{\nu} \left[\Delta w - (N-1)\kappa w_{\nu} - \frac{\lambda f(x)}{(w+\underline{u})^2} \right] \\ &= w_{\nu} [w_t - (N-1)\kappa w_{\nu}] = -(N-1)\kappa w_{\nu}^2 \leq 0 \end{aligned}$$

at (y, s) , and we are done. ■

The following lemma is dealt with the derivatives of higher order, and the idea of its proof is similar to Proposition 1 of [35].

Lemma 5.2.4. *Assume f satisfies (5.1.2) on a bounded domain Ω , and suppose u is a touchdown solution of (5.1.1) at finite time T . Assume touchdown set of u is a compact subset of Ω , and $x = a$ is any point of Ω_{η} for some small $\eta > 0$. Then there exists a positive constant M' such that*

$$|\nabla^m u(x, t)|(T-t)^{-\frac{1}{3} + \frac{m}{2}} \leq M', \quad m = 1, 2 \quad (5.2.15)$$

holds for $|x - a| \leq R$.

Proof: It suffices to consider the case $a = 0$ by translation, and we may focus on $\frac{1}{2}R^2 < r^2 < R^2$ and denote $Q_r = B_r \times (T[1 - (\frac{r}{R})^2], T)$.

Our first task is to show that $|\nabla u|$ and $|\nabla^2 u|$ are uniformly bounded on compact subsets of Q_R . Indeed, since $f(x)/u^2$ is bounded on any compact subset D of Q_R , standard L^p estimates for heat equations (cf. [47]) gives

$$\int \int_D (|\nabla^2 u|^p + |u_t|^p) dx dt < C, \quad 1 < p < \infty.$$

Choosing p to be large enough, we then conclude from Sobolev's inequality that $f(x)/u^2$ is Hölder continuous on D . Therefore, Schauder's estimates for heat equations (cf. [47]) show that $|\nabla u|$ and $|\nabla^2 u|$ are uniformly bounded on compact subsets of D . In particular, there exists M_1 such that

$$|\nabla u| + |\nabla^2 u| \leq M_1 \quad \text{for } (x, t) \in B_r \times (T[1 - (\frac{r}{R})^2], T[1 - \frac{1}{2}(1 - \frac{r}{R})^2]), \quad (5.2.16)$$

where M_1 depends only on R , N and M given in (5.1.3).

We next prove (5.2.15) for $|x| < r$ and $T[1 - \frac{1}{2}(1 - \frac{r}{R})^2] \leq t < T$. Fix such a point (x, t) , let $\mu = [\frac{2}{T}(T - t)]^{\frac{1}{2}}$ and consider

$$v(z, \tau) = \mu^{-\frac{2}{3}} u(x + \mu z, T - \mu^2(T - \tau)). \quad (5.2.17)$$

For above given point (x, t) , we now define $O := \{z : (x + \mu z) \in \Omega\}$ and $g(z) := f(x + \mu z) \geq 0$ on O . One can verify that $v(z, \tau)$ is a solution of

$$\begin{aligned} v_\tau - \Delta_z v &= -\frac{\lambda g(z)}{v^2} \quad z \in O, \\ v(z, 0) &= v_0(z) > 0; \quad v(z, \tau) = \mu^{-\frac{2}{3}} \quad z \in \partial O, \end{aligned} \quad (5.2.18)$$

where Δ_z denotes the Laplacian operator with respect to z , and $v_0(z) = \mu^{-\frac{2}{3}} u(x + \mu z, T - \mu^2 T) > 0$ satisfies $\Delta_z v_0 - \frac{\lambda g(z)}{v_0^2} \leq 0$ on O . The formula (5.2.17) implies that T is also the finite touchdown time of v , and the domain of v includes Q_{r_0} for some $r_0 = r_0(R) > 0$. Since touchdown set of u is assumed to be a compact subset of Ω , one can observe that touchdown set of v is also a compact subset of O . Therefore, the argument of Theorem 5.1.1(2) can be applied to (5.2.18), yielding that there exists a constant $M_2 > 0$ such that

$$v(z, \tau) \geq M_2(T - \tau)^{\frac{1}{3}}$$

where M_2 depends only on R , λ , f and Ω again. The argument used for (5.2.16) then yields that there exists $M'_1 > 0$, depending on R , N and M_2 , such that

$$|\nabla_z v| + |\nabla_z^2 v| \leq M'_1 \quad \text{for } (z, \tau) \in B_r \times (T[1 - (\frac{r}{r_0})^2], T[1 - \frac{1}{2}(1 - \frac{r}{r_0})^2]), \quad (5.2.19)$$

where we assume $\frac{1}{2}r_0^2 < r^2 < r_0^2$. Applying (5.2.17) and taking $(z, \tau) = (0, \frac{T}{2})$, this estimate reduces to

$$\mu^{-\frac{2}{3}+1} |\nabla u| + \mu^{-\frac{2}{3}+2} |\nabla^2 u| \leq M'_1.$$

Therefore, (5.2.15) follows since $\mu = [\frac{2}{T}(T - t)]^{\frac{1}{2}}$. ■

Before concluding this subsection, we now apply gradient estimates to establishing integral estimates.

Theorem 5.2.5. *Assume f satisfies (5.1.2) on a bounded domain Ω , and suppose u is a touchdown solution of (5.1.1) at finite time T . Assume touchdown set of u is a compact subset of Ω , then for $\gamma > \frac{3}{2}N$ we have*

$$\lim_{t \rightarrow T^-} \int_{\Omega} f(x) u^{-\gamma}(x, t) dx = +\infty.$$

Proof: For any given $t_0 \in (0, T)$ close to T , Lemma 5.2.3 implies that

$$\frac{1}{2}|\nabla u|^2 \leq \frac{C}{\underline{u}^2}(u - \underline{u}) \quad \text{in } \Omega \times (0, t_0) \quad (5.2.20)$$

for some bounded constant $C > 0$, where $\underline{u} = u(x_0, t_0) = \min_{x \in \Omega} u(x, t_0)$. Considering any t sufficiently close to t_0 , we now introduce polar coordinates (r, θ) about the point x_0 . Then in any direction θ , there is a smallest value of $r_0 = r_0(\theta, t)$ such that $u(r_0, t) = 2\underline{u}$. Note that r_0 is very small as $t < t_0$ sufficiently approach to T . Furthermore, since x_0 approaches to one of touchdown points of u as $t \rightarrow T^-$, Proposition 5.2.2 shows that as $t < t_0$ sufficiently approach to T , we have $f(x) \geq C_0 > 0$ in $\{r < r_0\}$ for some $C_0 > 0$. Since (5.2.20) and the definition of \underline{u} imply that $\frac{ur}{\sqrt{u-\underline{u}}} \leq \frac{\sqrt{2C}}{\underline{u}}$, which is $2\sqrt{u-\underline{u}} \leq \frac{\sqrt{2C}}{\underline{u}}r$, we attain $\sqrt{\frac{2}{C}}\underline{u}^{3/2} \leq r_0$ by taking $r = r_0$. Therefore, for $\gamma > \frac{3}{2}N$ we have

$$\begin{aligned} \int_{\Omega} u^{-\gamma} dx &\geq C \int_{\Omega} f(x)u^{-\gamma} dx \geq CC_0 \int_{\{r \leq r_0\}} u^{-\gamma} dx \geq C \int_{\theta} dS_{\theta} \int_{\{r \leq r_0\}} u^{-\gamma} r^{N-1} dr \\ &\geq C \int_{\theta} dS_{\theta} \int_{\{r \leq r_0\}} (2\underline{u})^{-\gamma} r^{N-1} dr \\ &\geq C \int_{\theta} dS_{\theta} \underline{u}^{-\gamma} r_0^N \geq C \int_{\theta} dS_{\theta} \underline{u}^{-\gamma + \frac{3}{2}N} = +\infty \end{aligned}$$

as $t \rightarrow T^-$, which completes the proof of Theorem 5.2.5. \blacksquare

5.2.3 Upper bound estimate

In this subsection, we discuss the upper bound estimate of touchdown solution u by applying energy methods.

First, we note the following local upper bound estimate.

Proposition 5.2.6. *Suppose u is a touchdown solution of (5.1.1) at finite time T . Then, there exists a bounded constant $C = C(\lambda, f, \Omega) > 0$ such that*

$$\min_{x \in \Omega} u(x, t) \leq C(T-t)^{\frac{1}{3}} \quad \text{for } 0 < t < T. \quad (5.2.21)$$

Proof: Set

$$U(t) = \min_{x \in \Omega} u(x, t), \quad 0 < t < T,$$

and let $U(t_i) = u(x_i, t_i)$ ($i = 1, 2$) with $h = t_2 - t_1 > 0$. Then,

$$U(t_2) - U(t_1) \leq u(x_1, t_2) - u(x_1, t_1) = hu_t(x_1, t_1) + o(h),$$

$$U(t_2) - U(t_1) \geq u(x_2, t_2) - u(x_2, t_1) = hu_t(x_2, t_2) + o(h).$$

It follows that $U(t)$ is Lipschitz continuous. Hence, for $t_2 > t_1$ we have

$$\frac{U(t_2) - U(t_1)}{t_2 - t_1} \geq u_t(x_2, t_2) + o(1).$$

On the other hand, since $\Delta u(x_2, t_2) \geq 0$ we obtain,

$$u_t(x_2, t_2) \geq -\frac{\lambda f(x_2)}{u^2(x_2, t_2)} = -\frac{\lambda f(x_2)}{U^2(t_2)} \geq -\frac{C}{U^2(t_2)} \quad \text{for } 0 < t_2 < T.$$

Consequently, at any point of differentiability of $U(t)$, it deduces from above inequalities that

$$U^2 U_t \geq -C \quad \text{a.e. } t \in (0, T). \quad (5.2.22)$$

Integrating (5.2.22) from t to T we obtain (5.2.21). \blacksquare

For the touchdown solution $u = u(x, t)$ of (5.1.1) at finite time T , we now introduce the associated similarity variables

$$y = \frac{x - a}{\sqrt{T - t}}, \quad s = -\log(T - t), \quad u(x, t) = (T - t)^{\frac{1}{3}} w_a(y, s), \quad (5.2.23)$$

where a is any point of Ω_η for some small $\eta > 0$. Then $w_a(y, s)$ is defined in

$$W_a := \{(y, s) : a + ye^{-s/2} \in \Omega, s > s' = -\log T\},$$

and it solves

$$\frac{\partial}{\partial s} w_a - \Delta w_a + \frac{1}{2} y \cdot \nabla w_a - \frac{1}{3} w_a + \frac{\lambda f(a + ye^{-s/2})}{w_a^2} = 0. \quad (5.2.24)$$

Here $w_a(y, s)$ is always strictly positive in W_a . Note that the form of w_a defined by (5.2.23) is motivated by Theorem 5.1.1 and Proposition 5.2.6. The slice of W_a at a given time s^1 will be denoted by $\Omega_a(s^1)$:

$$\Omega_a(s^1) := W_a \cap \{s = s^1\} = e^{s^1/2}(\Omega - a).$$

Then for any $a \in \Omega_\eta$, there exists $s_0 = s_0(\eta, a) > 0$ such that

$$B_s := \{y : |y| < s\} \subset \Omega_a(s) \quad \text{for } s \geq s_0. \quad (5.2.25)$$

From now on, we often suppress the subscript a , writing w for w_a , etc.

In view of (5.2.23), one can combine Theorem 5.1.1 and Lemma 5.2.4 to reaching the following estimates on $w = w_a$:

Corollary 5.2.7. *Assume f satisfies (5.1.2) on a bounded domain Ω , and suppose u is a touchdown solution of (5.1.1) at finite time T . Assume touchdown set of u is a compact subset of Ω , then the rescaled solution $w = w_a$ satisfies*

$$M \leq w \leq e^{\frac{s}{3}}, \quad |\nabla w| + |\Delta w| \leq M' \quad \text{in } W,$$

where M is a constant as in Theorem 5.1.1 and while M' is a constant as in Lemma 5.2.4. Moreover, it satisfies

$$M \leq w(y_1, s) \leq w(y_2, s) + M'|y_2 - y_1|$$

for any $(y_i, s) \in W$, $i = 1, 2$.

We now rewrite (5.2.24) in divergence form:

$$\rho w_s - \nabla \cdot (\rho \nabla w) - \frac{1}{3} \rho w + \frac{\lambda \rho f(a + ye^{-\frac{s}{2}})}{w^2} = 0, \quad (5.2.26)$$

where $\rho(y) = e^{-|y|^2/4}$. We also introduce the frozen energy functional

$$E_s[w](s) = \frac{1}{2} \int_{B_s} \rho |\nabla w|^2 dy - \frac{1}{6} \int_{B_s} \rho w^2 dy - \int_{B_s} \frac{\lambda \rho f(a)}{w} dy, \quad (5.2.27)$$

which is defined in the compact set B_s of $\Omega_a(s)$ for $s \geq s_0$.

Lemma 5.2.8. *Assume f satisfies (5.1.2) on a bounded domain Ω , and suppose u is a touchdown solution of (5.1.1) at finite time T . Assume touchdown set of u is a compact subset of Ω , then the rescaled solution $w = w_a$ satisfies*

$$\frac{1}{2} \int_{B_s} \rho |w_s|^2 dy \leq -\frac{d}{ds} E_s[w](s) + g_\eta(s) \quad \text{for } s \geq s_0, \quad (5.2.28)$$

where $g_\eta(s)$ is positive and satisfies $\int_{s_0}^\infty g_\eta(s) ds < \infty$.

Proof: Multiply (5.2.26) by w_s and use integration by parts to get

$$\begin{aligned} \int_{B_s} \rho |w_s|^2 dy &= \int_{B_s} w_s \nabla (\rho \nabla w) dy + \frac{1}{3} \int_{B_s} \rho w w_s dy - \int_{B_s} \frac{\lambda \rho w_s f(a + ye^{-\frac{s}{2}})}{w^2} dy \\ &= -\frac{1}{2} \int_{B_s} \frac{d}{ds} |\nabla w|^2 \rho dy + \int_{B_s} \frac{d}{ds} \left(\frac{1}{6} w^2 + \frac{\lambda f(a)}{w} \right) \rho dy \\ &\quad + \int_{\partial B_s} \rho w_s \frac{\partial w}{\partial \nu} dS + \int_{B_s} \frac{\lambda \rho w_s [f(a) - f(a + ye^{-\frac{s}{2}})]}{w^2} dy \\ &= -\frac{d}{ds} E_s[w](s) + \int_{\partial B_s} \rho w_s \frac{\partial w}{\partial \nu} dS + \frac{1}{2s} \int_{\partial B_s} \rho |\nabla w|^2 (y \cdot \nu) dS \\ &\quad - \frac{1}{s} \int_{\partial B_s} \rho \left(\frac{1}{6} w^2 + \frac{\lambda f(a)}{w} \right) (y \cdot \nu) dS + \int_{B_s} \frac{\lambda \rho w_s [f(a) - f(a + ye^{-\frac{s}{2}})]}{w^2} dy \\ &\leq -\frac{d}{ds} E_s[w](s) + \int_{\partial B_s} \rho w_s \frac{\partial w}{\partial \nu} dS + \frac{1}{2s} \int_{\partial B_s} \rho |\nabla w|^2 (y \cdot \nu) dS \\ &\quad + \int_{B_s} \frac{\lambda \rho w_s [f(a) - f(a + ye^{-\frac{s}{2}})]}{w^2} dy \\ &:= -\frac{d}{ds} E_s[w](s) + I_1 + I_2 + I_3, \end{aligned} \quad (5.2.29)$$

where ν is the exterior unit norm vector to $\partial\Omega$ and dS is the surface area element. The following formula is applied in the third equality of (5.2.29): if $g(y, s) : W \mapsto R$ is a smooth

function, then

$$\begin{aligned}
 \frac{d}{ds} \int_{B_s} g(y, s) dy &= \frac{d}{ds} \int_{B_1} g(sz, s) s^N dz \\
 &= N \int_{B_1} g(sz, s) s^{N-1} dz + \int_{B_1} g_s(sz, s) s^N dz + \int_{B_1} (\nabla_y g \cdot z) s^N dz \\
 &= \int_{B_s} g_s(y, s) dy + N \int_{B_s} g(y, s) \frac{dy}{s} + \int_{B_s} (\nabla g \cdot \frac{y}{s}) dy \\
 &= \int_{B_s} g_s(y, s) dy + \frac{1}{s} \int_{\partial B_s} g(y, s) (y \cdot \nu) dS.
 \end{aligned}$$

For $s \geq s_0$, we next estimate integration terms I_1 , I_2 and I_3 as follows:

Considering $|y| \leq S$ in B_s , Corollary 5.2.7 gives

$$|w_s| = \left| \Delta w - \frac{1}{2} y \cdot \nabla w + \frac{1}{3} w - \frac{\lambda f(a + ye^{-\frac{s}{2}})}{w^2} \right| \leq C(1 + |y|) + \frac{1}{3} w \leq C_1 s + \frac{1}{3} e^{\frac{s}{3}},$$

which implies

$$I_1 \leq C s^{N-1} e^{-\frac{s^2}{4}} \left(C_1 s + \frac{1}{3} e^{\frac{s}{3}} \right) \leq C_2 s^N e^{-\frac{s^2}{4} + \frac{s}{3}}. \quad (5.2.30)$$

It is easy to observe that

$$I_2 \leq C_3 s^{N-1} e^{-\frac{s^2}{4}}. \quad (5.2.31)$$

As for I_3 , since w has a lower bound and since $f(x) \in C^\alpha(\bar{\Omega})$ for some $\alpha \in (0, 1]$, we apply Young's inequality to deduce

$$I_3 \leq C e^{-\frac{\alpha}{2}s} \int_{B_s} \rho |y|^\alpha w_s dy \leq C e^{-\frac{\alpha}{2}s} \left[\varepsilon \int_{B_s} \rho w_s^2 dy + C(\varepsilon) \int_{B_s} \rho |y|^{2\alpha} dy \right],$$

where the constant $\varepsilon > 0$ is arbitrary. Because $e^{-\frac{\alpha}{2}s} < \infty$, one can take sufficiently small ε such that

$$I_3 \leq \frac{1}{2} \int_{B_s} \rho w_s^2 dy + C_4 e^{-\frac{\alpha}{2}s}. \quad (5.2.32)$$

Combining (5.2.29) – (5.2.32) then yields

$$\begin{aligned}
 \frac{1}{2} \int_{B_s} \rho |w_s|^2 dy &\leq -\frac{d}{ds} E_s[w](s) + \bar{C}_1 s^N e^{-\frac{s^2}{4} + \frac{s}{3}} + \bar{C}_2 e^{-\frac{\alpha}{2}s} \\
 &:= -\frac{d}{ds} E_s[w](s) + g_\eta(s),
 \end{aligned}$$

where $g_\eta(s)$ is positive and satisfies $\int_{s_0}^\infty g_\eta(s) ds < \infty$, and we are done. \blacksquare

Remark 5.2.2. Supposing the convexity of Ω , one can establish an energy estimate in the whole domain $\Omega_a(s)$:

$$\int_{\Omega_a(s)} \rho |w_s|^2 dy \leq -\frac{d}{ds} E_{\Omega_a(s)}[w](s) + K_\eta(s) \quad \text{for } s \geq s_0, \quad (5.2.33)$$

where $K_\eta(s)$ is positive and satisfies $\int_{s_0}^\infty K_\eta(s)ds < \infty$, and $E_{\Omega_a(s)}[w](s)$ is defined by

$$E_{\Omega_a(s)}[w](s) = \frac{1}{2} \int_{\Omega_a(s)} \rho |\nabla w|^2 dy - \frac{1}{6} \int_{\Omega_a(s)} \rho w^2 dy - \int_{\Omega_a(s)} \frac{\lambda \rho f(a)}{w} dy. \quad (5.2.34)$$

However, by estimating the energy functional $E_s[w](s)$ in B_s , instead of $\Omega_a(s)$, it is sufficient to obtain the desirable upper bound estimate of w , see Theorem 5.2.10 below.

The following lemma is also necessary for establishing the desirable upper bound estimate.

Lemma 5.2.9. *Assume f satisfies (5.1.2) on a bounded domain Ω , and suppose u is a touchdown solution of (5.1.1) at finite time T . Assume touchdown set of u is a compact subset of Ω , and a is any point of Ω_η for some $\eta > 0$. Then there exists a constant $\varepsilon > 0$, depending only on λ , f and Ω , such that if*

$$u(x, t)(T - t)^{-\frac{1}{3}} \geq \varepsilon \quad (5.2.35)$$

for all $(x, t) \in Q_\delta := \{(x, t) : |x - a| < \delta, T - \delta < t < T\}$, then a is not a touchdown point for u . Here $\delta > 0$ is an arbitrary constant.

Proof: Setting $v(x, t) = \frac{1}{u(x, t)}$, then $v(x, t)$ blows up at finite time T , and v satisfies

$$v_t - \Delta v = -\frac{2|\nabla v|^2}{v} + \lambda f(x)v^4 \leq K(1 + v^4) \quad \text{in } Q_\delta, \quad (5.2.36)$$

where $K := \lambda \sup_{x \in \bar{\Omega}} f(x) > 0$. We now apply Theorem 2.1 of [37] to (5.2.36), which gives that there exists a constant $\frac{1}{\varepsilon} > 0$, depending only on λ , f and Ω , such that if

$$v(x, t) \leq \frac{1}{\varepsilon}(T - t)^{-\frac{1}{3}} \quad \text{in } Q_\delta,$$

then a is not a blow-up point for v , and hence (5.2.35) follows. \blacksquare

Theorem 5.2.10. *Assume f satisfies (5.1.2) on a bounded domain Ω , and suppose u is a touchdown solution of (5.1.1) at finite time T . Assume touchdown set of u is a compact subset of Ω , and a is any point of Ω_η for some $\eta > 0$. If $w_a(y, s) \rightarrow \infty$ as $s \rightarrow \infty$ uniformly for $|y| \leq C$, where C is any positive constant, then a is not a touchdown point for u .*

Proof: We first claim that if $w_a(y, s) \rightarrow \infty$ as $s \rightarrow \infty$ uniformly for $|y| \leq C$, then

$$E_s[w_a](s) \rightarrow -\infty \quad \text{as } s \rightarrow \infty. \quad (5.2.37)$$

Indeed, it is obvious from Corollary 5.2.7 that the first term and the third term in $E_s[w_a](s)$ are uniformly bounded. As for the second term, we can write

$$\int_{B_s} \rho w^2 dy = \int_{B_C} \rho w^2 dy + \int_{B_s \setminus B_C} \rho w^2 dy \geq \int_{B_C} \rho w^2 dy.$$

Since $w_a \rightarrow \infty$ as $s \rightarrow \infty$ uniformly on B_C , we have $\int_{B_C} \rho w^2 dy \rightarrow \infty$ as $s \rightarrow \infty$, which gives $-\frac{1}{6} \int_{B_C} \rho w^2 dy \rightarrow -\infty$ as $s \rightarrow \infty$, and hence (5.2.37) follows.

Let K be a large positive constant to be determined later. Then (5.2.37) implies that there exists an \bar{s} such that $E_{\bar{s}}[w_a](\bar{s}) \leq -4K$. Using the same argument as in [36], it is easy to show that for any fixed s , $E_s[w_a](s)$ varies smoothly with $a \in \Omega$. Therefore, there exists an $r_0 > 0$ such that

$$E_{\bar{s}}[w_b](\bar{s}) \leq -3K \quad \text{for } |b - a| < r_0.$$

Since touchdown set of u is assumed to be a compact subset of Ω , we have $\text{dist}(a, \partial\Omega) > \eta$ for some $\eta > 0$. Therefore, it now follows from Lemma 5.2.8 that

$$E_s[w_b](s) \leq -2K \quad \text{for } |b - a| < r_0, s \geq \bar{s}$$

provided $K \geq M_1 := \int_{s_0}^{\infty} g_{\eta}(s) ds$, where $g_{\eta}(s)$ is as in Lemma 5.2.8. Since the first term and the third term in $E_s[w_b](s)$ are uniformly bounded, we have

$$\int_{B_s} \rho w_b^2 dy \geq 6K \quad \text{for } |b - a| < r_0, s \geq \bar{s}. \quad (5.2.38)$$

Recalling from Corollary 5.2.7,

$$w_b^2(y, s) \leq 2(w_b^2(0, s) + M'^2|y|^2),$$

we obtain from (5.2.38) that

$$3K \leq w_b^2(0, s) \int_{B_s} \rho dy + M'^2 \int_{B_s} \rho |y|^2 dy \leq C_1 w_b^2(0, s) + C_2.$$

We now choose $K \geq \max\{M_1, \frac{2}{3}C_2\}$ so large that

$$w_b(0, s) \geq \sqrt{\frac{3K}{2C_1}} := \varepsilon. \quad (5.2.39)$$

Setting $\bar{t} := T - e^{-\bar{s}}$, it reduces from (5.2.39) that

$$u(b, t)(T - t)^{-\frac{1}{3}} \geq \varepsilon \quad \text{for } |b - a| < r_0, \bar{t} < t < T.$$

Applying Lemma 5.2.9 with a small r_0 , we finally conclude that a is not a touchdown point for u , and the theorem is proved. \blacksquare

5.3 Refined touchdown profiles

In this section we first establish touchdown rates by applying self-similar method [35]. Then the refined touchdown profiles for $N = 1$ and $N = 2$ will be separately derived by using center manifold analysis of a PDE [25], which will be discussed for $N = 1$ in §5.3.1 and for $N \geq 2$ in §5.3.2, respectively. It should be pointed out that for $N = 1$ we may establish the refined touchdown profiles for any touchdown point, see Theorem 5.3.3; while for $N \geq 2$, we are only able to deal with the refined touchdown profiles in the radial situation for the special touchdown point $r = 0$, see Theorem 5.3.5. Throughout this section and unless mentioned otherwise, touchdown set for u is assumed to be a compact subset of Ω , and a is always

assumed to be any touchdown point of u . Therefore, all a priori estimates of last section can be adapted here.

Our starting point of studying touchdown profiles is a similarity variable transformation of (5.1.1). For the touchdown solution $u = u(x, t)$ of (5.1.1) at finite time T , as before we use the associated similarity variables

$$y = \frac{x - a}{\sqrt{T - t}}, \quad s = -\log(T - t), \quad u(x, t) = (T - t)^{\frac{1}{2}} w(y, s), \quad (5.3.1)$$

where a is any touchdown point of u . Then $w(y, s)$ is defined in $W = \{(y, s) : |y| < Re^{s/2}, s > s' = -\log T\}$, where $R = \max\{|x - a| : x \in \Omega\}$, and it solves

$$w_s - \frac{1}{\rho} \nabla(\rho \nabla w) - \frac{1}{3} w + \frac{\lambda f(a + ye^{-\frac{s}{2}})}{w^2} = 0 \quad (5.3.2)$$

with $\rho(y) = e^{-|y|^2/4}$, where $f(a) > 0$ since a is assumed to be a touchdown point. Therefore, studying touchdown behavior of u is equivalent to studying large time behavior of w .

Lemma 5.3.1. *Suppose w is a solution of (5.3.2). Then, $w(y, s) \rightarrow w_\infty(y)$ as $s \rightarrow \infty$ uniformly on $|y| \leq C$, where $C > 0$ is any bounded constant, and $w_\infty(y)$ is a bounded positive solution of*

$$\Delta w - \frac{1}{2} y \cdot \nabla w + \frac{1}{3} w - \frac{\lambda f(a)}{w^2} = 0 \quad \text{in } \mathbb{R}^N, \quad (5.3.3)$$

where $f(a) > 0$.

Proof: We adapt the arguments from the proofs of Propositions 6 and 7 in [35]: let $\{s_j\}$ be a sequence such that $s_j \rightarrow \infty$ and $s_{j+1} - s_j \rightarrow \infty$ as $j \rightarrow \infty$. We define $w_j(y, s) = w(y, s + s_j)$. According to Theorem 5.1.1, Corollary 5.2.7 and Arzela-Ascoli theorem, there is a subsequence of $\{w_j\}$, still denoted by w_j , such that

$$w_j(y, s) \rightarrow w_\infty(y, s)$$

uniformly on compact subsets of W , and

$$\nabla w_j(y, m) \rightarrow \nabla w_\infty(y, m)$$

for almost all y and for each integer m . We obtain from Corollary 5.2.7 that either $w_\infty \equiv \infty$ or $w_\infty < \infty$ in \mathbb{R}^{N+1} . Since a is a touchdown point for u , the case $w_\infty \equiv \infty$ is ruled out by Theorem 5.2.10, and hence $w_\infty < \infty$ in \mathbb{R}^{N+1} . Therefore, we conclude again from Corollary 5.2.7 that

$$w \leq C_1(1 + |y|) \quad (5.3.4)$$

for some constant $C_1 > 0$.

Define the associated energy of w at time s ,

$$E_R[w](s) = \frac{1}{2} \int_{B_R} \rho |\nabla w|^2 dy - \frac{1}{6} \int_{B_R} \rho w^2 dy - \int_{B_R} \frac{\lambda \rho f(a)}{w} dy. \quad (5.3.5)$$

Taking $R(s) = s$, the same calculations as in (5.2.29) give

$$-\frac{d}{ds}E_s[w](s) = \int_{B_s} \rho(y)|w_s|^2 dy - K(s) \quad (5.3.6)$$

with

$$\begin{aligned} K(s) = & \int_{\partial B_s} \rho w_s \frac{\partial w}{\partial \nu} dS + \frac{1}{2s} \int_{\partial B_s} \rho |\nabla w|^2 (y \cdot \nu) dS - \frac{1}{s} \int_{\partial B_s} \rho \left(\frac{1}{6} w^2 + \frac{\lambda f(a)}{w} \right) (y \cdot \nu) dS \\ & + \lambda \int_{B_s} \frac{\rho w_s [f(a) - f(a + ye^{-s/2})]}{w^2} dy. \end{aligned}$$

We note that the expression $K(s)$ can be estimated as $s \gg 1$. Essentially, since $f(x) \in C^\alpha(\bar{\Omega})$ for some $\alpha \in (0, 1]$, using (5.3.4) and applying the same estimates as in Lemma 5.2.8 one can deduce that

$$K(s) - \frac{1}{2} \int_{B_s} \rho w_s^2 dy \leq G(s) := C_1 s^N e^{-\frac{s^2}{4}} + C_2 e^{-\frac{\alpha}{2}s} \quad \text{for } s \gg 1. \quad (5.3.7)$$

Together with (5.3.7), integrating (5.3.6) in time yields an energy inequality

$$\frac{1}{2} \int_a^b \int_{B_s} \rho |w_s|^2 dy ds \leq E_a[w](a) - E_b[w](b) + \int_a^b G(s) ds, \quad (5.3.8)$$

whenever $a < b$.

We now use (5.3.8) to prove that w_∞ is independent of s . We set $a = s_j + m$ and $b = s_{j+1} + m$ in (5.3.8) to obtain

$$\frac{1}{2} \int_m^{m+s_{j+1}-s_j} \int_{B_{s_j+s}} \rho |w_{js}|^2 dy ds \leq E_{s_j+m}[w_j](m) - E_{s_{j+1}+m}[w_{j+1}](m) + \int_{s_j+m}^{s_{j+1}+m} G(s) ds \quad (5.3.9)$$

for any integer m , where we use $w_j(y, s) = w(y, s + s_j)$. Since $\nabla w_j(y, m)$ is bounded and independent of j , and since we have assumed that $\nabla w_j(y, m) \rightarrow \nabla w_\infty(y, m)$ a.e. as $j \rightarrow \infty$, the dominated convergence theorem shows that

$$\int \rho(y) |\nabla w_j(y, m)|^2 dy \rightarrow \int \rho(y) |\nabla w_\infty(y, m)|^2 dy \quad \text{as } j \rightarrow \infty.$$

Arguing similarly for the other terms we can deduce that

$$\lim_{j \rightarrow \infty} E_{s_j+m}[w_j](m) = \lim_{j \rightarrow \infty} E_{s_{j+1}+m}[w_{j+1}](m) := E[w_\infty]. \quad (5.3.10)$$

On the other hand, because $m + s_j \rightarrow \infty$ as $j \rightarrow \infty$, (5.3.7) assures that the term involving G in (5.3.9) tends to zero as $j \rightarrow \infty$. Therefore, the right side of (5.3.9) tends to zero as $j \rightarrow \infty$. It now follows from $s_{j+1} - s_j \rightarrow \infty$ that

$$\lim_{j \rightarrow \infty} \int_m^{M} \int_{B_{s_j+s}} \rho |w_{js}|^2 dy ds = 0 \quad (5.3.11)$$

for each pair of integers $m < M$. Further, since (5.3.4) implies $|w_{js}(y, s)| \leq C(1 + |y|)$ with C independently of j , one can deduce that w_{js} converges weakly to $w_{\infty s}$. Because ρ decreases exponentially as $|y| \rightarrow \infty$, the integral of (5.3.11) is lower semi-continuous, and hence

$$\int_m^M \int_{\mathbb{R}^N} \rho |w_{\infty s}|^2 dy ds = 0,$$

where m and M are arbitrary, which shows that w_{∞} is independent of the choice of s .

We now notice from (5.3.5) that (5.3.10) defines $E[w_{\infty}]$ by

$$E[v] = \frac{1}{2} \int_{\mathbb{R}^N} \rho |\nabla_y v|^2 dy - \frac{1}{6} \int_{\mathbb{R}^N} \rho |v|^2 dy - \int_{\mathbb{R}^N} \frac{\lambda \rho f(a)}{v} dy.$$

We claim that $E[w_{\infty}]$ is independent of the choice of the sequence $\{s_j\}$. If this is not the case, then there is another $\{\bar{s}_j\}$ such that $E[w_{\infty}] \neq E[\bar{w}_{\infty}]$, where $\bar{w}_{\infty} = \lim_{j \rightarrow \infty} \bar{w}_j$ with $\bar{w}_j(y, s) = w(y, s + \bar{s}_j)$. Relabeling and passing to a sequence if necessary, we may suppose that $E[w_{\infty}] < E[\bar{w}_{\infty}]$ with $s_j < \bar{s}_j$. Now the energy inequality (5.3.8), with $a = s_j$ and $b = \bar{s}_j$, gives that

$$\frac{1}{2} \int_{s_j}^{\bar{s}_j} \int_{B_s} \rho |w_s|^2 dy ds \leq E_{s_j}[w_j](0) - E_{\bar{s}_j}[\bar{w}_j](0) + \int_{s_j}^{\bar{s}_j} G(s) ds. \quad (5.3.12)$$

Since $E_{s_j}[w_j](0) - E_{\bar{s}_j}[\bar{w}_j](0) \rightarrow E[w_{\infty}] - E[\bar{w}_{\infty}] < 0$ and $\int_{s_j}^{\bar{s}_j} G(s) ds \rightarrow 0$ as $j \rightarrow \infty$, the right side of (5.3.12) is negative for sufficiently large j . This leads to a contradiction, because the left side of (5.3.12) is non-negative. Hence $E[w_{\infty}] = E[\bar{w}_{\infty}]$, which implies that $E[w_{\infty}]$ is independent of the choice of the sequence $\{s_j\}$.

Therefore, we conclude that $w(y, s) \rightarrow w_{\infty}(y)$ as $s \rightarrow \infty$ uniformly on $|y| \leq C$, where C is any bounded constant, and $w_{\infty}(y)$ is a bounded positive solution of (5.3.3). \blacksquare

5.3.1 Refined touchdown profiles for $N = 1$

In this subsection, we establish refined touchdown profiles for the deflection $u = u(x, t)$ in one dimensional case. We begin with the discussions on the solution $w_{\infty}(y)$ of (5.3.3). For one dimensional case, Fila and Hulshof proved in Theorem 2.1 of [23] that every non-constant solution $w(y)$ of

$$w_{yy} - \frac{1}{2} y w_y + \frac{1}{3} w - \frac{1}{w^2} = 0 \quad \text{in } (-\infty, \infty)$$

must be strictly increasing for all $|y|$ sufficiently large, and $w(y)$ tends to ∞ as $|y| \rightarrow \infty$. So it reduces from Lemma 5.3.1 that it must have $w_{\infty}(y) \equiv \text{const.}$. Therefore, by scaling we conclude that

$$\lim_{s \rightarrow \infty} w(y, s) \equiv (3\lambda f(a))^{\frac{1}{3}}$$

uniformly on $|y| \leq C$ for any bounded constant C . This gives the following touchdown rate.

Lemma 5.3.2. *Assume f satisfies (5.1.2) on a bounded domain $\Omega \subset \mathbb{R}^1$, and suppose u is a unique touchdown solution of (5.1.1) at finite time T . Assume touchdown set for u is a compact subset of Ω . If $x = a$ is a touchdown point of u , then we have*

$$\lim_{t \rightarrow T^-} u(x, t)(T - t)^{-\frac{1}{3}} \equiv (3\lambda f(a))^{\frac{1}{3}}$$

uniformly on $|x - a| \leq C\sqrt{T-t}$ for any bounded constant C .

We next determine the refined touchdown profiles for one dimensional case. Our method is based on the center manifold analysis of a PDE that results from a similarity group transformation of (5.1.1). Such an approach was used in [32] for the uniform permittivity profile $f(x) \equiv 1$. A closely related approach was used in [25] to determine the refined blow-up profile for a semilinear heat equation. We now briefly outline this method and the results that can be extended to the varying permittivity profile $f(x)$:

Continuing from (5.3.2) with touchdown point $x = a$, for $s \gg 1$ and $|y|$ bounded we have $w \sim w_\infty + v$, where $v \ll 1$ and $w_\infty \equiv (3\lambda f(a))^{1/3} > 0$. Keeping the quadratic terms in v , we obtain for $N = 1$ that

$$\begin{aligned} v_s - v_{yy} + \frac{y}{2}v_y - v &= \frac{w_\infty}{3} \left[1 - \frac{f(a + ye^{-s/2})}{f(a)} \right] + \frac{2[f(a + ye^{-s/2}) - f(a)]}{3f(a)} v \\ &\quad - \frac{3\lambda f(a + ye^{-s/2})}{w_\infty^4} v^2 + O(v^3) \\ &\approx -(3\lambda f(a))^{-\frac{1}{3}} v^2 + O(v^3 + e^{-\frac{\alpha}{2}s}), \end{aligned} \quad (5.3.13)$$

for $s \gg 1$ and bounded $|y|$, due to the assumption (5.1.2) that $f(x) \in C^\alpha(\bar{\Omega})$ for some $0 < \alpha \leq 1$. As shown in [25] (see also [32]), the linearized operator in (5.3.13) has a one-dimensional nullspace when $N = 1$. By projecting the nonlinear term in (5.3.13) against the nullspace of the linearized operator, the following far-field behavior of v for $s \rightarrow +\infty$ and $|y|$ bounded is obtained (see (1.7) of [25]):

$$v \sim -\frac{(3\lambda f(a))^{1/3}}{4s} \left(1 - \frac{|y|^2}{2} \right), \quad N = 1. \quad (5.3.14)$$

The refined touchdown profile is then obtained from $w \sim w_\infty + v$, (5.3.1) and (5.3.14), which is for $t \rightarrow T^-$,

$$u \sim [3\lambda f(a)(T-t)]^{1/3} \left(1 - \frac{1}{4|\log(T-t)|} + \frac{|x-a|^2}{8(T-t)|\log(T-t)|} + \dots \right), \quad N = 1. \quad (5.3.15)$$

Combining Lemma 5.3.2 and (5.3.15) directly gives the following refined touchdown profile.

Theorem 5.3.3. *Assume f satisfies (5.1.2) on a bounded domain Ω in \mathbb{R}^N , and suppose u is a touchdown solution of (5.1.1) at finite time T . Assume touchdown set of u is a compact subset of Ω , and suppose $N = 1$ and $x = a$ is a touchdown point of u . Then we have*

$$\lim_{t \rightarrow T^-} u(x, t)(T-t)^{-\frac{1}{3}} \equiv (3\lambda f(a))^{1/3} \quad (5.3.16)$$

uniformly on $|x - a| \leq C\sqrt{T-t}$ for any bounded constant C . Moreover, when $t \rightarrow T^-$,

$$u \sim [3\lambda f(a)(T-t)]^{1/3} \left(1 - \frac{1}{4|\log(T-t)|} + \frac{|x-a|^2}{8(T-t)|\log(T-t)|} + \dots \right), \quad N = 1. \quad (5.3.17)$$

We finally remark that applying formal asymptotic methods, when $N = 1$ the refined touchdown profile of (5.1.1) is also established in (4.5.12). By making a binomial approximation, it is easy to compare that (5.3.15) agrees asymptotically with (4.5.12).

5.3.2 Refined touchdown profiles for $N \geq 2$

For obtaining refined touchdown profiles in higher dimension, in this subsection we assume that $f(r) = f(|x|)$ is radially symmetric and $\Omega = B_R(0)$ is a bounded ball in \mathbb{R}^N with $N \geq 2$. Then the uniqueness of solutions for (5.1.1) implies that the solution u of (5.1.1) must be radially symmetric. We study the refined touchdown profile for the special touchdown point $r = 0$ of u at finite time T . In this situation, the fact that the solution u of (5.1.1) is radially symmetric implies the radial symmetry of $w(y, s)$ in y , and hence the radial symmetry of $w_\infty(y)$ (cf. [34]). Note that $w_\infty(y)$ is a radially symmetric solution of

$$w_{yy} + \left(\frac{N-1}{y} - \frac{y}{2}\right)w_y + \frac{1}{3}w - \frac{\lambda f(0)}{w^2} = 0 \quad \text{for } y > 0, \quad (5.3.18)$$

where $w_y(0) = 0$ and $f(0) > 0$. For this case, applying Theorem 1.6 of [39] yields that every non-constant radial solution $w(y)$ of (5.3.18) must be strictly increasing for all y sufficiently large, and $w(y)$ tends to ∞ as $y \rightarrow \infty$. It now reduces again from Lemma 5.3.1 that

$$\lim_{s \rightarrow \infty} w(y, s) \equiv (3\lambda f(0))^{\frac{1}{3}}$$

uniformly on $|y| \leq C$ for any bounded constant C . This gives the following touchdown rate.

Lemma 5.3.4. *Assume $f(r) = f(|x|)$ satisfies (5.1.2) on a bounded ball $B_R(0) \subset \mathbb{R}^N$ with $N \geq 2$, and suppose u is a unique touchdown solution of (5.1.1) at finite time T . Assume touchdown set for u is a compact subset of Ω . If $r = 0$ is a touchdown point of u , then we have*

$$\lim_{t \rightarrow T^-} u(r, t)(T - t)^{-\frac{1}{3}} \equiv (3\lambda f(0))^{\frac{1}{3}}$$

uniformly for $r \leq C\sqrt{T-t}$ for any bounded constant C .

We next derive a refined touchdown profile (5.3.20). Similar to one dimensional case, indeed we can establish the refined touchdown profiles for varying permittivity profile $f(|x|)$ defined in higher dimension $N \geq 2$. Specially, applying a result from [25], the refined touchdown profile for $N = 2$ is given by

$$u \sim [3\lambda f(0)(T-t)]^{1/3} \left(1 - \frac{1}{2|\log(T-t)|} + \frac{|x-a|^2}{4(T-t)|\log(T-t)|} + \dots \right), \quad N = 2.$$

This leads to the following refined touchdown profile for higher dimensional case.

Theorem 5.3.5. *Assume f satisfies (5.1.2) on a bounded domain Ω in \mathbb{R}^N , and suppose u is a touchdown solution of (5.1.1) at finite time T . Assume touchdown set of u is a compact subset of Ω , and suppose $\Omega = B_R(0) \subset \mathbb{R}^N$ is a bounded ball with $N \geq 2$ and $f(r) = f(|x|)$ is radially symmetric. If $r = 0$ is a touchdown point of u , then we have*

$$\lim_{t \rightarrow T^-} u(r, t)(T-t)^{-\frac{1}{3}} \equiv (3\lambda f(0))^{\frac{1}{3}} \quad (5.3.19)$$

uniformly on $r \leq C\sqrt{T-t}$ for any bounded constant C . Moreover, when $t \rightarrow T^-$,

$$u \sim [3\lambda f(0)(T-t)]^{1/3} \left(1 - \frac{1}{2|\log(T-t)|} + \frac{r^2}{4(T-t)|\log(T-t)|} + \dots \right), \quad N = 2. \quad (5.3.20)$$

Remark 5.3.1. Applying analytical and numerical techniques, next section we shall show that Theorem 5.3.5 does hold for a larger class of profiles $f(r) = f(|x|)$.

Before concluding this section, it is interesting to compare the solution of (5.1.1) with that of the ordinary differential equation obtained by omitting Δu . For that we focus on one dimensional case, and we compare the solutions of

$$u_t - u_{xx} = -\frac{\lambda f(x)}{u^2} \quad \text{in } (-a, a), \quad (5.3.21a)$$

$$u(\pm a, t) = 1; \quad u(x, 0) = 1, \quad (5.3.21b)$$

and

$$v_t = -\frac{\lambda f(x)}{v^2} \quad \text{in } (-a, a), \quad (5.3.22a)$$

$$v(\pm a, t) = 1; \quad v(x, 0) = 1, \quad (5.3.22b)$$

where f is assumed to satisfy (5.1.2) and (5.2.1). The ordinary differential equation (5.3.22) is explicitly solvable, and the solution touches down at finite time

$$v(x, t) = (1 - 3\lambda f(x)t)^{\frac{1}{3}}, \quad (5.3.23)$$

which shows that touchdown point of v is the maximum value point of $f(x)$. In the partial differential equation (5.3.21), there is a contest between the dissipating effect of the Laplacian u_{xx} and the singularizing effect of the nonlinearity $f(x)/u^2$; when u touches down at $x = x_0$ in finite time T , then the nonlinear term dominates (essentially, for some special cases, touchdown point x_0 of u is also the maximum value point of $f(x)$, see Theorem 5.1.4 for details).

However, we claim that a smoothing effect of the Laplacian can be still observed in the different character of touchdown. Indeed, letting $f(y_0) = \max\{f(x) : x \in (-a, a)\}$, then $f'(y_0) = 0$ and $f''(y_0) \leq 0$. And (5.3.23) gives the finite touchdown time T_0 for v satisfying $T_0 = 1/[3\lambda f(y_0)]$. Furthermore, we can get from (5.3.23), together with the Taylor series of $f(x)$,

$$\lim_{t \rightarrow T_0^-} (T_0 - t)^{-\frac{1}{3}} v(y_0 + (T_0 - t)^{\frac{1}{2}} y, t) = (3\lambda f(y_0))^{\frac{1}{3}} \left[1 - \frac{f''(y_0)}{2f^2(y_0)} |y|^2\right]^{\frac{1}{3}} \geq (3\lambda f(x_0))^{\frac{1}{3}}. \quad (5.3.24)$$

And our Theorem 5.3.3 says that for such u we have

$$\lim_{t \rightarrow T^-} (T - t)^{-\frac{1}{3}} u(x_0 + (T - t)^{\frac{1}{2}} y, t) = (3\lambda f(x_0))^{\frac{1}{3}}. \quad (5.3.25)$$

Comparing (5.3.24) with (5.3.25), we see that the touchdown of the partial differential equation (5.3.21) is “flatter” than that of the ordinary differential equation (5.3.22).

5.4 Set of touchdown points

This section is focussed on the set of touchdown points for (5.1.1), which may provide useful information on the design of MEMS devices. In §5.4.1, we consider the radially symmetric case where $f(r) = f(|x|)$ with $r = |x|$ is a radial function and Ω is a ball $B_R = \{|x| \leq R\} \subset \mathbb{R}^N$ with $N \geq 1$. In §5.4.2, numerically we compute some simulations for one dimensional case, from which we discuss the compose of touchdown points for some explicit permittivity profiles $f(x)$.

5.4.1 Radially symmetric case

In this subsection, $f(r) = f(|x|)$ is assumed to be a radial function and Ω is assumed to be a ball $B_R = \{|x| \leq R\} \subset \mathbb{R}^N$ with any $N \geq 1$. For this radially symmetric case, the uniqueness of solutions for (5.1.1) implies that the solution $u = u(x, t)$ of (5.1.1) must be radially symmetric. We begin with the following lemma for proving Theorem 5.1.4:

Lemma 5.4.1. *Suppose $f(r)$ satisfies (5.1.2) and $f'(r) \leq 0$ in B_R , and let $u = u(r, t)$ be a touchdown solution of (5.1.1) at finite time T . Then $u_r > 0$ in $\{0 < r < R\} \times (t_0, T)$ for some $0 < t_0 < T$.*

Proof: Setting $w = r^{N-1}u_r$, then (5.1.1) gives

$$u_t - \frac{1}{r^{N-1}}w_r = -\frac{\lambda f(r)}{u^2}, \quad 0 < t < T. \quad (5.4.1)$$

Differentiating (5.4.1) with respect to r , we obtain

$$w_t - w_{rr} + \frac{N-1}{r}w_r - \frac{2\lambda f}{u^3}w = -\frac{\lambda f' r^{N-1}}{u^2} \geq 0, \quad 0 < t < T, \quad (5.4.2)$$

since $f'(r) \leq 0$ in B_R . Therefore, w can not attain negative minimum in $\{0 < r < R\} \times (0, T)$. Since $w(0, t) = w(r, 0) = 0$ and $u_t < 0$ for all $t \in (0, T)$, we have $w = r^{N-1}u_r > 0$ on $\partial B_R \times (0, T)$. So the maximum principle shows that $w \geq 0$ in $\{0 < r < R\} \times (0, T)$. This gives

$$w_t - w_{rr} + \frac{N-1}{r}w_r \geq 0 \quad \text{in } \{0 < r < R\} \times (t_1, T),$$

where $t_1 > 0$ is chosen so that $w(r, t_1) \not\equiv 0$ in $\{0 < r < R\}$.

Now compare w with the solution z of

$$z_t - z_{rr} + \frac{N-1}{r}z_r = 0 \quad \text{in } \{0 < r < R\} \times (t_1, T)$$

subject to $z(r, t_1) = w(r, t_1)$ for $0 \leq r \leq R$, $z(R, t) = w(R, t) > 0$ and $z(0, t) = 0$ for $t_1 \leq t < T$. The comparison principle yields $w \geq z$ in $\{0 < r < R\} \times (t_1, T)$. On the other hand, for any $t_0 > t_1$ we have $z > 0$ in $\{0 < r < R\} \times (t_0, T)$. Consequently we conclude that $w > 0$, i.e. $u_r > 0$ in $\{0 < r < R\} \times (t_0, T)$. \blacksquare

Proof of Theorem 5.1.4: For $w = r^{N-1}u_r$, we set $J(r, t) = w - \varepsilon \int_0^{r^\theta} f(s)ds$, where $\theta \geq N$ and $\varepsilon = \varepsilon(\theta) > 0$ are constants to be determined. We calculate from (5.4.1) and (5.4.2) that

$$\begin{aligned} J_t - J_{rr} + \frac{N-1}{r}J_r &= b_1 J + \frac{2\lambda \varepsilon f \int_0^{r^\theta} f(s)ds}{u^3} - \frac{\lambda f' r^{N-1}}{u^2} + \theta \varepsilon r^{\theta-1} f' \\ &\geq b_1 J - r^{N-1}(\lambda - \theta \varepsilon r^{\theta-N}) f' \geq b_1 J, \end{aligned}$$

provided ε is sufficiently small, where b_1 is a locally bounded function. Here we have applied the assumption $f'(r) \leq 0$ and the relations $u_r = w/r^{N-1}$ and $w = J + \varepsilon \int_0^{r^\theta} f(s)ds$. Note that $J(0, t) = 0$, and hence it follows that J can not obtain negative minimum in $B_R \times (0, T)$.

We next observe that J can not obtain negative minimum on $\{r = R\}$ provided ε is sufficiently small, which comes from the fact

$$J_r(R, t) = w_r - \theta \varepsilon R^{\theta-1} f(R) = \frac{\lambda R^{N-1} f(R)}{u^2} - \theta \varepsilon R^{\theta-1} f(R) \geq R^{N-1} f(R) [\lambda - \theta \varepsilon R^{\theta-N}] \geq 0$$

for sufficiently small $\varepsilon > 0$, where (5.4.1) is applied. We now choose some $0 < t_0 < T$ such that $w(r, t_0) > 0$ for $0 < r \leq R$ in view of Lemma 5.4.1. This gives $u_r(r, t_0) > 0$ for $0 < r \leq R$. Since $u_r(0, t_0) = 0$, there exists some $\alpha > 0$ such that

$$u_{rr}(0, t_0) = \lim_{r \rightarrow 0} \frac{u_r(r, t_0)}{r^\alpha} = \lim_{r \rightarrow 0} \frac{w(r, t_0)}{r^{N+\alpha-1}} > 0.$$

We now choose $\theta = \max\{N, N + \alpha - 1\}$, from which one can further deduce that $J(r, t_0) \geq 0$ for $0 \leq r < R$ provided $\varepsilon = \varepsilon(t_0, \theta) > 0$ is sufficiently small.

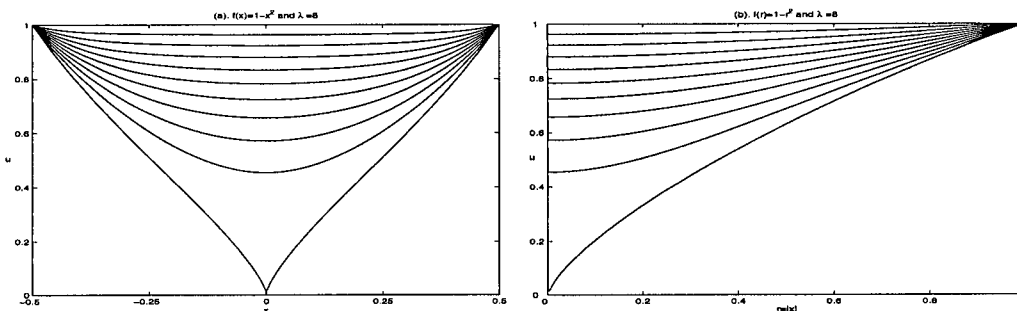


Figure 5.1: Left figure: plots of u versus x at different times with $f(x) = 1 - x^2$ in the slab domain, where the unique touchdown point is $x = 0$. Right figure: plots of u versus $r = |x|$ at different times with $f(r) = 1 - r^2$ in the unit disk domain, where the unique touchdown point is $r = 0$ too.

It now concludes from the maximum principle that $J \geq 0$ in $B_R \times (t_0, T)$ provided $\varepsilon = \varepsilon(t_0) > 0$ is sufficiently small. This leads to

$$u(r, t) \geq u(r, t) - u(0, t) \geq \varepsilon \int_0^r \frac{\int_0^{s^\theta} f(\mu) d\mu}{s^{N-1}} ds. \quad (5.4.3)$$

Given small $C_0 > 0$, then the assumption of $f(r)$ implies that there exists $0 < r_0 = r_0(C_0) \leq R$ such that $f(r) \geq C_0$ on $[0, r_0]$. Denote $r_m = \min\{r_0, r\}$, and then (5.4.3) gives

$$u(r, t) \geq \varepsilon \int_0^{r_m} \frac{\int_0^{s^\theta} f(\mu) d\mu}{s^{N-1}} ds \geq \varepsilon \int_0^{r_m} \frac{C_0 s^\theta}{s^{N-1}} ds = \frac{1}{\theta - N + 2} \varepsilon C_0 r_m^{\theta - N + 2}, \quad \text{where } \theta - N + 2 \geq 2,$$

which implies that $r = 0$ must be the unique touchdown point of u . ■

Before ending this subsection, we now present a few numerical simulations on Theorem 5.1.4. Here we apply the implicit Crank-Nicholson scheme. In the following simulations 1 ~ 3,

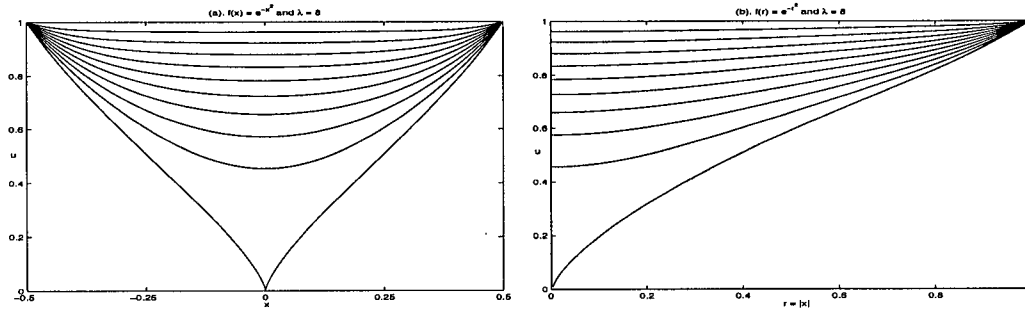


Figure 5.2: Left figure: plots of u versus x at different times with $f(x) = e^{-x^2}$ in the slab domain, where the unique touchdown point is $x = 0$. Right figure: plots of u versus $r = |x|$ at different times with $f(r) = e^{-r^2}$ in the unit disk domain, where the unique touchdown point is $r = 0$ too.

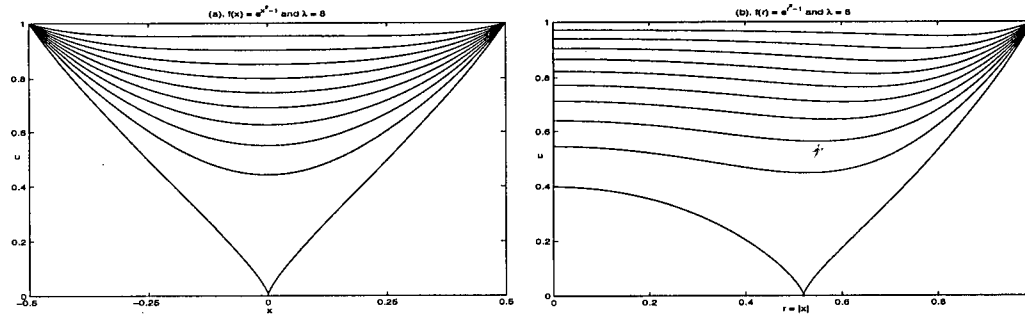


Figure 5.3: Left figure: plots of u versus x at different times with $f(x) = e^{x^2-1}$ in the slab domain, where the unique touchdown point is still at $x = 0$. Right figure: plots of u versus $r = |x|$ at different times with $f(r) = e^{r^2-1}$ in the unit disk domain, where the touchdown points satisfy $r = 0.51952$.

we always take $\lambda = 8$ and the number of meshpoints $N = 1000$, and consider (5.1.1) in the following symmetric slab or unit disk domains:

$$\Omega : [-1/2, 1/2] \quad (\text{Slab}); \quad \Omega : x^2 + y^2 \leq 1 \quad (\text{Unit Disk}). \quad (5.4.4)$$

Simulation 1: $f(|x|) = 1 - |x|^2$ is chosen as a permittivity profile. In Figure 5.1(a), u versus x is plotted at different times for (5.1.1) in the symmetric slab domain. For this touchdown behavior, touchdown time is $T = 0.044727$ and the unique touchdown point is $x = 0$. In Figure 5.1(b), u versus $r = |x|$ is plotted at different times for (5.1.1) in the unit disk domain. For this touchdown behavior, touchdown time is $T = 0.0455037$ and the unique touchdown point is $r = 0$.

Simulation 2: $f(|x|) = e^{-|x|^2}$ is chosen as a permittivity profile. In Figure 5.2(a), u versus x is plotted at different times for (5.1.1) in the symmetric slab domain. For this touchdown behavior, touchdown time is $T = 0.044675$ and the unique touchdown point is $x = 0$. In Figure 5.2(b), u versus $r = |x|$ is plotted at different times for (5.1.1) in the unit disk domain. For this touchdown behavior, touchdown time is $T = 0.0450226$ and the unique touchdown point is $r = 0$ too.

Simulation 3: $f(|x|) = e^{|x|^2 - 1}$ is chosen as a permittivity profile. In Figure 5.3(a), u versus x is plotted at different times for (5.1.1) in the symmetric slab domain. For this touchdown behavior, touchdown time is $T = 0.147223$ and touchdown point is still uniquely at $x = 0$. In Figure 5.3(b), u versus $r = |x|$ is plotted at different times for (5.1.1) in the unit disk domain. For this touchdown behavior, touchdown time is $T = 0.09065363$, but touchdown points are at $r_0 = 0.51952$, which compose into the surface of $B_{r_0}(0)$. This simulation shows that the assumption $f'(r) \leq 0$ in Theorem 5.1.4 is just sufficient, not necessary.

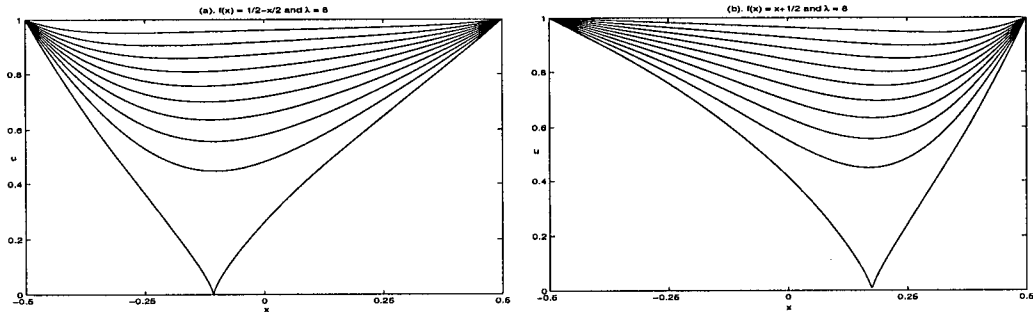


Figure 5.4: Left figure: plots of u versus x at different times with $f(x) = 1/2 - x/2$ in the slab domain, where the unique touchdown point is $x = -0.10761$. Right figure: plots of u versus $r = |x|$ at different times with $f(x) = x + 1/2$ in the slab domain, where the unique touchdown point is $x = 0.17467$.

5.4.2 One dimensional case

For one dimensional case, Theorem 5.1.4 already gives that touchdown points must be unique if the permittivity profile $f(x)$ is uniform. In the following, we choose some explicit varying

permittivity profiles $f(x)$ to perform two numerical simulations. Here we apply the implicit Crank-Nicholson scheme again.

Simulation 4: Monotone Function $f(x)$:

We take $\lambda = 8$ and the number of meshpoints $N = 1000$, and we consider (5.1.1) in the slab domain Ω defined in (5.4.4). In Figure 5.4(a), the monotonically decreasing profile $f(x) = 1/2 - x/2$ is chosen, and u versus x is plotted for (5.1.1) at different times. For this touchdown behavior, the touchdown time is $T = 0.09491808$ and the unique touchdown point is $x = -0.10761$. In Figure 5.4(b), the monotonically increasing profile $f(x) = x + 1/2$ is chosen, and u versus x is plotted for (5.1.1) at different times. For this touchdown behavior, the touchdown time is $T = 0.0838265$ and the unique touchdown point is $x = 0.17467$. For the general case where $f(x)$ is monotone in a slab domain, it is interesting to look insights into whether the touchdown points must be unique.

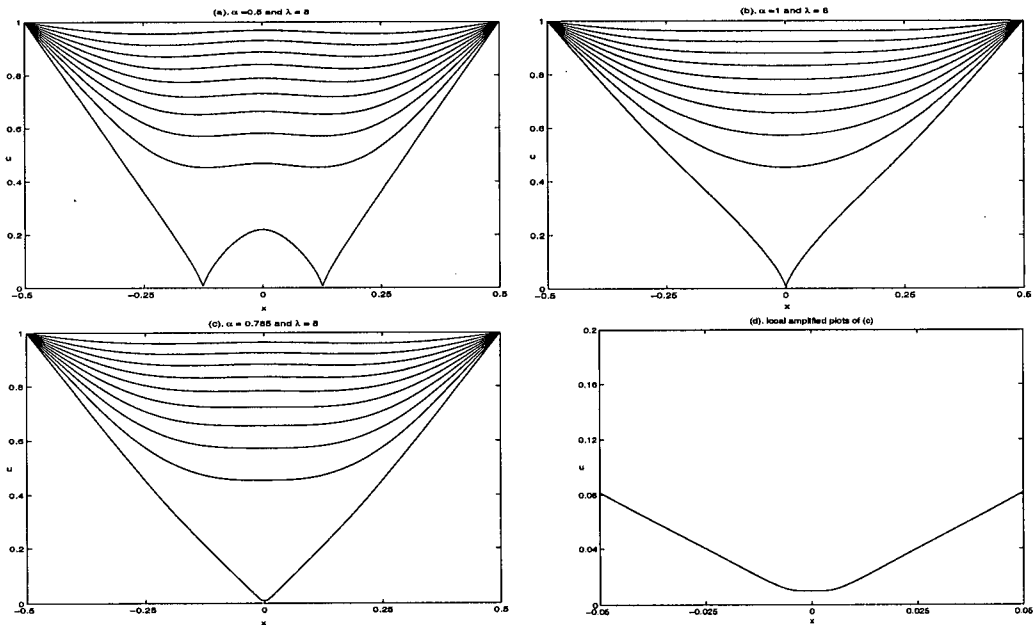


Figure 5.5: Plots of u versus x at different times in the slab domain, for different permittivity profiles $f[\alpha](x)$ given by (5.4.5). Top left (a): when $\alpha = 0.5$, two touchdown points are at $x = \pm 0.12631$. Top right (b): when $\alpha = 1$, the unique touchdown point is at $x = 0$. Bottom Left (c): when $\alpha = 0.785$, touchdown points are observed to consist of a closed interval $[-0.0021255, 0.0021255]$. Bottom right (d): local amplified plots of (c).

Simulation 5: “M”-Form Function $f(x)$:

In this simulation, we consider (5.1.1) in the slab domain Ω defined in (5.4.4). Here we take $\lambda = 8$ and the number of the meshpoints $N = 2000$, and the varying dielectric permittivity

profiles satisfies

$$f[\alpha](x) = \begin{cases} 1 - 16(x + 1/4)^2, & \text{if } x < -1/4; \\ \alpha + (1 - \alpha)|\sin(2\pi x)|, & \text{if } |x| \leq 1/4; \\ 1 - 16(x - 1/4)^2, & \text{if } x > 1/4 \end{cases} \quad (5.4.5)$$

with $\alpha \in [0, 1]$, which has “M”-form. In Figure 5.5, u versus x is plotted at different times for (5.1.1) for different α , *i.e.* for different permittivity profiles $f[\alpha](x)$. In Figure 5.5(a): when $\alpha = 0.5$, the touchdown time is $T = 0.05627054$ and two touchdown points are at $x = \pm 0.12631$. In Figure 5.5(b): when $\alpha = 1$, the touchdown time is $T = 0.0443323$ and the unique touchdown point is at $x = 0$. In Figure 5.5(c): when $\alpha = 0.785$, the touchdown time is $T = 0.04925421$ and touchdown points are observed to compose into a closed interval $[-0.0021255, 0.0021255]$. In Figure 5.5(d): local amplified plots of (c) at touchdown time $t = T$. This simulation shows for dimension $N = 1$ that the set of touchdown points may be composed of finite points or finite compact subsets of the domain, if the permittivity profile is ununiform.

Chapter 6

Thesis Summary

In this thesis, we have used both analytical and numerical methods to analyze the most basic mathematical model describing the dynamics of an elastic membrane in an electrostatic MEMS. We have answered mathematical questions dealing with existence, uniqueness and regularity of solutions. We have also addressed problems of more applicable nature such as stability, as well as estimates on pull-in voltages and touchdown times in terms of the shape of the domain and the permittivity profile of the membrane. The thesis consists of two main parts:

6.1 Stationary Case

This reflects the state of the membrane at equilibrium when the voltage is below the critical threshold. We have given a detailed and rigorous analysis of the pull-in voltage and the deflection profile, as described by the solutions of the equation that models Electrostatic MEMS.

By applying various numerical and analytic methods, we have given several useful upper and lower bounds for the pull-in voltage λ^* , by using modern mathematical tools such as Pohozaev-type estimates and Bandle's Schwarz symmetrization techniques. We do believe however that our estimates are not optimal and better ones, depending on the distribution of the permittivity profile and the shape of the domain, can still be obtained.

We have studied the branch of stable and semi-stable solutions by using energy estimates and have shown how the problem is dependent on the dimension, the shape of the membrane and the permittivity profile. We have also used sophisticated blow-up analysis to give a rigorous analysis of the unstable solutions. We also established partial results about uniqueness and multiplicity of solutions at various voltage ranges. The case where we have a power law permittivity profile on a round ball is however completely understood.

6.2 Dynamic Case

Here we analyze the evolution of the membrane's deflection with time. The system exhibits three types of behavior. We have global convergence to a stable stationary state whenever the voltage is below the critical threshold. We have touchdown in finite time when we are beyond, and we have possible touchdown in infinite time at the critical pull-in voltage.

We give several useful estimates for the touchdown time in terms of the domain, the permittivity profile and the applied voltage. A detailed analysis of the geometry and "size" of the touchdown set is given, showing in particular how the permittivity profile and the shape of the membrane can be used to affect both the duration and the functioning of the MEMS. It is shown for example that the zero points of the profile f cannot be touchdown points.

The pull-in distance is also discussed and several interesting phenomena are observed numerically and established mathematically. For example, for the case of a power law profile

$(f(x) = |x|^\alpha)$ on a 2-dimensional disk, one can show that the pull-in distance is independent of the voltage, while numerical estimates show that the membrane develops a boundary-layer structure near the boundary of the domain as the power α is increased.

Bibliography

- [1] A. Ambrosetti, H. Brezis and G. Cerami, *Combined effects of concave and convex nonlinearities in some elliptic problems*, J. Funct. Anal. **122** (1994), 519–543.
- [2] U. Ascher, R. Christiansen and R. Russell, *Collocation software for boundary value ODE's*, Math. Comp. **33** (1979), 659–679.
- [3] A. Ambrosetti and P. Rabinowitz, *Dual variational methods in critical point theory and application*, J. Funct. Anal. **14** (1973), 349–381.
- [4] S. Alama and G. Tarantello, *Elliptic problems with nonlinearities indefinite in sign*, J. Funct. Anal. **141** (1996), 159–215.
- [5] S. Alama and G. Tarantello, *On the solvability of a semilinear elliptic equation via an associated eigenvalue problem*, Math. Z. **221** (1996), 467–493.
- [6] C. Bandle, *Isoperimetric inequalities and applications*, Monographs and Studies in Mathematics, Boston, Mass.-London, Pitman, 1980.
- [7] R. E. Bank, *PLTMG: A software package for solving elliptic partial differential equations*, User's guide 8.0, Software, Environments, and Tools, SIAM, Philadelphia, PA, 1998.
- [8] H. Bellout, *A criterion for blow-up of solutions to semilinear heat equations*, SIAM, J. Math. Anal. **18** (1987), 722–727.
- [9] D. Bernstein, P. Guidotti and J. A. Pelesko, *Analytic and numerical analysis of electrostatically actuated MEMS devices*, Proc. of Modeling and Simulation of Microsystems **2000** (2000), 489–492.
- [10] H. Brezis, T. Cazenave, Y. Martel and A. Ramiandrisoa, *Blow up for $u_t - \Delta u = g(u)$ revisited*, Adv. Diff. Eqns. **1** (1996), 73–90.
- [11] C. M Brauner and B. Nicolaenko, *Sur une classe de problèmes elliptiques non linéaires*, C. R. Acad. Sci. Paris **286** (1978), 1007–1010.
- [12] H. Brezis and L. Nirenberg, *H^1 versus C^1 local minimizers*, C. R. Math. Acad. Sci. Paris **317** (1993), 465–472.
- [13] H. Brezis, L. A. Peletier and D. Terman, *A very singular solution of the heat equation with absorption*, Arch. Ration. Mech. Anal. **95** (1986), 185–209.
- [14] H. Brezis and J. L. Vazquez, *Blow-up solutions of some nonlinear elliptic problems*, Rev. Mat. Univ. Compl. Madrid **10** (1997), 443–469.

Bibliography

- [15] X. Cabré, *Extremal solutions and instantaneous complete blow-up for elliptic and parabolic problems*, Contemporary Math., Amer. Math. Soc. 2007, in: "Perspectives in Nonlinear Partial Differential Equations: In honor of Haim Brezis", to appear.
- [16] X. Cabré and A. Capella, *On the stability of radial solutions of semilinear elliptic equations in all of \mathbb{R}^n* , C. R. Math. Acad. Sci. Paris **338** (2004), 769–774.
- [17] E. K. Chan and R. W. Dutton, *Effects of capacitors, resistors and residual change on the static and dynamic performance of electrostatically actuated devices*, Proceedings of SPIE **3680** (1999), 120–130.
- [18] X. Cabré and Y. Martel, *Weak eigenfunctions for the linearization of extremal elliptic problems*, J. Funct. Anal. **156** (1998), 30–56.
- [19] M. G. Crandall and P. H. Rabinowitz, *Bifurcation, perturbation of simple eigenvalues and linearized stability*, Arch. Rational Mech. Anal. **52** (1973), 161–180.
- [20] M. G. Crandall and P. H. Rabinowitz, *Some continuation and variational methods for positive solutions of nonlinear elliptic eigenvalue problems*, Arch. Ration. Mech. Anal. **58** (1975), 207–218.
- [21] L. Evans, *Partial differential equations*, Graduate Studies in Mathematics, 19. AMS, Providence, RI, 1998.
- [22] P. Esposito, N. Ghoussoub and Y. Guo, *Compactness along the branch of semi-stable and unstable solutions for an elliptic problem with a singular nonlinearity*, Comm. Pure Appl. Math., to appear (2006).
- [23] M. Fila and J. Hulshof, *A note on the quenching rate*, Proc. Amer. Math. Soc. **112** (1991), 473–477.
- [24] M. Fila, J. Hulshof and P. Quittner, *The quenching problem on the N -dimensional ball*, Nonlinear Diffusion Equations and their Equilibrium States 3, Birkhäuser, Boston, (1991), 183–196.
- [25] S. Filippas and R. V. Kohn, *Refined asymptotics for the blow up of $u_t - \Delta u = u^p$* , Comm. Pure Appl. Math. **45** (1992), 821–869.
- [26] G. Flores, G. A. Mercado and J. A. Pelesko, *Dynamics and touchdown in electrostatic MEMS*, Proceedings of ICMENS **2003** (2003), 182–187.
- [27] A. Friedman and B. McLeod, *Blow-up of positive solutions of semilinear heat equations*, Indiana Univ. Math. J. **34** (1985), 425–447.
- [28] P. Feng and Z. Zhou, *Multiplicity and symmetry breaking for positive radial solutions of semilinear elliptic equations modelling MEMS on annular domains*, Electron. J. Diff. Eqns. **146** (2005), 1–14.
- [29] N. Ghoussoub and Y. Guo, *On the partial differential equations of electrostatic MEMS devices: stationary case*, SIAM, J. Math. Anal. **38** (2007), 1423–1449.

Bibliography

- [30] N. Ghoussoub and Y. Guo, *On the partial differential equations of electrostatic MEMS devices II: dynamic case*, NoDEA Nonlinear Diff. Eqns. Appl., to appear (2007).
- [31] Y. Guo, *On the partial differential equations of electrostatic MEMS devices III: refined touchdown behavior*, submitted (2006).
- [32] Y. Guo, Z. Pan and M. J. Ward, *Touchdown and pull-in voltage behavior of a MEMS device with varying dielectric properties*, SIAM, J. Appl. Math. **66** (2005), 309–338.
- [33] F. Gazzola and A. Malchiodi, *Some remarks on the equation $-\Delta u = \lambda(1 + u)^p$ for varying λ , p and varying domains*, Comm. Part. Diff. Eqns. **27** (2002), 809–845.
- [34] B. Gidas, W. M. Ni and L. Nirenberg, *Symmetry and related properties via the maximum principle*, Comm. Math. Phys. **68** (1979), 209–243.
- [35] Y. Giga and R. V. Kohn, *Asymptotically self-similar blow-up of semilinear heat equations*, Comm. Pure and Appl. Math. (1985), 297–319.
- [36] Y. Giga and R. V. Kohn, *Characterizing blow-up using similarity variables*, Indiana Univ. Math. J. **36** (1987), 1–40.
- [37] Y. Giga and R. V. Kohn, *Nondegeneracy of blow-up for semilinear heat equations*, Comm. Pure Appl. Math. **42** (1989), 845–884.
- [38] J. S. Guo, *On the quenching behavior of the solution of a semilinear parabolic equation*, J. Math. Anal. Appl. **151** (1990), 58–79.
- [39] J. S. Guo, *On the semilinear elliptic equation $\Delta w + \frac{1}{2}y \cdot \nabla w + \lambda w - w^{-\beta} = 0$ in R^n* , Chinese J. Math. **19** (1991), 355–377.
- [40] D. Gilbarg and N. S. Trudinger, *Elliptic partial differential equations of second order*, 2nd, Springer, Berlin, 1983.
- [41] A. Haraux and F. B. Weissler, *Non-uniqueness for a semilinear initial value problem*, Indiana Univ. Math. J. **31** (1982), 167–189.
- [42] J. D. Jackson, *Classical electrodynamics*, John Wiley, New York, 1999.
- [43] D. D. Joseph and T. S. Lundgren, *Quasilinear Dirichlet problems driven by positive sources*, Arch. Ration. Mech. Anal. **49** (1973), 241–268.
- [44] J. P. Keener and H. B. Keller, *Positive solutions of convex nonlinear eigenvalue problems*, J. Diff. Eqns: **16** (1974), 103–125.
- [45] J. B. Keller, J. Lowengrub, *Asymptotic and numerical results for blowing-up solutions to semilinear heat equations*, Singularities in Fluids, Plasmas, and Optics (1992), 11–38.
- [46] H. A. Levine, *Quenching, nonquenching, and beyond quenching for solution of some parabolic equations*, Annali Matematica Pura Appl. **155** (1989), 243–260.
- [47] O. A. Ladyzhenskaya, V. A. Solonnikov and N. N. Uralceva, *Linear and quasilinear equations of parabolic type*, Translations of Mathematical Monographs AMS **23**, 1968.

Bibliography

- [48] F. Mignot and J. P. Puel, *Sur une classe de problèmes non linéaires avec non linéarité positive, croissante, convexe*. Comm. Partial Differential Equations **5** (1980), 791–836.
- [49] H. C. Nathanson, W. E. Newell and R. A. Wickstrom, J. R. Davis, *The resonant gate transistor*, IEEE Trans. on Elect. Devices **14** (1967), 117–133.
- [50] J. A. Pelesko, *Mathematical modeling of electrostatic MEMS with tailored dielectric properties*, SIAM J. Appl. Math. **62** (2002), 888–908.
- [51] J. A. Pelesko, D. Bernstein and J. McCuan, *Symmetry and symmetry breaking in electrostatic MEMS*, Proceedings of MSM **2003** (2003), 304–307.
- [52] J. A. Pelesko and D. H. Bernstein, *Modeling MEMS and NEMS*, Chapman Hall and CRC Press, (2002).
- [53] J. A. Pelesko and A. A. Triolo, *Nonlocal problems in MEMS device control*, J. Eng. Math. **41** (2001), 345–366.
- [54] I. Stackgold, *Green's functions and boundary value problems*, Wiley, New York, (1998).
- [55] G. I. Taylor, *The coalescence of closely spaced drops when they are at different electric potentials*, Proc. Roy. Soc. A. **306** (1968), 423–434.
- [56] G. Zheng, *New results on the formation of singularities for parabolic problems*, Chinese University of Hongkong, PhD Thesis, 2005.